

NOAA Technical Memorandum ERL PMEL-59

WAVE AND CURRENT OBSERVATIONS AT THE COLUMBIA  
RIVER ENTRANCE, 10-13 SEPTEMBER 1981

F. I. Gonzalez  
M. R. Mulhern  
E. D. Cokelet  
T. C. Kaiser

Pacific Marine Environmental Laboratory

J. F. R. Gower  
J. Wallace

Institute of Ocean Sciences  
Sidney, B.C.  
Canada V8L 4B2

Pacific Marine Environmental Laboratory  
Seattle, Washington  
December 1984



**UNITED STATES  
DEPARTMENT OF COMMERCE**

**Malcolm Baldrige,  
Secretary**

**NATIONAL OCEANIC AND  
ATMOSPHERIC ADMINISTRATION**

**Environmental Research  
Laboratories**

**Vernon E. Derr  
Director**

## NOTICE

Mention of a commercial company or product does not constitute an endorsement by NOAA Environmental Research Laboratories. Use for publicity or advertising purposes of information from this publication concerning proprietary products or the tests of such products is not authorized.

## CONTENTS

		<u>Page</u>
0.	ACKNOWLEDGEMENTS . . . . .	1
	ABSTRACT . . . . .	3
1.	INTRODUCTION . . . . .	4
2.	OBSERVATION METHODS . . . . .	8
2.1	Surface Wave Data . . . . .	8
2.1.1	Waverider . . . . .	8
2.1.2	NDBC Buoys . . . . .	12
2.1.3	Side-Looking Airborne Radar (SLAR) . . . . .	12
2.2	Current Data . . . . .	16
2.2.1	NOS Subsurface Current Meters . . . . .	16
2.2.2	Surface Drifter Program . . . . .	16
	<i>Surface Drifter Deployments . . . . .</i>	16
	<i>Cape Disappointment Radar Tracking . . . . .</i>	20
	<i>Jetty A Radar Tracking . . . . .</i>	22
2.3	Surface Wind . . . . .	25
2.3.1	NOS Meteorological Station . . . . .	25
2.3.2	NDBC Buoy 46010 . . . . .	25
2.3.3	Clatsop County Airport . . . . .	25
3.	DATA SUMMARY . . . . .	26
3.1	Regional Data . . . . .	26
3.2	Local Data . . . . .	26
4.	PRELIMINARY DATA ANALYSIS . . . . .	49
4.1	Wave Decay Upriver of Buoy 8 . . . . .	49
4.2	Wave-Current Interaction Seaward of Buoy 8 . . . . .	56
4.2.1	The Observations . . . . .	56
4.2.2	Comparison with Linear, 1-D Theory . . . . .	58
5.	SUMMARY AND CONCLUSIONS . . . . .	73
6.	RECOMMENDATIONS FOR FURTHER RESEARCH . . . . .	74
6.1	Real-time, Long-term Monitoring . . . . .	74
6.2	Theory and Numerical Modeling . . . . .	75
6.3	Field Experiments . . . . .	75
7.	REFERENCES . . . . .	76

	<u>Page</u>
APPENDIX. INTENSIVE OBSERVATION PERIODS DATA SUMMARY . . . . .	79
<u>Flood of 10 September 1981</u> . . . . .	85
<i>Waverider Log, Tracks, and Spectra</i>	
<i>Cape Disappointment Radar Log and Surface Drifter Tracks</i>	
<i>Jetty A Radar Log and Surface Drifter Tracks</i>	
<u>Ebb of 10 September 1981</u> . . . . .	101
<i>Waverider Log, Tracks, and Spectra</i>	
<i>Cape Disappointment Radar Log and Surface Drifter Tracks</i>	
<i>Jetty A Radar Log and Surface Drifter Tracks</i>	
<i>SLAR Imagery</i>	
<u>Slack of 11 September 1981</u> . . . . .	119
<i>Waverider Log, Tracks, and Spectra</i>	
<i>Cape Disappointment Radar Log and Surface Drifter Tracks</i>	
<i>Jetty A Radar Log and Surface Drifter Tracks</i>	
<i>SLAR Imagery</i>	
<u>Ebb of 11 September 1981</u> . . . . .	137
<i>Waverider Log, Tracks, and Spectra</i>	
<i>Cape Disappointment Radar Log and Surface Drifter Tracks</i>	
<i>Jetty A Radar Log and Surface Drifter Tracks</i>	
<i>SLAR Imagery</i>	
<u>Flood of 12 September 1981</u> . . . . .	149
<i>Waverider Log, Tracks, and Spectra</i>	
<i>Cape Disappointment Radar Log and Surface Drifter Tracks</i>	
<i>Jetty A Radar Log and Surface Drifter Tracks</i>	
<i>SLAR Imagery</i>	
<u>Ebb of 12 September 1981</u> . . . . .	171
<i>Waverider Log, Tracks, and Spectra</i>	
<i>Cape Disappointment Radar Log and Surface Drifter Tracks</i>	
<i>Jetty A Radar Log and Surface Drifter Tracks</i>	
<i>SLAR Imagery</i>	
<u>Flood of 13 September 1981</u> . . . . .	187
<i>Waverider Log, Tracks, and Spectra</i>	
<i>Cape Disappointment Radar Log and Surface Drifter Tracks</i>	
<i>Jetty A Radar Log and Surface Drifter Tracks</i>	
<i>SLAR Imagery</i>	

Ebb of 13 September 1981 . . . . . 211

*Waverider Log, Tracks, and Spectra*  
*Cape Disappointment Radar Log and Surface Drifter Tracks*  
*Jetty A Radar Log and Surface Drifter Tracks*  
*SLAR Imagery*

LIST OF FIGURES

	<u>Page</u>
Figure 1. Map of U.S. West Coast, showing location of Columbia River entrance relative to various sources of environmental observations. SOWM locations refer to positions of grid points for which the Fleet Numerical Oceanographic Center (FNOC) provides wave spectrum nowcasts and forecasts computed by the FNOC Spectral Ocean Wave Model (SOWM). . . . .	5
Figure 2. Reference map of Columbia River entrance. . . . .	6
Figure 3. PMEL Waverider 67135 predeployment calibration curve. . . . .	9
Figure 4. NOAA data buoy 46010 at dockside in Astoria, Oregon. . . . .	11
Figure 5. Oregon Army National Guard Mohawk on a reconnaissance flight of Mount St. Helens, Oregon. The SLAR antenna can be seen mounted under the cockpit. . . . .	14
Figure 6. Nominal Mohawk SLAR flight lines 1 to 8. Circled numbers indicate the start of each flight line and coverage extends 25 km to the right of each track. . . . .	15
Figure 7. Sketch of surface drifter buoy equipped with radar corner reflector. . . . .	19
Figure 8(a). Surface pressure analysis for 1800Z, 8 September 1981. . . . .	27
Figure 8(b). Surface pressure analysis for 1800Z, 9 September 1981. . . . .	28
Figure 8(c). Surface pressure analysis for 1800Z, 10 September 1981. . . . .	29
Figure 8(d). Surface pressure analysis for 1800Z, 11 September 1981. . . . .	30
Figure 8(e). Surface pressure analysis for 1800Z, 12 September 1981. . . . .	31
Figure 8(f). Surface pressure analysis for 1800Z, 13 September 1981. . . . .	32
Figure 9(a). Wind and wave observations at NDBC 46002 for period 7-13 Sept. . . . .	33

	<u>Page</u>
Figure 9(b). Wind and wave observations at NDBC 46004 for period 7-13 Sept. . . . .	34
Figure 9(c). Wind and wave observations at NDBC 46005 for period 7-13 Sept. . . . .	35
Figure 9(d). Wind and wave observations at NDBC 46006 for period 7-13 Sept. . . . .	36
Figure 9(e). Wind and wave observations at NDBC 46010 for period 7-13 Sept. . . . .	37
Figure 10. Wind observations at Clatsop County Airport for period 9-14 Sept. 1981. . . . .	38
Figure 11. NOS current meter observations for stations C1 at depths 5, 25, and 35 feet from the bottom for the period 10-13 September. . . . .	39
Figure 12. Waverider and NDBC 46010 intercomparison spectra. . .	48
Figure 13a. Waverider significant wave height estimates as a function of distance east of buoy 8 for 10 Sept. 1981. . . . .	50
Figure 13b. Waverider significant wave height estimates as a function of distance east of buoy 8 for 11 Sept. 1981. . . . .	51
Figure 13c. Waverider significant wave height estimates as a function of distance east of buoy 8 for 12 Sept. 1981. . . . .	52
Figure 13d. Waverider significant wave height estimates as a function of distance east of buoy 8 for 13 Sept. 1981. . . . .	53
Figure 14. Drifter derived surface current vectors near the time of peak ebb. (a) 10 Sept. 1981. (b) 11 Sept. 1981. (c) 12 Sept. 1981. (d) 13 Sept. 1981. . . . .	55

LIST OF TABLES

		<u>Page</u>
Table 1.	Predeployment calibration of Waverider 67135. . . . .	10
Table 2.	Characteristics of Motorola APS-94E SLAR. . . . .	13
Table 3.	NOS Data Station summary. . . . .	17
Table 4.	Specifications for Aanderaa Recording Current Meter Model 4. . . . .	18
Table 5.	Characteristics of Corps of Engineers Wave Imaging Radar. . . . .	21
Table 6.	Daily Jetty A Radar fixes for determination of van orientation. . . . .	24
Table 7.	Daytime slack, peak ebb, or peak flood predictions for intensive observation periods. . . . .	40
Table 8.	Summary of Waverider deployments. . . . .	41
Table 9.	Summary of Cape Disappointment Radar observation periods. . . . .	42
Table 10.	Summary of Jetty A Radar observation periods. . . . .	43
Table 11.	Summary of Mohawk SLAR observation periods. . . . .	44
Table 12.	Summary of selected surface drifter speed and Waverider significant wave height observations. . . . .	45
Table 13.	Drifter information for current vectors presented in Figure 14. . . . .	54
Table 14.	Summary of observed wave and current characteristics and computed transfer function, $T$ , during the intensive observation periods. . . . .	57
Table 15a.	Wave height amplification $T$ (Eq. 3) for $d = 10$ m, $\theta_o = 0^\circ$ . . . . .	60
Table 15b.	Wave height amplification $T$ (Eq. 3) for $d = 10$ m, $\theta_o = 30^\circ$ . . . . .	61
Table 15c.	Wave height amplification $T$ (Eq. 3) for $d = 10$ m, $\theta_o = 60^\circ$ . . . . .	62
Table 15d.	Wave height amplification $T$ (Eq. 3) for $d = 15$ m, $\theta_o = 0^\circ$ . . . . .	63



	$\theta_o = 30^\circ$ . . . . .	64
Table 15f.	Wave height amplification $T$ (Eq. 3) for $d = 15$ m, $\theta_o = 60^\circ$ . . . . .	65
Table 15g.	Wave height amplification $T$ (Eq. 3) for $d = 20$ m, $\theta_o = 0^\circ$ . . . . .	66
Table 15h.	Wave height amplification $T$ (Eq. 3) for $d = 20$ m, $\theta_o = 30^\circ$ . . . . .	67
Table 15i.	Wave height amplification $T$ (Eq. 3) for $d = 20$ m, $\theta_o = 60^\circ$ . . . . .	68



## 0. ACKNOWLEDGEMENTS

It is a pleasure to acknowledge here the numerous organizations and individuals which contributed to the success of this field experiment.

The cooperation and assistance of the U.S. Coast Guard is gratefully acknowledged, particularly that of the USCG Search and Rescue Station at Cape Disappointment, commanded by LCDR J. Sprague. Coast Guard ET-1 K. Stokes provided able and valuable assistance in tracking radar reflectors as part of the surface current measurement program.

The National Marine Fisheries Service provided surface vessel support during the September experiment. Our sincere thanks to the crews of the EGRET, N. Zorich, R. Pettit, and W. Muir, and the NERKA, L. Davis, M. Laird, and E. Keller, for their cheerful assistance in frequently unpleasant conditions.

We are grateful to R. Patchen of the National Ocean Survey for permitting access to the important subsurface current meter data, to CDR O. Stephen, Commanding Officer of the NOAA Ship McARTHUR, for his enthusiastic cooperation and support, and to Lt. A. Snella for timely provision of the data in a useful format.

Much of the meteorological data was provided by R. Anderson, W. Burton, and K. Short of the National Weather Service, Seattle Ocean Services Unit, and by C. Krepke, R. Storey, and R. Tomes of the NWS Astoria field office. The valuable sea state and meteorological data collected by NOAA data buoys were provided by G. Hamilton, F. Abbell, and A. Johnson of the NOAA Data Buoy Center Data Systems Division of the National Space Technology Laboratories (NSTL) Station in Mississippi.

M. Stapp of PMEL ably solved numerous problems associated with the Waverider data transmission during the experiment. D. Zopf and C. Creech of Oregon State University provided seismic wavemeter records, and were assisted by W. Watkins of NWS, Astoria.

We appreciate the contributions of S. Noble of the Portland District Corps of Engineers, who provided valuable assistance and expertise, who arranged for deployment of the Corps wave imaging radar, and who made the resulting radar data available to us. Similarly, we are grateful to G. Arnott of EPSCO, who arranged the loan of a demonstration radar van for our use in tracking surface current drifters.

The spectacular side-looking airborne radar (SLAR) imagery was provided by the 1042nd MICAS unit of the Oregon Army National Guard. The consistently excellent quality of this imagery testifies to the high professionalism and technical competence of the entire organization--aircraft and sensor maintenance and support crews, technical observers and pilots. Especially appreciated is the cooperation and support of the Commanding Officer, Major S. Hammons, the invaluable advice and assistance of Capt. C. Rosenfeld (who pioneered the use of SLAR at the Columbia River Bar), and SFC R. Hartmann, who bore the primary responsibility for scheduling and coordinating all flights.

The assistance of the Office of Naval Research (ONR) is also very gratefully acknowledged. The field experiment was partially funded by an ONR grant overseen by H. Dolezalek of the ONR Coastal Sciences Program.

Finally, we acknowledge the support of the Ocean Services Division of the National Ocean Service, which provided partial support for this preliminary analysis.

Wave and Current Observations at the Columbia  
River Entrance, 10-13 September 1981.

F. I. Gonzalez  
M. R. Mulhern  
E. D. Cokelet  
T. C. Kaiser  
J. F. R. Gower  
J. Wallace

ABSTRACT. This technical memorandum presents the results of a joint exercise undertaken by PMEL and IOS to measure waves and currents at the Columbia River Bar during 10-13 September 1981. The waves were measured *in situ* with a vertical accelerometer buoy (Waverider) and observed aloft with Side Looking Airborne Radar (SLAR). Drifters tracked by an independent radar system provided surface-current velocities within the river mouth.

Wave refraction occurs in this area owing to depth and current gradients. Upriver of Buoy 8 waves decay on ebb and flood currents due to depth refraction away from the channel axis. During strong ebbs wave decay may be enhanced by breaking within the channel itself. Seaward of Buoy 8 waves amplify during peak ebbs and attenuate during peak floods. Most of the time the amplification and decay factors are predicted to within 20% by linear, one-dimensional theory. However, during one extreme ebb event the wave height was *underpredicted* by up to 50%. This was likely due to the crossing of wave crests produced by the current jet. The accurate prediction of such an event awaits the application of a two-dimensional theory for both the currents and the waves.

Predictions of hazardous sea state on the Columbia River Bar could certainly be improved by implementing recent analytical and numerical advances in wave refraction-diffraction theory. This should be complemented by Bar wave-height observations made available in real-time. These would provide accurate nowcasts and short-term forecasts and improve the intuition of forecasters and mariners. The observations would also provide a data base to tune the theoretical models and verify forecasts.

---

Contribution Number 717 from the Pacific Marine Environmental Laboratory.

## 1. INTRODUCTION

The entrance to the Columbia River (Figs. 1 and 2) is one of the most hazardous navigational regions in the world. Hundreds of search and rescue missions are run yearly by the Coast Guard facility at Cape Disappointment and the Coast Guard Air Station at Astoria. Nonetheless, tragic loss of life continues to occur; 22 were lost in Fiscal Year 1982 alone, during which the Coast Guard performed 400 search and rescue missions (saving 21 lives in the process).

Briefly stated, the physical processes which lead to dangerous sea state conditions are the interactions of incident swell and wind wave energy at the entrance with local bathymetry and opposing surface tidal currents. Peak ebb velocities of 6 knots and more can double the significant wave height on the bar within a few hours. The process of wave steepening and amplification is dependent not only on the tidal stage, but also on the period and direction of the incident wave energy.

The National Oceanic and Atmospheric Administration (NOAA) is responsible for forecasting sea state conditions at the Columbia River entrance, as well as a number of other potentially dangerous sites on the United States coasts. Thus, NOAA's National Weather Service (NWS) has supported research which resulted in a semi-automated procedure for predicting sea state conditions on the Columbia River Bar (Enfield, 1973). This investigation, though comprehensive, was nonetheless hampered by a lack of direct environmental measurements at the river entrance, especially with regard to wave direction.

Some sea state observations at the river entrance were obtained by NOAA for the U.S. Corps of Engineers Coastal Engineering Research Center (CERC) for short periods during 1979 and 1980. In addition, the Corps deployed the CERC wave imaging radar, which provided wavelength and direction estimates out to a distance of about 3 nm from Cape Disappointment. In February of 1980, an intensive three-week field experiment was organized and conducted by NOAA, during which airborne remote sensing data was gathered to supplement the *in-situ* observations. In particular, units of the Oregon Army National Guard provided side-looking airborne radar (SLAR) imagery of nearshore and deep water swell wavelength and direction. The use of such imagery at the Columbia River entrance had been pioneered by Rosenfeld and Bell (1978).

A major field variable which was not directly measured in the February 1980 experiment was the tidal current velocity. In September of 1981, an opportunity arose to gather *in-situ* and remotely sensed wave data coincident with the deployment of a number of subsurface current meters near the river entrance by the National Ocean Service. To supplement these subsurface measurements, a modest surface current measurement program was also implemented, which involved tracking surface drifters with two shore based radar units. This technique was developed by the Canadian Department of Fisheries and Oceans and was successfully employed in an earlier effort to map surface currents in the Strait of Georgia near the mouth of the Fraser River. The resulting environmental information collected at the Columbia River entrance during the 4-day period 10-13 September comprises the bulk of this report.

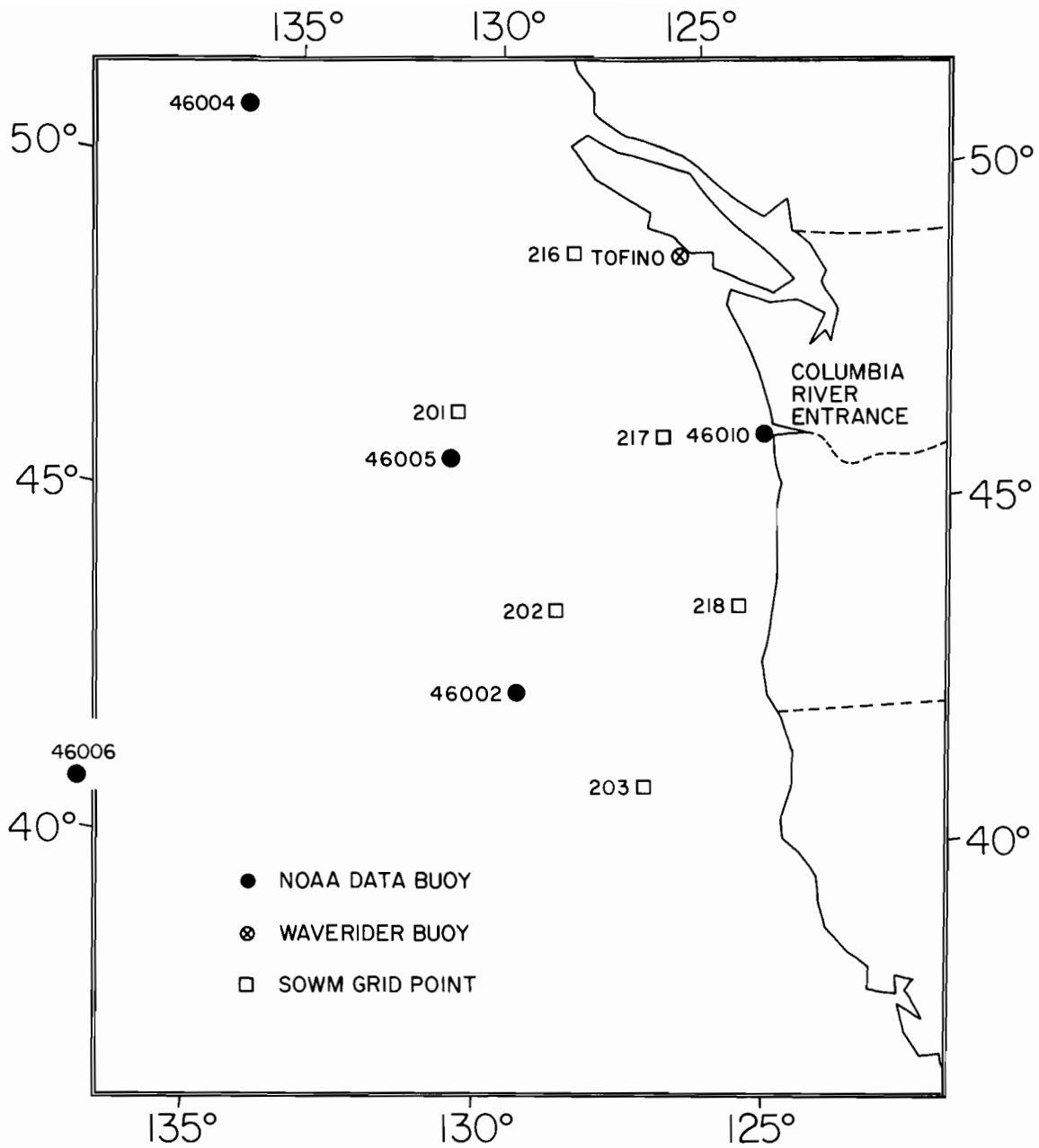


Figure 1. Map of U.S. West Coast, showing location of Columbia River entrance relative to various sources of environmental observations. SOWM locations refer to positions of grid points for which the Fleet Numerical Oceanographic Center (FNOC) provides wave spectrum nowcasts and forecasts computed by the FNOC Spectral Ocean Wave Model (SOWM).

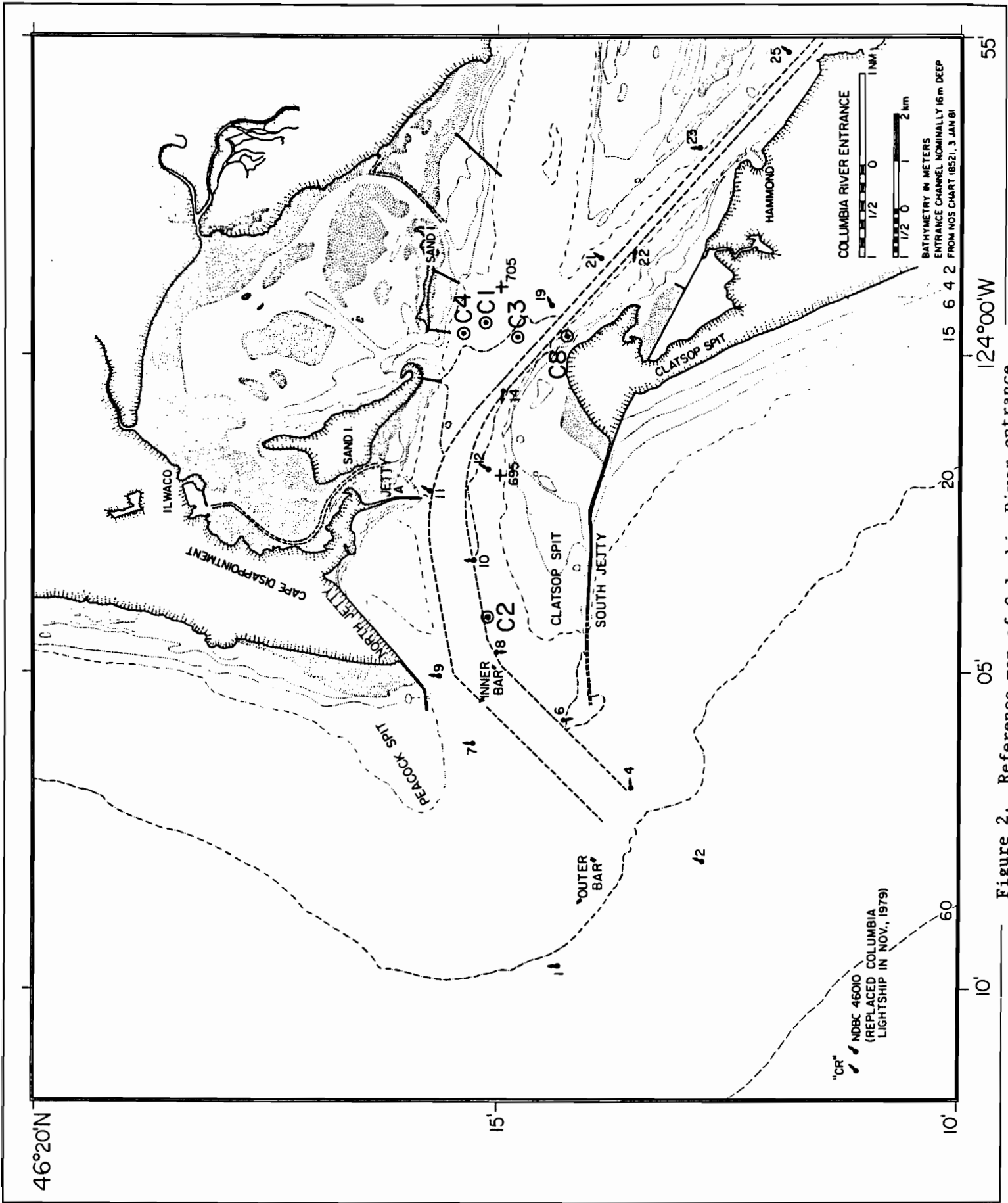


Figure 2. Reference map of Columbia River entrance.



This report is organized in the following way. In §2 we discuss the methods for observing and recording surface waves, currents and wind velocities. Section 3 is a summary of the data collected on both the regional and local scales. In §4 we analyze and interpret the data in terms of wave-current-bathymetry interaction at the Columbia River Entrance. Section 5 contains a summary, and §6 has recommendations for further research. One of the primary purposes of this report is to amalgamate the information gathered from various instruments and sources, to organize it on an event-by-event basis and to place it in one reference. The Appendix serves that purpose.

## 2. OBSERVATION METHODS

In this section, we describe the instrumentation and techniques employed to obtain estimates of surface waves, current speed and direction, and surface winds.

### 2.1 Surface Wave Data

Three sources of surface wave information are presented in this report: a Waverider buoy was deployed nearshore and inside of the entrance during eight separate intensive observation periods; NOAA Data Buoy Center (NDBC) buoys acquired data 5 nm southwest of the entrance every hour (NDBC 46010) and about 300 nm due west of the entrance every three hours (NDBC 46005) (see Fig. 1); Side Looking Airborne Radar (SLAR) imagery was obtained coincident with each Waverider deployment on approximately eight separate flight lines.

Details of the instruments and their deployment are given below.

#### 2.1.1 Waverider

This instrument is manufactured by the Datawell Corporation, and was calibrated at the NOAA Ocean Wave Instrument facility just prior to its use in this experiment. A new modulator printed circuit board was also installed as recommended by Datawell; the board is designed to correct measurements for water temperature variations from the 22.4° C at which the buoy was calibrated. The calibration results are given in Table 1 and in Figure 3. The buoy sampling rate was 2 Hertz, and the data was telemetered to shore and recorded both on a continuous strip chart and on a digital magnetic tape.

The buoy was deployed from a surface vessel on the end of a 300 foot tether line attached to a 3-point buoy bridle. Stationary and drifting modes of deployment were used. In the stationary mode, the launch was kept on station by steaming against the current, so that the Waverider streamed out behind the boat. Usually, this maneuver was performed near a channel marker buoy, which served as a reference point. In the drifting mode, the vessel was allowed to drift with the current in such a manner that the Waverider tether remained slack.

During each intensive observation period, a typical observation profile would consist of alternating 20-minute drifting and stationary records. Sextant fixes were taken periodically on a number of landmarks. The surface vessel used for the deployment was a 43-foot National Marine Fisheries Service (NMFS) vessel, the EGRET. During the observation periods, the EGRET was assigned the call sign "Waverider" for all field communications and log entries. In the Appendix, the logs, plotted tracks, and wave spectra for each of the observational periods are presented.

Each Waverider spectrum was obtained by subjecting a 17.07 minute record (2048 data points taken at 0.5 second sampling interval) to de-trending, a 10% cosine bell filter, fast Fourier transform, and 11 point

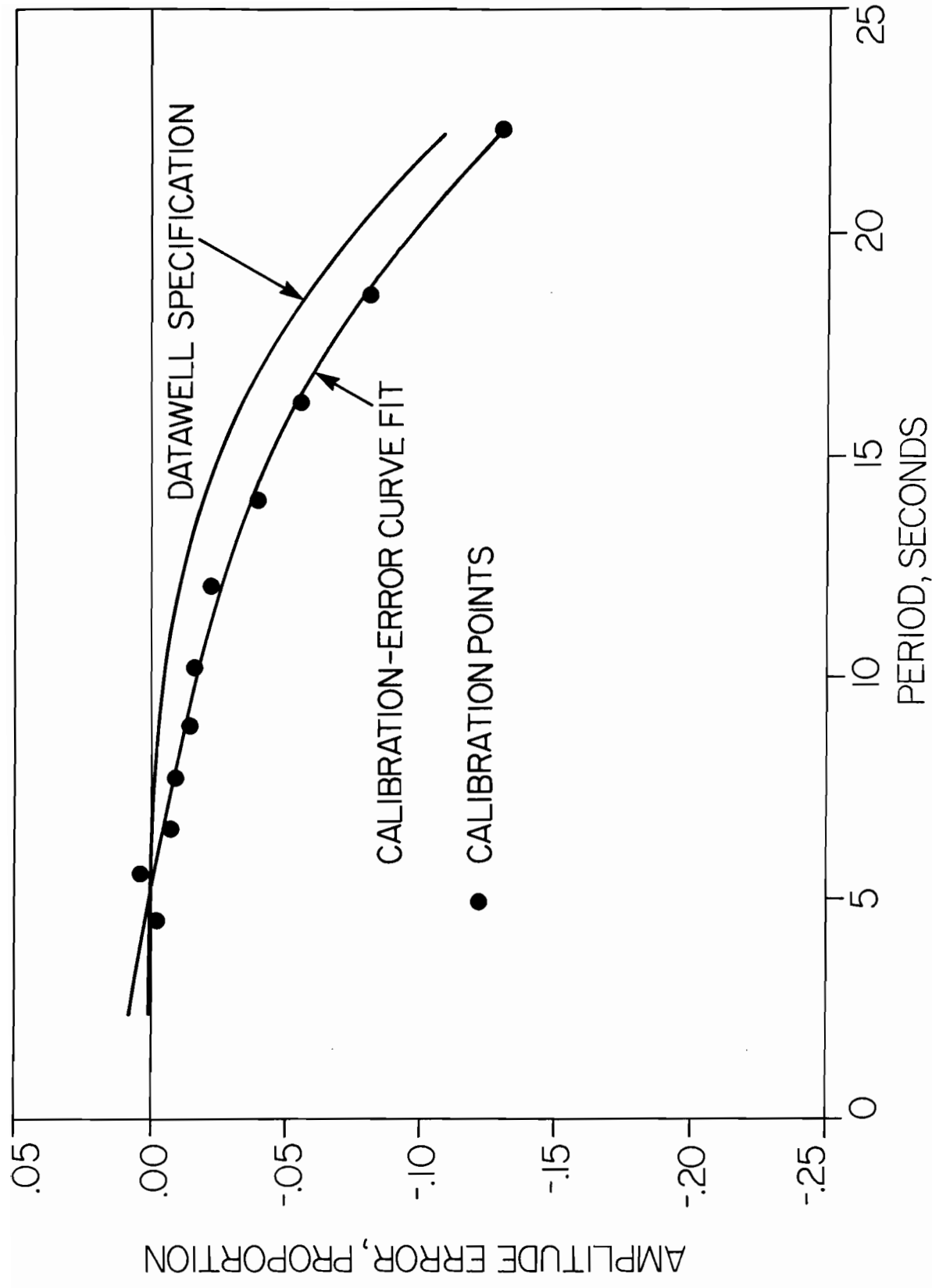


Figure 3. PMEL Waverider 67135 predeployment calibration curve.

TABLE 1. Predeployment Calibration of Waverider 67135.  
 Performed on August 25, 1981.

Y Actual Proportion	X Actual Seconds	Error Proportion
-0.0023	4.33	0.004
0.0040	5.37	-0.006
-0.0066	6.38	0.002
-0.0078	7.54	0.001
-0.0113	8.71	0.001
-0.0110	10.03	-0.002
-0.0118	11.85	-0.004
-0.0201	13.80	0.002
-0.0211	16.02	0.001
-0.0229	18.48	0.002
-0.0191	22.17	-0.001

Residual Standard Error is = 0.003 Proportion

Second Order Regression is for Waverider Calibration Minus Datawell Prediction Error.

Y is Waverider	X is Period	Degree Fit = 2
Term	Coefficient	
0	1.6046E-02	
1	-3.8403E-03	
2	9.8909E-05	



Figure 4. NOAA data buoy 46010 at dockside in Astoria, Oregon.

smoothing in the frequency domain. Because a running mean was employed, successive spectral estimates are not independent. Those which are 11 frequency bands apart are independent, however, and characterized by 22 degrees of freedom. For a Chi-square distribution, there is 90% confidence that the true spectral density is between 0.65 and 1.78 of the computed value.

### 2.1.2 NDBC Buoys

Hourly wave spectral estimates were provided by buoy 46010, located about 5 nm southwest of the entrance in 200 feet of water (see Figs. 2 and 4). The wave data analyzer (WDA), consisting of an axial linear accelerometer, provided spectral estimates with a resolution of .01 Hz over a range of 1.01 to 0.05 Hz, with 48 degrees of freedom and 80% confidence that the true value lies between 0.788 and 1.335 of the estimated value. This value must then be corrected for system noise and the power transfer function of the buoy as described by Steele and Earle (1979). Similar data buoys have been compared with a 0.9 meter diameter Waverider buoy; the average percentage error in significant wave height estimates was found to be about 7%. It is believed that the performance of NDBC 46010 is comparable or better. Examples of such spectral estimates are presented in Section 3 and the Appendix. Figure 4 is a photo of NDBC 46010 at dockside in Astoria, Oregon.

Similar spectral estimates were provided hourly at locations 46002, 46004, 46005, and 46006 (Fig. 1). Summaries of the spectra from these buoys for the experimental period are also presented in Section 3.

### 2.1.3 Side-Looking Airborne Radar (SLAR)

SLAR imagery was acquired during seven of the eight intensive observation periods and on two additional days when no Waverider or surface drifter measurements were made. The radar units are Motorola APS-94E models with the characteristics listed in Table 2. These radar units are mounted on Grumman OV-1 Mohawk aircraft (Fig. 5), flown by the Oregon Army National Guard from the Army Aviation Support Facility in Salem, Oregon.

Eight flight lines were flown on each mission, which was timed to be coincident with Waverider and surface current drifter data acquisition. The nominal flight lines and extent of the SLAR coverage are presented in Figure 6. The aircraft were flown at approximately 1000 m, and the swaths extended from nadir to the right of the aircraft for a distance of 25 km.

One of the best of the eight scenes acquired during each mission was chosen as an example, and these are presented in the Appendix. The primary SLAR information of interest in this experiment is the direction and length of swell which are evident in most scenes, and in the refraction due to bathymetry and currents which is obvious near shore. Wavelength and direction estimates can be obtained from this imagery by means of two-dimensional digital Fourier transforms.

---

TABLE 2. Characteristics of Motorola APS-94E SLAR

---

Frequency:	9100 to 9400 MHz (Variable)
Wavelength:	3.3 to 3.2 cm
Range:	25, 50, or 100 km
Offset from nadir:	0 to 60 km in 10 km steps
Modulation:	Pulse
Pulse Width:	0.2 ± 0.025 microsecond
Pulse repetition frequency:	750 pps
Resolution:	30 meters in range 0.45 degrees beamwidth in azimuth

---

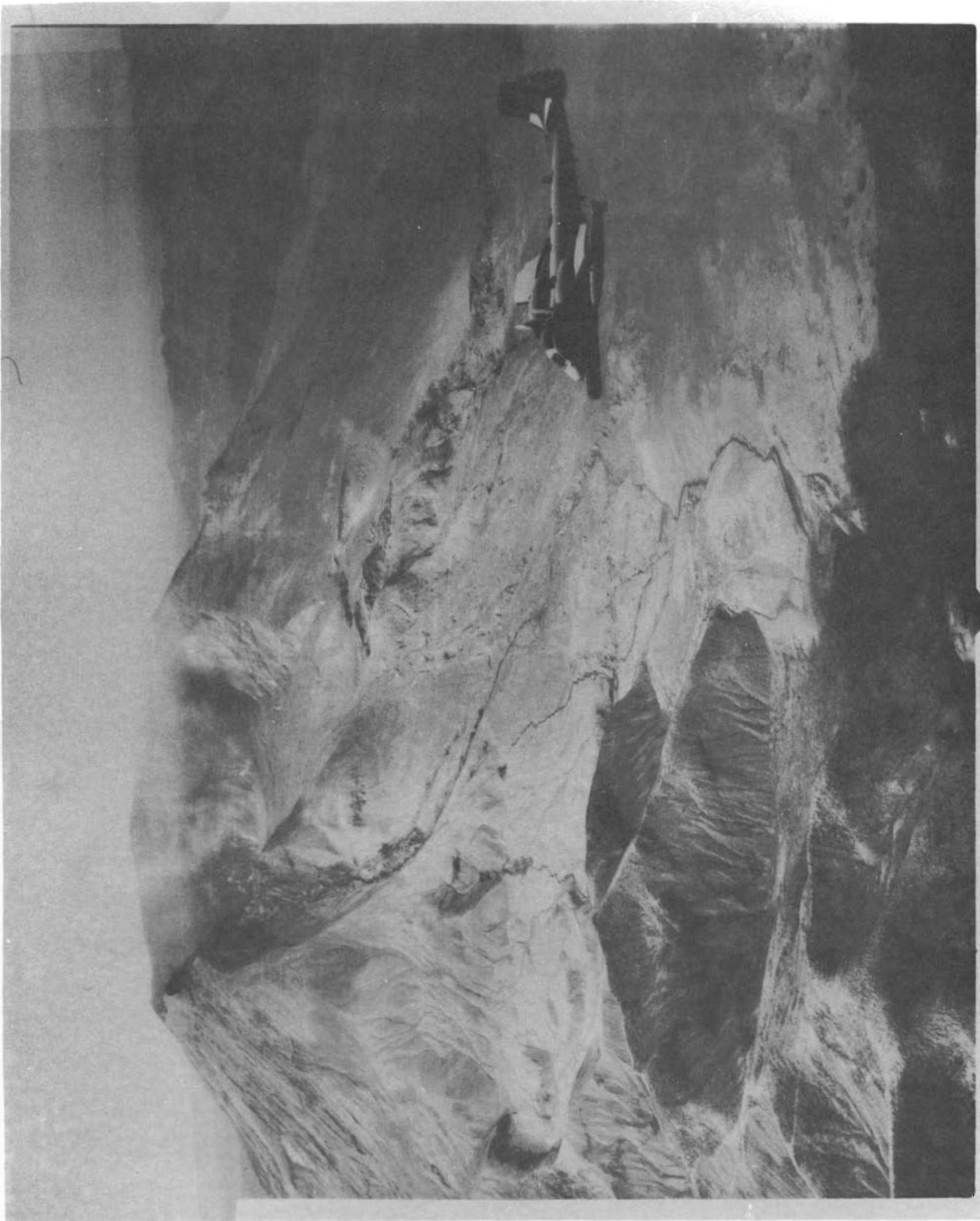


Figure 5. Oregon Army National Guard Mohawk on a reconnaissance flight of Mount St. Helens, Oregon. The SLAR antenna can be seen mounted under the cockpit.



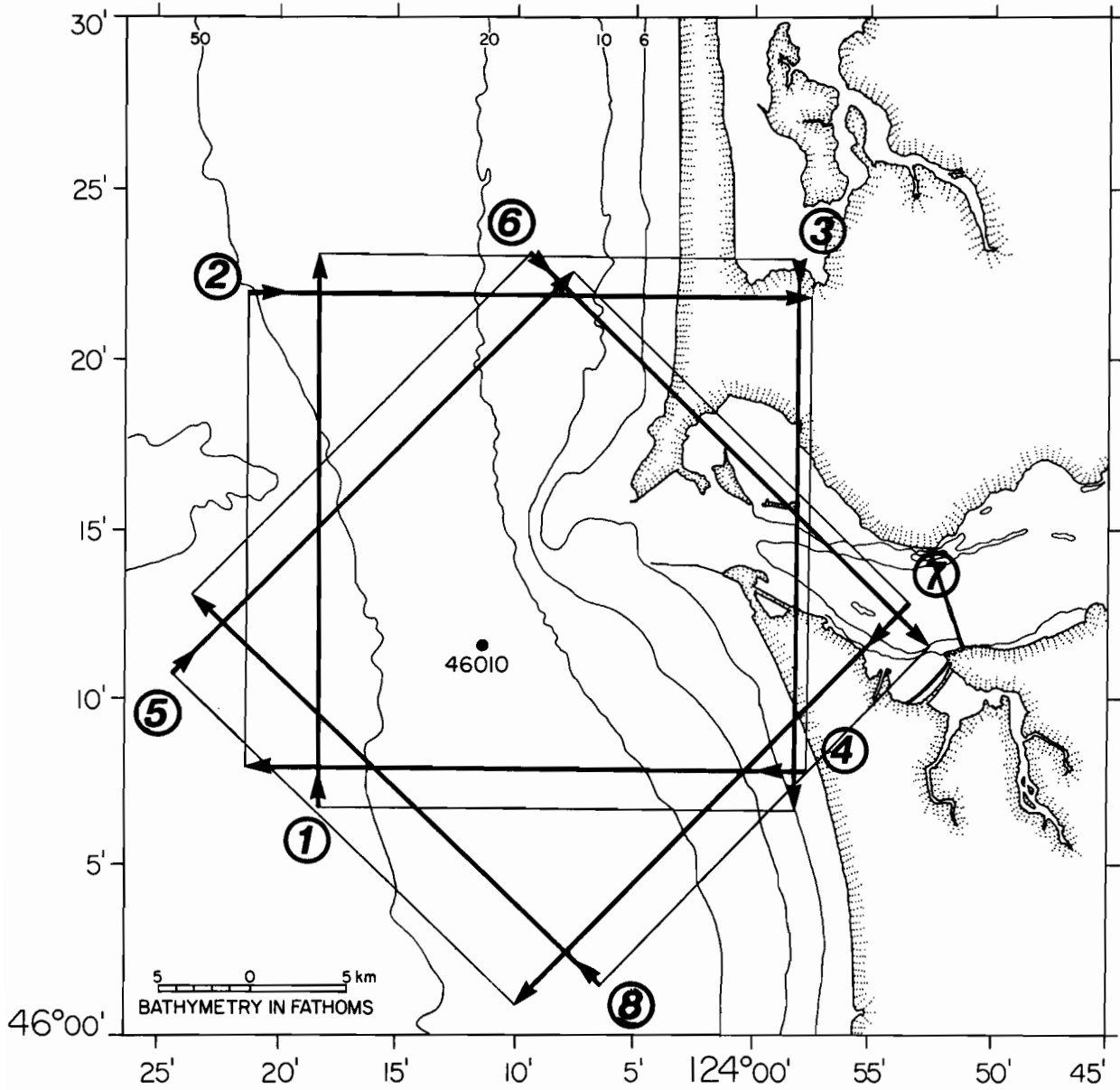


Figure 6. Nominal Mohawk SLAR flight lines 1 to 8. Circled numbers indicate the start of each flight line and coverage extends 25 km to the right of each track.

## 2.2 Current Data

There were two coordinated programs to obtain estimates of currents near the Columbia River entrance: the National Ocean Service (NOS) current meter moorings, and the PMEL/IOS surface drifter program.

### 2.2.1 NOS Subsurface Current Meters

As part of a larger scale Columbia River circulation survey, NOS deployed 19 subsurface current meters at a total of 8 separate moorings. The location of the five stations nearest the river entrance are shown in Figure 2. Table 3 lists the current meter depths, additional instrumentation at each mooring and other NOS stations occupied during the experiment. Unfortunately, the wave pressure gage at location C2 and the near-surface current meter at C3 were lost.

The instruments used were Aanderaa recording current meters Model 4, with temperature, conductivity and pressure sensors. The current meter specifications are given in Table 4, and examples of the output are presented in the Appendix. It should be noted here that the data presented in this report is raw field data quality, is unedited, and is uncorrected for errors due to effects of such things as sensor tilting.

Mulhern (1982) provides a detailed analysis of the data collected at stations C1, C3, C4 and C8, located at river mile 5 (RM 5).

### 2.2.2 Surface Drifter Program

As a supplement to the NOS subsurface current meter data, a modest surface drifter program was implemented. Two shore-based radar were used to track surface drifters equipped with 16-inch corner reflectors on 8-foot masts (Fig. 7). This technique was developed and used successfully by the Canadian Department of Fisheries and Oceans in a previous study of surface currents in the Strait of Georgia near the mouth of the Fraser River. During that study the drifters were tracked over ranges out to 20 nautical miles using the fixed observing stations of the Canadian Coast Guard's Vessel Traffic Management System. Tracking and position recording made use of the large display screens and positioning cursors of this system, and also benefitted from a computerized predictor system linked to the cursor. Tracking used here was greatly simplified to make use of available equipment. Several of the problems listed below could be avoided with a more sophisticated system. The drifter tracks are presented in the Appendix.

#### Surface Drifter Deployments.

The surface drifters were deployed from the 43 foot NMFS vessel NERKA. Four men were required: a helmsman, two persons to deploy and recover drifters, and a fourth person to communicate by radio with the radar operators on shore. Good radio communication was a critical part of the operation. Sea clutter and small craft would frequently obscure the

TABLE 3. NOS Data Station Summary

Station No.	Bottom Depth (Ft. below MLLW)	Current Meter Depth (Ft. above bottom)	Other Instrumentation	Location
C1	50	5, 25, 35	CTD	RM5
C2	50	20	Pressure	RM1
C3	70	5, 43, 53	CTD	RM5
C4	49	5, 21, 31	CTD	RM5
C5	35	5	CTD, Tidal Height	RM5
C8	36	5, 18	CTD, Tidal Height	RM5
C17	34	5, 20	CTD, Tidal Height	RM6.5
C18	38	5, 18, 25	CTD, Tidal Height	RM6.5
M1	--	--	Wind Speed, Direction, Air Temperature, Pressure	RM12.5 (Pilings on Desdemona Sands)
0572	--	--	Tidal Height	Jetty A
0573	--	--	Tidal Height	Chinook, WA
9008	--	--	Tidal Height	Ft. Steven, OR
0512	--	--	Tidal Height	Oak Point, WA
9040	--	--	Tidal Height	Astoria, OR

---

TABLE 4. Specifications for Aanderaa recording current meter Model 4.

---

CURRENT SPEED

Sensor: A rotor with magnetic coupling through the instrument case. Electronic counter registers the number of rotations during the period between two samplings.  
Range: 2.5 to 250 cm/sec  
Accuracy:  $\pm 1$  cm/sec or  $\pm 2\%$  of actual speed, whichever is greater  
Starting velocity: 2.0 cm/sec

CURRENT DIRECTION

Sensor: Magnetic compass with needle clamped onto potentiometer ring  
Resolution:  $0.35^\circ$   
Accuracy:  $\pm 7.5^\circ$  for speeds of 2.5 to 5 cm/sec or 100 to 200 cm/sec  
 $\pm 5^\circ$  for speeds of 5 to 100 cm/sec  
Maximum Compass Tilt:  $12^\circ$  from horizontal

TEMPERATURE

Sensor: Thermistor (Fenwal GB32JM19)  
Range:  $-2.46^\circ\text{C}$  to  $21.48^\circ\text{C}$   
Accuracy:  $\pm 0.15^\circ\text{C}$   
Resolution:  $0.02^\circ\text{C}$   
63% Response Time: 12 seconds

CONDUCTIVITY

Sensor: Inductive cell  
Range: 0 to 70 mmho/cm  
Resolution: 0.07 mmho/cm

PRESSURE

Sensor: Bourdon tube driving a potentiometer  
Range: 0-100 PSI  
Accuracy:  $\pm 1$  PSI  
Resolution:  $\pm 0.1$  PSI

---

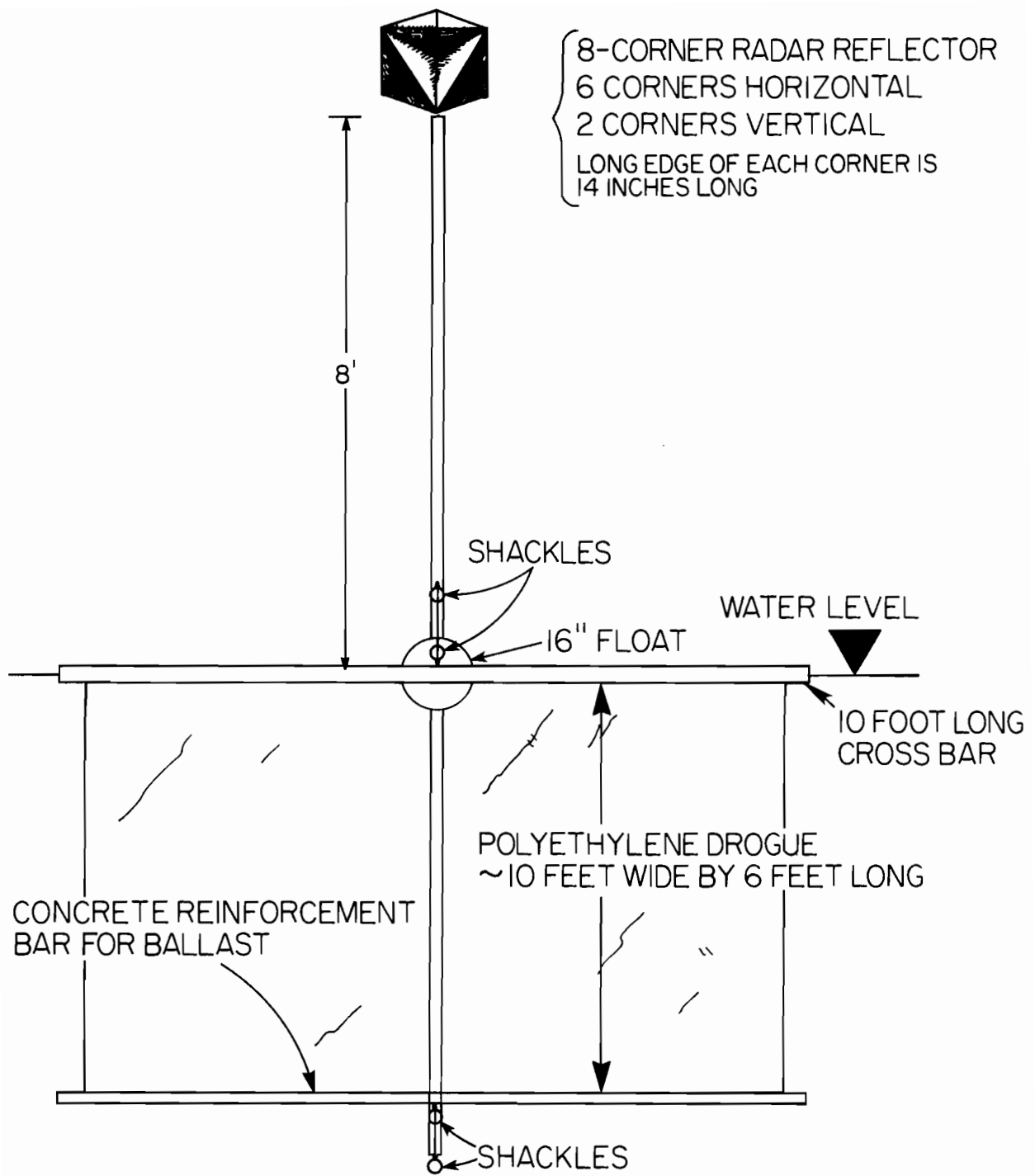


Figure 7. Sketch of surface drifter buoy equipped with radar corner reflector.

target or confuse the radar operator. When a maximum of four drifters had been deployed, the strategy called for the surface vessel to keep as many drifters in sight as possible, and make frequent visits to each drifter in turn, pulling alongside, then proceeding to the next, all the while keeping the radar operators advised of the vessel's position. In this way, the radar operators could make frequent checks on the validity of their target identification and tracking. If an operator was uncertain of a drifter target or had lost its signal on the radar scope, he would request that the NERKA pull alongside that drifter momentarily for positive identification.

#### Cape Disappointment Radar Tracking.

The Portland District of the Corps of Engineers deployed an X-band imaging radar near the Cape Disappointment lighthouse at an elevation of 220 feet above mean sea level. The system was designed to obtain wavelength and direction information out to a range of 3 nautical miles. Table 5 lists the specific design characteristics of this unit. An earlier, similar system is described by Mattie and Harris (1979).

The drifter buoys were tracked from Cape Disappointment using this radar, which was equipped with a variable range marker with a resolution in nautical miles to the second decimal place. All bearings taken were relative to the radar orientation which was referenced to charted features.

Once a buoy was deployed by the surface vessel, that fact was communicated by radio to the radar operator, and the target was identified on the screen. Thereafter, until buoy recovery, range, relative bearing, and local time were taken at nominal five minute intervals. Fixes were taken more frequently if the buoys moved at high speed. The observations and any appropriate comments were logged by an assistant.

Sea clutter and small craft drifting in the current created problems in correctly identifying the drifting buoys. This problem was substantially eliminated by requesting the deployment vessel to run between the buoys and identify them as the vessel paused alongside. The deployment vessel moved at high speed between buoys, and this made it an easy target for the radar operator to identify.

Another minor problem was the existence of dead sectors, or areas where the radar signal was blocked due to buildings, land masses, etc. In general, however, dead sectors were not a significant portion of the area of interest; furthermore, the dead sectors of the Cape Disappointment and Jetty A radars were different, so that a drifter fix could usually be taken by the unblocked radar.

Calibration fixes were taken to a few known fixed targets in the field of view. These showed good accuracy when compared to charted distances and bearings, and excellent repeatability from day to day.

The drifter tracks obtained in this manner were then plotted, and are presented in the Appendix.

---

TABLE 5. Characteristics of Corps of Engineers Wave Imaging Radar

---

Model:	Raytheon RM 1650/12XR
Frequency:	9375 $\pm$ 30 MHz (X-band)
Wavelength:	3.2 cm
Pulse width:	0.06 microsecond for .75 to 3 nm ranges 0.5 microseconds for greater ranges
Range resolution:	20 yards or 1% of range, whichever is greater
Vertical beam width:	22 degrees
Horizontal beam width:	0.65 degrees at 3 decibels
Antenna length:	12 feet
Power:	50 kilowatts
Rotation rate:	27 rpm
Display scope:	16 inch diameter plan position indicator (PPI) cathode ray and tube, with fast decay phosphor.
Scope camera:	Bolex 16mm reflex

---

### Jetty A Radar Tracking

In this section we describe how a mobile radar van was used to track the drifters. This radar system provided independent check on the positions of the drifters as determined from the Cape Disappointment radar and it provided the opportunity to evaluate the concept of using such a mobile radar unit for future drifter studies.

The radar van was on loan from Epsco Marine, 1030 Industry Drive, Seattle, WA. The vehicle was a Ford van of the type normally used for private transportation. It was equipped with an Epsco model S14 radar which operates at 10KW of peak power on an X-band frequency of 9275 MHz corresponding to an electromagnetic wavelength of 3.23 cm. The radar had an optional 6 foot scanning antenna and a variable range marker (VRM). The latter is an illuminated ring which appears on the 7" radar scope and whose diameter can be adjusted by the operator. The ring is expanded to intersect a specific target on the scope, and the range to that target is displayed on a digital meter. The bearing to a target can be ascertained by aligning a radial line through the target and reading the bearing from a bearing ring graduated in degrees at the outer edge of the display.

The radar can operate on one of the following ranges:  $\frac{1}{2}$ ,  $1\frac{1}{2}$ , 3, 6, 12, 34 and 50 nm. A short pulse length of 0.08 $\mu$ -sec. characterizes the  $\frac{1}{2}$  to  $1\frac{1}{2}$  nm range settings, and a longer pulse length of 0.8  $\mu$ -sec. is used for the 6 to 50 nm settings. At the 3 nm setting, however, either pulse length is permitted. For the entire experiment the 3 nm-short pulse setting was used. At this setting the drifting buoy images subtended an angle of 2° and were 0.02 nm in radial width when at a typical operating range of 1 to  $1\frac{1}{2}$  nm. Epsco sales literature advertises a bearing accuracy of 2° or better and a range resolution of less than 30 yards. These values are not at variance with what we observed. During operation a radar fix was taken by placing the radial bearing line through the center of the target and the range ring on the nearside of the target.

The radar range and bearing to a target gives the position of the target relative to the radar. In order to find the absolute location of the target the position and orientation of the radar must be determined. For each day of the experiment the radar van was positioned within 3 m of the same location. This location was determined from the following horizontal sextant fixes, in which the numbers in parenthesis refer to the objects listed in Table A1 of the Appendix.

left target:		(3) Large Sand Island Obs. Tower
left angle:	44° 47'	
center target:		(5) Jetty A light, "F1 4 sec. 31 ft. 10 M"
right angle:	114° 20'	
right target:		(2) Cape Disappointment lighthouse, "Alt. F1 R&W 30. sec. 220 ft. 18 M"
right check angle:	37° 37'	
right check target:		(18) Light on S tip large Sand Island, "F1 G 4 sec. 15 ft. '1'"



This position is on the landward end of Jetty A at  $124^{\circ} 02' 26''$  W,  $46^{\circ} 16' 33''$  N according to NOAA chart 18521, 51st Ed., Jan. 3, 1981. The van was oriented in such a way that  $0^{\circ}$  bearing on the radar corresponded to  $0^{\circ} \pm 1^{\circ}$  True. This was achieved by aligning the van visually with a pair of Dayglo-orange signal cloth markers placed on the ground at distances from the van of approximately 10 and 20 m. On most occasions a final determination of the orientation of the van was obtained by taking radar fixes to known landmarks. These fixes are given in Table 6. Those to the Clatsop Spit lookout tower are best since the localized steel structure gave a strong radar echo. The radar range recorded for this tower could be used to calibrate the remaining radar fixes. This has not been done for the drifter fixes reported here, but in general observed ranges should be multiplied by a factor of actual distance/observed distance =  $3.18/3.13 = 1.02$ .

The technique of tracking the drifters on the radar scope was refined during the course of the experiment. On the first two days, 10 and 11 September, a hood and magnifier were attached to the scope. Although this had the advantage of giving good picture contrast and an enlarged image, there was no convenient way for the operator to follow individual targets except by simply keeping a watch on them. It proved impossible to follow more than 2 drifters by this approach since the radar scope was often cluttered with too many other returns from as many as 30 to 40 small fishing boats in the area. On 12 and 13 September, the hood and magnifier were removed, and clear plastic overlays were placed directly on the scope. The track of each drifter was marked on the plastic with a grease pencil. For each drifter this gave the radar operator a reference line to which he could return if his attention were diverted. Individual drifter fixes were taken every 2 minutes or as often as possible. The operator would set the variable range ring and bearing line on the target image and call out the readings to an assistant who would log them. Time was recorded to the nearest minute, with the actual fix usually occurring within  $\pm 15$  seconds of this time.

The radar operator used a portable FM radio transceiver to exchange information on drifter deployment and location with the NERKA and with the Cape Disappointment radar operator. When a drifter location was in doubt, verification was obtained by requesting that the deployment vessel rapidly approach, and then move away from, the drifter. The concomitant merging and separating of the two radar blips then enabled the radar operator to identify the drifter target.

Tracking the surface drifter corner reflectors with the Epsco radar and the Corps radar was a success. It appears that useful surface current estimates can be obtained in this manner. However, eye strain and fatigue were severe in the case of the Epsco radar operation. This would be alleviated with a larger radar screen, on the order of at least 12 inches in diameter. Even better would be the projection of the image onto a large television screen equipped with a light pen for the automatic logging of range and bearing to target. Such systems are presently on the market.

Notwithstanding the inherent difficulty of gathering these data and the necessary caveats regarding their quality, these field efforts are necessary if we are to gain sufficient understanding of the physical processes involved to improve the accuracy of Bar forecasting procedures.

TABLE 6. Daily Jetty A Radar Fixes to determine radar van orientation.

<u>Date &amp; Tidal Stage</u>	<u>Landmark</u>	<u>Range (nm)</u>	<u>Radar Bearing (°)</u>
10 September Flood	(19) Clatsop Spit lookout tower	3.14	157.5
	(20) Bend in South Jetty	2.46	180
10 September Slack	(19) Clatsop Spit lookout tower	3.14	157
	(20) Bend in South Jetty	2.46	179
	(21) Light on S tip of line of piles on S central side of small Sand Island	2.73	114
	(22) Seaward end of North Jetty	2.11	248
12 September Flood	(19) Clatsop Spit lookout tower	3.13	156
	(20) Bend in South Jetty	2.44	181
	(18) Light on S tip of line of piles near SE corner of large Sand Island	1.61	122
12 September Ebb	(Van orientation unchanged from Flood)		
13 September Flood	(Van orientation not logged)		
13 September Ebb	(19) Clatsop Spit lookout tower	3.12	157
	(20) Bend in South Jetty	2.45	181
	(18) Light on S tip of line of piles near SE end of large Sand Island	1.61	123

## 2.3 Surface Wind

Observations of surface wind speed and direction were made at three locations: a meteorological station deployed by NOS, NOAA data buoy 46010, and the NWS station at the Clatsop County airport.

### 2.3.1 NOS meteorological station.

The National Ocean Service meteorological station was located about 2 miles northwest of the Port of Astoria, at river mile 12.5, on pilings at Desdemona Sands, at 46°12'38" North latitude and 123°52'30" West longitude. The meteorological package is manufactured by Aanderaa. Wind direction is an instantaneous measurement, and wind speed is a 10 minute average recorded every 10 minutes.

### 2.3.2 NDBC buoy 46010

NOAA data buoy 46010 consists of a Coast Guard large navigation buoy (LNB) outfitted with a General Service Buoy Payload (GSBP) manufactured by Magnavox. Wind speed and maximum wind gust estimates are obtained by means of a vortex shedder; one second samples are averaged for 8.5 minutes to get average wind speed, while the highest 8 second average in that record is retained as the maximum gust. A vane and fluxgate compass also samples wind direction every second to provide an 8.5 minute average.

### 2.3.3 Clatsop County Airport.

The National Weather Service (NWS) maintains a standard F420C wind sensor at the Clatsop County Airport, about 20 nm southeast of the Columbia River entrance. The sensor is manufactured by Electric Speed Indicator Company, and is mounted at an elevation of 10 meters. Both speed and direction are instantaneous and continuous measurements. The outputs are displayed in the NWS office on needle gauges, which are read and logged every hour by the NWS personnel on watch.

### 3. DATA SUMMARY

#### 3.1 Regional Data

In this section, we present a general overview of the regional meteorology and wave conditions for the period 8-13 September. Figures 8a-f present the 1800Z (1100 PDT) surface pressure analyses for the period 8-13 September, and Figures 9a-e summarize the wind and wave conditions at NOAA data buoys 46002, 46004, 46005, 46006, and 46010 for the period 7-13 September. Figure 10 presents the wind speed and direction measured at Clatsop County airport from 9 to 13 September. Figure 11 presents the NOS current meter measurements for station C1 at depths 5, 25, and 35 feet from the bottom, for the period 10-13 September.

The timing of the experimental period, 10-13 September, was fortuitous. From 8-10 September, the low pressure systems shown in Figures 8a-c dominated the Northeast Pacific. As a result, significant wave height in deep water off the Washington-Oregon coast rose from a value of 1 m on 7 September to 2.5 m on 10 September (Figs. 9a,c). Even higher waves were produced west of Vancouver Island; on 10 September, heights of 4 m were observed at 0000 PDT (Fig. 9b), as the southeast storm sector, characterized by 50 knot winds, made landfall on the Canadian coast (Figs. 8b,c).

Similarly, at the Columbia River entrance, significant wave height rose steadily from a minimum of 1 m on 7 September to a peak value of 3 m at 0000 PDT on 12 September (Fig. 9e). Substantial swell energy from the low pressure systems was therefore present during the four-day experimental period. Furthermore, in contrast to the previous three days, an offshore high pressure system dominated the Northwest's coast on 11-13 September, bringing northerly winds of up to 10 m/s and adding significant local wind wave energy to that of the swell already present (Fig. 9e).

#### 3.2 Local Data

During the four days (10-13 September) of the experiment, there were 8 periods of a few hours each of intensive data collection. The intention was to collect data at predicted times of slack current, peak ebb current, or peak flood current. These times and the predicted tidal current speeds for NOS Station 695 are presented in Table 7. Table 8 summarizes the times and modes of deployment for the Waverider. Tables 9 and 10 summarize the periods during which surface drifters were tracked by the shore-based radar units at Cape Disappointment and Jetty A, and Table 11 summarizes the periods during which SLAR imagery was acquired by OANG Mohawks. The data for these intensive observation periods are collected together and presented in the Appendix.

Table 12 summarizes the significant waveheight estimates derived from Waverider observations obtained during the eight intensive observation periods. The table also provides surface current estimates near the time of Waverider deployments; these estimates are derived from two sources-- surface drifter speeds, and the NOS algorithm for current speed at station 695. In addition, the SLAR image for each observation period is indicated in the last column. The Waverider records are of varying length because the

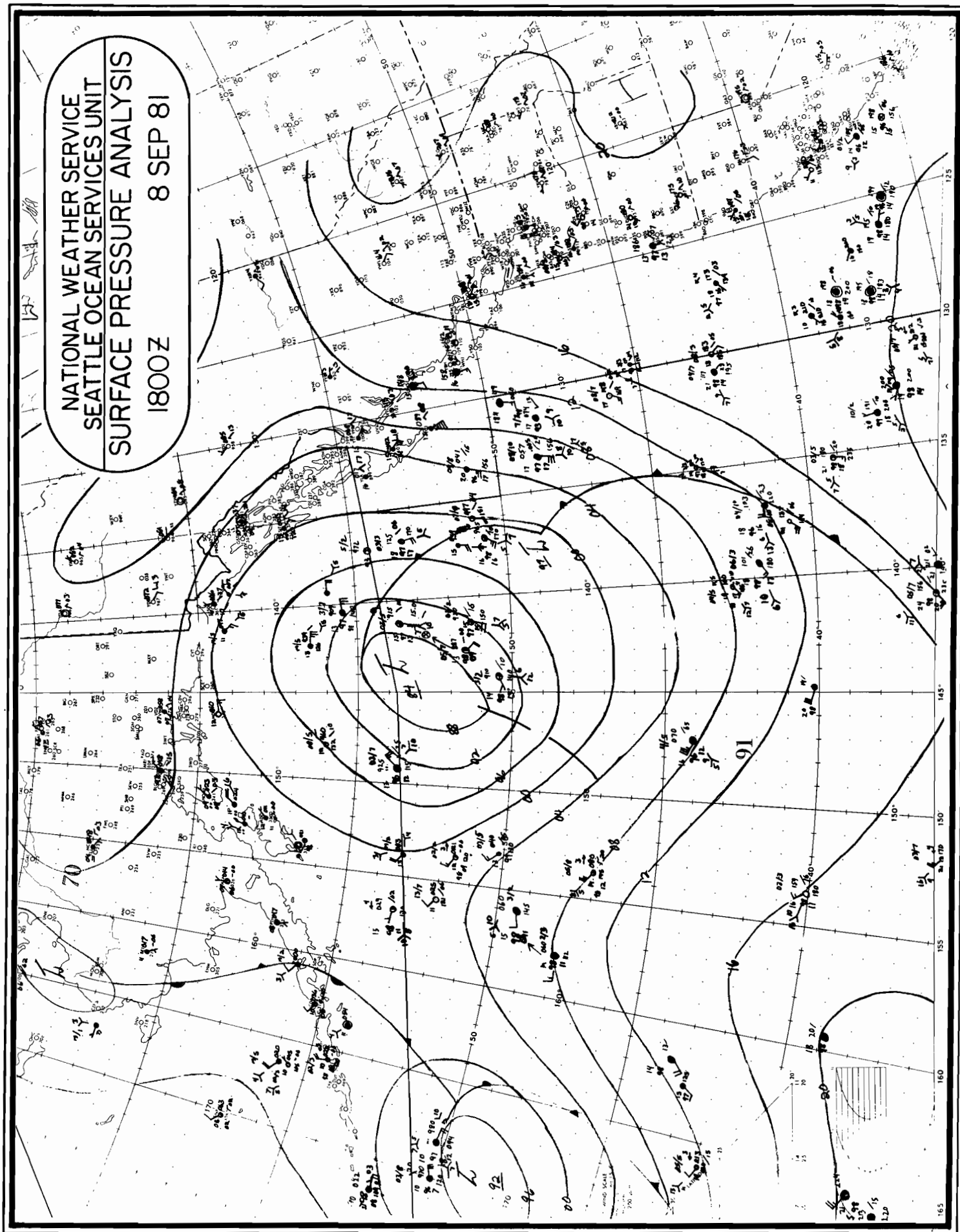


Figure 8(a). Surface pressure analysis for 1800Z, 8 September 1981.

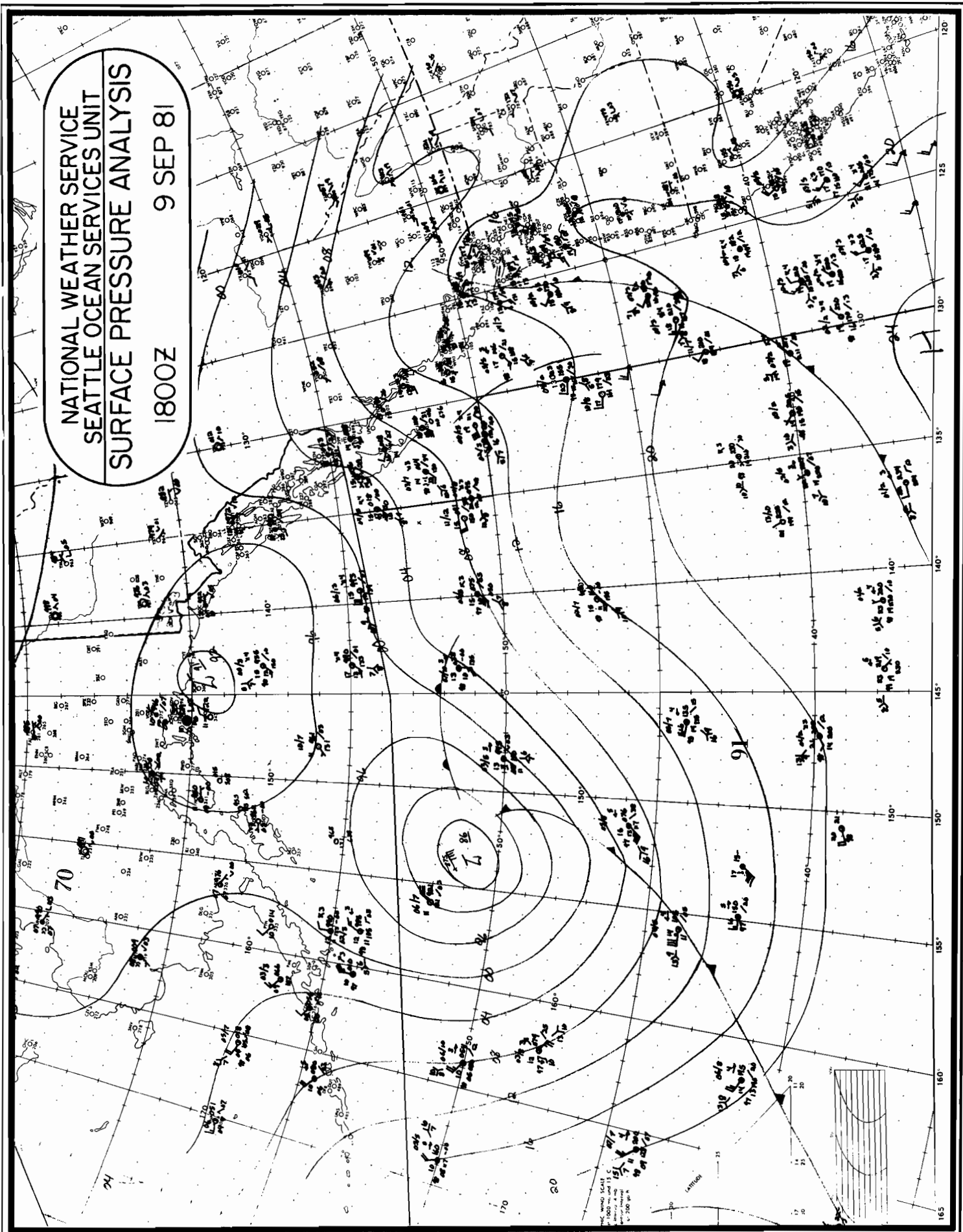


Figure 8(b). Surface pressure analysis for 1800Z, 9 September 1981.

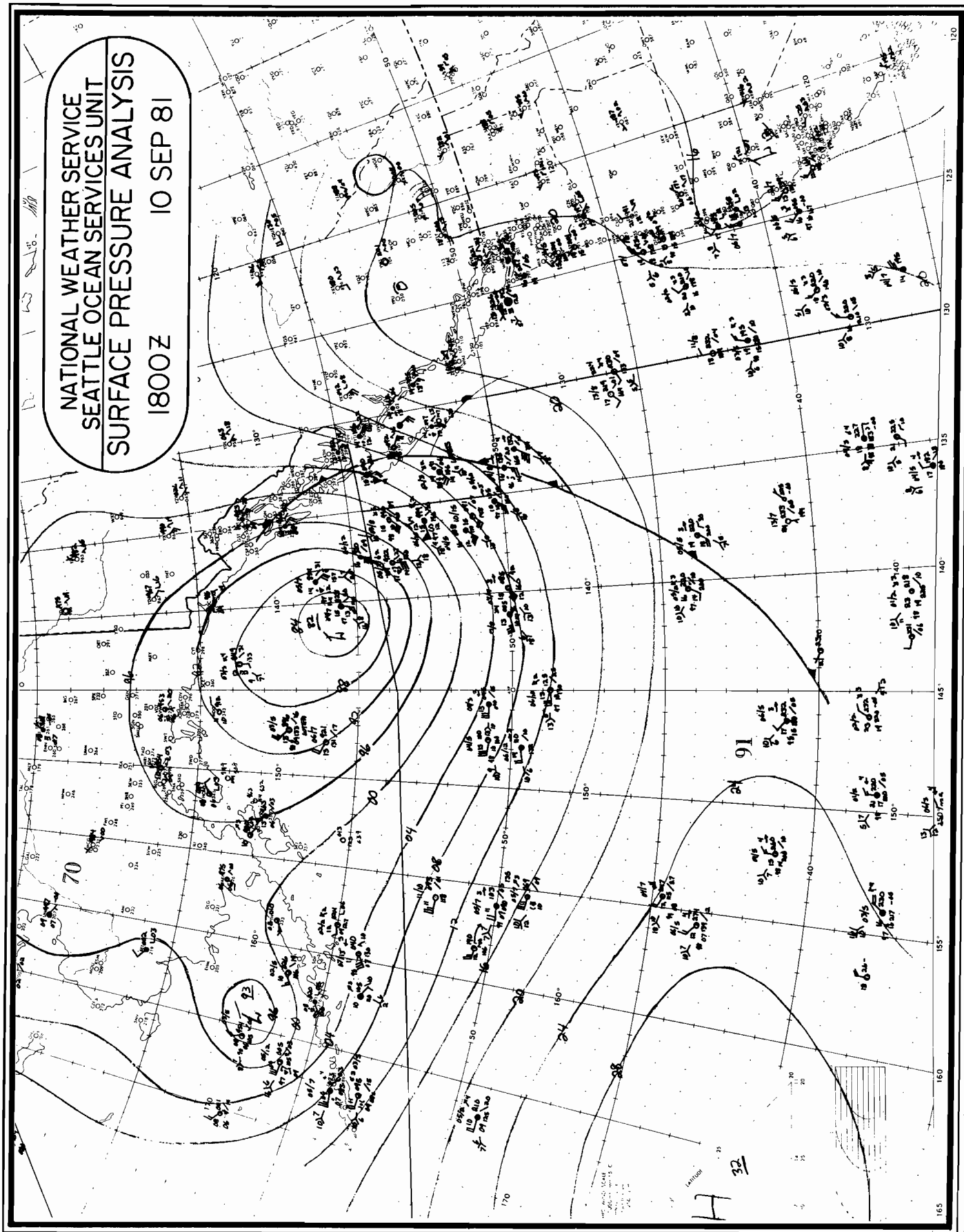


Figure 8(c). Surface pressure analysis for 1800Z, 10 September 1981.

NATIONAL WEATHER SERVICE  
SEATTLE OCEAN SERVICES UNIT  
SURFACE PRESSURE ANALYSIS

1800Z 11 SEP 81

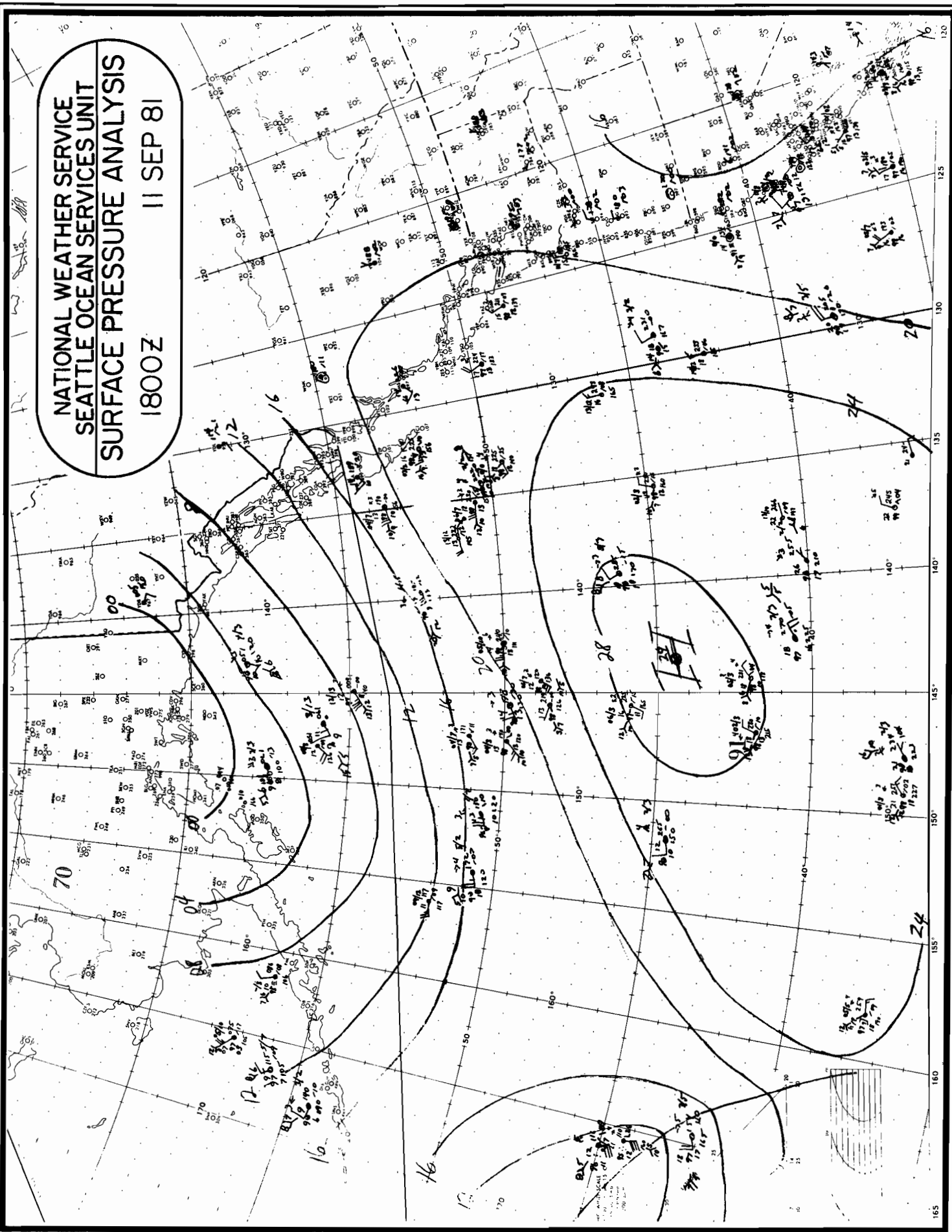


Figure 8(d). Surface pressure analysis for 1800Z, 11 September 1981.



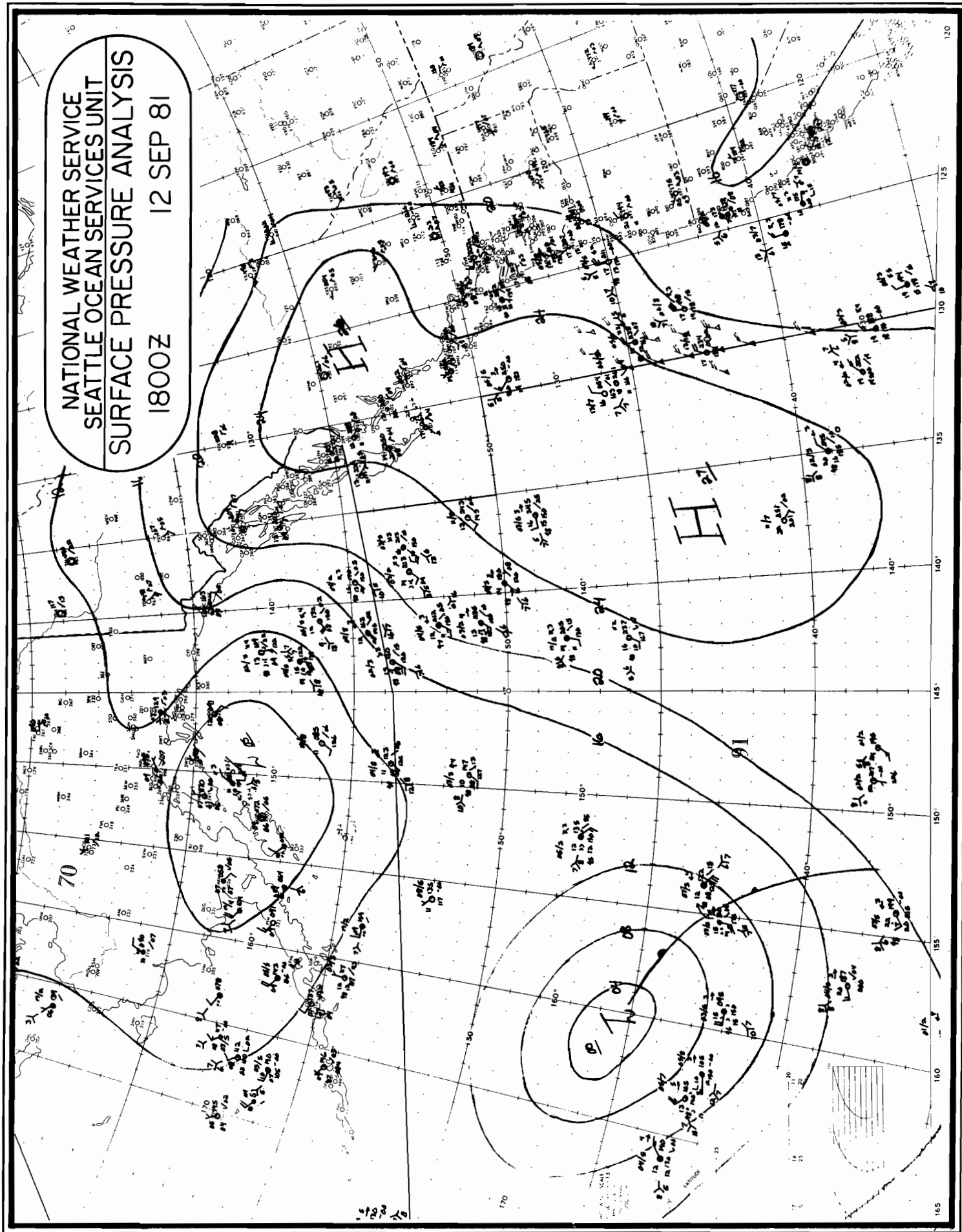


Figure 8(e). Surface pressure analysis for 1800Z, 12 September 1981.

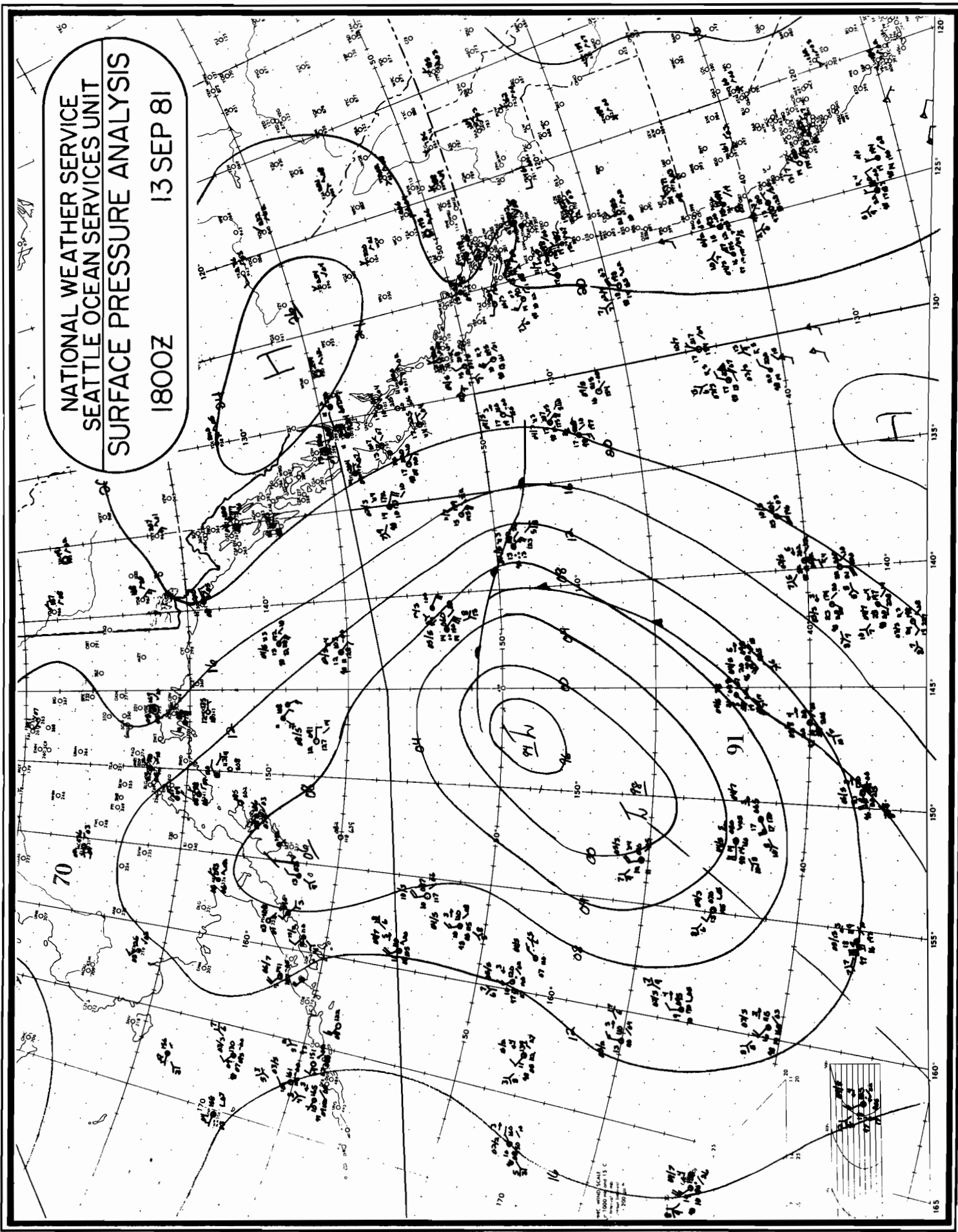


Figure 8(f). Surface pressure analysis for 1800Z, 13 September 1981.

NOAA DATA BUOY 46002

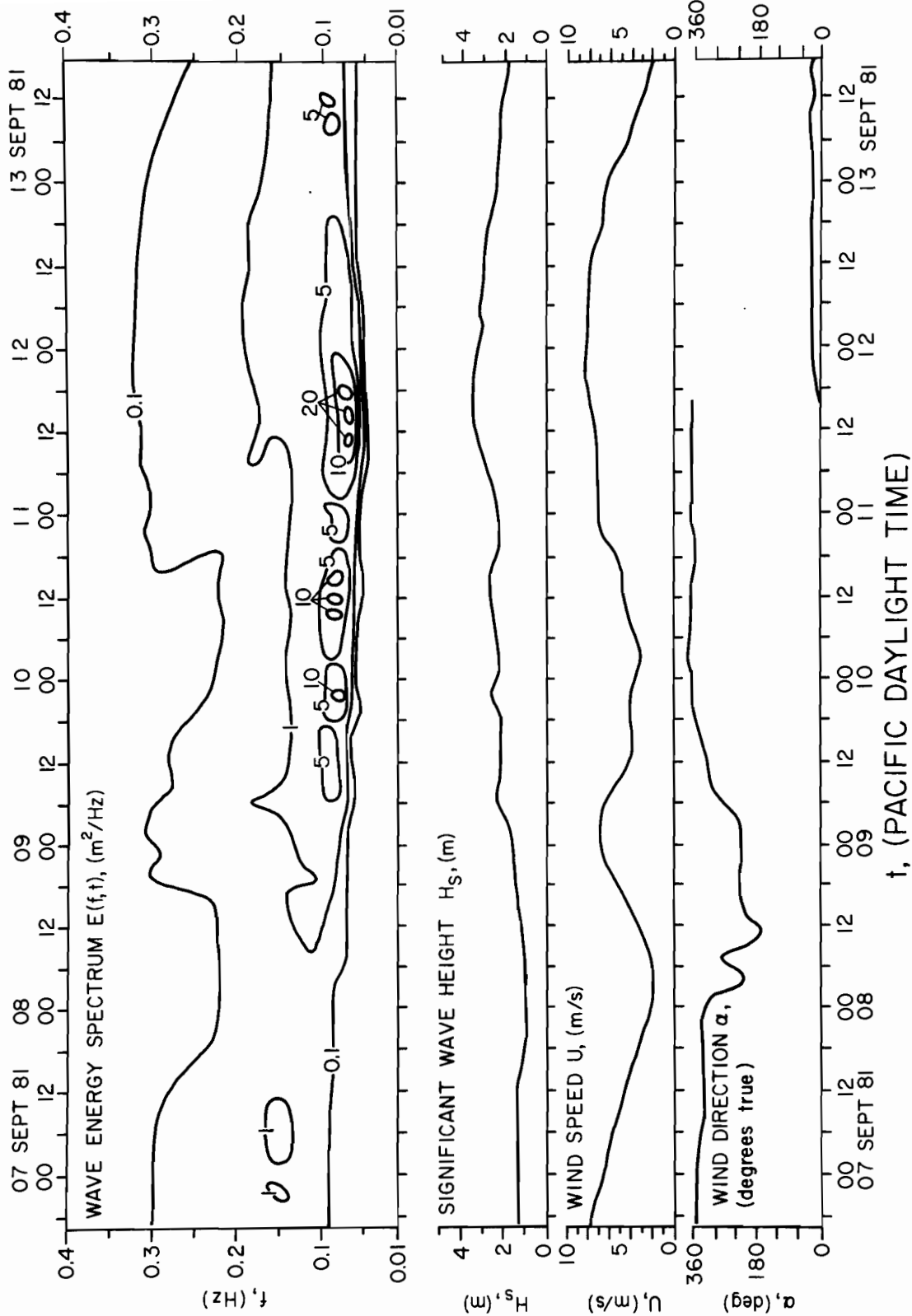


Figure 9(a). Wind and wave observations at NDBC 46002 for period 7-13 Sept.

NOAA DATA BUOY 46004

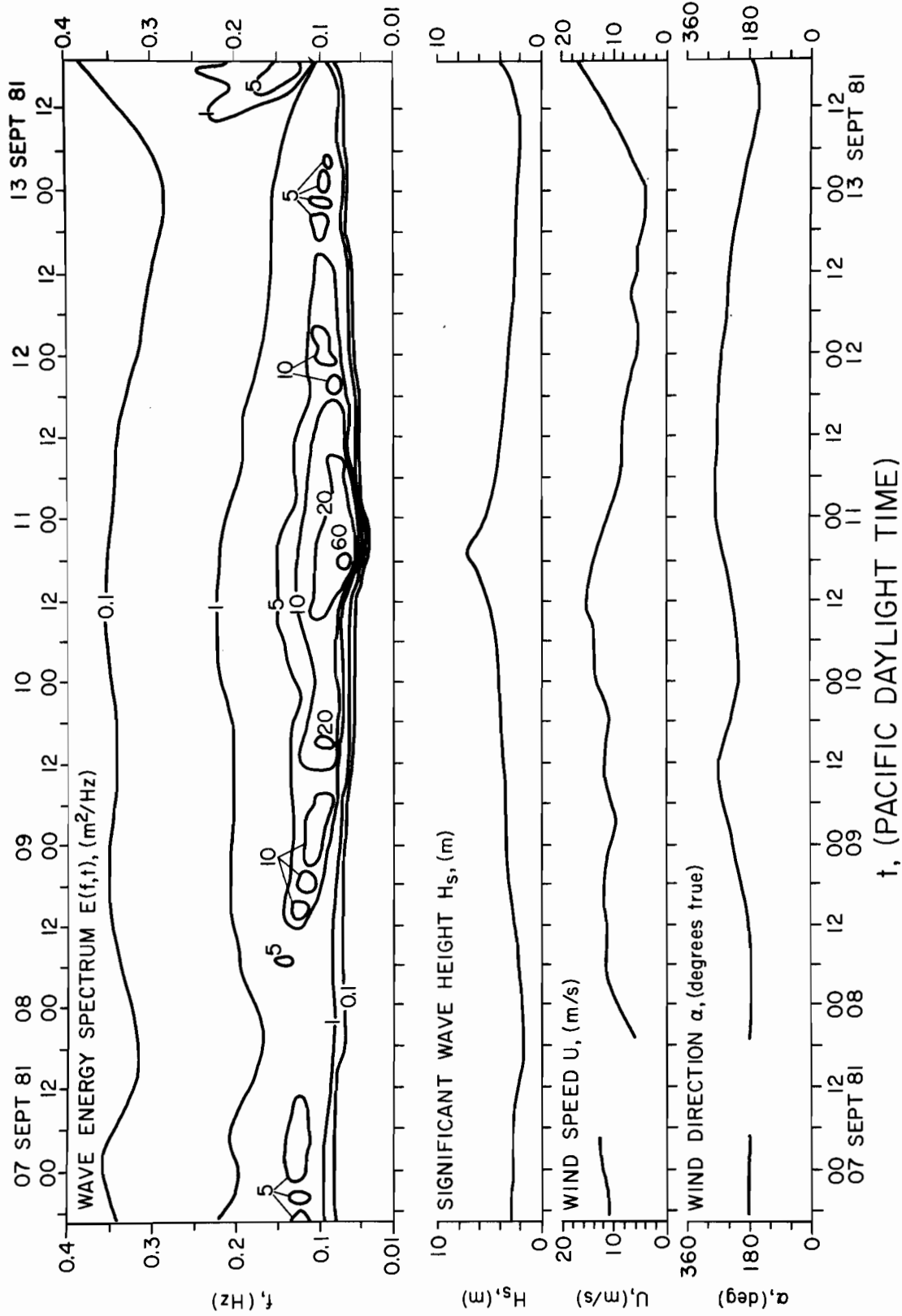


Figure 9(b). Wind and wave observations at NDBC 46004 for period 7-13 Sept.

NOAA DATA BUOY 46005

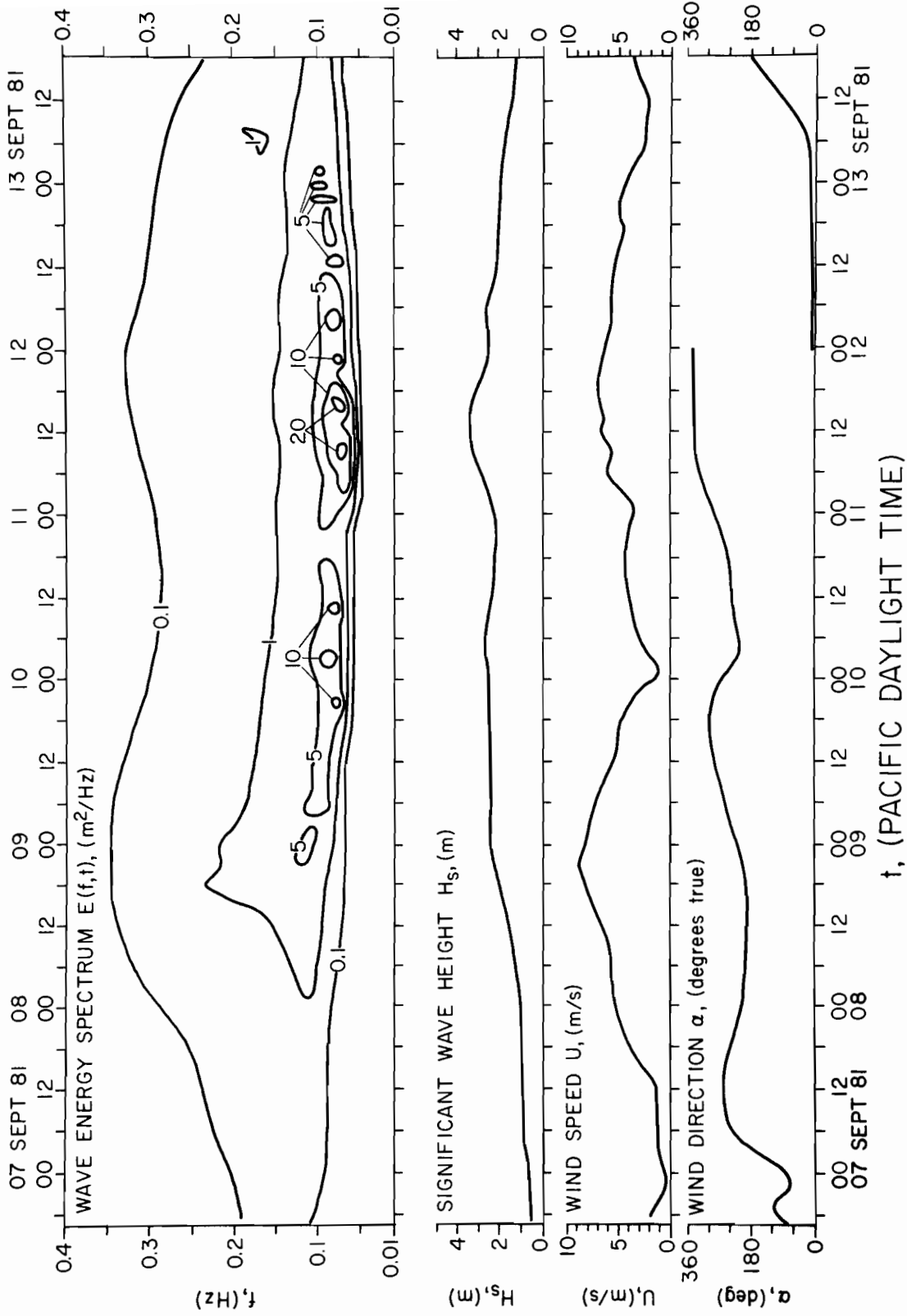


Figure 9(c). Wind and wave observations at NDBC 46005 for period 7-13 Sept.

NOAA DATA BUOY 46006

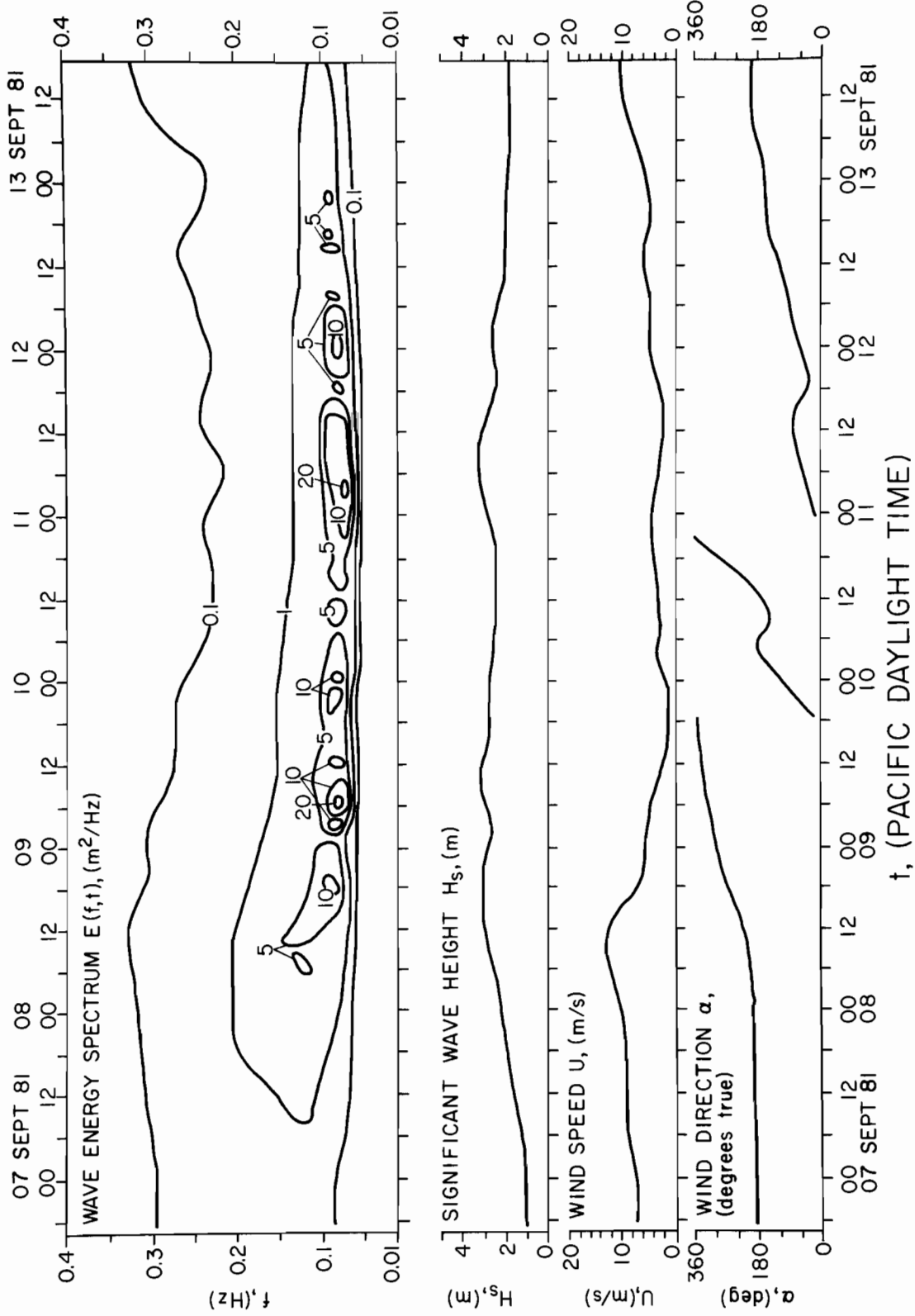


Figure 9(d). Wind and wave observations at NDBC 46006 for period 7-13 Sept.

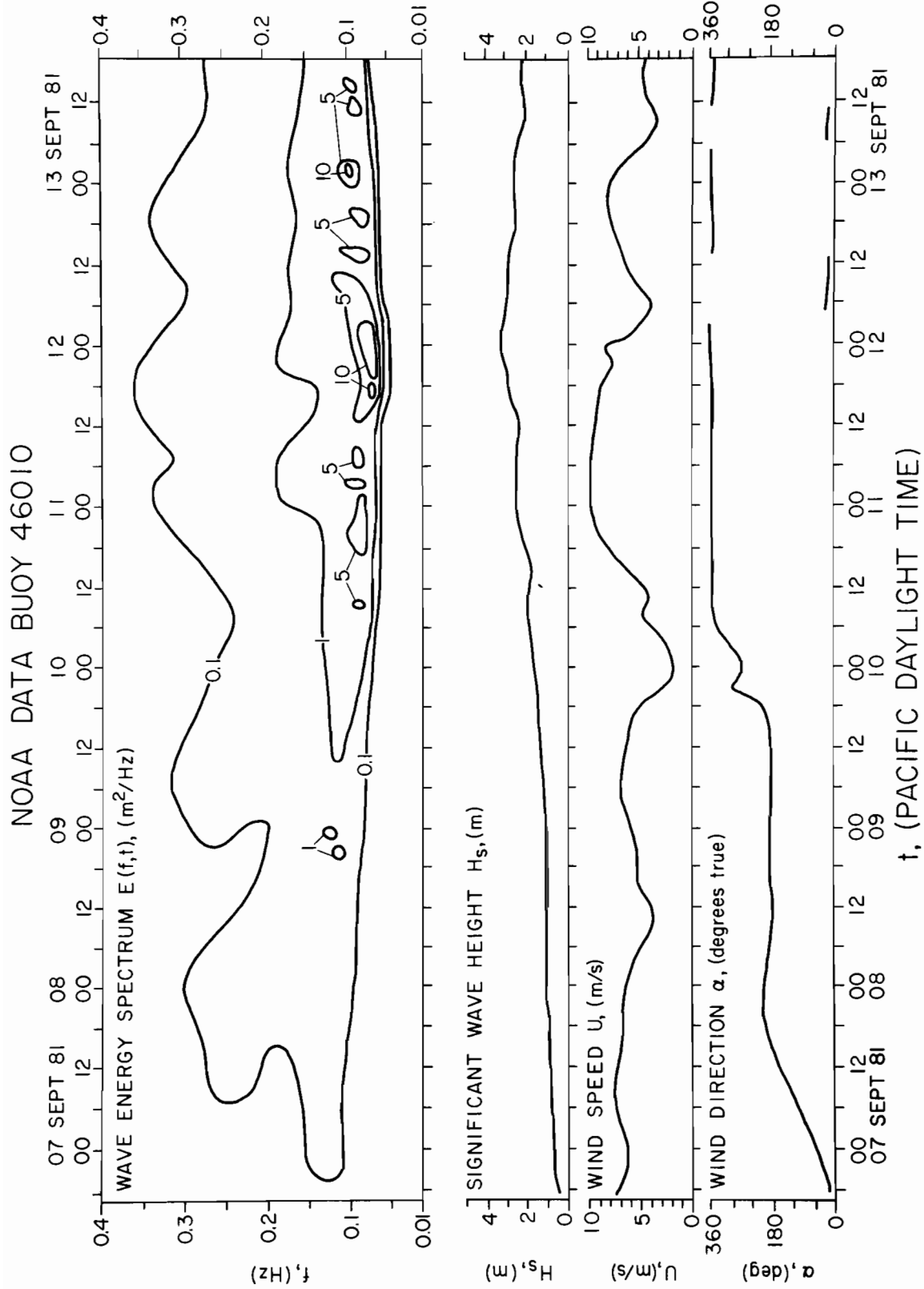


Figure 9(e). Wind and wave observations at NDBC 46010 for period 7-13 Sept.

CLATSOP COUNTY AIRPORT (WSO-ASTORIA, OREGON)

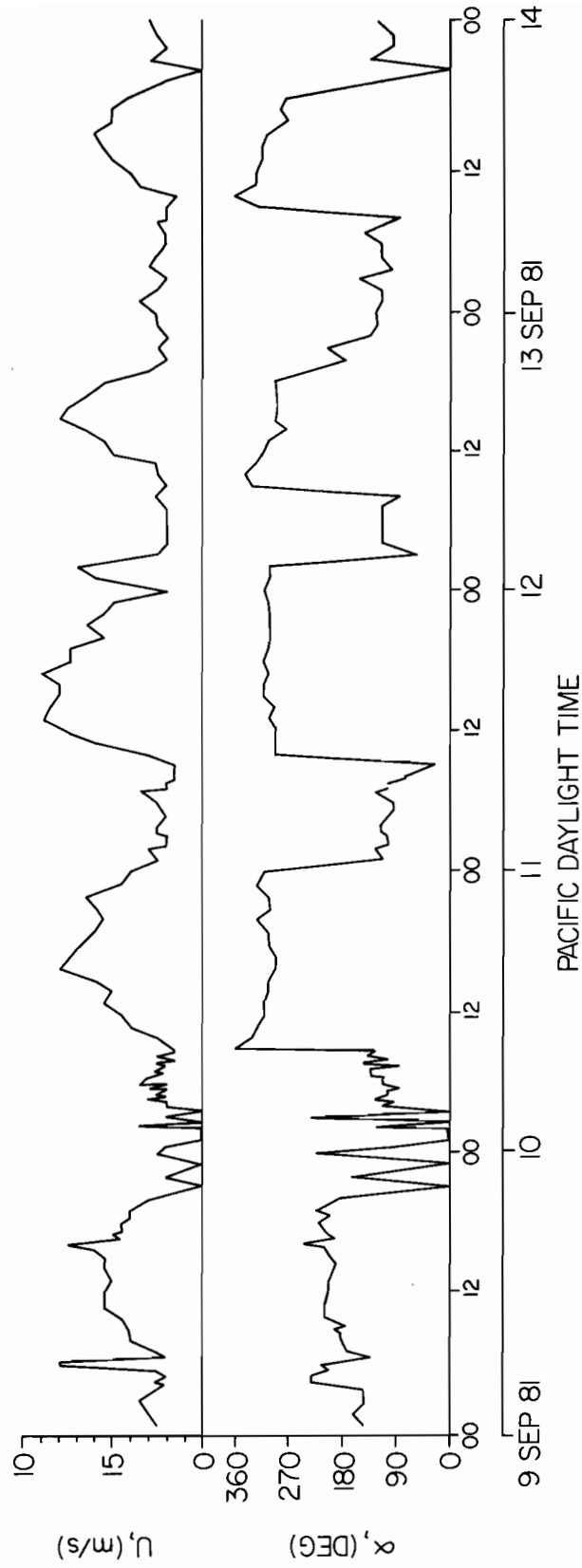


Figure 10. Wind observations at Clatsop County Airport for period 9-14 Sept. 1981.



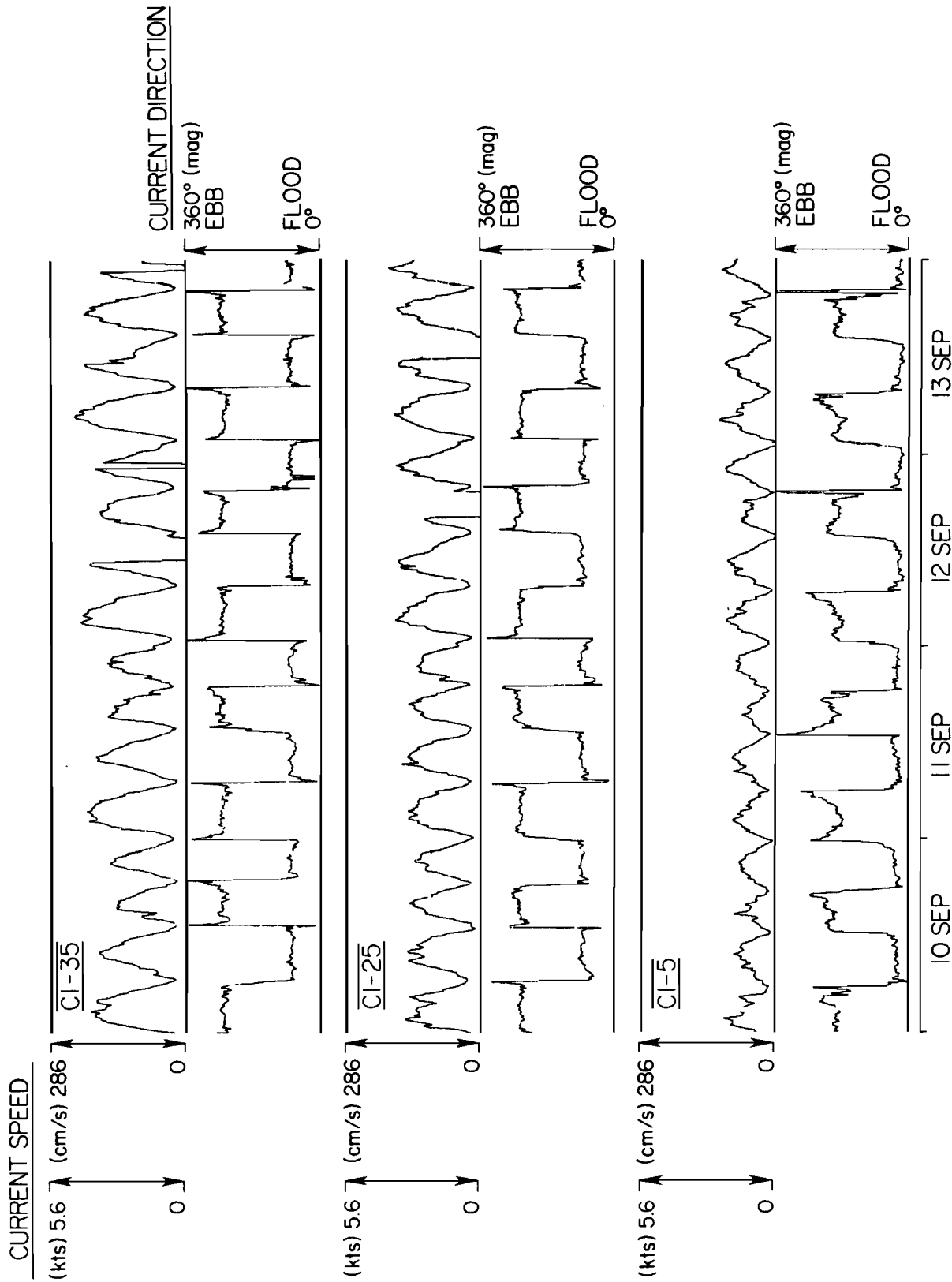


Figure 11. NOS current meter observations for stations C1 at depths 5, 25, and 35 feet from the bottom for the period 10-13 September. From Mulhern (1982).

TABLE 7. Daytime slack, peak ebb, or peak flood current predictions for intensive observation periods. Predictions refer to NOS station 695.

<u>Day</u>	<u>Date</u>	<u>Predicted Tidal Current</u>		
		<u>Time</u> (PDT)	<u>Speed</u> (m/s)	<u>Stage</u>
Thursday	10 September	1015	1.3	FLOOD
Thursday	10 September	1545	-1.4	EBB
Friday	11 September	1330	0.0	SLACK
Friday	11 September	1630	-1.7	EBB
Saturday	12 September	1115	1.8	FLOOD
Saturday	12 September	1715	-2.1	EBB
Sunday	13 September	1145	2.0	FLOOD
Sunday	13 September	1745	-2.4	EBB

TABLE 8. Summary of Waverider deployments. Entries under stationary and drifting columns refer to buoys.

<u>Date</u>	<u>Tidal Stage</u>	<u>Time Period</u> (PDT)	<u>Deployment Mode</u>		
			Stationary	Drifting	
10 September	FLOOD	1030-1055	8		
		1055-1120		8→10	
		1131-1157	10		
		1157-1221		10→12	
	EBB	1444-1506	10		
		1506-1528		10→8	
		1528-1555	8		
		1555-1629		8→1	
11 September	SLACK	1348-1409	10		
		1409-1447		10→8	
	EBB	1548-1610		12→10	
		1612-1633	10		
12 September	FLOOD	0921-0955	46010		
		1041-1101	4		
		1127-1148	8		
		1200-1234	10		
		1248-1300	8		
		1300-1318		8→10	
	EBB	1644-1704		12→10	
		1758-1822	12		
	13 September	FLOOD	1117-1137	8	
			1139-1202		8→10
1223-1245			8		
1245-1310				8→10	
EBB		1658-1724		19→11	
		1724-1746	11		
		1746-1808		11→9	
		1825-1856	10		

---

TABLE 9. Summary of Cape Disappointment Radar observation periods.

---

<u>Date</u>	<u>Tidal Stage</u>	<u>Time Period</u> (PDT)
10 September	FLOOD	1050-1225
10 September	EBB	1450-1625
11 September	SLACK	1301-1450
11 September	EBB	1605-1628
12 September	FLOOD	1041-1315
12 September	EBB	1639-1833
13 September	FLOOD	1130-1307
13 September	EBB	1704-1830

---

TABLE 10. Summary of Jetty A Radar observation periods.

<u>Date</u>	<u>Tidal Stage</u>	<u>Time Period</u> (PDT)
10 September	FLOOD	1050-1202
10 September	EBB	No Data
11 September	SLACK	1307-1426
11 September	EBB	No Data
12 September	FLOOD	1040-1314
12 September	EBB	1640-1833
13 September	FLOOD	1112-1304
13 September	EBB	1703-1846

---

TABLE 11. Summary of Mohawk SLAR observation periods

---

<u>Date</u>	<u>Tidal Stage</u>	<u>Time Period</u>	<u>Comments</u>
10 September	FLOOD		No flight.
10 September	EBB	1519-1731	A/C 925: Kaufman/Coursey. ADAS and log agree. High altitude test runs at 5100 feet yielded no return. Flight line #1 (1519-1526) printed for report.
11 September	SLACK	1232-1345	A/C 925: Rolfness/Coursey. ADAS and log time agree to within 15 minutes. ADAS and log time agree to within 15 minutes. ADAS date is incorrect (10 Sept.). Flight line #1 (1311-1319) printed for report.
11 September	EBB	1610-1736	AC/925: ? / Anderson. ADAS and log date incorrect (10 Sept. '81). Print line #1 (1628-1636).
12 September	FLOOD	1110-1227	A/C 957: Rux/Fough. ADAS and log agree. Print line #1 (1110-1123).
12 September	EBB	1645-1748	A/C 957: Burns/Fogg. ADAS incorrect.
13 September	FLOOD	1115-1300	A/C 957: Evans/Lakawsi. ADAS times incorrect. Print line #3 (1138-?).
13 September	EBB	1710-1835	A/C 957: Dwyer/Galvin. ADAS and log agree.

---

TABLE 12. Summary of Selected Surface Drifter Speed and Waverider Significant Wave Height Observations.

Date	Start Time (PDT)	End Time (PDT)	Mid Time (PDT)	Position (km east of Buoy 8)	Drifter ID (Fig/Buoy)	Drift Distance (m)	Drifter Time (min)	Drifter Speed (m/s)	NOS Speed (Sta. 695) (m/s)	Waverider Rec. Length (sec)	H <sub>s</sub> (m)	SLAR Image (Fig.)
10 Sep	1030	1047	1038	0.0					1.3	1024	1.5	
10 Sep	1050	1058	1054	1.6	A8/1	640	8	1.3	1.2			
10 Sep	1050	1059	1055	1.8	A7/1	640	9	1.2	1.2			
10 Sep	1056	1104	1100	0.3					1.2	512	1.4	
10 Sep	1104	1113	1108	0.8					1.2	512	1.5	
10 Sep	1113	1120	1116	1.4					1.1	429	1.2	
10 Sep	1131	1148	1139	1.9					1.0	1024	0.8	
10 Sep	1157	1204	1200	2.1					0.6	443	0.9	
10 Sep	1204	1213	1208	2.3					0.4	512	0.8	
10 Sep	1213	1221	1217	2.8					0.2	478	0.8	
10 Sep	1444	1501	1452	1.7					-1.2	1024	1.3	
10 Sep	1506	1511	1509	1.4					-1.3	324	1.6	
10 Sep	1511	1520	1516	0.8					-1.3	512	1.9	
10 Sep	1520	1528	1524	0.0					-1.4	478	2.1	
10 Sep	1523	1530	1527	3.0	A16/5	1110	7	-2.6	-1.4			A18
10 Sep	1527	1535	1531	2.1	A16/4	825	8	-1.7	-1.4			A18
10 Sep	1528	1545	1536	-0.3					-1.4	1024	2.2	
10 Sep	1541	1550	1546	1.3	A16/2	1090	8	-2.3	-1.4			A18
10 Sep	1537	1545	1546	1.7	A16/3	1040	9	-1.9	-1.4			A18
10 Sep	1555	1603	1559	-0.7					-1.4	473	2.4	
10 Sep	1603	1611	1607	-1.4					-1.4	512	2.1	
10 Sep	1611	1620	1616	-2.1					-1.4	512	2.4	
10 Sep	1620	1629	1625	-2.7					-1.3	512	2.4	
11 Sep	1315	1330	1323	2.2	A26/3	350	15	-0.4	0.1			A28
11 Sep	1315	1330	1323	1.1	A26/4	250	15	-0.3	0.1			A28
11 Sep	1348	1405	1356	1.7					-0.5	512	1.5	
11 Sep	1400	1410	1405	0.1	A26/4	400	10	-0.7	-0.6			
11 Sep	1409	1416	1413	1.6					-0.8	431	1.9	
11 Sep	1410	1420	1415	-0.3	A26/4	490	10	-0.8	-0.8			
11 Sep	1416	1425	1421	1.4					-0.9	512	2.0	
11 Sep	1420	1430	1425	-0.7	A26/4	525	10	-0.9	-0.9			
11 Sep	1425	1433	1429	1.1					-0.9	512	2.3	
11 Sep	1430	1440	1435	-1.2	A26/4	640	10	-1.1	-1.0			
11 Sep	1433	1442	1437	0.7					-1.0	512	2.9	
11 Sep	1442	1447	1443	0.3					-1.1	302	2.6	
11 Sep	1440	1450	1445	-1.8	A26/4	750	10	-1.3	-1.1			
11 Sep	1552	1601	1556	2.9					-1.7	512	1.5	
11 Sep	1601	1609	1605	2.3					-1.7	512	2.4	
11 Sep	1610	1618	1614	2.6	A34/3	900	8	-1.9	-1.7			A35
11 Sep	1615	1623	1619	1.3	A34/2	950	8	-2.0	-1.7			A35
11 Sep	1620	1628	1624	1.2	A34/1	950	8	-2.0	-1.7			A35
11 Sep	1612	1629	1620	1.8					-1.7	1024	3.4	
12 Sep	1110	1120	1115	2.6	A45/3	890	10	1.5	1.8			A47
12 Sep	1110	1124	1117	3.4	A45/1	1275	14	1.5	1.8			A47
12 Sep	1120	1130	1125	3.4	A46/3	850	10	1.4	1.8			A47
12 Sep	1127	1144	1135	0.1					1.8	1024	1.6	
12 Sep	1155	1205	1200	0.9	A45/5	1040	10	1.7	1.7			
12 Sep	1200	1210	1205	1.0	A45/6	1090	10	1.8	1.7			
12 Sep	1200	1217	1208	2.0					1.6	1024	0.9	
12 Sep	1206	1220	1213	0.2	A45/4	675	14	0.8	1.6			
12 Sep	1640	1644	1642	2.3	A55/1	525	4	-2.2	-2.0			A56
12 Sep	1642	1648	1645	1.9	A55/2	675	6	-1.9	-2.0			A56
12 Sep	1639	1651	1645		A54/1	1525	12	-2.1	-2.0			A56
12 Sep	1645	1651	1647	1.7	A54/2	750	6	-2.1	-2.0			A56
12 Sep	1644	1650	1648	3.2					-2.0	386	1.7	A56
12 Sep	1646	1700	1653	0.8	A55/1	1900	14	-2.3	-2.0			A56
12 Sep	1651	1657	1654	0.7	A54/1	750	6	-2.1	-2.0			A56
12 Sep	1650	1659	1654	2.4					-2.0	512	2.2	A56
12 Sep	1659	1704	1702	1.4					-2.0	297	3.9	A56
12 Sep	1758	1815	1806	3.4					-1.9	1024	2.4	

TABLE 12. (Continued)

Date	Start Time (PDT)	End Time (PDT)	Mid Time (PDT)	Position (km east of Buoy 8)	Drifter ID (Fig/Buoy)	Drift Distance (m)	Drifter Time (min)	Drifter Speed (m/s)	NOS Speed (sta. 695) (m/s)	Waverider Rec. Length (sec)	H <sub>s</sub> (m)	SLAR Image (Fig.)
13 Sep	1115	1130	1123	-0.5	A65/2	1225	15	1.4	2.0			A69
13 Sep	1117	1134	1125	-0.4					2.0	1024	1.5	A69
13 Sep	1117	1135	1126	-1.1	A65/3	1190	18	1.1	2.0			A69
13 Sep	1121	1135	1128	0.0	A67/2	1300	14	1.6	2.0			A69
13 Sep	1125	1136	1130	1.0	A67/1	1300	11	2.0	2.0			A69
13 Sep	1125	1140	1133	-1.3	A65/4	820	15	0.9	2.0			A69
13 Sep	1127	1140	1134	-1.2	A67/4	650	13	0.8	2.0			A69
13 Sep	1133	1141	1137	-0.3	A67/3	725	8	1.5	2.0			A69
13 Sep	1130	1145	1138	1.9	A65/1	1700	15	1.9	2.0			A69
13 Sep	1139	1144	1142	0.2					2.0	273	1.4	A69
13 Sep	1140	1151	1146	2.8	A67/1	1180	11	1.8	2.0			A69
13 Sep	1143	1150	1147	0.6	A67/3	790	7	1.9	2.0			A69
13 Sep	1143	1150	1147	-0.3	A67/4	560	7	1.3	2.0			A69
13 Sep	1144	1152	1148	0.6					2.0	512	1.3	
13 Sep	1146	1155	1151	2.4	A67/2	830	9	1.5	2.0			
13 Sep	1152	1201	1156	1.3					2.0	512	0.9	
13 Sep	1215	1227	1221	0.5	A66/5	1075	12	1.5	2.0			
13 Sep	1220	1230	1225	0.5	A66/6	900	10	1.5	2.0			
13 Sep	1222	1230	1226	-0.1	A66/7	700	8	1.5	2.0			
13 Sep	1658	1702	1700	6.7					-2.2	226	0.7	
13 Sep	1702	1710	1706	6.0					-2.2	512	0.7	
13 Sep	1710	1719	1714	5.2					-2.3	512	0.7	
13 Sep	1710	1720	1715	5.1	A76/1	1000	10	-1.7	-2.3			
13 Sep	1710	1720	1715	5.4	A76/2	1275	10	-2.1	-2.3			
13 Sep	1710	1720	1715	5.4	A76/3	1350	10	-2.3	-2.3			
13 Sep	1709	1721	1715	5.4	A78/1	1425	12	-2.0	-2.3			
13 Sep	1709	1722	1715	5.5	A78/2	1475	13	-1.9	-2.3			
13 Sep	1710	1720	1715	5.5	A78/3	1250	10	-2.1	-2.3			A80
13 Sep	1719	1724	1722	4.2					-2.3	304	0.8	A80
13 Sep	1720	1730	1725	4.1	A76/1	1250	10	-2.1	-2.3			A80
13 Sep	1720	1730	1725	4.2	A76/2	1275	10	-2.1	-2.3			A80
13 Sep	1720	1730	1725	4.2	A76/3	1410	10	-2.4	-2.3			A80
13 Sep	1721	1731	1726	4.1	A78/1	1150	10	-1.9	-2.3			A80
13 Sep	1722	1731	1726	4.3	A78/2	1300	9	-2.4	-2.3			A80
13 Sep	1720	1732	1726	4.3	A78/3	1650	12	-2.3	-2.3			A80
13 Sep	1724	1741	1732	4.0					-2.3	512	1.0	A80
13 Sep	1735	1741	1738	2.6	A78/2	750	6	-2.1	-2.3			
13 Sep	1735	1745	1740	1.9	A76/1	1475	10	-2.5	-2.3			
13 Sep	1737	1744	1741	1.9	A78/1	1160	7	-2.8	-2.3			
13 Sep	1746	1753	1750	3.5					-2.4	436	1.0	
13 Sep	1753	1802	1757	2.7					-2.4	512	1.3	
13 Sep	1802	1808	1805	1.4					-2.4	367	1.2	
13 Sep	1803	1814	1809	3.9	A77/5	1525	11	-2.3	-2.3			
13 Sep	1803	1814	1809	3.9	A79/5	1525	11	-2.3	-2.3			
13 Sep	1805	1815	1810	4.2	A77/6	1475	10	-2.5	-2.3			
13 Sep	1805	1817	1811	4.0	A79/6	1700	12	-2.4	-2.3			
13 Sep	1814	1824	1819	2.4	A79/5	1525	10	-2.5	-2.3			
13 Sep	1815	1825	1820	2.2	A77/5	1490	10	-2.5	-2.3			
13 Sep	1820	1830	1825	2.0	A77/6	1550	10	-2.6	-2.2			
13 Sep	1821	1830	1826	2.0	A79/6	1260	9	-2.3	-2.2			
13 Sep	1825	1842	1833	1.7					-2.2	512	2.2	



electronics was set to acquire individual records of length 512 seconds, with a 1-second gap between them. In some cases, two records were combined to form a 1024-second record; these were processed to a power spectrum, as described above, and plots of these spectra are presented in the Appendix. In other cases, the Waverider was deployed after the start of a new record, so that the first portion of that record was discarded, leaving a record shorter than 512 seconds. The significant wave height for these records of length 512 seconds or shorter was then computed as  $H_s = 4\sigma$ , where  $\sigma$  is the square root of the record variance.

The river entrance is an extremely hostile environment. Large waves and strong currents frequently stress *in-situ* instrumentation and moorings to failure and, if the instrument survives these natural forces, there is still a high likelihood that it will succumb to the heavy commercial and recreational vessel traffic in that region. The technique of tethering a Waverider to a surface vessel was used primarily to avoid the risk of instrument loss, but while observations made this way are preferable to a complete lack of data, the procedure does have potentially serious shortcomings. There is a question of how the currents, which frequently exceed 5 knots, and the tether and bridle arrangement affect the response of the Waverider. Beyond this question of data interpretation, there is the considerable expense incurred in vessel support, and the inconvenience and potential hazard involved in collection of the data in this manner.

On the morning of 12 September, a Waverider deployment was made at a location within 100 yards of NDBC buoy 46010. The purpose was to check the method of Waverider deployment using the tether arrangement described above. Figure 12 displays the resulting Waverider spectra and the two NDBC 46010 spectra which bracket the time of the Waverider deployment. The Waverider spectra has been subjected to 11-point frequency band averaging, so that the resulting frequency resolution of 0.0107 Hz is comparable to the 0.01 Hz resolution of buoy 46010. As can be seen, there is good agreement in significant wave height, and in the qualitative features of the individual spectra. Thus, although there were no currents present during this intercomparison (unlike deployments in the river entrance), this result does give some confidence in the accuracy of the rest of the Waverider observations.

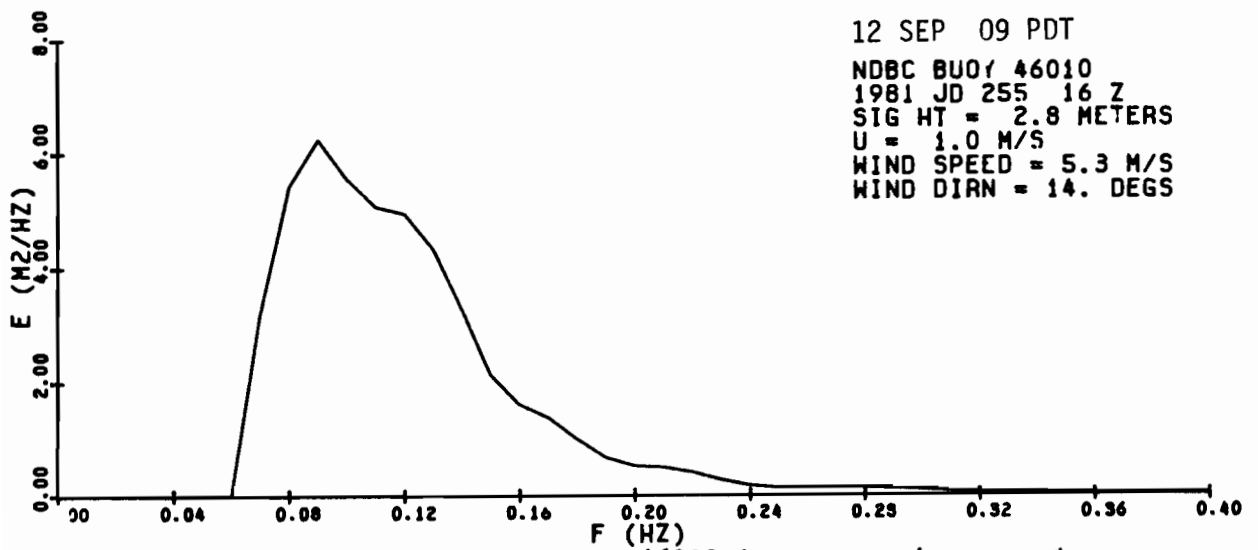
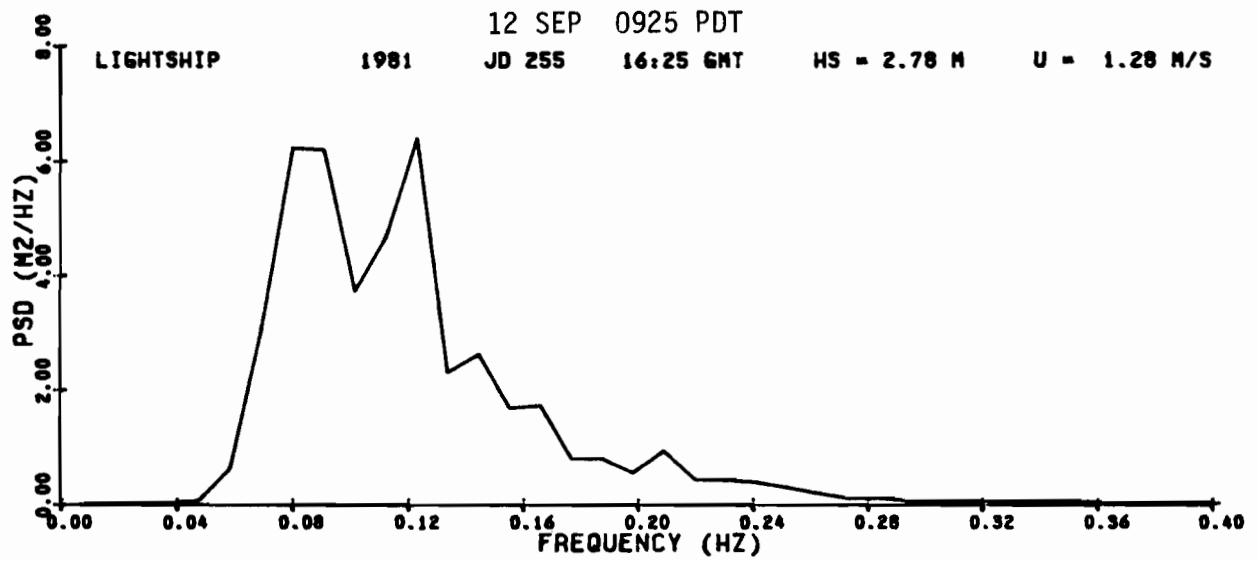
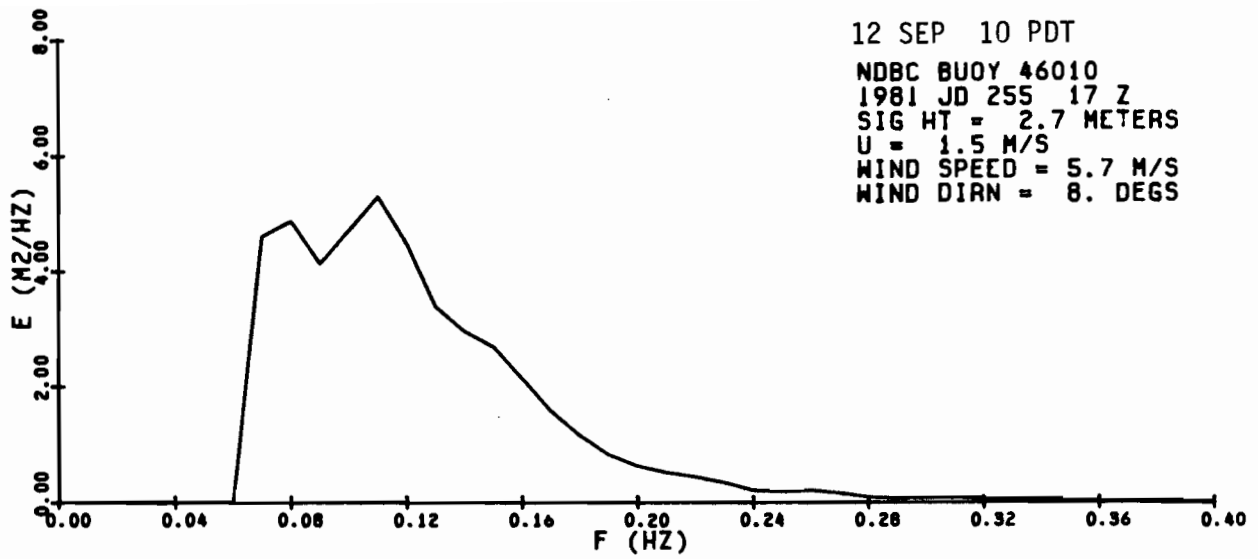


Figure 12. Waverider and NDBC 46010 intercomparison spectra.

#### 4. PRELIMINARY DATA ANALYSIS

We hypothesize that Buoy 8 roughly represents the boundary between two wave regions. Landward of this site the waves decay due to bathymetric refraction away from the main axis of the navigation channel, where the depth is maintained at ~15m, toward the shallower regions to the north and south. Seaward of this site waves grow or decay along their propagation path due both to wave-current interaction with ebb or flood currents and to shoaling.

##### 4.1 Wave Decay Upriver of Buoy 8

Evidence for wave decay landward of Buoy 8 is presented in Figures 13a-d. The significant wave height,  $H_s$ , is plotted as a function of the distance,  $x$ , upriver of Buoy 8. These measurements were obtained from the tethered waverider deployments. Notice that during both ebb and flood conditions the waves decay upriver. The bending of the waves toward the shoals on either side of the navigation channel can be seen in most of the SLAR imagery, but it is clearest during the slack-to-ebb tide of 11 September (Figs. A28 and A29) when the current plays a lesser role. We conjecture that depth refraction is the primary source of the wave decay. Diffraction from the tips of the jetties may also contribute.

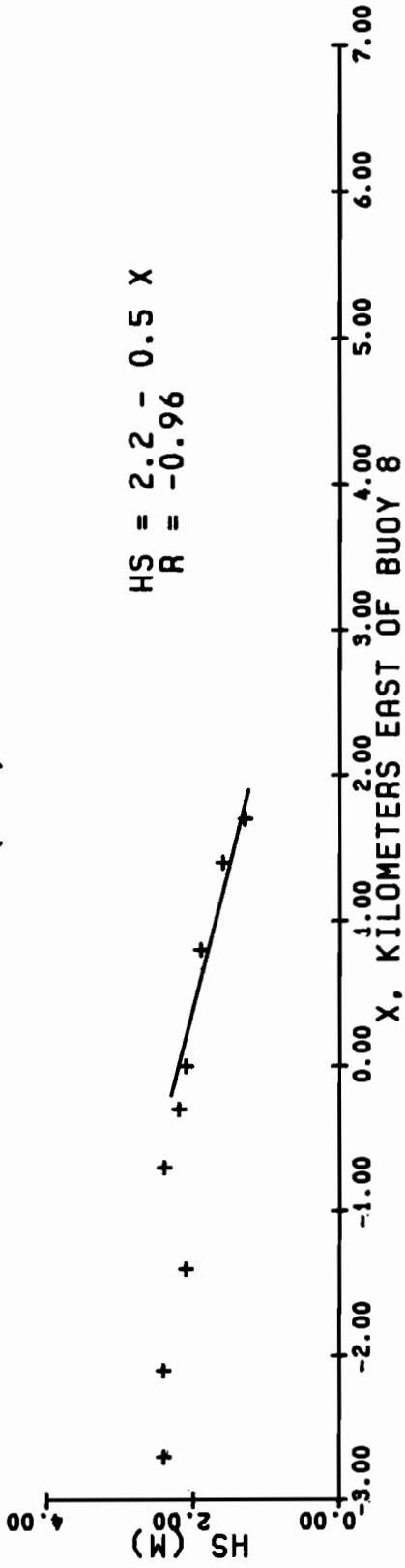
Linear least squares fits have been made to the data of Figure 13 for  $0 \leq x \leq 5$  km. Each line, its equation, and the correlation coefficient of each fit are shown in the figure. The fact that the absolute values of the correlations are near unity indicates that the linear fit is a good approximation. The slopes range in value from -0.3 m/km on the first flood (Figure 13a) to -1.7 m/km on the second ebb (Figure 13b).

The ebbs have larger upriver decay rates than the floods. This seems strange at first because an ebb current should refract the waves toward its axis hence mitigating the effects of bathymetric refraction toward the shoals. A flood current, on the other hand, should enhance the refraction away from the channel axis.

One possible explanation for the behavior observed here is that the mid-channel current magnitude decreases upriver from the vicinity of the jetty tips near Buoy 8 at  $x=0$ . If this happens on an ebb current the gradient would cause waves to refract *away* from the channel axis hence enhancing the decay rate, and *vice versa* on flood. This agrees qualitatively with the observations. The converging jetty tips were designed to accelerate the current to scour the channel. We might expect another current-speed maximum upriver between Jetty A and Clatsop Spit.

Confirmation of the current gradients awaits a complete analysis of the drifter tracks and perhaps further observations. However, a preliminary analysis has been conducted near the time of peak ebb during four of the intensive observation periods. Tabulated results of the drift-distance over periods of a few minutes are presented in Table 13. The inferred surface-current vectors are shown in Figure 14. The ebb currents were mostly in excess of 2 m/s. Figure 14a shows some divergence just upriver of the jetty tips.

10 SEPT 1981 1444-1629 PDT (EBB)



10 SEPT 1981 1030-1221 PDT (FLOOD)

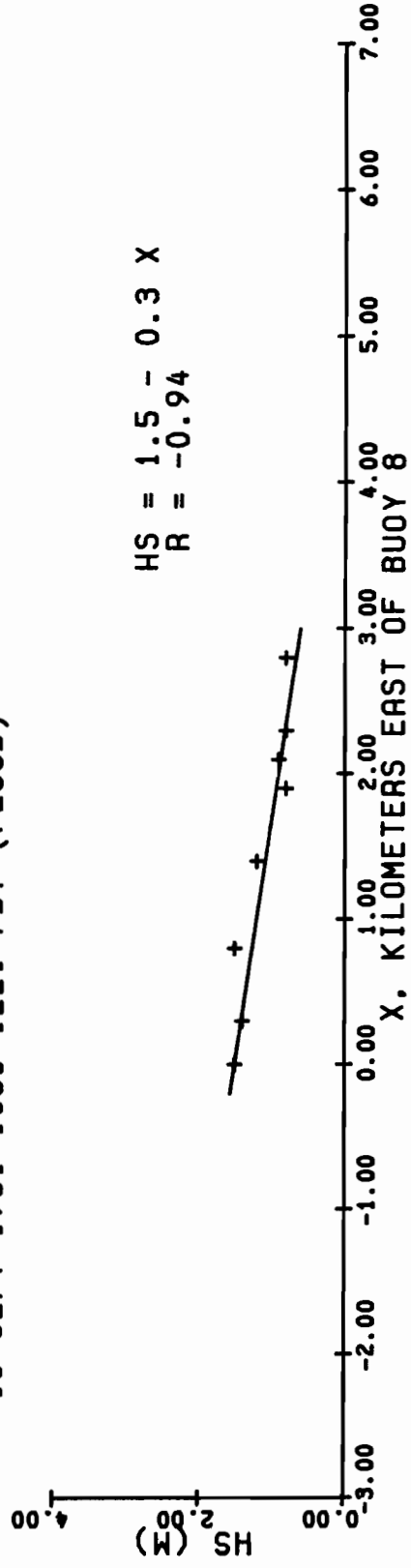
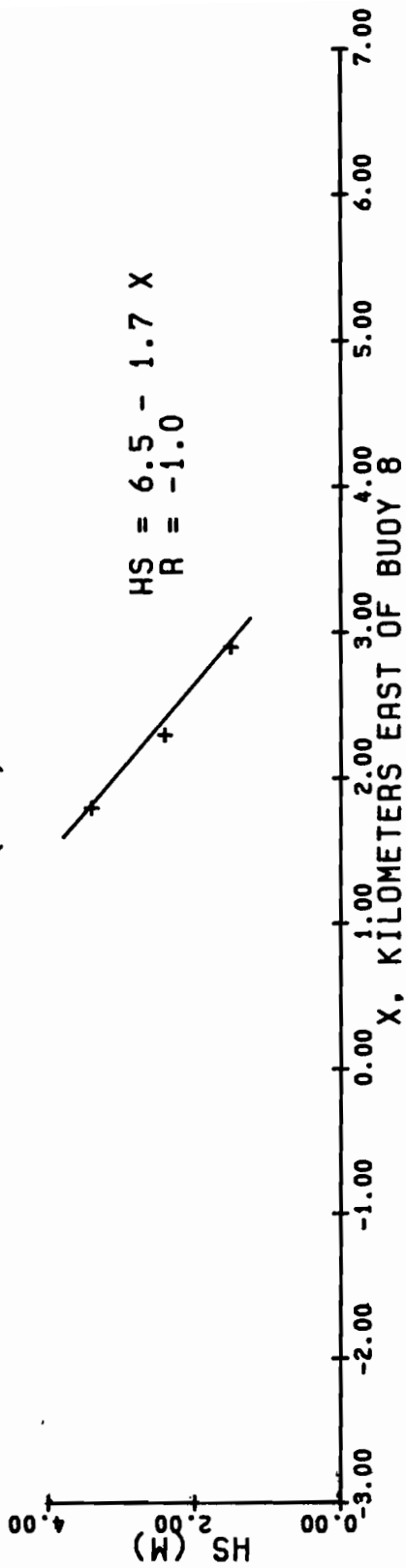


Figure 13a. Waverider significant wave height estimates as a function of distance east of buoy 8 for 10 Sept. 1981.

11 SEPT 1981 1552-1629 PDT (EBB)



11 SEPT 1981 1348-1447 PDT (SLACK-EBB)

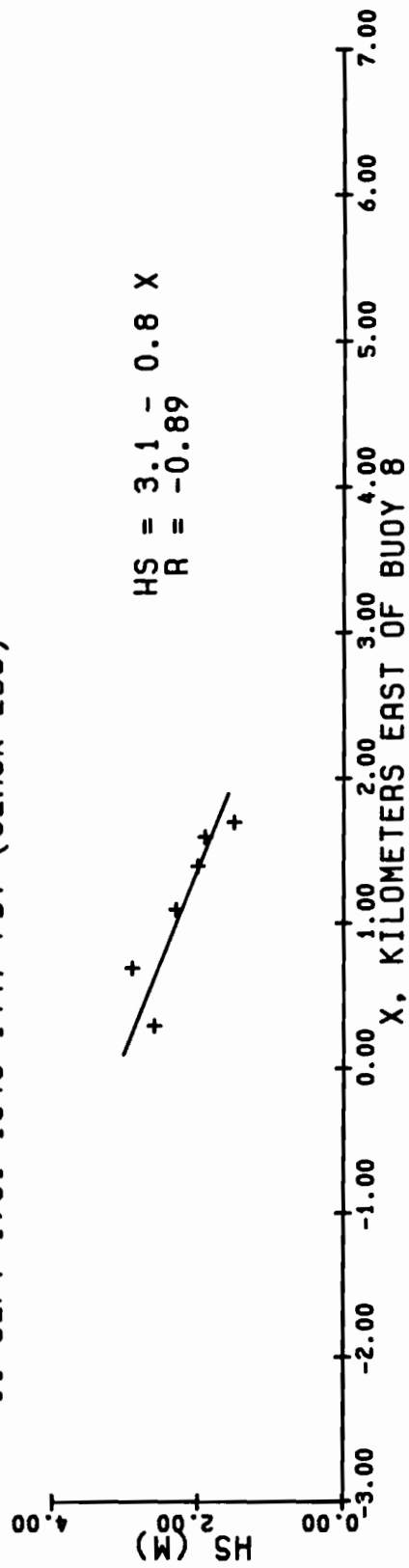


Figure 13b. Waverider significant wave height estimates as a function of distance east of buoy 8 for 11 Sept. 1981.

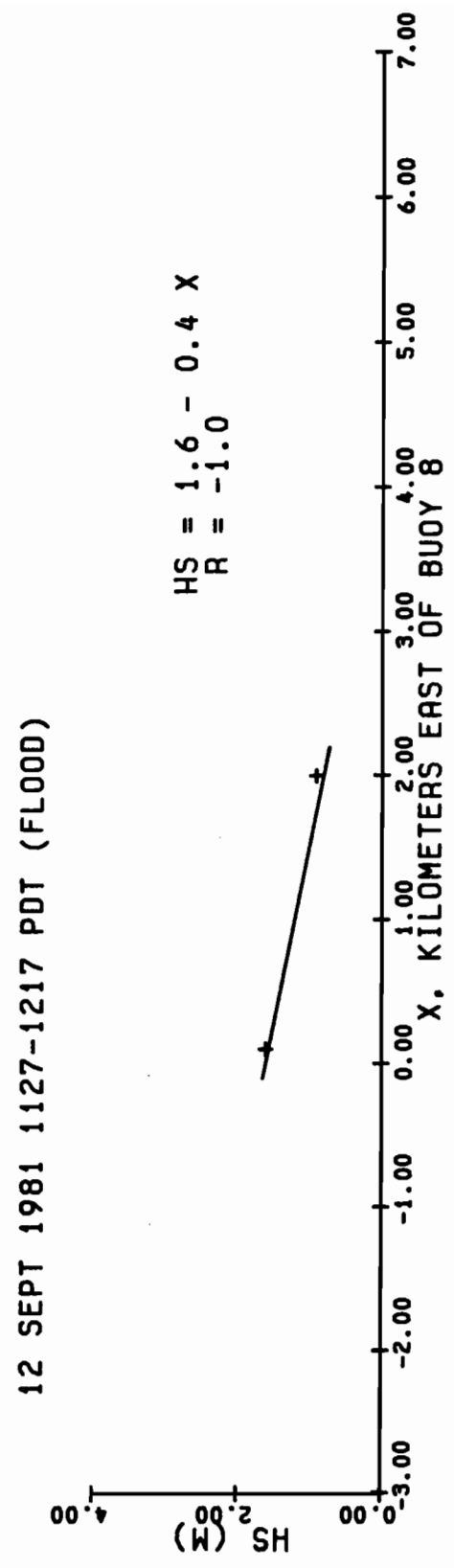
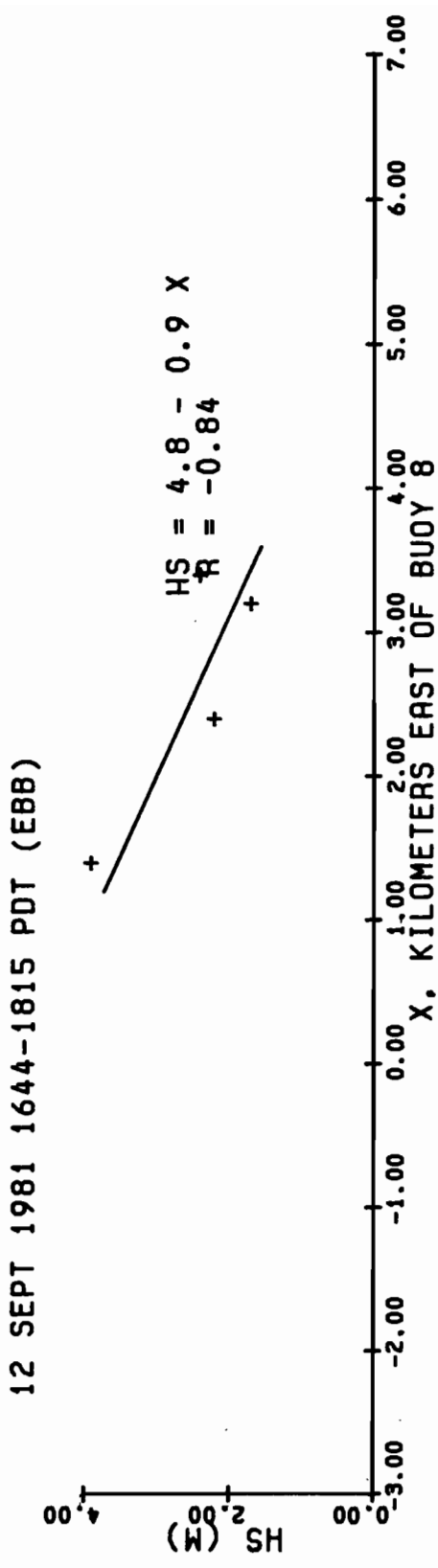
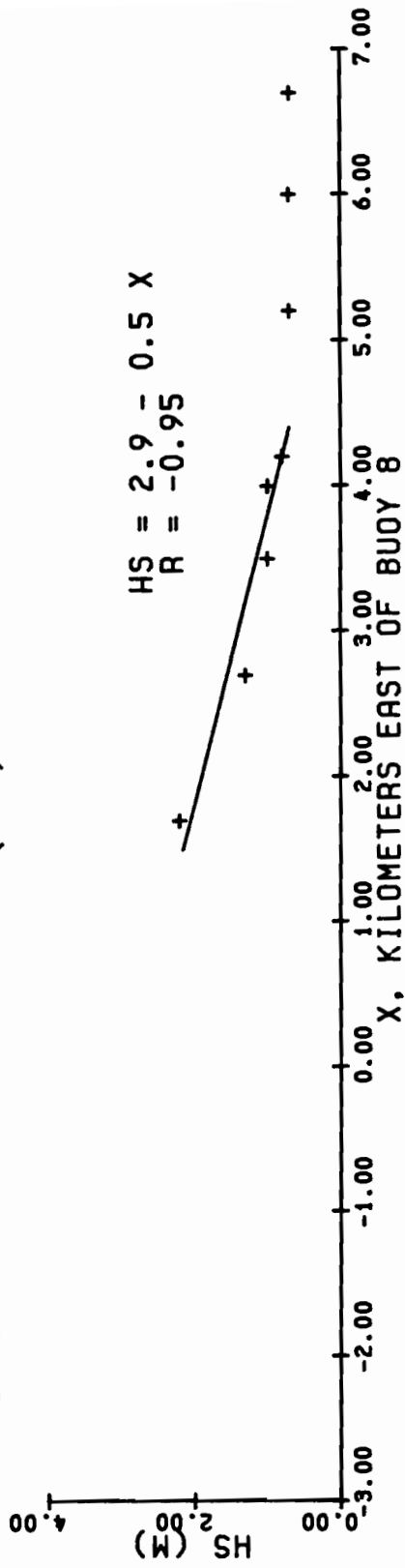


Figure 13c. Waverider significant wave height estimates as a function of distance east of buoy 8 for 12 Sept. 1981.

13 SEPT 1981 1658-1842 PDT (EBB)



13 SEPT 1981 1117-1202 PDT (FLOOD)

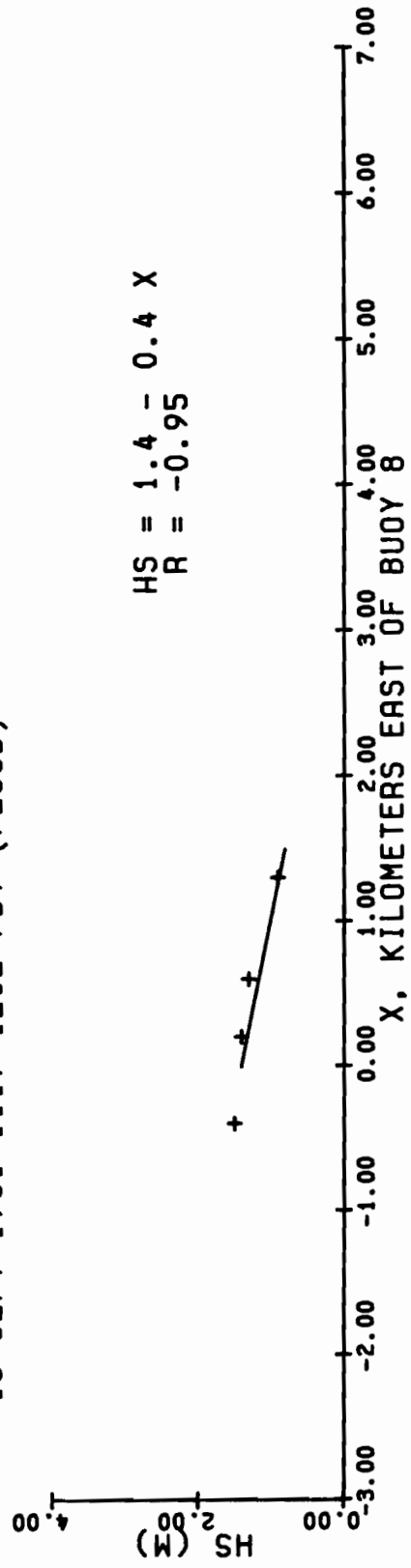


Figure 13d. Waverider significant wave height estimates as a function of distance east of buoy 8 for 13 Sept. 1981.

TABLE 13. Drifter Information for Current Vectors Presented in Figure 14.

Date	Start Time (PDT)	End Time (PDT)	Drifter ID (Fig./Buoy)	Drift Distance (m)	Drift Time (min)	Drift Speed m/s
10 Sep	1540	1600	A16/2	2225	20	1.9
10 Sep	1550	1610	A16/3	2100	20	1.8
10 Sep	1540	1600	A16/5	2025	20	1.7
11 Sep	1610	1618	A34/1	975	8	2.0
11 Sep	1610	1618	A34/2	1150	8	2.4
11 Sep	1610	1618	A34/3	925	8	1.9
12 Sep	1642	1651	A54/1	1250	9	2.3
12 Sep	1642	1651	A54/2	1110	9	2.1
13 Sep	1735	1741	A76/1	925	6	2.6
13 Sep	1735	1741	A76/2	850	6	2.4
13 Sep	1735	1739	A76/3	475	4	2.0
13 Sep	1727	1734	A76/4	850	7	2.0



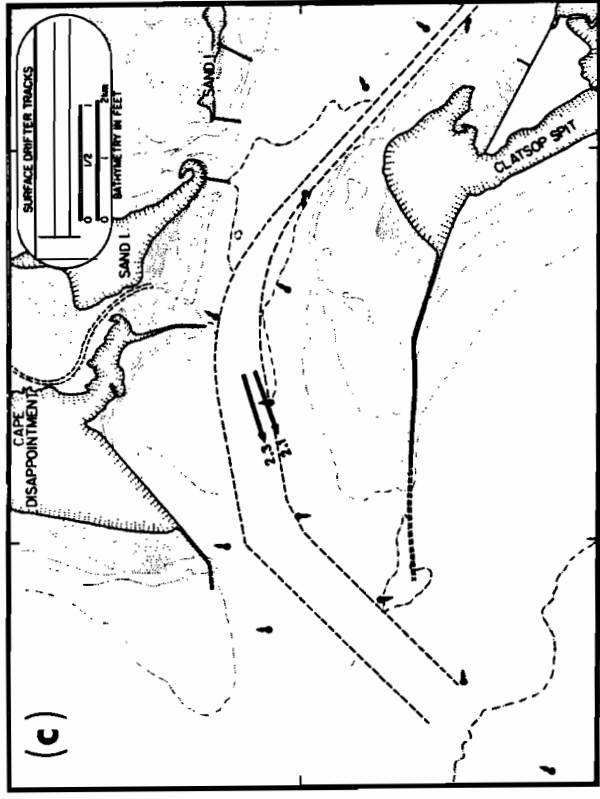
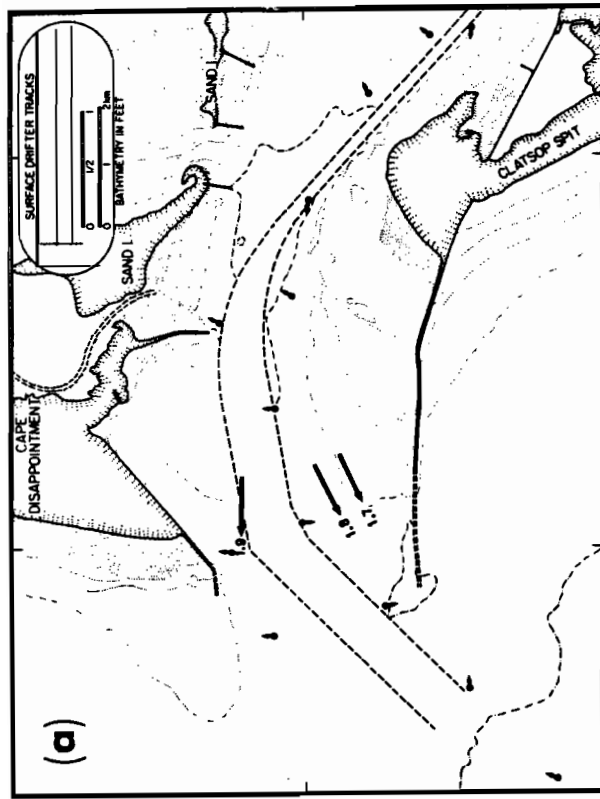
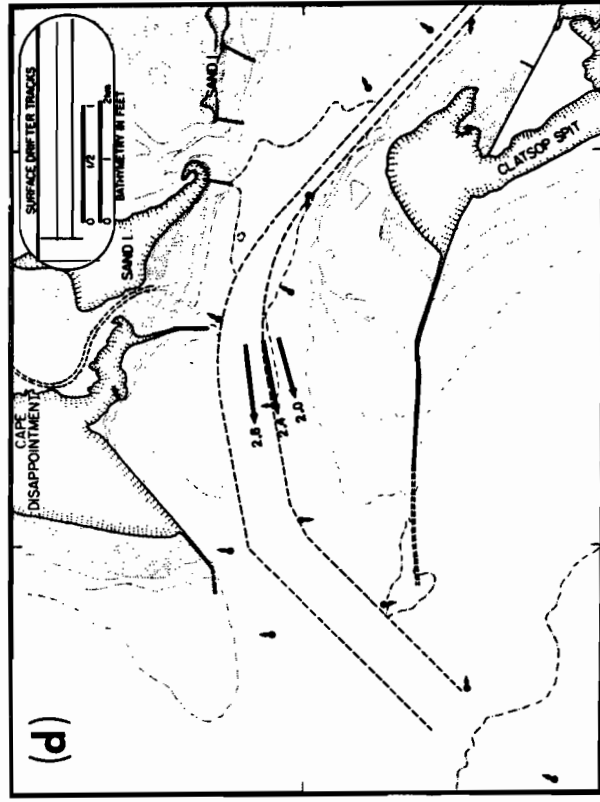
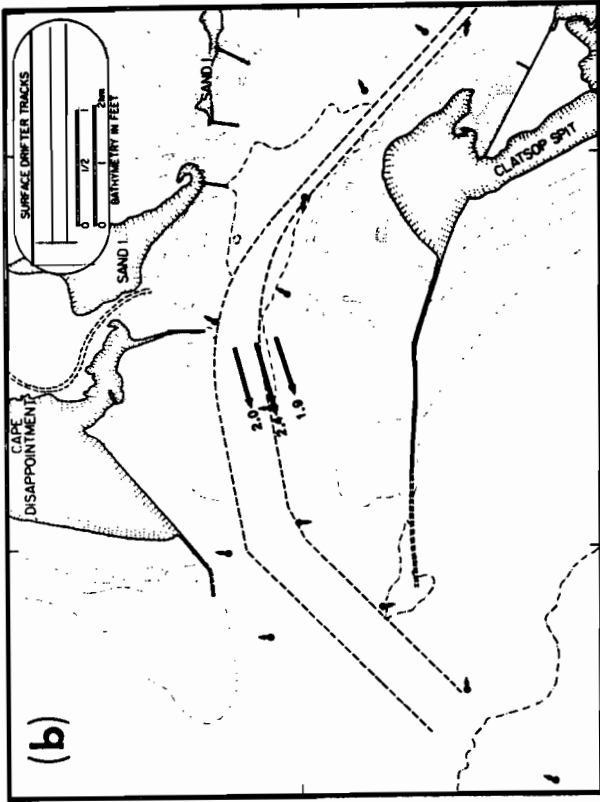


Figure 14. Drifter derived surface current vectors near the time of peak ebb. (a) 10 Sept. 1981. (b) 11 Sept. 1981. (c) 12 Sept. 1981. (d) 13 Sept. 1981.

The enhanced wave decay rate on ebb may be due in part to wave breaking. The instance of greatest decay is on the ebb of 11 September, when breaking swell were observed visually. It is possible to estimate the wave steepness near Buoy 8 and compare this with maximum values limited by breaking. For a wave spectrum we take the characteristic steepness to be  $\frac{1}{2}H_s k$ . The wavenumber,  $k$ , can be estimated (rather inappropriately) from linear theory applied to slowly varying waves. Details are given in §4.2.2.  $H_s$  is extrapolated from Figure 13. The characteristic steepness is given in column 10 of Table 14 for each of the ebb and flood events observed. For regular, periodic waves the theoretical maximum steepness is given approximately by (Miche, 1944)

$$(ak)_{\max} = 0.44 \tanh kd. \quad (1)$$

where  $a$  is the wave amplitude and  $d$  is the depth. Due to the inherent unsteadiness of a real sea and the existence of wave groups, significant sporadic breaking can occur if the characteristic steepness is somewhat lower than this. For random waves in deltaic regions Battjes (1982) suggests the following empirical formula

$$\left(\frac{1}{2}H_s k\right)_{\max} \approx 0.2 \tanh kd. \quad (2)$$

For the full ebb on 11 September at 1615 the extrapolated characteristic steepness exceeded this value. This points to wave breaking as being a cause of the enhanced decay rate. SLAR images on this date (Figs. A35 and A36) show numerous highly radar-reflective regions in the channel entrance which are similar in size and shape to surf on nearby beaches. This provides further evidence for mid-channel breaking, but it must be cautioned that similar images occur in other locations and other scenes where breaking could not be occurring. Thus there is not a unique correspondence between breaking waves and such images.

#### 4.2 Wave-Current Interaction Seaward of Buoy 8

Due to logistical and safety considerations we did not often measure wave heights in the vicinity of the channel entrance seaward of Buoy 8. Therefore to test the hypothesis that the waves grow or decay along their propagation path due to ebb or flood currents, respectively, we must content ourselves with a comparison between two point measurements, one offshore and one at Buoy 8. The offshore wave measurements are those from NDBC Buoy 46010.

##### 4.2.1 The Observations

For each of the eight intensive observation periods the measurements are summarized in Table 14 which is divided horizontally into two portions corresponding to ebb and flood conditions. (Actually nine rows are shown since at 1127 on 12 September the offshore spectrum had two peaks; hence these are analyzed as two independent wave systems.) Columns 1 and 2 give the date and time of the offshore and channel-entrance comparisons.

TABLE 14. Summary of Observed Wave and Current Characteristics and Computed Transfer Function, T, During the Intensive Observation Periods

1 Date	2 Time (PDT)	3 Buoy 46010 <sup>1</sup> $f_p$ (H <sub>z</sub> )	4 H <sub>s46</sub> (m)	5 Buoy 8 H <sub>s8</sub> (m)	6 Current Speed <sup>2</sup> (m/s)	7 $T_o =$ H <sub>s8</sub> /H <sub>s46</sub>	8 $T_c$ Eq. (1) $\theta_o = 0^\circ$ ( $\theta_o = 30^\circ$ )	9 $T_o/T_c$ $\theta_o = 0^\circ$ ( $\theta_o = 30^\circ$ )	10 Steepness $\frac{1}{2}H_{s8}k$
EBB									
10 Sept	1528	0.09	1.7	2.2	-2.1	1.3	1.4 (1.3)	0.9 (1.0)	0.07
11 Sept	1445	0.07	2.7	3.1	-1.3	1.1	1.3 (1.2)	0.8 (0.9)	0.07
11 Sept	1615	0.07	2.9	5.2 <sup>4</sup> -6.5	-2.0	1.8 <sup>4</sup> -2.2	1.5 (1.4)	1.2 <sup>4</sup> -1.5 (1.3 <sup>4</sup> -1.6)	0.12 <sup>4</sup> -0.16
12 Sept	1700	0.08	2.8	4.8 <sup>3</sup>	-2.2	1.7	1.5 (1.4)	1.1 (1.2)	0.14
13 Sept	1825	0.09	1.9	2.9 <sup>3</sup>	-2.3	1.5	1.5 (1.4)	1.0 (1.1)	0.10
FLOOD									
10 Sept	1030	0.08	1.8	1.5	1.3	0.8	0.9 (0.9)	0.9 (0.9)	0.03
12 Sept	1127	0.08	1.4	1.0	1.5	0.7	0.9 (0.9)	0.8 (0.8)	0.02
12 Sept	1127	0.11	2.4	1.2	1.5	0.5	0.8 (0.8)	0.6 (0.6)	0.03
13 Sept	1117	0.09	2.1	1.5	1.4	0.7	0.9 (0.8)	0.8 (0.9)	0.03

<sup>1</sup> H<sub>s</sub> and peak frequency f<sub>p</sub> were interpolated from observations bracketing the time of Waverider observations.

<sup>2</sup> From drifter speed estimates in Table 12. Ebb currents are negative, flood are positive.

<sup>3</sup> From least square fit to data presented in Figs. 13b-d.

<sup>4</sup> Lower value corresponds to limiting breaking height given by Equation (2).

Columns 3 and 4 give the frequency of the offshore spectral peak,  $f_p$ , and the significant wave height at Buoy 46010,  $H_{s46}$ . The significant wave height at Buoy 8,  $H_{s8}$ , is presented in column 5. Directly measured values were used when available, and when not, the linear least-squares extrapolations from upriver of Buoy 8 were used. Figure 13a shows that these fits represent the data well when a comparison is possible. The current-speed estimates at Buoy 8 based on the drifter data of Table 12 are shown in column 6. Finally, column 7 lists the observed wave height transfer function from offshore to onshore, i.e., the ratio of the significant wave heights,  $T_o = H_{s8}/H_{s46}$ .

Column 7 of Table 14 shows that for all ebb currents the waves were amplified ( $T_o > 1$ ) from offshore to the channel entrance, and for all flood currents they decayed ( $T_o < 1$ ). Thus our hypothesis that wave-current interaction is responsible for wave height changes seaward of Buoy 8 is confirmed qualitatively, at least during maximum ebb and flood conditions. The amplification reached values as high as 2.2 on ebb (or perhaps 1.8 if the waves at Buoy 8 were indeed limited by the empirical breaking criterion of (2)) with an attenuation of up to 0.5 on flood.

#### 4.2.2 Comparison with Linear, 1-D Theory

In a previous study, Gonzalez (1984) compared existing linear, one-dimensional wave-current interaction theory with Waverider observations taken hourly over ten tidal cycles at an offshore location and near Buoy 8. A theoretical amplification factor or transfer function,  $T$ , based on conservation of wave action density,  $A = E/\sigma$ , is given by (see, for example, Phillips, §2.7, 1977)

$$T(\omega, U; \theta_0, d, d_0, U_0) \equiv \left( \frac{E}{E_0} \right)^{\frac{1}{2}} = \frac{a}{a_0} = \left( \frac{U_0 + c_{g0} \cos \theta_0}{U + c_g \cos \theta} \right)^{\frac{1}{2}} \left( \frac{\sigma}{\sigma_0} \right)^{\frac{1}{2}} \quad (3)$$

where unscripted parameters refer to the river entrance and the subscript "o" indicates initial conditions, or offshore (deep water) values, and where

- $E$  = spectral energy density values,
- $a$  = wave height amplitude,
- $U$  = surface current velocity,
- $c_g$  = wave group velocity,
- $\theta$  = relative wave-current direction
- $\sigma$  = *intrinsic* wave frequency,
- $\omega$  = *observed* wave frequency,
- $d$  = water depth.

This expression accounts for shoaling, radiation stress (momentum transfer from currents to waves), and offshore wave direction. It does not account

for 2-dimensional effects which produce convergence or divergence of wave rays by features such as bathymetric headlands and current jets. Furthermore, the physical assumptions are that wave motion is purely periodic, that wave amplitude is small compared to wavelength and depth, that wave and current properties vary slowly over scales of many wavelengths, that wave periods are small compared to tidal periods, that all quantities vary only along the main axis of the current (no lateral variations), and that there is no lateral current component across the main axis.

The theory also provides the following relations between the parameters in (3)

$$\begin{aligned} \omega &= \sigma + kU\cos\theta \\ \sigma &= (gk \tanh kd)^{\frac{1}{2}} \\ C_g &= \frac{1}{2} \left( 1 + \frac{2kd}{\sinh 2kd} \right) \frac{\sigma}{k} \end{aligned} \quad (4)$$

where  $k$  is the wave number, and where an analogous set of equations can be written for the subscripted variables. A final relationship

$$k \sin\theta = k_0 \sin\theta_0 \quad (5)$$

closes the system of transcendental equations which can be solved iteratively to compute values of  $T$  as given by equation (3). For convenience, we have here computed Tables 15a-i, which present  $T$  as a function of  $f (= \omega/2\pi)$  and  $U$ . Each of these nine tables correspond to specific values for the pair  $(d, \theta_0)$ , where the river entrance depth  $d$  takes on the values  $d = 10, 15,$  and  $20$  meters, and the offshore wave direction relative to the current's main axis takes on the values  $\theta_0 = 0, 30,$  and  $60$  degrees. All tables assume that the offshore current  $U_0 = 0$  and that the offshore depth  $d_0 = 60$  m (corresponding to the buoy 46010 location).

Strictly speaking, equations (3)-(5) apply to monochromatic waves. To relate the predicted amplifications in Table 15 to the observed waves we approximate the spectrum with a monochromatic wave whose frequency is that at the spectral peak,  $f_p$ , and whose height is the significant wave height,  $H_s$ .

The theoretically computed wave height transfer function,  $T_c$ , at Buoy 8 in 15 m of water is given in column 8 of Table 14 for each of the intensive observation periods. Values without parentheses refer to incident angles of  $0^\circ$  and values with parentheses refer to  $30^\circ$  incidence. Qualitatively, the theory predicts wave amplification during ebbs and wave decay during floods just as has been observed. The change of the assumed angle of incidence from  $0^\circ$  to  $30^\circ$  lowers the predicted amplification on ebb by about 10% and does not affect the flood values in the first decimal place.

For convenience, the ratio of observed to computed wave amplifications is presented in column 9. For all but one ebb the ratio is within 20% of unity. There is no clear preference for one offshore incident angle over the other. However for the ebb of 11 September at 1615 hours the wave height was underpredicted by up to 50% at  $0^\circ$  incidence. It is for this

TABLE 15a. Wave height amplification  $T$  (Eq. 3) for  $d = 10m$ ,  $\theta_0 = 0^\circ$ .

F	T	D		CURRENT SPEED																			
		THETAO	U0	-2.50	-2.25	-2.00	-1.75	-1.50	-1.25	-1.00	-.75	-.50	-.25	0.00	.25	.50	.75	1.00	1.25	1.50	1.75	2.00	2.25
050	20.0	1.92	1.84	1.77	1.71	1.65	1.60	1.55	1.50	1.46	1.41	1.38	1.34	1.30	1.27	1.24	1.21	1.18	1.15	1.12	1.10	1.07	1.05
055	18.2	1.89	1.81	1.74	1.67	1.61	1.56	1.51	1.46	1.42	1.38	1.34	1.30	1.27	1.24	1.21	1.18	1.15	1.12	1.10	1.07	1.05	
060	16.7	1.85	1.77	1.70	1.63	1.57	1.52	1.47	1.42	1.38	1.34	1.30	1.26	1.23	1.20	1.17	1.14	1.11	1.09	1.06	1.04	1.02	
065	15.4	1.82	1.74	1.66	1.59	1.53	1.48	1.43	1.38	1.34	1.30	1.26	1.22	1.19	1.16	1.13	1.10	1.08	1.05	1.03	1.00	98	
070	14.3	1.79	1.70	1.62	1.55	1.49	1.44	1.39	1.34	1.30	1.25	1.22	1.18	1.15	1.12	1.09	1.06	1.04	1.01	99	97	95	
075	13.3	1.75	1.66	1.58	1.51	1.45	1.40	1.34	1.30	1.25	1.21	1.18	1.14	1.11	1.08	1.05	1.02	1.00	98	95	93	91	
080	12.5	1.73	1.63	1.55	1.48	1.41	1.36	1.30	1.26	1.21	1.17	1.14	1.10	1.07	1.04	1.01	98	95	92	90	88	84	
085	11.8	1.70	1.60	1.52	1.44	1.38	1.32	1.27	1.22	1.18	1.14	1.10	1.07	1.03	1.00	97	95	92	90	87	85	83	81
090	11.1	1.69	1.58	1.49	1.41	1.35	1.29	1.23	1.19	1.14	1.10	1.07	1.03	1.00	97	94	92	89	87	85	83	81	79
095	10.5	1.69	1.57	1.47	1.39	1.32	1.26	1.21	1.16	1.11	1.07	1.04	1.00	97	94	92	89	87	85	83	81	79	76
100	10.0	1.69	1.56	1.46	1.37	1.30	1.24	1.18	1.13	1.09	1.05	1.01	98	95	92	89	87	84	82	80	78	76	74
105	9.5	1.71	1.57	1.46	1.36	1.29	1.22	1.16	1.11	1.07	1.03	99	96	92	89	86	83	80	78	76	74	72	70
110	9.1	1.75	1.58	1.46	1.36	1.28	1.21	1.15	1.10	1.05	1.01	97	94	91	88	85	82	80	77	75	73	71	69
115	8.7	1.80	1.61	1.47	1.36	1.28	1.20	1.14	1.09	1.04	99	96	92	89	86	83	81	79	76	74	73	71	69
120	8.3	1.87	1.65	1.49	1.37	1.28	1.20	1.13	1.08	1.03	98	94	91	88	85	82	80	77	75	73	71	69	68
125	8.0	1.96	1.70	1.52	1.39	1.29	1.20	1.13	1.07	1.02	97	93	89	86	83	80	77	75	73	71	69	67	66
130	7.7	2.09	1.76	1.56	1.41	1.30	1.21	1.13	1.07	1.02	97	92	88	85	82	79	77	74	72	70	68	66	65
135	7.4	2.27	1.85	1.60	1.44	1.31	1.22	1.14	1.07	1.01	97	92	88	85	82	79	77	74	72	70	68	66	65
140	7.1	2.52	1.95	1.66	1.47	1.33	1.23	1.14	1.07	1.01	96	92	88	84	81	78	75	73	71	69	67	65	64
145	6.9	3.65	2.27	1.81	1.55	1.38	1.26	1.16	1.08	1.01	96	91	87	84	80	77	75	72	70	68	66	64	63
150	6.7	6.71	2.51	1.91	1.61	1.41	1.28	1.17	1.09	1.02	96	91	87	83	80	77	74	72	70	68	66	64	63
155	6.5	****	2.85	2.03	1.67	1.45	1.30	1.19	1.10	1.02	96	91	87	83	79	76	74	71	69	67	65	63	62
160	6.3	****	3.41	2.18	1.74	1.49	1.32	1.20	1.11	1.03	97	91	87	83	79	76	73	71	68	66	64	62	62
165	6.1	****	4.67	2.36	1.82	1.54	1.35	1.22	1.12	1.04	97	92	87	83	79	76	73	70	68	65	63	62	62
170	5.9	****	****	2.60	1.91	1.59	1.38	1.24	1.13	1.04	98	92	87	83	79	75	72	70	68	65	63	61	61
175	5.7	****	****	****	2.02	1.64	1.41	1.26	1.14	1.05	98	92	87	82	79	75	72	69	67	65	63	61	61
180	5.6	****	****	****	3.39	2.14	1.70	1.48	1.28	1.16	1.06	99	92	87	82	78	75	72	69	67	64	62	60
185	5.4	****	****	****	4.30	2.28	1.76	1.48	1.30	1.17	1.07	99	93	87	82	78	75	72	69	66	64	62	60
190	5.3	****	****	****	8.42	2.45	1.83	1.52	1.33	1.19	1.08	1.00	93	87	83	78	75	72	69	66	64	61	59
195	5.1	****	****	****	****	2.65	1.91	1.56	1.35	1.20	1.09	1.00	93	88	83	78	75	71	68	66	63	61	59
200	5.0	****	****	****	****	3.29	2.08	1.60	1.38	1.22	1.11	1.01	94	88	83	78	75	71	68	65	63	61	59
205	4.9	****	****	****	****	3.89	2.17	1.65	1.40	1.23	1.11	1.02	94	88	83	78	74	71	68	65	63	61	58
210	4.8	****	****	****	****	3.89	2.17	1.65	1.43	1.25	1.12	1.03	95	88	83	78	74	71	68	65	63	60	58
215	4.7	****	****	****	****	5.36	2.28	1.74	1.45	1.27	1.13	1.03	95	89	83	78	74	71	68	65	62	60	58
220	4.5	****	****	****	****	****	2.41	1.79	1.48	1.28	1.14	1.04	96	89	83	78	74	71	68	65	62	60	58
225	4.4	****	****	****	****	****	2.56	1.84	1.50	1.30	1.15	1.05	96	89	83	78	74	71	68	65	62	60	58
230	4.3	****	****	****	****	****	2.74	1.89	1.53	1.31	1.16	1.05	97	89	84	79	74	71	67	64	62	60	57
235	4.3	****	****	****	****	****	2.97	1.94	1.56	1.33	1.17	1.06	97	90	84	79	74	70	67	64	62	59	57
240	4.2	****	****	****	****	****	3.29	2.00	1.58	1.34	1.18	1.06	97	90	84	79	74	70	67	64	61	59	57
245	4.1	****	****	****	****	****	3.78	2.07	1.61	1.36	1.19	1.07	98	90	84	79	74	70	67	64	61	59	57
250	4.0	****	****	****	****	****	3.78	2.07	1.61	1.36	1.19	1.07	98	90	84	79	74	70	67	64	61	59	57

TABLE 15b. Wave height amplification  $T$  (Eq. 3) for  $d = 10$  m,  $\theta_0 = 30^\circ$ .

D	THETAO	DO	UO	CURRENT SPEED																			
				-2.50	-2.00	-1.75	-1.50	-1.25	-1.00	-.75	-.50	-.25	0.00	.25	.50	.75	1.00	1.25	1.50	1.75	2.00	2.25	2.50
10.0	30.0	60.0	0.0																				
F	T																						
.050	20.0	1.80	1.73	1.66	1.61	1.55	1.50	1.45	1.41	1.37	1.33	1.30	1.26	1.23	1.20	1.17	1.15	1.12	1.10	1.07	1.05	1.03	
.055	18.2	1.77	1.70	1.63	1.57	1.52	1.47	1.42	1.38	1.34	1.30	1.26	1.23	1.20	1.17	1.14	1.11	1.09	1.06	1.04	1.02	1.00	
.060	16.7	1.74	1.66	1.60	1.53	1.48	1.43	1.38	1.34	1.30	1.26	1.22	1.19	1.16	1.13	1.10	1.07	1.04	1.01	0.99	0.97	0.94	
.065	15.4	1.70	1.63	1.56	1.50	1.44	1.39	1.34	1.30	1.26	1.22	1.19	1.16	1.13	1.10	1.07	1.04	1.02	1.00	0.98	0.96	0.94	
.070	14.3	1.67	1.59	1.52	1.46	1.40	1.35	1.30	1.26	1.22	1.19	1.15	1.12	1.09	1.06	1.03	1.01	0.99	0.96	0.94	0.92	0.90	
.075	13.3	1.64	1.56	1.49	1.42	1.37	1.31	1.27	1.22	1.18	1.15	1.11	1.08	1.05	1.02	1.00	0.97	0.95	0.93	0.91	0.89	0.87	
.080	12.5	1.62	1.53	1.45	1.39	1.33	1.28	1.23	1.19	1.15	1.11	1.08	1.04	1.01	0.98	0.96	0.94	0.92	0.90	0.88	0.86	0.84	
.085	11.8	1.60	1.50	1.43	1.36	1.30	1.24	1.20	1.15	1.11	1.08	1.04	1.01	0.98	0.95	0.93	0.91	0.89	0.87	0.85	0.83	0.81	
.090	11.1	1.58	1.48	1.40	1.33	1.27	1.21	1.17	1.12	1.08	1.05	1.01	0.98	0.95	0.93	0.90	0.88	0.86	0.84	0.82	0.80	0.78	
.095	10.5	1.58	1.47	1.38	1.31	1.25	1.19	1.14	1.10	1.06	1.02	0.99	0.96	0.93	0.90	0.88	0.85	0.83	0.81	0.79	0.78	0.76	
.100	10.0	1.58	1.47	1.37	1.29	1.23	1.17	1.12	1.07	1.03	1.00	0.96	0.93	0.90	0.88	0.85	0.83	0.81	0.79	0.77	0.76	0.74	
.105	9.5	1.60	1.47	1.37	1.29	1.21	1.15	1.10	1.06	1.01	0.98	0.94	0.91	0.89	0.86	0.84	0.81	0.79	0.77	0.75	0.74	0.72	
.110	9.1	1.63	1.48	1.37	1.28	1.21	1.14	1.09	1.04	1.00	0.96	0.93	0.90	0.87	0.84	0.82	0.80	0.78	0.76	0.74	0.72	0.71	
.115	8.7	1.68	1.51	1.38	1.29	1.21	1.14	1.08	1.03	0.99	0.95	0.92	0.89	0.86	0.83	0.81	0.78	0.76	0.74	0.73	0.71	0.69	
.120	8.3	1.74	1.54	1.40	1.29	1.21	1.14	1.08	1.03	0.98	0.94	0.91	0.88	0.85	0.82	0.80	0.77	0.75	0.73	0.72	0.70	0.68	
.125	8.0	1.82	1.59	1.43	1.31	1.22	1.14	1.08	1.02	0.98	0.94	0.90	0.86	0.83	0.81	0.78	0.76	0.74	0.72	0.70	0.68	0.67	
.130	7.7	1.93	1.64	1.46	1.33	1.23	1.15	1.08	1.02	0.98	0.93	0.89	0.86	0.83	0.80	0.77	0.75	0.73	0.71	0.69	0.68	0.66	
.135	7.4	2.09	1.72	1.50	1.35	1.24	1.15	1.08	1.02	0.97	0.93	0.89	0.86	0.82	0.80	0.77	0.75	0.73	0.71	0.69	0.67	0.66	
.140	7.1	2.30	1.81	1.55	1.38	1.26	1.17	1.09	1.03	0.98	0.93	0.89	0.86	0.82	0.80	0.77	0.75	0.73	0.71	0.69	0.67	0.66	
.145	6.9	2.62	1.93	1.61	1.42	1.28	1.18	1.10	1.03	0.98	0.93	0.89	0.85	0.82	0.79	0.77	0.74	0.72	0.70	0.68	0.66	0.65	
.150	6.7	3.19	2.08	1.69	1.46	1.31	1.20	1.11	1.04	0.98	0.93	0.89	0.85	0.82	0.79	0.76	0.74	0.72	0.70	0.68	0.66	0.65	
.155	6.5	4.77	2.29	1.77	1.51	1.34	1.21	1.12	1.05	0.99	0.93	0.89	0.85	0.82	0.79	0.76	0.74	0.72	0.70	0.68	0.66	0.64	
.160	6.3	***	2.57	1.88	1.56	1.37	1.24	1.13	1.06	0.99	0.94	0.89	0.85	0.82	0.79	0.76	0.74	0.71	0.69	0.67	0.65	0.64	
.165	6.1	***	3.02	2.01	1.63	1.41	1.26	1.15	1.07	1.00	0.94	0.89	0.85	0.82	0.79	0.76	0.73	0.71	0.69	0.67	0.65	0.64	
.170	5.9	***	3.89	2.17	1.70	1.45	1.28	1.17	1.08	1.01	0.95	0.90	0.86	0.82	0.79	0.76	0.73	0.71	0.69	0.67	0.65	0.64	
.175	5.7	***	***	2.37	1.78	1.49	1.31	1.19	1.09	1.01	0.95	0.90	0.86	0.82	0.79	0.76	0.73	0.71	0.69	0.67	0.65	0.64	
.180	5.6	***	***	2.64	1.88	1.54	1.34	1.20	1.10	1.02	0.96	0.91	0.86	0.82	0.79	0.76	0.73	0.71	0.69	0.67	0.65	0.63	
.185	5.4	***	***	3.02	1.98	1.60	1.37	1.23	1.13	1.03	0.97	0.91	0.86	0.82	0.79	0.76	0.73	0.71	0.69	0.67	0.65	0.63	
.190	5.3	***	***	3.68	2.11	1.66	1.41	1.25	1.13	1.04	0.97	0.91	0.87	0.83	0.79	0.76	0.73	0.71	0.69	0.67	0.65	0.63	
.195	5.1	***	***	5.73	2.25	1.72	1.44	1.27	1.15	1.05	0.98	0.92	0.87	0.83	0.79	0.76	0.73	0.71	0.69	0.67	0.65	0.63	
.200	5.0	***	***	***	2.43	1.79	1.48	1.29	1.16	1.06	0.99	0.93	0.87	0.83	0.79	0.76	0.73	0.71	0.69	0.66	0.65	0.63	
.205	4.9	***	***	***	2.65	1.86	1.52	1.32	1.18	1.07	0.99	0.93	0.88	0.83	0.80	0.76	0.73	0.71	0.69	0.66	0.65	0.63	
.210	4.8	***	***	***	2.95	1.94	1.56	1.34	1.19	1.09	1.00	0.94	0.88	0.84	0.80	0.76	0.73	0.71	0.69	0.66	0.65	0.63	
.215	4.7	***	***	***	3.41	2.02	1.60	1.36	1.21	1.10	1.01	0.94	0.89	0.84	0.80	0.77	0.74	0.71	0.69	0.66	0.65	0.63	
.220	4.5	***	***	***	4.31	2.12	1.64	1.39	1.22	1.11	1.02	0.95	0.89	0.84	0.80	0.77	0.74	0.71	0.69	0.66	0.65	0.63	
.225	4.4	***	***	***	***	2.23	1.68	1.41	1.24	1.12	1.02	0.95	0.89	0.84	0.80	0.77	0.74	0.71	0.69	0.66	0.65	0.63	
.230	4.3	***	***	***	***	2.36	1.73	1.44	1.25	1.13	1.03	0.96	0.90	0.85	0.81	0.77	0.74	0.71	0.69	0.66	0.65	0.63	
.235	4.3	***	***	***	***	2.51	1.78	1.46	1.27	1.14	1.04	0.96	0.90	0.85	0.81	0.77	0.74	0.71	0.69	0.66	0.65	0.63	
.240	4.2	***	***	***	***	2.71	1.83	1.48	1.28	1.15	1.04	0.97	0.90	0.85	0.81	0.77	0.74	0.71	0.69	0.66	0.65	0.63	
.245	4.1	***	***	***	***	2.96	1.88	1.51	1.30	1.15	1.05	0.97	0.91	0.85	0.81	0.77	0.74	0.71	0.69	0.66	0.65	0.63	
.250	4.0	***	***	***	***	3.33	1.94	1.53	1.31	1.16	1.06	0.97	0.91	0.86	0.81	0.77	0.74	0.71	0.69	0.66	0.65	0.64	

TABLE 15c. Wave height amplification  $T$  (Eq. 3) for  $d = 10$  m,  $\theta_0 = 60^\circ$ .

D	THETA	DO	UO	CURRENT SPEED																		
				-2.50	-2.25	-2.00	-1.75	-1.50	-1.25	-1.00	-.75	-.50	-.25	0.00	.25	.50	.75	1.00	1.25	1.50	1.75	2.00
050	20.0	1.39	1.33	1.29	1.24	1.20	1.16	1.13	1.10	1.07	1.04	1.01	99	96	94	92	90	88	86	85	83	82
055	18.2	1.36	1.31	1.26	1.22	1.18	1.14	1.10	1.07	1.04	1.01	99	96	94	92	90	88	86	84	83	81	79
060	16.7	1.34	1.28	1.23	1.19	1.15	1.11	1.08	1.04	1.01	99	96	94	91	89	87	85	83	82	80	79	77
065	15.4	1.31	1.26	1.21	1.16	1.12	1.08	1.05	1.02	99	96	93	91	89	87	85	83	81	79	78	76	75
070	14.3	1.29	1.23	1.18	1.13	1.09	1.05	1.02	99	96	93	90	88	86	84	82	80	78	77	75	74	72
075	13.3	1.27	1.21	1.15	1.11	1.06	1.02	99	96	93	90	88	85	83	81	79	78	76	74	73	71	70
080	12.5	1.25	1.18	1.13	1.08	1.04	1.00	96	93	90	88	85	83	81	79	77	75	74	72	71	69	68
085	11.8	1.23	1.16	1.11	1.06	1.01	97	94	91	88	85	83	81	78	77	75	73	71	70	69	67	66
090	11.1	1.22	1.15	1.09	1.04	99	95	92	89	86	83	81	79	77	75	73	71	69	68	67	65	64
095	10.5	1.22	1.14	1.08	1.02	98	94	90	87	84	81	79	77	75	73	71	69	68	66	65	64	63
100	10.0	1.22	1.14	1.07	1.01	96	92	89	85	82	80	77	75	73	71	69	68	66	65	64	62	61
105	9.5	1.23	1.14	1.07	1.01	96	91	88	84	81	79	76	74	72	70	68	67	65	64	63	62	60
110	9.1	1.26	1.15	1.07	1.01	95	91	87	84	81	78	75	73	71	69	68	66	65	63	62	61	60
115	8.7	1.29	1.17	1.08	1.01	95	91	87	83	80	77	75	73	71	69	67	66	64	63	61	60	59
120	8.3	1.33	1.19	1.09	1.02	96	91	87	83	80	77	75	72	70	68	67	65	64	62	61	60	59
125	8.0	1.39	1.23	1.11	1.03	97	91	87	83	80	77	75	72	70	68	67	65	64	62	61	60	59
130	7.7	1.46	1.27	1.14	1.05	98	92	87	84	80	77	75	72	70	68	67	65	64	62	61	60	59
135	7.4	1.56	1.32	1.17	1.07	99	93	88	84	81	78	75	73	70	68	67	65	64	62	61	60	59
140	7.1	1.69	1.38	1.21	1.09	1.01	94	89	85	81	78	75	73	71	69	67	66	64	63	62	60	59
145	6.9	1.88	1.46	1.25	1.12	1.03	96	90	86	82	79	76	73	71	69	68	66	64	63	62	61	60
150	6.7	2.18	1.56	1.30	1.15	1.05	97	91	87	83	79	76	74	72	70	68	66	65	64	62	61	60
155	6.5	2.78	1.69	1.36	1.19	1.07	99	93	88	84	80	77	75	72	70	69	67	65	64	63	62	60
160	6.3	****	1.86	1.43	1.23	1.10	1.01	94	89	85	81	78	75	73	71	69	68	66	65	63	62	61
165	6.1	****	2.11	1.52	1.27	1.13	1.03	96	90	86	82	79	76	74	72	70	68	67	65	64	63	62
170	5.9	****	2.52	1.62	1.33	1.16	1.05	97	92	87	83	80	77	75	73	71	69	67	66	65	63	62
175	5.7	****	3.48	1.75	1.38	1.20	1.08	99	93	88	84	81	78	76	73	71	69	67	66	65	63	62
180	5.6	****	7.31	1.92	1.45	1.23	1.10	1.01	95	89	85	82	79	77	74	72	70	68	67	65	64	63
185	5.4	****	6.10	2.14	1.53	1.27	1.13	1.03	96	91	87	83	80	78	75	73	71	70	68	67	65	64
190	5.3	****	****	2.47	1.61	1.32	1.16	1.05	98	92	88	84	81	79	76	74	72	71	69	67	66	65
195	5.1	****	****	3.08	1.71	1.36	1.19	1.07	99	94	89	85	82	80	77	75	73	71	70	68	67	65
200	5.0	****	****	7.15	1.82	1.41	1.22	1.09	1.01	95	90	86	83	81	78	76	74	72	70	69	67	66
205	4.9	****	****	****	1.96	1.47	1.25	1.12	1.03	96	92	88	84	82	79	77	75	73	71	69	68	66
210	4.8	****	****	****	2.14	1.52	1.28	1.14	1.04	98	93	89	85	83	80	78	76	73	72	70	68	66
215	4.7	****	****	****	2.38	1.59	1.31	1.16	1.06	99	94	90	86	84	81	78	76	74	72	70	68	67
220	4.5	****	****	****	2.75	1.65	1.34	1.18	1.08	1.00	95	91	87	85	82	80	77	75	73	71	69	67
225	4.4	****	****	****	****	1.72	1.37	1.20	1.09	1.02	96	92	88	84	82	80	77	75	73	71	69	67
230	4.3	****	****	****	****	1.81	1.41	1.22	1.11	1.03	97	93	89	86	83	81	78	76	73	71	69	67
235	4.3	****	****	****	****	1.90	1.44	1.24	1.12	1.04	98	94	90	87	84	81	78	76	74	71	69	67
240	4.2	****	****	****	****	2.02	1.48	1.26	1.13	1.05	99	95	91	87	84	82	79	76	74	72	69	67
245	4.1	****	****	****	****	2.16	1.51	1.28	1.14	1.06	1.00	95	91	88	85	82	79	77	74	72	69	67
250	4.0	****	****	****	****	2.35	1.55	1.29	1.16	1.07	1.01	96	92	89	85	82	79	77	74	72	69	67



TABLE 15d. Wave height amplification  $T$  (Eq. 3) for  $d = 15$  m,  $\theta_0 = 0^\circ$ .

D	THETAO	DO	UO	CURRENT SPEED																		
				-2.50	-2.00	-1.75	-1.50	-1.25	-1.00	-.75	-.50	-.25	0.00	.25	.50	.75	1.00	1.25	1.50	1.75	2.00	2.25
050	20.0	1.66	1.61	1.56	1.51	1.47	1.43	1.39	1.35	1.32	1.29	1.26	1.23	1.20	1.18	1.15	1.13	1.11	1.08	1.06	1.04	1.02
055	18.2	1.64	1.58	1.53	1.48	1.44	1.40	1.36	1.32	1.29	1.26	1.23	1.20	1.17	1.15	1.12	1.10	1.08	1.05	1.03	1.01	1.00
060	16.7	1.62	1.56	1.50	1.46	1.41	1.37	1.33	1.29	1.26	1.23	1.20	1.17	1.14	1.11	1.09	1.07	1.04	1.02	1.00	98	97
065	15.4	1.59	1.53	1.48	1.43	1.38	1.34	1.30	1.26	1.22	1.19	1.16	1.13	1.11	1.08	1.06	1.03	1.01	99	97	95	93
070	14.3	1.57	1.51	1.45	1.40	1.35	1.30	1.26	1.23	1.19	1.16	1.13	1.10	1.07	1.05	1.02	1.00	98	96	94	92	90
075	13.3	1.55	1.48	1.42	1.37	1.32	1.27	1.23	1.19	1.16	1.13	1.09	1.07	1.04	1.01	99	97	95	93	91	89	87
080	12.5	1.54	1.47	1.40	1.34	1.29	1.24	1.20	1.16	1.13	1.09	1.06	1.03	1.01	98	96	94	91	89	88	86	84
085	11.8	1.53	1.45	1.38	1.32	1.27	1.22	1.17	1.13	1.10	1.06	1.03	1.00	98	95	93	91	88	86	85	83	81
090	11.1	1.53	1.44	1.37	1.30	1.25	1.20	1.15	1.11	1.07	1.04	1.01	98	95	92	90	88	86	84	82	80	78
095	10.5	1.54	1.44	1.36	1.29	1.23	1.18	1.13	1.09	1.05	1.01	98	95	92	90	88	85	83	81	79	78	76
100	10.0	1.56	1.45	1.36	1.29	1.22	1.16	1.12	1.07	1.03	1.00	96	93	90	88	85	83	81	79	77	76	74
105	9.5	1.60	1.47	1.37	1.29	1.22	1.16	1.11	1.06	1.02	98	95	92	89	86	84	81	79	77	75	74	72
110	9.1	1.65	1.50	1.39	1.30	1.22	1.16	1.10	1.05	1.01	97	93	90	87	85	82	80	78	76	74	72	71
115	8.7	1.72	1.55	1.42	1.31	1.23	1.16	1.10	1.05	1.00	96	93	89	86	84	81	79	77	75	73	71	69
120	8.3	1.82	1.60	1.45	1.34	1.24	1.17	1.10	1.05	1.00	96	92	89	86	83	80	78	76	74	72	70	68
125	8.0	1.94	1.67	1.50	1.36	1.26	1.18	1.11	1.05	1.00	96	92	88	85	82	79	77	75	73	71	69	67
130	7.7	2.10	1.76	1.55	1.40	1.29	1.19	1.12	1.06	1.00	96	91	88	85	82	79	76	74	72	70	68	66
135	7.4	2.30	1.87	1.62	1.44	1.31	1.21	1.13	1.06	1.01	96	91	88	84	81	78	76	73	71	69	67	66
140	7.1	2.59	2.00	1.69	1.49	1.35	1.23	1.15	1.07	1.01	96	92	88	84	81	78	75	73	71	69	67	65
145	6.9	3.01	2.16	1.78	1.54	1.38	1.26	1.16	1.09	1.02	97	92	88	84	81	78	75	73	71	69	66	65
150	6.7	3.74	2.35	1.88	1.60	1.42	1.29	1.18	1.10	1.03	97	92	88	84	81	78	75	72	70	68	66	64
155	6.5	6.59	2.61	1.99	1.67	1.46	1.31	1.20	1.11	1.04	98	93	88	84	81	77	75	72	70	67	65	64
160	6.3	***	2.95	2.12	1.74	1.51	1.34	1.22	1.13	1.05	99	93	88	84	81	77	74	72	69	67	65	63
165	6.1	***	3.49	2.27	1.82	1.55	1.38	1.25	1.14	1.06	99	94	89	84	81	77	74	72	69	67	65	63
170	5.9	***	4.73	2.44	1.90	1.60	1.41	1.27	1.16	1.07	1.00	94	89	85	81	77	74	71	69	67	64	62
175	5.7	***	***	2.67	1.99	1.65	1.44	1.29	1.17	1.08	1.01	95	89	85	81	77	74	71	69	66	64	62
180	5.6	***	***	2.97	2.09	1.71	1.47	1.31	1.19	1.09	1.02	95	90	85	81	77	74	71	68	66	64	62
185	5.4	***	***	3.43	2.20	1.76	1.51	1.33	1.21	1.11	1.03	96	90	85	81	77	74	71	68	66	64	62
190	5.3	***	***	4.32	2.33	1.82	1.54	1.36	1.22	1.12	1.03	96	90	85	81	77	74	71	68	66	63	61
195	5.1	***	***	***	2.48	1.88	1.57	1.38	1.23	1.13	1.04	97	91	86	81	77	74	71	68	66	63	61
200	5.0	***	***	***	2.68	1.95	1.61	1.40	1.25	1.14	1.05	97	91	86	81	77	74	71	68	65	63	61
205	4.9	***	***	***	2.93	2.02	1.64	1.42	1.26	1.14	1.05	98	91	86	81	77	74	71	68	65	63	61
210	4.8	***	***	***	3.29	2.10	1.68	1.44	1.27	1.15	1.06	98	92	86	81	77	74	71	68	65	63	60
215	4.7	***	***	***	3.89	2.19	1.72	1.46	1.29	1.16	1.06	98	92	86	82	77	74	70	67	65	62	60
220	4.5	***	***	***	5.36	2.29	1.76	1.48	1.30	1.17	1.07	99	92	86	82	77	74	70	67	65	62	60
225	4.4	***	***	***	***	2.42	1.80	1.50	1.31	1.18	1.07	99	92	86	81	77	73	70	67	64	62	60
230	4.3	***	***	***	***	2.56	1.85	1.52	1.32	1.18	1.08	99	92	86	81	77	73	70	67	64	62	60
235	4.3	***	***	***	***	2.74	1.90	1.54	1.33	1.19	1.08	99	92	86	81	77	73	70	67	64	62	59
240	4.2	***	***	***	***	2.98	1.95	1.57	1.35	1.19	1.08	99	92	86	81	77	73	70	67	64	61	59
245	4.1	***	***	***	***	3.29	2.01	1.59	1.36	1.20	1.09	1.00	92	86	81	77	73	69	66	64	61	59
250	4.0	***	***	***	***	3.78	2.07	1.62	1.37	1.21	1.09	1.00	92	86	81	77	73	69	66	63	61	59



TABLE 15f. Wave height amplification  $T$  (Eq. 3) for  $d = 15$  m,  $\theta_0 = 60^\circ$ .

F	D	THETAO	DO	UO	CURRENT SPEED																	
					-2.50	-2.00	-1.75	-1.50	-1.25	-1.00	-.75	-.50	-.25	0.00	.25	.50	.75	1.00	1.25	1.50	1.75	2.00
.050	20.0	1.22	1.18	1.15	1.12	1.09	1.06	1.03	1.01	.99	.97	.95	.93	.91	.89	.88	.86	.85	.83	.82	.81	.79
.055	18.2	1.20	1.16	1.13	1.10	1.07	1.04	1.01	.99	.97	.95	.93	.91	.89	.87	.86	.84	.83	.81	.80	.79	.77
.060	16.7	1.19	1.15	1.11	1.08	1.05	1.02	.99	.97	.95	.93	.91	.89	.87	.85	.84	.82	.81	.79	.78	.77	.75
.065	15.4	1.17	1.13	1.09	1.06	1.03	1.00	.97	.95	.92	.90	.88	.86	.85	.83	.81	.80	.78	.77	.76	.75	.73
.070	14.3	1.15	1.11	1.07	1.04	1.01	.98	.95	.93	.90	.88	.86	.84	.82	.81	.79	.78	.76	.75	.74	.73	.71
.075	13.3	1.14	1.10	1.06	1.02	.99	.96	.93	.90	.88	.86	.84	.82	.80	.79	.77	.76	.74	.73	.72	.71	.69
.080	12.5	1.13	1.08	1.04	1.00	.97	.94	.91	.88	.86	.84	.82	.80	.78	.77	.75	.74	.72	.71	.70	.69	.68
.085	11.8	1.13	1.07	1.03	.99	.95	.92	.89	.87	.84	.82	.80	.78	.77	.75	.73	.72	.71	.69	.68	.67	.66
.090	11.1	1.13	1.07	1.02	.98	.94	.91	.88	.85	.83	.81	.79	.77	.75	.73	.72	.71	.69	.68	.67	.66	.65
.095	10.5	1.13	1.07	1.02	.97	.93	.90	.87	.84	.82	.79	.77	.75	.74	.72	.71	.69	.68	.67	.66	.65	.63
.100	10.0	1.15	1.08	1.02	.97	.93	.89	.86	.83	.81	.79	.77	.75	.74	.72	.71	.69	.68	.67	.66	.65	.63
.105	9.5	1.17	1.09	1.03	.98	.93	.89	.86	.83	.81	.78	.76	.74	.72	.71	.69	.68	.67	.66	.65	.64	.63
.110	9.1	1.20	1.11	1.04	.98	.94	.90	.86	.83	.81	.78	.76	.74	.72	.71	.69	.68	.66	.65	.64	.63	.62
.115	8.7	1.25	1.14	1.06	1.00	.95	.90	.86	.84	.81	.78	.76	.74	.72	.71	.69	.68	.66	.65	.64	.63	.62
.120	8.3	1.30	1.18	1.09	1.02	.96	.91	.88	.84	.81	.78	.76	.74	.72	.71	.69	.68	.66	.65	.64	.63	.62
.125	8.0	1.38	1.23	1.12	1.04	.98	.93	.89	.85	.82	.80	.77	.75	.73	.72	.70	.69	.67	.66	.65	.64	.63
.130	7.7	1.47	1.28	1.16	1.07	1.00	.95	.90	.86	.83	.80	.78	.76	.74	.72	.71	.69	.68	.67	.66	.65	.63
.135	7.4	1.59	1.35	1.20	1.10	1.02	.96	.92	.88	.84	.82	.79	.77	.75	.73	.71	.70	.69	.68	.67	.66	.64
.140	7.1	1.74	1.43	1.25	1.13	1.05	.99	.93	.89	.86	.83	.80	.78	.76	.74	.72	.71	.69	.68	.67	.66	.65
.145	6.9	1.96	1.52	1.31	1.17	1.08	1.01	.95	.91	.87	.84	.81	.79	.77	.75	.73	.72	.70	.69	.68	.67	.65
.150	6.7	2.28	1.64	1.37	1.22	1.11	1.03	.97	.93	.89	.86	.83	.80	.78	.76	.75	.73	.71	.70	.69	.68	.66
.155	6.5	2.87	1.78	1.45	1.26	1.14	1.06	1.00	.94	.90	.87	.84	.82	.79	.77	.76	.74	.72	.71	.70	.69	.67
.160	6.3	7.16	1.97	1.53	1.31	1.18	1.09	1.02	.96	.92	.89	.86	.83	.81	.79	.77	.75	.73	.72	.71	.70	.68
.165	6.1	***	2.21	1.62	1.36	1.21	1.11	1.04	.98	.94	.90	.87	.84	.82	.80	.78	.76	.75	.73	.71	.70	.69
.170	5.9	***	2.61	1.73	1.42	1.25	1.14	1.06	1.00	.95	.92	.88	.86	.83	.81	.79	.77	.75	.74	.72	.71	.69
.175	5.7	***	***	1.85	1.48	1.29	1.17	1.08	1.02	.97	.93	.90	.87	.84	.82	.80	.78	.76	.75	.73	.71	.70
.180	5.6	***	***	2.00	1.54	1.32	1.19	1.10	1.04	.98	.94	.91	.88	.86	.83	.81	.79	.77	.75	.74	.72	.70
.185	5.4	***	***	2.21	1.61	1.36	1.22	1.12	1.05	1.00	.96	.92	.89	.87	.84	.82	.80	.78	.75	.74	.72	.71
.190	5.3	***	***	2.52	1.68	1.40	1.24	1.14	1.07	1.01	.97	.93	.90	.88	.85	.83	.81	.79	.77	.75	.73	.71
.195	5.1	***	***	3.11	1.77	1.44	1.27	1.16	1.08	1.02	.98	.94	.91	.88	.86	.83	.81	.79	.77	.75	.73	.71
.200	5.0	***	***	7.13	1.87	1.48	1.29	1.17	1.09	1.03	.99	.95	.92	.89	.87	.84	.82	.79	.77	.75	.73	.71
.205	4.9	***	***	***	2.00	1.52	1.31	1.19	1.11	1.04	1.00	.96	.93	.90	.87	.85	.82	.80	.77	.75	.73	.71
.210	4.8	***	***	***	2.16	1.57	1.34	1.20	1.12	1.05	1.01	.97	.93	.90	.88	.85	.82	.80	.77	.75	.73	.71
.215	4.7	***	***	***	2.39	1.62	1.36	1.22	1.13	1.06	1.01	.97	.94	.91	.88	.85	.82	.80	.77	.75	.73	.71
.220	4.5	***	***	***	2.76	1.68	1.38	1.23	1.13	1.07	1.02	.98	.94	.91	.88	.85	.83	.80	.78	.75	.73	.71
.225	4.4	***	***	***	***	1.74	1.41	1.24	1.14	1.07	1.02	.98	.95	.92	.89	.86	.83	.80	.77	.75	.73	.70
.230	4.3	***	***	***	***	***	1.82	1.43	1.26	1.15	1.08	1.03	.99	.95	.92	.89	.86	.83	.80	.77	.75	.72
.235	4.3	***	***	***	***	***	***	1.91	1.46	1.27	1.16	1.08	1.03	.99	.95	.92	.89	.86	.83	.80	.77	.70
.240	4.2	***	***	***	***	***	***	2.02	1.49	1.28	1.16	1.09	1.03	.99	.95	.92	.89	.86	.83	.80	.77	.70
.245	4.1	***	***	***	***	***	***	2.16	1.52	1.29	1.17	1.09	1.04	.99	.96	.92	.89	.86	.82	.77	.74	.69
.250	4.0	***	***	***	***	***	***	2.35	1.56	1.31	1.18	1.10	1.04	1.00	.96	.92	.89	.85	.82	.76	.74	.69

TABLE 15g. Wave height amplification  $T$  (Eq. 3) for  $d = 20$  m,  $\theta_0 = 0^\circ$ .

D	THETAO	DO	UO	CURRENT SPEED																				
				-2.50	-2.25	-2.00	-1.75	-1.50	-1.25	-1.00	-.75	-.50	-.25	0.00	.25	.50	.75	1.00	1.25	1.50	1.75	2.00	2.25	2.50
050	20.0	0.0	0.0	1.52	1.48	1.44	1.40	1.36	1.33	1.30	1.27	1.24	1.21	1.19	1.16	1.14	1.12	1.10	1.08	1.06	1.04	1.02	1.00	.98
055	18.2	1.51	1.46	1.42	1.38	1.34	1.31	1.27	1.24	1.21	1.19	1.16	1.14	1.11	1.09	1.06	1.03	1.01	0.99	0.97	0.95	0.94	0.92	.90
060	16.7	1.49	1.44	1.40	1.36	1.32	1.28	1.25	1.22	1.19	1.16	1.13	1.11	1.08	1.06	1.03	1.01	0.99	0.97	0.95	0.94	0.92	0.91	.89
065	15.4	1.48	1.43	1.38	1.33	1.29	1.26	1.22	1.19	1.16	1.13	1.11	1.08	1.05	1.03	1.00	0.98	0.95	0.93	0.91	0.90	0.88	0.87	.85
070	14.3	1.47	1.41	1.36	1.31	1.27	1.23	1.20	1.16	1.13	1.10	1.08	1.05	1.02	1.00	0.97	0.95	0.93	0.91	0.89	0.87	0.85	0.83	.82
075	13.3	1.46	1.40	1.34	1.29	1.25	1.21	1.17	1.14	1.11	1.08	1.05	1.02	1.00	0.97	0.95	0.92	0.90	0.88	0.86	0.84	0.82	0.81	.79
080	12.5	1.45	1.39	1.33	1.28	1.23	1.19	1.15	1.11	1.08	1.05	1.02	1.00	0.97	0.95	0.92	0.90	0.88	0.86	0.84	0.82	0.80	0.78	.77
085	11.8	1.46	1.38	1.32	1.26	1.21	1.17	1.13	1.09	1.06	1.03	1.00	0.97	0.95	0.92	0.90	0.88	0.86	0.84	0.82	0.80	0.78	0.76	.75
090	11.1	1.47	1.39	1.32	1.26	1.20	1.15	1.11	1.07	1.04	1.01	0.98	0.96	0.93	0.90	0.88	0.86	0.84	0.82	0.80	0.78	0.76	0.74	.73
095	10.5	1.49	1.40	1.32	1.25	1.20	1.14	1.10	1.06	1.02	0.99	0.96	0.93	0.90	0.88	0.86	0.84	0.82	0.80	0.78	0.76	0.74	0.73	.71
100	10.0	1.53	1.42	1.33	1.26	1.20	1.14	1.09	1.05	1.01	0.98	0.94	0.91	0.89	0.86	0.84	0.82	0.80	0.78	0.76	0.74	0.72	0.70	.69
105	9.5	1.58	1.46	1.35	1.27	1.20	1.14	1.09	1.04	1.00	0.97	0.93	0.90	0.87	0.85	0.83	0.81	0.79	0.77	0.75	0.73	0.71	0.70	.68
110	9.1	1.74	1.56	1.42	1.32	1.23	1.16	1.10	1.05	1.00	0.96	0.92	0.89	0.85	0.82	0.80	0.78	0.76	0.74	0.72	0.70	0.68	0.67	.65
115	8.7	1.85	1.63	1.47	1.35	1.25	1.17	1.11	1.05	1.00	0.96	0.92	0.88	0.85	0.82	0.80	0.77	0.75	0.73	0.71	0.69	0.67	0.65	.63
120	8.3	1.99	1.71	1.53	1.39	1.28	1.19	1.12	1.06	1.01	0.96	0.92	0.88	0.85	0.82	0.80	0.77	0.75	0.73	0.71	0.69	0.67	0.65	.63
125	8.0	2.16	1.81	1.59	1.43	1.31	1.22	1.14	1.07	1.02	0.97	0.93	0.89	0.85	0.82	0.80	0.77	0.75	0.73	0.71	0.69	0.67	0.65	.63
130	7.7	2.37	1.93	1.66	1.48	1.35	1.24	1.16	1.09	1.03	0.97	0.93	0.89	0.85	0.82	0.80	0.77	0.75	0.73	0.71	0.69	0.67	0.65	.63
135	7.4	2.65	2.06	1.74	1.54	1.38	1.27	1.18	1.10	1.04	0.98	0.93	0.89	0.85	0.82	0.80	0.77	0.75	0.73	0.71	0.69	0.67	0.65	.63
140	7.1	3.06	2.22	1.83	1.59	1.42	1.30	1.20	1.12	1.05	0.99	0.94	0.90	0.86	0.82	0.80	0.77	0.75	0.73	0.71	0.69	0.67	0.65	.63
145	6.9	3.78	2.40	1.93	1.65	1.46	1.33	1.22	1.13	1.06	1.00	0.95	0.90	0.86	0.82	0.80	0.77	0.75	0.73	0.71	0.69	0.67	0.65	.63
150	6.7	6.60	2.64	2.03	1.71	1.50	1.35	1.24	1.15	1.07	1.01	0.95	0.90	0.86	0.82	0.80	0.77	0.75	0.73	0.71	0.69	0.67	0.65	.63
155	6.5	****	2.97	2.15	1.78	1.55	1.38	1.26	1.16	1.08	1.02	0.96	0.91	0.87	0.83	0.80	0.77	0.75	0.73	0.71	0.69	0.67	0.65	.63
160	6.3	****	3.51	2.29	1.85	1.59	1.41	1.28	1.18	1.09	1.02	0.96	0.91	0.87	0.83	0.80	0.77	0.75	0.73	0.71	0.69	0.67	0.65	.63
165	6.1	****	4.73	2.46	1.92	1.63	1.44	1.30	1.19	1.10	1.03	0.97	0.92	0.87	0.83	0.80	0.77	0.75	0.73	0.71	0.69	0.67	0.65	.63
170	5.9	****	****	2.68	2.01	1.68	1.47	1.32	1.20	1.11	1.04	0.97	0.92	0.87	0.83	0.80	0.77	0.75	0.73	0.71	0.69	0.67	0.65	.63
175	5.7	****	****	2.98	2.10	1.72	1.50	1.34	1.22	1.12	1.04	0.98	0.93	0.88	0.83	0.80	0.77	0.75	0.73	0.70	0.68	0.66	0.64	.62
180	5.6	****	****	3.43	2.21	1.77	1.52	1.35	1.23	1.13	1.05	0.98	0.93	0.88	0.83	0.80	0.77	0.75	0.73	0.70	0.68	0.66	0.64	.62
185	5.4	****	****	4.32	2.33	1.83	1.55	1.37	1.24	1.14	1.06	0.99	0.93	0.88	0.83	0.80	0.77	0.75	0.73	0.70	0.68	0.66	0.64	.62
190	5.3	****	****	****	2.49	1.89	1.58	1.39	1.25	1.15	1.06	0.99	0.93	0.88	0.83	0.80	0.77	0.75	0.73	0.70	0.68	0.66	0.64	.62
195	5.1	****	****	****	2.68	1.95	1.62	1.41	1.26	1.15	1.06	0.99	0.93	0.88	0.83	0.80	0.77	0.75	0.73	0.70	0.68	0.66	0.64	.62
200	5.0	****	****	****	2.93	2.02	1.65	1.43	1.27	1.16	1.07	0.99	0.93	0.88	0.83	0.80	0.77	0.75	0.73	0.70	0.68	0.66	0.64	.62
205	4.9	****	****	****	3.29	2.10	1.68	1.44	1.28	1.16	1.07	1.00	0.93	0.88	0.83	0.80	0.77	0.75	0.73	0.70	0.68	0.66	0.64	.62
210	4.8	****	****	****	3.89	2.19	1.72	1.46	1.29	1.17	1.07	1.00	0.93	0.88	0.83	0.80	0.77	0.75	0.73	0.70	0.68	0.66	0.64	.62
215	4.7	****	****	****	5.36	2.29	1.76	1.48	1.30	1.18	1.08	1.00	0.93	0.88	0.83	0.80	0.77	0.75	0.73	0.70	0.68	0.66	0.64	.62
220	4.5	****	****	****	****	2.42	1.80	1.50	1.31	1.18	1.08	1.00	0.93	0.88	0.83	0.80	0.77	0.75	0.73	0.70	0.68	0.66	0.64	.62
225	4.4	****	****	****	****	2.56	1.85	1.52	1.32	1.19	1.08	1.00	0.93	0.87	0.83	0.80	0.77	0.75	0.73	0.70	0.68	0.66	0.64	.61
230	4.3	****	****	****	****	2.74	1.90	1.55	1.34	1.19	1.08	1.00	0.93	0.87	0.83	0.80	0.77	0.75	0.73	0.70	0.68	0.66	0.64	.61
235	4.3	****	****	****	****	2.98	1.95	1.57	1.35	1.20	1.09	1.00	0.93	0.87	0.83	0.80	0.77	0.75	0.73	0.70	0.68	0.66	0.64	.61
240	4.2	****	****	****	****	3.29	2.01	1.59	1.36	1.20	1.09	1.00	0.93	0.87	0.83	0.80	0.77	0.75	0.73	0.70	0.68	0.66	0.64	.61
245	4.1	****	****	****	****	3.78	2.07	1.62	1.37	1.21	1.09	1.00	0.93	0.87	0.83	0.80	0.77	0.75	0.73	0.70	0.68	0.66	0.64	.61
250	4.0	****	****	****	****	****	2.07	1.62	1.37	1.21	1.09	1.00	0.93	0.87	0.83	0.80	0.77	0.75	0.73	0.70	0.68	0.66	0.64	.61



TABLE 15i. Wave height amplification  $T$  (Eq. 3) for  $d = 20$  m,  $\theta_0 = 60^\circ$ .

F	T	D	THETAO	DO	UNO	CURRENT SPEED																
						-2.50	-2.00	-1.75	-1.50	-1.25	-1.00	-.75	-.50	-.25	0.00	.25	.50	.75	1.00	1.25	1.50	1.75
050	20.0	1.13	1.10	1.08	1.05	1.03	1.01	.99	.97	.95	.93	.91	.90	.88	.87	.85	.84	.83	.82	.81	.79	.78
055	18.2	1.12	1.09	1.06	1.04	1.01	.99	.97	.95	.93	.91	.90	.88	.86	.85	.84	.82	.81	.80	.79	.78	.77
060	16.7	1.11	1.08	1.05	1.02	1.00	.98	.95	.93	.91	.90	.88	.86	.85	.83	.82	.81	.79	.78	.77	.76	.75
065	15.4	1.10	1.07	1.04	1.01	.98	.96	.94	.92	.90	.88	.86	.84	.83	.81	.80	.78	.76	.75	.74	.73	.73
070	14.3	1.09	1.06	1.03	1.00	.97	.94	.92	.90	.88	.86	.84	.83	.81	.80	.78	.77	.75	.74	.73	.72	.72
075	13.3	1.09	1.05	1.01	.98	.96	.93	.91	.88	.86	.84	.83	.81	.80	.78	.77	.75	.74	.73	.72	.71	.70
080	12.5	1.09	1.04	1.01	.97	.94	.92	.89	.87	.85	.83	.81	.80	.78	.77	.75	.74	.73	.72	.70	.69	.68
085	11.8	1.09	1.04	1.00	.97	.94	.91	.88	.86	.84	.82	.80	.78	.77	.75	.74	.73	.71	.70	.69	.68	.67
090	11.1	1.10	1.05	1.00	.96	.93	.90	.87	.85	.83	.81	.79	.77	.76	.74	.73	.72	.70	.69	.68	.67	.66
095	10.5	1.11	1.06	1.01	.97	.93	.90	.87	.84	.82	.80	.78	.77	.75	.73	.72	.71	.70	.68	.67	.66	.65
100	10.0	1.14	1.07	1.02	.97	.93	.90	.87	.84	.82	.80	.78	.76	.75	.73	.72	.70	.69	.68	.67	.66	.65
105	9.5	1.17	1.10	1.03	.98	.94	.91	.88	.85	.82	.80	.78	.76	.75	.73	.72	.70	.69	.68	.67	.66	.65
110	9.1	1.22	1.13	1.06	1.00	.96	.92	.88	.85	.83	.81	.79	.77	.75	.73	.72	.71	.69	.68	.67	.66	.65
115	8.7	1.27	1.17	1.09	1.03	.97	.93	.89	.87	.84	.81	.79	.77	.76	.74	.73	.71	.70	.69	.68	.67	.66
120	8.3	1.34	1.22	1.12	1.05	1.00	.95	.91	.88	.85	.83	.80	.78	.77	.75	.73	.72	.71	.70	.68	.67	.66
125	8.0	1.43	1.27	1.16	1.08	1.02	.97	.93	.89	.87	.84	.82	.80	.78	.76	.74	.73	.72	.70	.69	.68	.67
130	7.7	1.54	1.34	1.21	1.12	1.05	.99	.95	.91	.88	.85	.83	.81	.79	.77	.76	.74	.73	.72	.70	.69	.68
135	7.4	1.66	1.41	1.26	1.16	1.08	1.02	.97	.93	.90	.87	.85	.82	.80	.79	.77	.75	.74	.73	.71	.70	.69
140	7.1	1.82	1.50	1.32	1.20	1.11	1.05	.99	.95	.92	.89	.86	.84	.82	.80	.78	.76	.75	.74	.72	.71	.70
145	6.9	2.03	1.60	1.38	1.24	1.14	1.07	1.02	.97	.93	.90	.88	.85	.83	.81	.79	.77	.75	.74	.72	.71	.70
150	6.7	2.33	1.71	1.44	1.28	1.18	1.10	1.04	.99	.95	.92	.89	.87	.85	.83	.81	.79	.77	.76	.74	.73	.72
155	6.5	2.90	1.84	1.51	1.33	1.21	1.12	1.06	1.01	.97	.94	.91	.88	.86	.84	.82	.80	.79	.77	.75	.74	.72
160	6.3	7.13	2.01	1.58	1.37	1.24	1.15	1.08	1.03	.99	.95	.92	.90	.88	.86	.84	.82	.80	.78	.76	.75	.73
165	6.1	****	2.24	1.66	1.42	1.27	1.17	1.10	1.04	1.00	.96	.93	.91	.88	.86	.84	.82	.80	.78	.76	.75	.73
170	5.9	****	2.63	1.76	1.46	1.30	1.19	1.12	1.06	1.01	.98	.95	.92	.89	.87	.85	.83	.81	.79	.77	.75	.74
175	5.7	****	****	1.87	1.51	1.33	1.21	1.13	1.07	1.03	.99	.96	.93	.90	.88	.86	.84	.81	.79	.78	.76	.74
180	5.6	****	****	2.02	1.57	1.36	1.23	1.15	1.08	1.04	1.00	.96	.94	.91	.89	.86	.84	.82	.80	.78	.76	.74
185	5.4	****	****	2.22	1.63	1.39	1.25	1.16	1.10	1.05	1.01	.97	.94	.92	.89	.87	.84	.82	.80	.78	.76	.74
190	5.3	****	****	2.52	1.70	1.42	1.27	1.17	1.10	1.05	1.01	.98	.95	.92	.89	.87	.85	.82	.80	.78	.76	.74
195	5.1	****	****	3.11	1.78	1.45	1.29	1.18	1.11	1.06	1.02	.98	.95	.92	.89	.87	.85	.82	.80	.78	.75	.73
200	5.0	****	****	7.13	1.88	1.49	1.31	1.20	1.12	1.07	1.02	.99	.96	.93	.90	.87	.85	.82	.80	.77	.75	.73
205	4.9	****	****	****	2.00	1.53	1.32	1.21	1.13	1.07	1.03	.99	.96	.93	.90	.87	.85	.82	.80	.77	.75	.73
210	4.8	****	****	****	2.16	1.57	1.34	1.22	1.13	1.07	1.03	.99	.96	.93	.90	.87	.85	.82	.80	.77	.75	.72
215	4.7	****	****	****	2.39	1.62	1.36	1.23	1.14	1.08	1.03	.99	.96	.93	.90	.87	.84	.82	.79	.77	.74	.72
220	4.5	****	****	****	2.76	1.68	1.39	1.24	1.15	1.09	1.03	.99	.96	.93	.90	.87	.84	.81	.79	.76	.74	.72
225	4.4	****	****	****	****	1.74	1.41	1.25	1.15	1.09	1.04	1.00	.96	.93	.90	.87	.84	.81	.78	.76	.73	.71
230	4.3	****	****	****	****	1.82	1.43	1.26	1.16	1.09	1.04	1.00	.96	.93	.90	.87	.84	.81	.78	.75	.73	.71
235	4.3	****	****	****	****	1.91	1.46	1.27	1.16	1.09	1.04	1.00	.96	.93	.90	.87	.84	.81	.78	.75	.73	.70
240	4.2	****	****	****	****	2.02	1.49	1.28	1.17	1.09	1.04	1.00	.96	.93	.90	.86	.83	.80	.77	.75	.72	.70
245	4.1	****	****	****	****	2.16	1.52	1.30	1.17	1.10	1.04	1.00	.96	.93	.89	.86	.83	.80	.77	.74	.72	.69
250	4.0	****	****	****	****	2.35	1.56	1.31	1.18	1.10	1.04	1.00	.96	.93	.89	.86	.83	.80	.77	.74	.71	.69

case that a linear extrapolation from measured wave heights upriver leads to a wave height at Buoy 8 which exceeds the empirical breaking criteria of (2). If we presume the waves are limited by breaking then the wave height could be the lower value in this table entry, and the "observed" height would exceed the predicted by 20%. It appears that the ebb of 11 September falls into the category of an "extreme event" such as that observed previously at the Columbia River Entrance on 18 October 1979 by Gonzalez (1984) and for which the simple one-dimensional theory fails to predict accurately. For the rest of the October 1979 observations Gonzalez found generally good agreement between theory and observation.

If for the moment we assume that the one-dimensional, linear theory is applicable and that the current at Buoy 46010 is zero, then there are three variables in Eq. (3) which should be examined in search of some significant difference which characterizes the 11 September ebb relative to the other cases. These are the current speed  $U$ , the wave frequency  $\omega = \sigma_0$ , and the incident wave direction  $\theta_0$ . From Table 14, we see that the estimated surface currents were comparable for each peak ebb, ranging from 2.0 to 2.3 m/s. Figure 9e also shows that the peak frequency of the wave spectrum gradually increased from a low of 0.07 Hz on the ebb of 11 September to a value of 0.09 Hz on the ebb of 13 September. This frequency shift is the characteristic signature of dispersive waves detected at a distant point after propagating from a localized source. An examination of the weather maps of Figure 8 suggests that the source was the well-defined fetch region in the south-to-southwest sector of the low pressure system dominating the central Gulf of Alaska on 10 September (Fig. 8c). An important implication of this is that the direction of swell incident on the Columbia River entrance was approximately constant for the last three ebbs observed over the period 11 to 13 September. It thus appears that both current speed and incident wave direction were comparable on the last three ebbs, but that there was a significant difference in wave frequency. However Table 15d, say, for  $0^\circ$  incidence indicates that this frequency difference is not enough to account for an inferred amplification of 1.8 from offshore to Buoy 8.

Although less relevant for the sole prediction of hazardous waves, a better test for the linear, one-dimensional theory is to compare observed and predicted wave heights at flood tides since nonlinear effects will be minimized due to reduced wave heights. Column 9 of Table 14 shows that the observed values are consistently lower than the predicted ones for flood conditions. In one case their ratio is 0.6, but this was for one peak of a two-peaked deep-water spectrum observed at 46010 (Fig. A44). At Buoy 8, three peaks were observed (Fig. A40); hence some uncertainty is associated with the interpretation of this case.

The most likely reason why the simple theory fails to the extent it does is due to two-dimensional effects. It is clear that within the entrance the bathymetry varies markedly in a north-south direction, going from a dredged channel to a shoal, to a jetty, to another shoal, to coastwise-parallel bottom contours. The currents must also vary laterally especially outside the entrance. On ebb the current most likely takes the form of a confined jet with marked lateral shear at its edges. On flood it is probably more like a sink flow at the edge of a long, straight boundary with streamlines converging from a wider fan-shaped region. SLAR imagery on the slack-to-ebb of 11 September (Fig. A28) shows more or less straight

and parallel swell crests across the entrance. In contrast, 3 hours later at peak ebb current (Fig. A35) the wave crests are strongly curved, and the distinctive grid pattern of crossed waves is now apparent. Two-dimensional effects would explain why the wave heights are consistently overpredicted on floods since wave ray divergence, not accounted for by the theory would lead to lower actual wave heights. The converse - that the theory should underpredict wave heights on ebbs - need not be true. Bathymetric refraction over the deeper channel could mitigate the effects of wave focussing due to currents. For the first two ebbs wave heights were overpredicted while SLAR imagery showed little wave crossing. For the next two ebbs the wave heights were underpredicted when wave crossing was observed.

If wave crossing is known to occur then a rough correction to the predicted transfer function can be made by assuming that, although the offshore energy  $E_o$  remains constant, the energy  $E$  on the bar is double that predicted without wave crossing as if two independent wave systems were present. Thus, from Eq. (3),  $T' = \left(\frac{2E}{E_o}\right)^{\frac{1}{2}} = \sqrt{2}T$ , where  $T'$  implies two-dimensional refraction severe enough to induce crossing wave crests. If this correction is applied to the entries for 11 September in Table 14, we then obtain  $T'_c(\theta = 0^\circ) = 2.1$  and  $T'_c(\theta = 30^\circ) = 2.0$ . The entries of column 9 become

$$T_o/T'_c(\theta = 0^\circ) = 0.9 \text{ to } 1.0 \quad \text{and}$$

$T_o/T'_c(\theta = 30^\circ) = 0.9 \text{ to } 1.1$ , so that the agreement between observed and predicted wave height amplification is thereby improved. The difficulty with this method is we still have to predict when wave crossing will occur. This is probably best done with a proper two-dimensional theory; one for which the calculation just completed will be accounted for automatically.

On the basis of this result, let us assume that two-dimensional wave refraction and focusing by a current with jet-like lateral shear can be an important mechanism for wave height amplification on the Columbia River Bar. We have in mind here a physical setting similar to the wave/rip-current interaction problem examined by Arthur (1950), in which wave rays initially parallel to the main axis of a jet-like current were sufficiently refracted to induce crossing farther upstream. We should then ask what set of parameters might control the magnitude of this effect on any particular ebb. These include: (1) the incident wave frequency,  $f$ , (2) the relative angle between the incident wave and the main axis of the current,  $\theta_o$ , and (3) the two-dimensional distribution of current shear at peak ebb.

The question is: Were any of these factors significantly different on the ebb of 11 September, such that wave refraction and focusing was intensified to the point that two-dimensional effects became important and the simple one-dimensional theory of Eq. (1) therefore failed?

For a given incidence angle and current shear, two-dimensional convergence should be greater for higher frequency waves, since wave group velocity decreases with increasing frequency and the ratio  $U/C_g$  thereby



increases, indicating the current U is more effective in inducing refraction. Since peak wave frequency increased from 0.07 Hz on 11 September to 0.09 Hz on 13 September, this effect would have made two-dimensional refraction more important on the ebbs of 12 and 13 September. However, this may have been offset by a relative wave/current incidence angle  $\theta_0$  which was closer to  $0^\circ$  on 11 September than on 12 and 13 September. This is because bathymetric effects are frequency dependent, and the crests of lower frequency waves tend to become aligned with bathymetry faster than higher frequency waves. Since the set of the current at the river entrance is more or less perpendicular to the depth contours offshore, this suggests that the waves on 11 September were more nearly in direct opposition to the current, thereby increasing the importance of two-dimensional wave refraction effects.

Later analyses of the SLAR data will yield wave direction estimates directly. However, we can make a rough estimate now of the frequency-dependent bathymetric effects on the incident wave direction at buoy 46010 by using Eqs. (4) and (5). As noted above, all swell arriving at the Columbia River entrance during the period 11 to 13 September appear to have been generated in the same well-defined fetch area evident in Figure 8c. If we assume for simplicity that waves arrived from the northwest and were incident on a region with parallel bathymetric contours oriented north-south, then  $\theta_0$  in Eq. (5) is  $45^\circ$  and we can combine (4) and (5) to get

$$\theta(f) \cong \sin^{-1}(\sin\theta_0 \tanh kd)$$

where k satisfies the second relation in (4) and  $d = 60$  m at buoy 46010. Using the observed peak frequency values on 11 and 13 September, we obtain

$$\Delta\theta \cong \theta(0.09 \text{ Hz}) - \theta(0.07 \text{ Hz}) \cong 43.1^\circ - 38.2^\circ \cong 4.9^\circ$$

as an estimate of the change in incident wave direction from ebb to ebb.

Although wave ray convergence may be quite sensitive to incident wave direction, it seems unlikely that a 5 degree difference in wave direction induced by bathymetry would produce the dramatic differences in observed wave height amplification. Judgement on this factor must thus await the analysis of the SLAR imagery for incident wave direction.

We must also consider the possibility that the surface current properties changed significantly from ebb to ebb. The direction of the main axis of the current and the degree of lateral shear might be influenced by the stage of the spring/neap tidal cycle, the amount of fresh water discharge, the wind induced surface drift, and the magnitude and direction of alongshore currents (either large-scale, seasonal, geostrophic phenomena, or local, short-term wind-induced effects).

Unfortunately, there is very little current drifter data available with which to assess these possibilities. Figure 14 displays selected current vectors corresponding to drifter tracks which were obtained near the time of each peak ebb. (The drifter information and current computations are summarized in Table 13.) The data sparseness is painfully evident, and few conclusions could be drawn. Mean direction is approximately the same on 11, 12, and 13 September. Jet-like lateral shear is evident on

11 September, but the data are insufficient to draw conclusions on the presence or absence of similar shear structure on the other ebbs. Furthermore, the persistence of such structure downstream of these observations and in the region outside the entrance is unknown.

Nonlinear effects may play a role in the crossing wave patterns observed at the Columbia River entrance as, for example, in the SLAR imagery on 11 September (Fig. A35). In a series of wave tank experiments Su (1982) has documented the evolution of similar patterns in steep, deep water wavetrains through a process governed by nonlinear skew bifurcation. The initial steepness of these waves was in the range  $0.16 \leq ak \leq 0.18$ . Using Eq. (4) with  $U = -2.0$  m/s,  $\omega = 2\pi(.07)$  s<sup>-1</sup> and  $d = 15$  m, we obtain  $k = 0.048$ . For  $a \cong 6.5/2$  m = 3.3 m we then have an estimate of  $ak \cong 0.16$  for the wave steepness on 11 September. Su's experiments do not include the effects of currents or finite depth, but it is conceivable that these could induce similar instabilities. Column 10 of Table 14 gives steepness estimates for all the cases we observed, and there does seem to be a correlation between estimated wave steepness and the presence of the grid-like pattern in the SLAR imagery. Thus, on 10 September ( $ak \sim 0.07$ ) the pattern is not clearly evident (Figs. A18 and A19), on 13 September ( $ak \sim 0.10$ ) the pattern is not clearly evident (Figs. A80 and A81), on 12 September ( $ak \sim 0.14$ ) the pattern exists but somewhat indistinctly (Figs. A56 and A57), and on 11 September ( $ak \sim 0.16$ ) the pattern is very distinct (Figs. A35 and A36). However, we feel that wave-current-bathymetry interaction, a zero-order effect, is the primary cause of wave amplification/attenuation at the Columbia River entrance. It is this effect that leads primarily to the steep waves and ultimately to wave crossing during extreme ebb events.

## 5. SUMMARY AND CONCLUSIONS

Waves and currents have been observed with a unique mixture of instruments at the Columbia River entrance during the period 10-13 September 1981. Offshore wave spectra were calculated by NDBC Buoy 46010. Bar wave records were measured by a Waverider tethered in strong currents, and SLAR imagery gives a two-dimensional picture of the swell both offshore and in the entrance. The technique of tracking surface drifters at short range with a portable radar set rather than a large, fixed system was successful.

Navigational Buoy 8 in the river entrance is the approximate boundary between two wave regimes. Upriver of this site waves decay on both ebb and flood tides. This is probably due to depth refraction away from the main channel axis toward the shoals on either side. Surprisingly, ebbs give a larger decay rate perhaps because of a decrease in current speed as one moves upriver away from the converging jetty tips. Another possibility is that the enhanced attenuation rate is due to wave breaking induced by the strong adverse current. Sporadic breaking was observed visually and on SLAR images.

Seaward of Buoy 8 waves amplify during peak ebbs and attenuate during peak floods thus confirming the important effect of the current. With the current specified, linear, one-dimensional theory can predict wave heights to within 20% of observed values most of the time. Heights were consistently overpredicted during flood tides while no consistent bias was observed during ebbs. This is most likely due to two-dimensional effects.

During an extreme wave event on 11 September the waves were underpredicted by 50% on ebb. These were the highest and steepest waves observed during the experiment and were breaking sporadically. SLAR images indicate that wave crests were crossing due to current refraction. An approximate calculation suggests that the wave-height prediction should be increased by a factor of  $\sqrt{2}$  which would bring it closer to that observed. For better wave predictions a two-dimensional theory which automatically accounts for this factor should be applied.

It must be cautioned that strong ebb currents of up to 3.5 m/sec can occur at the Columbia River entrance. Such currents, not encountered during this experimental period, can actually stop typical deep ocean swell, causing them to break for almost any initial, deep-water steepness. The linear, one-dimensional theory applied here becomes inappropriate near that limit, and we expect that prediction and observation will diverge radically.

## 6. RECOMMENDATIONS FOR FURTHER RESEARCH

There is a clear need for a systematic effort to improve operational capabilities to monitor, nowcast, and forecast hazardous navigational conditions at coastal tidal inlets of which the Columbia River entrance is an example. This effort should concentrate on:

- (1) real-time, long-term monitoring,
- (2) theory and numerical modeling, and
- (3) field experiments.

### 6.1 Real-time, Long-term Monitoring

The essential parameters to be measured are:

- (1) nondirectional wave spectra at the inlet entrance, and
- (2) directional wave spectra offshore.

The technology to attempt these measurements is available now. Timpe (1983) has described the successful use of 6-meter long, boat-shaped Navy Oceanographic Meteorological Automatic Device (NOMAD) buoys in very severe environments, and such a system may be well-suited for service at coastal inlets. It is recommended that a buoy of this type be deployed on the Columbia River Bar.

Also, NDBC has developed directional wave data analyzers (DWDA) (Steele, 1983). A successful deployment was recently accomplished aboard a 10-meter discus hull off the California Coast (Steele, 1984). Such a system would provide valuable directional wave data which can be used in conjunction with equation (3) to predict wave height as a function of deep water wave direction.

Benefits from such a monitoring system are as follows:

(1) Accurate nowcasts would be available. Such real-time information on inlet conditions is valuable to mariners. A decision to attempt a bar crossing could then be based on measurements, rather than on visual observations which may be unreliable and are not available during fog and darkness.

(2) Short-term forecasts would be improved. Influence of short-term meteorological or other local effects resulting in under or over forecast of wave height would be apparent to the forecaster and could be adjusted for.

(3) Forecasts could be verified. At present, there is no way to test the accuracy of bar forecasts.

(4) The intuition of forecasters and local mariners would be improved as measurements provide "corrective feed-back" to judgements regarding future wave height on the bar.

(5) A data base would be available for research.

## 6.2 Theory and Numerical Modeling

We have demonstrated at the Columbia River that two-dimensional effects should be accounted for if Bar forecasts are to be improved. Jet-like ebb currents contribute to unusually large waves on the Bar. The dynamics of tidal jets should be investigated and modeled. A similarity solution with a few parameters such as jet half-width and centerline velocity is one approach (Özsoy and Unlüata, 1982).

If the surface current field can be so specified, then along with efforts to better define the surface current field, recent analytical and numerical techniques for computing the wave field should be investigated. Liu (1983) has re-examined the wave/rip current problem studied by Arthur (1950), and has derived a mild-slope equation which includes currents. This, combined with a parabolic approximation, leads to a computationally efficient solution. The significant advantage of this approach is that, unlike wave-ray computations, the wave field is computed everywhere including where caustics arise and ray theory fails.

This research will result in products to guide forecasters, such as tables, charts, nomograms, and computer algorithms.

## 6.3 Field Experiments

This experiment has provided a valuable data set for the study of wave-current interaction. However it has several deficiencies. First, due to hazardous conditions, only limited observations were made at Buoy 8. Second, surface drifter measurements were not dense enough in space and time to give good current estimates, nor were they available seaward of Buoy 8. Third, while SLAR imagery can provide excellent information on long swell, the resolution of the radar is too coarse to yield similar data on shorter, locally generated wind waves, which are an important consideration as a navigational hazard.

A comprehensive field experiment must therefore measure, as a minimum,

- (1) nondirectional wave spectra on the Bar, near Buoy 8,
- (2) directional wave spectra offshore
- (3) surface current fields in the entrance and offshore.

In addition, these observations should be supplemented by SLAR overflights to map out the two-dimensional wave field and by vertical salinity and temperature profiles to determine the density structure which may play a role in the dynamics of the surface current especially during freshets.

Item (1) and (2), above, could be provided by the wave measurement technology mentioned earlier. Item (3) might be provided by a remote sensing technique such as the Coastal Ocean Dynamics Applications Radar (CODAR) developed by the NOAA/ERL Wave Propagation Laboratory (Barrick and Lipa, 1979; Holbrook and Frisch, 1981). Ideally, an experiment would be at least a month long, and coincident wave/current observations could be made at each peak ebb and at intervals of 1 to 3 hours between peak ebbs. A winter experiment and summer experiment would be desirable, since seasonal extremes in offshore wave energy and in fresh water runoff occur.

## 7. REFERENCES

- Arthur, R. S., (1950): Refraction of shallow water waves: the combined effect of currents and underwater topography. *Transactions, American Geophysical Union*, 31, 4, 549-552.
- Battjes, J.A. (1982): A case study of wave height variations due to currents in a tidal entrance. *Coastal Engineering*, 6, 47-57.
- Barrick, D. E., and B. J. Lipa (1979): Ocean surface features observed by HF coastal ground-wave radars: a progress review. In: *Ocean Wave Climate*, M.D. Earle and A. Malahoff (eds.), Plenum Press, New York, 129-152.
- Enfield, D. (1973): Prediction of Hazardous Columbia River Bar Conditions. Final Report, Dept. of Commerce Contract I-35356, 204 pp.
- Gonzalez, F. I. (1984): A case study of wave-current-bathymetry interactions at the Columbia River entrance. *J. Phys. Ocean.* (in press).
- Gonzalez, F. I., and C. L. Rosenfeld (1984): SLAR and *in-situ* observations of ocean swell modification due to currents and bathymetry at the Columbia River entrance. *IEEE Trans. Geosc. and Remote Sensing* (in review).
- Holbrook, J. R., and A. S. Frisch (1981): A comparison of near-surface CODAR and VACM measurements in the Strait of Juan de Fuca, August 1978. *J. Geophys. Res.*, 86, 10908-10912.
- Liu, P. L-F. (1983): Wave-current interactions on a slowly varying topography. *J. Geophys. Res.*, 88, 4421-4426.
- Mattie, M. G., and D. L. Harris (1979): A System for Using Radar to Record Wave Direction. U.S. Army Corps of Engineers Coastal Engineering Research Center Technical Report No. 79-1, 50 pp.
- Miche, R. (1944): Mouvements ondulatoires des mers en profondeur constante ou décroissante. *Ann. des Ponts et Chaussées*, pp. 25-78, 131-164, 270-292, 369-406.
- Mulhern, R. M. (1982): Current measurements in the Columbia River estuary. Dept. of Civil Engineering, University of Washington, Masters Report, 60 pp.
- Özsoy, E. and U. Unluata (1982): Ebb-tidal flow characteristics near inlets. *Estuarine, Coastal and Shelf Science*, 14, 251-263.
- Phillips, O.M. (1977): *Dynamics of the Upper Ocean*, Second edition, Cambridge University Press, Cambridge, 336 pp.
- Rosenfeld, C. L., and J. W. Bell (1978): Monitoring Ocean Wave Refraction Utilizing Side-Looking Airborne Radar. Presented at APCG 1978, Portland, Oregon.

Steele, K. E. and M. D. Earle (1979): The Status of Data Produced by NDBO Wave Data Analyzer (WDA) Systems. In: *Proceeding of the Oceans '79 Conference*, 212-220.

Steele, K. E. (1983): NDBC wave measurement activities and plans. In: *Proceedings 1983 Symposium on Buoy Technology*, Marine Technology Society, 182-188.

Steele, K. E. (1984): Personal communication.

Su, M.-Y., (1982): Three-dimensional deep-water waves. Part 1. Experimental measurement of skew and symmetric wave patterns, *J. Fluid Mech.*, 124, 73-108.

Timpe, G. L. (1983): The use of NOMAD hulls as severe environment buoys. In: *Proceedings 1983 Symposium on Buoy Technology*, Marine Technology Society, 72-78.





APPENDIX

Intensive Observation Periods

DATA SUMMARY



## APPENDIX

### Data for Individual Intensive Observations Periods

In this appendix, we present the data collected during each individual intensive observation period. The data is grouped by observation period and consists of:

1. The Waverider (EGRET) positions, as plotted from the log.
2. Waverider Spectral estimates and time series.
3. NDBC 46010 Spectral estimates.
4. The Cape Disappointment surface drifter tracks, as plotted from the log.
5. The Jetty A surface drifter tracks, as plotted from the log.
6. Large scale print of the SLAR image judged to be the best of those collected during the observation period.
7. Small scale print of the SLAR image judged to be the best of those collected during the observation period.
8. The Waverider (Surface Vessel EGRET) log.
9. The Cape Disappointment radar log.
10. The Jetty A radar log.

In the logs of the EGRET, the following conventions have been used. Entries for vessel position through sextant fixes have the format

Sextant Fixes	Objects
Left angle	Left object
	Center object
Right angle	Right object
Left or right check angle (L√ or R√)	Left or right check object (L√ or R√)

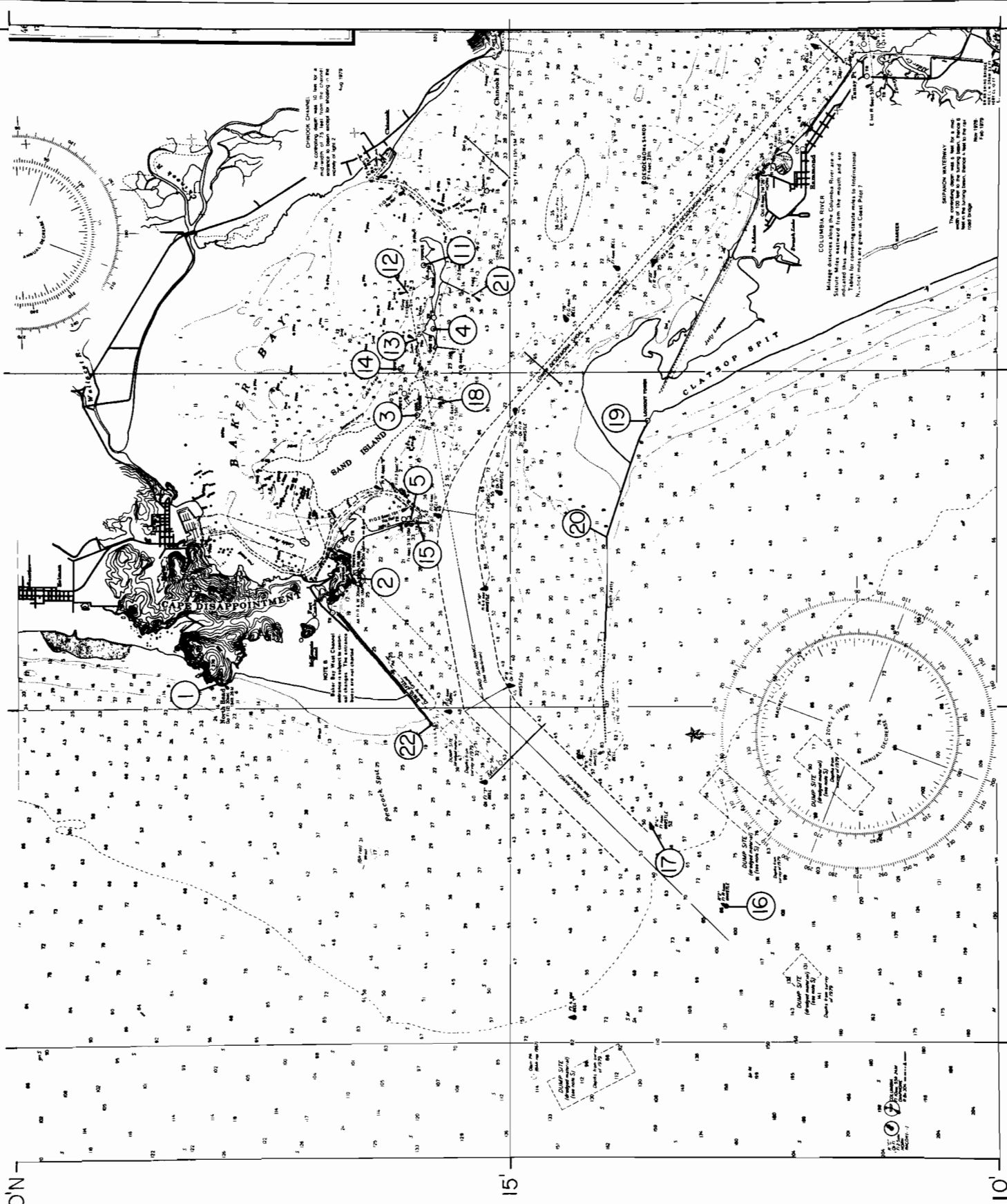
All angles are measured left or right from the center object. The identification of all landmark objects was confirmed by check angles on independent objects. Table A1 lists the description given for each landmark object on the 1981 NOS chart 18521, shown in Figure A0.

In the Remarks column, the notations UW and WR imply "underway" and "Waverider." "Drift log" entries refer to current speed estimates obtained by timing the drift of a small floater to the end of a 25 meter tether. Entries for ships heading are magnetic, referred to the compass on the EGRET, without correction for variation or deviation unless stated otherwise. From comparison of the compass with known directions, it appeared that deviation values were minimal and within the precision with which the

compass could be read (about 10 degrees). The magnetic variation is listed on the 1981 NOS chart 18521 as 20°30' East.

Range and bearing corrections determined from radar fixes on the landmarks have not been applied to the drifter tracks. Neither have the tracks from two independent radar systems been corrected to coincide with one another. These corrections will be made in later analyses.

46°20'N



10' 05' 124°00'W 55'

Figure A0. A portion of NOS chart 18521, showing Table A1 landmark locations.

TABLE A1. Description of sextant fix objects as given by 1981 NOS Chart 18521.

<u>Object Number</u>	<u>Description</u>
1	North Head Gp Fl(2) 30 sec 194 ft 26M
2	Alt Fl R & W 30 sec 220 ft 18M
3	OBS. TOWER
4	OBS. TOWER
5	Fl 4 sec 31 ft 10M
11	TOWER
12	E Int 6 sec 61 ft
13	Qk Fl
14	TOWER
15	TR
16	R "2" Fl R 4 sec WHISTLE (Buoy 2)
17	R "4" Fl 4 sec WHISTLE (Buoy 4)
18	Light on S. tip of large Sand Island, "Fl G 4 sec. 15 ft. '1'"
19	Clatsop Spit "Lookout Tower"
20	E side of bend in South Jetty
21	Light on S. tip of line of piles on central S. Side of small Sand Island, "Fl 4 sec '5'"
22	Seaward end of N. Jetty

10 September 1981

FLOOD





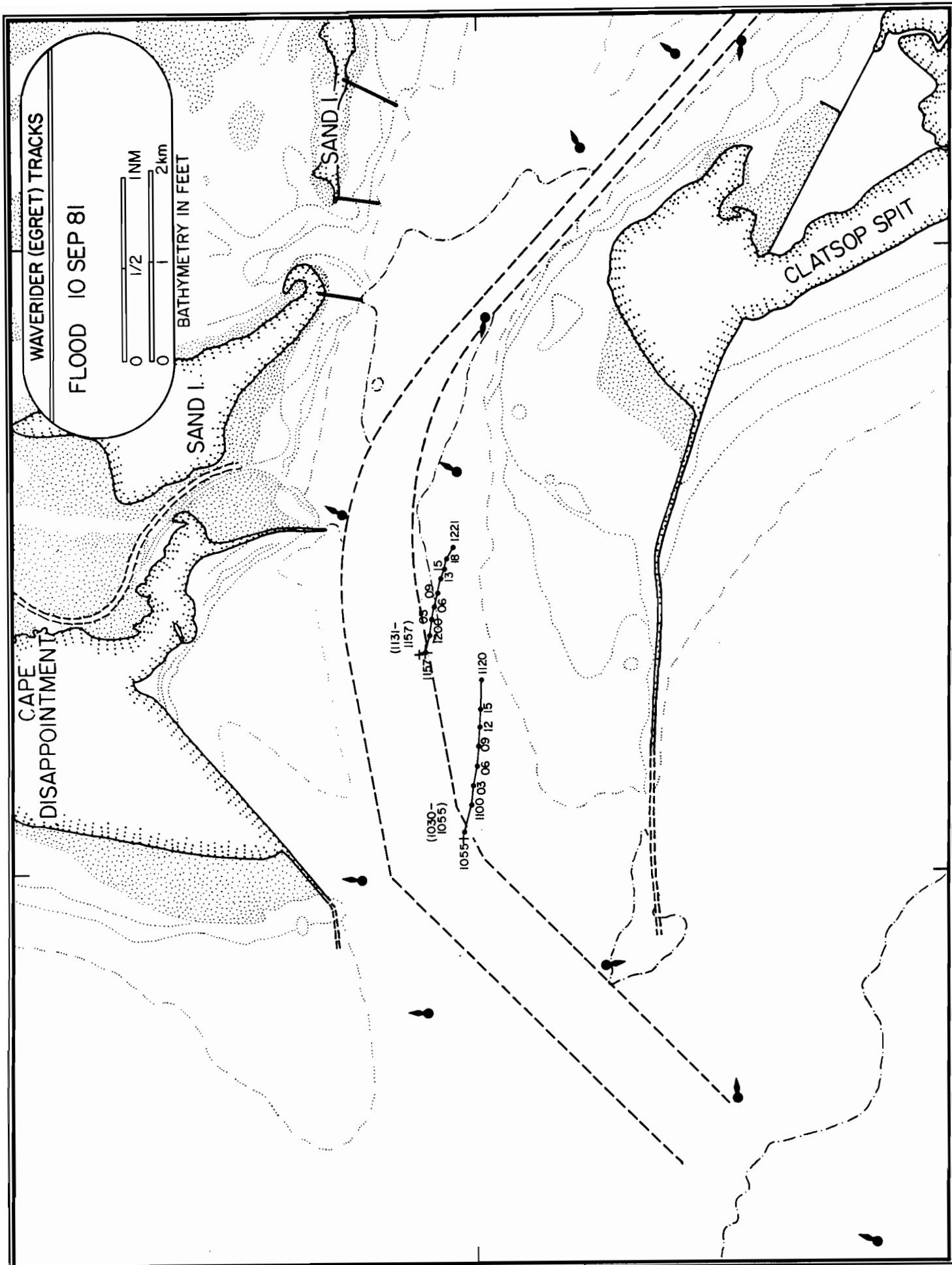


Figure A1. Waverider (EGRET) tracks for flood period of 10 Sept. 1981.

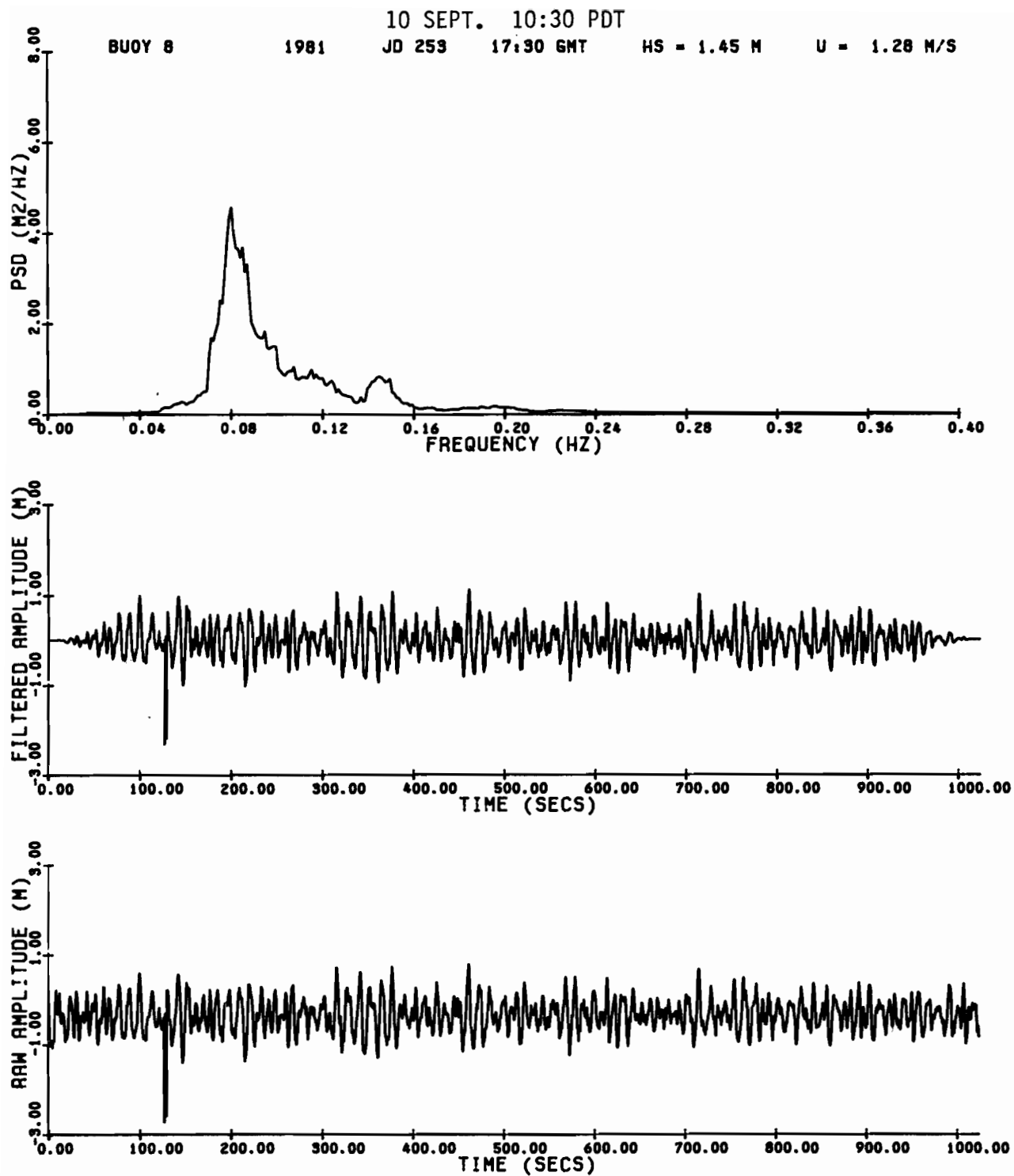


Figure A2. Waverider raw amplitude, filtered amplitude, and power spectral density for 1030 PDT, 10 Sept. 1981.

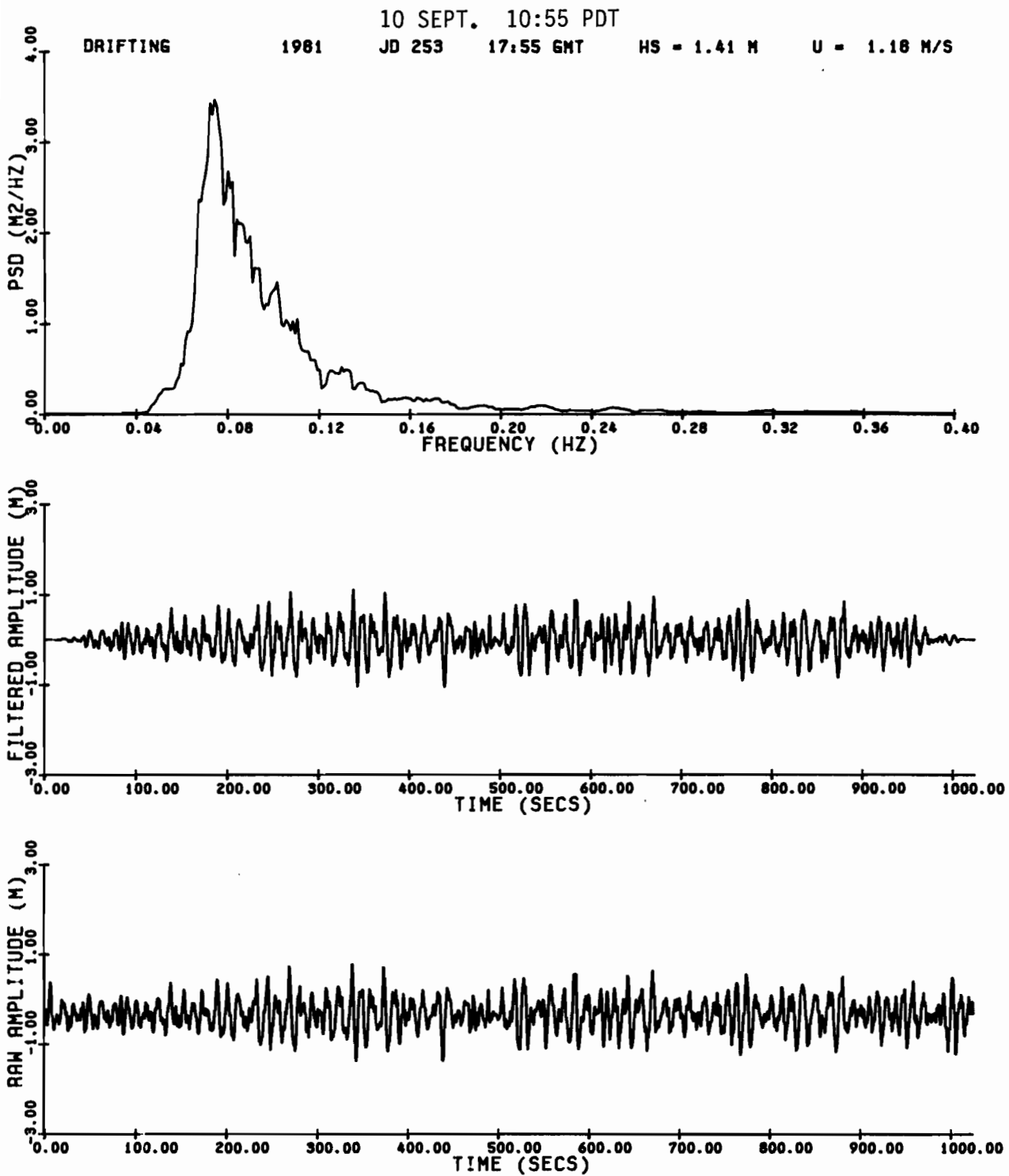


Figure A3. Waverider raw amplitude, filtered amplitude, and power spectral density for 1055 PDT, 10 Sept. 1981.

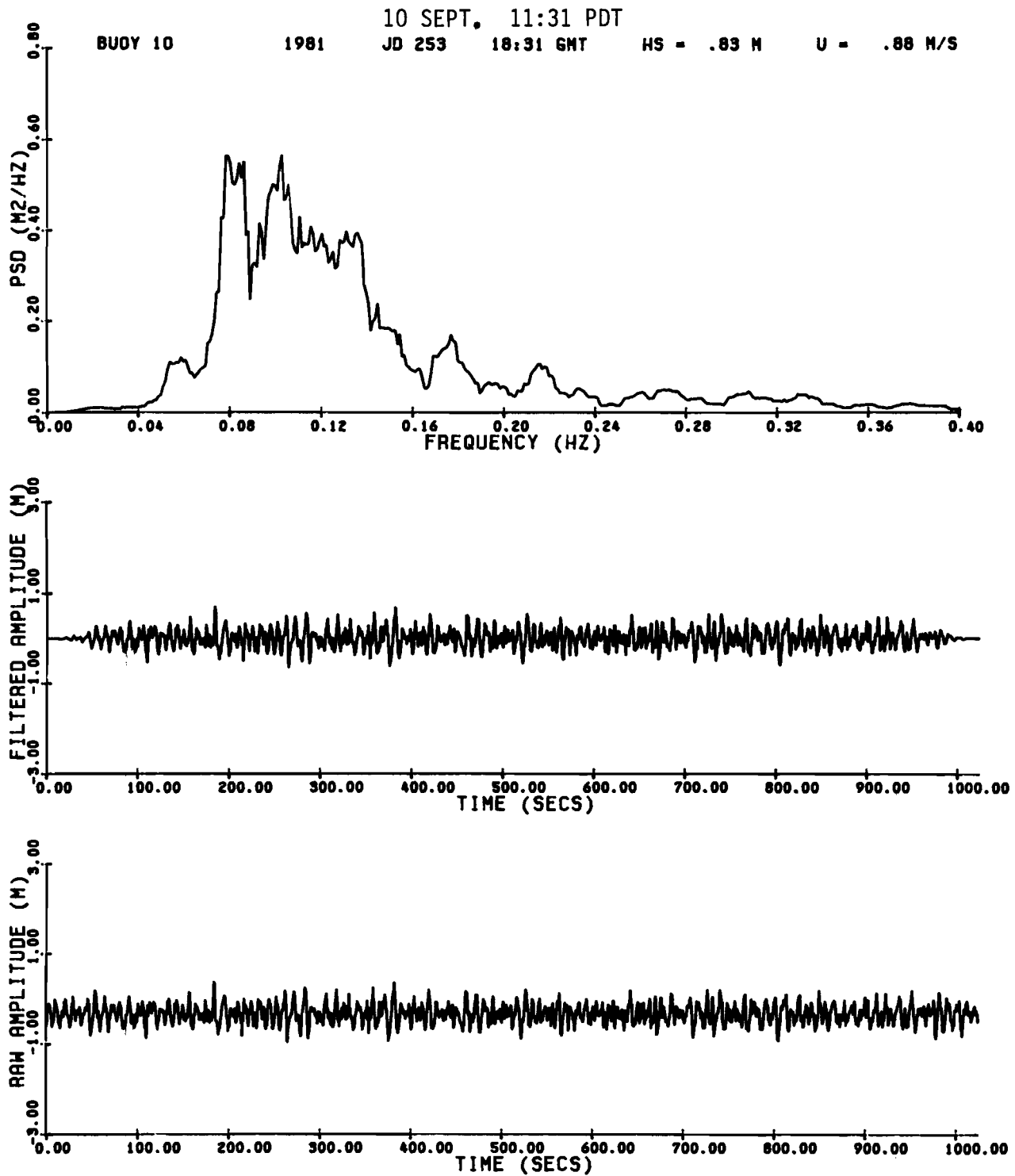


Figure A4. Waverider raw amplitude, filtered amplitude, and power spectral density for 1131 PDT, 10 Sept. 1981.

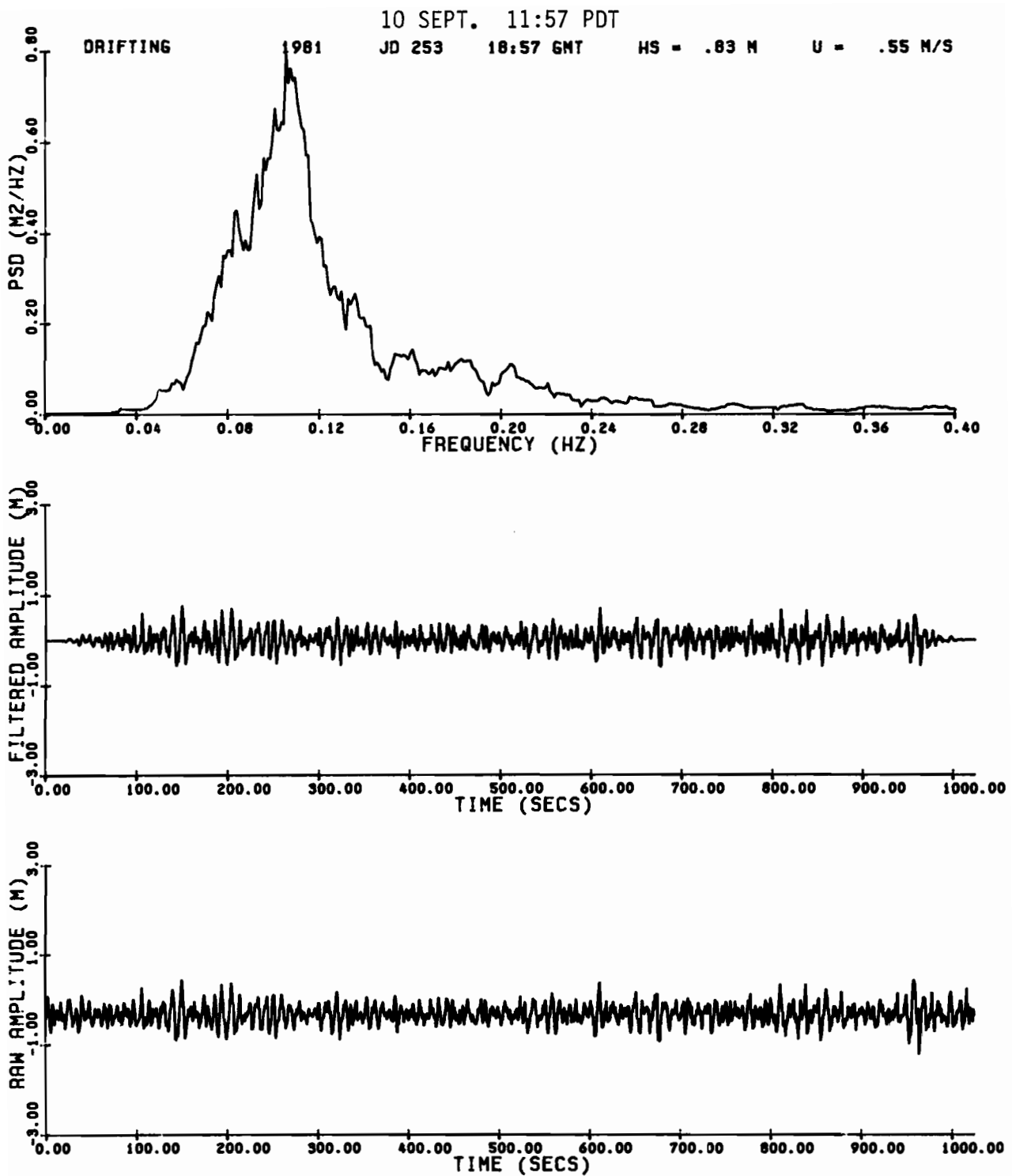


Figure A5. Waverider raw amplitude, filtered amplitude, and power spectral density for 1157 PDT, 10 Sept. 1981.

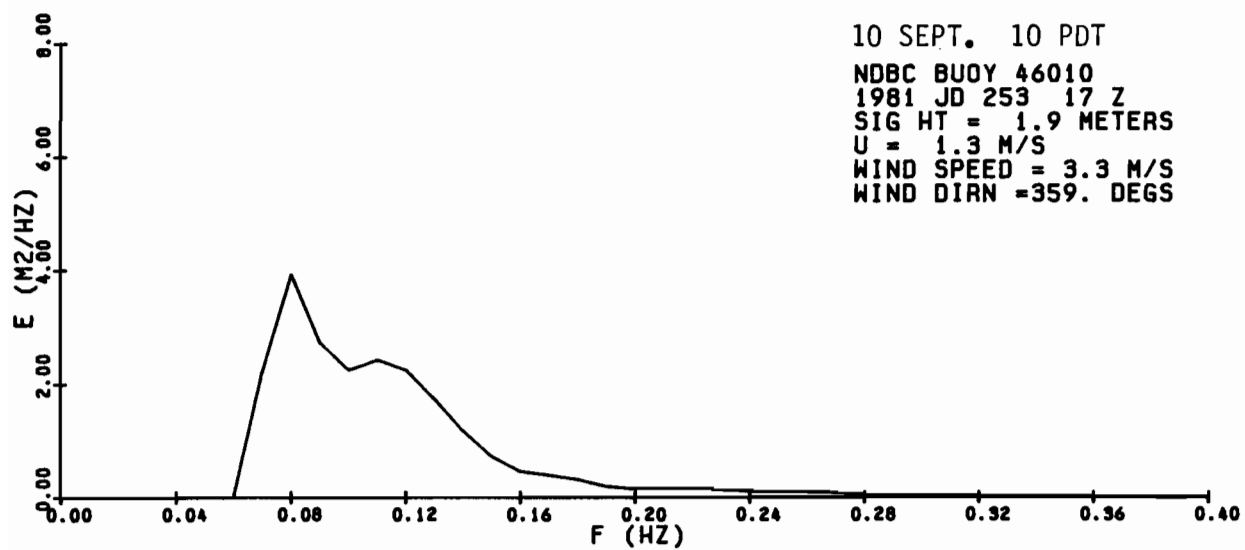
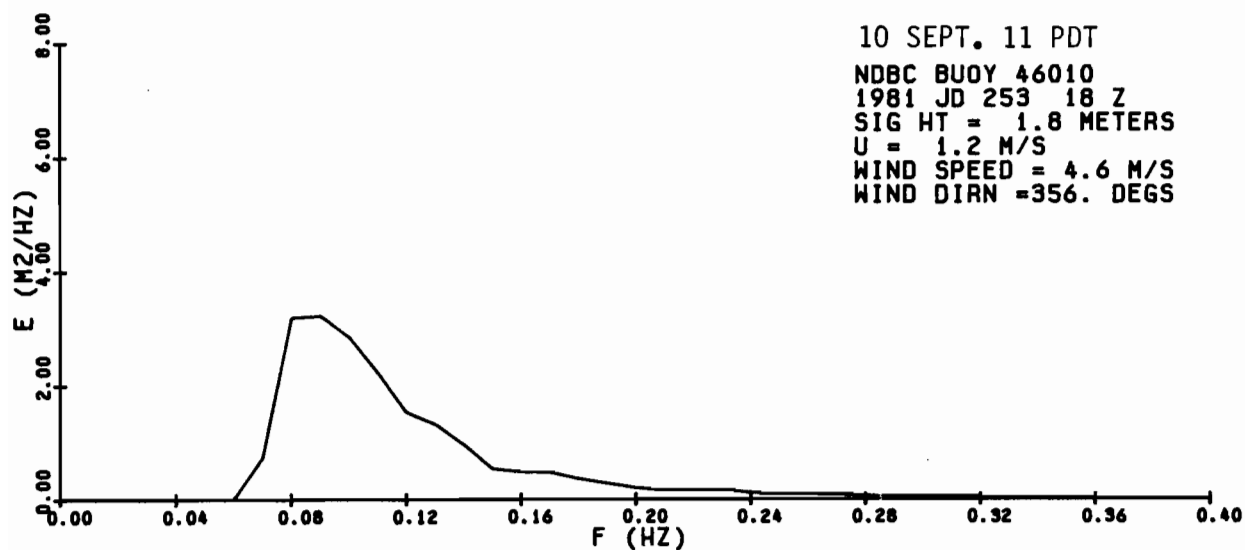
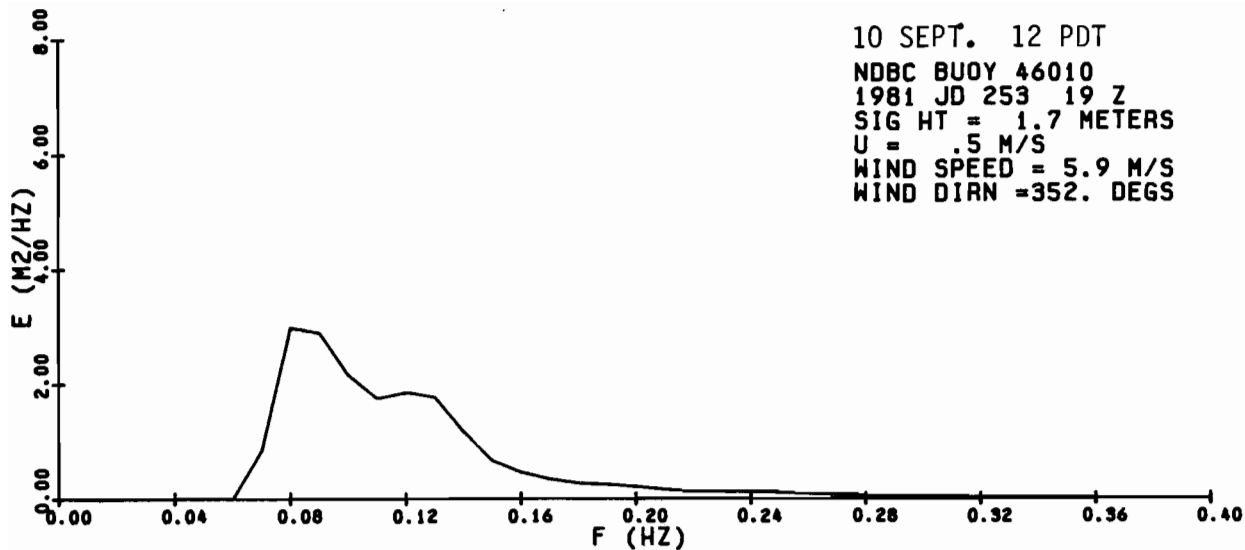


Figure A6. NDBC 46010 power spectral density for 1000, 1100, and 1200 PDT, 10 Sept. 1981.

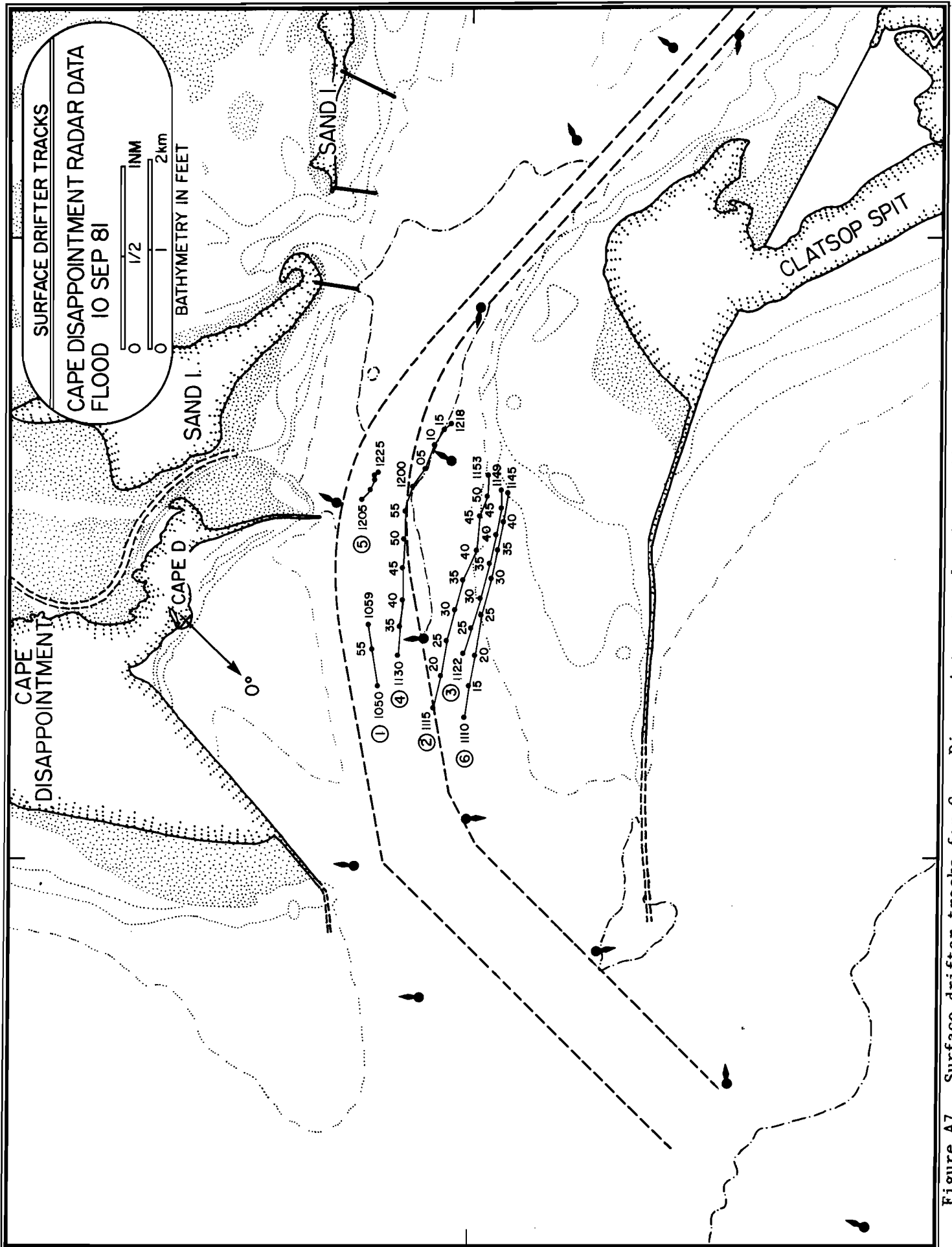


Figure A7. Surface drifter tracks for Cape Disappointment radar data collected during flood of 10 Sept. 1981.

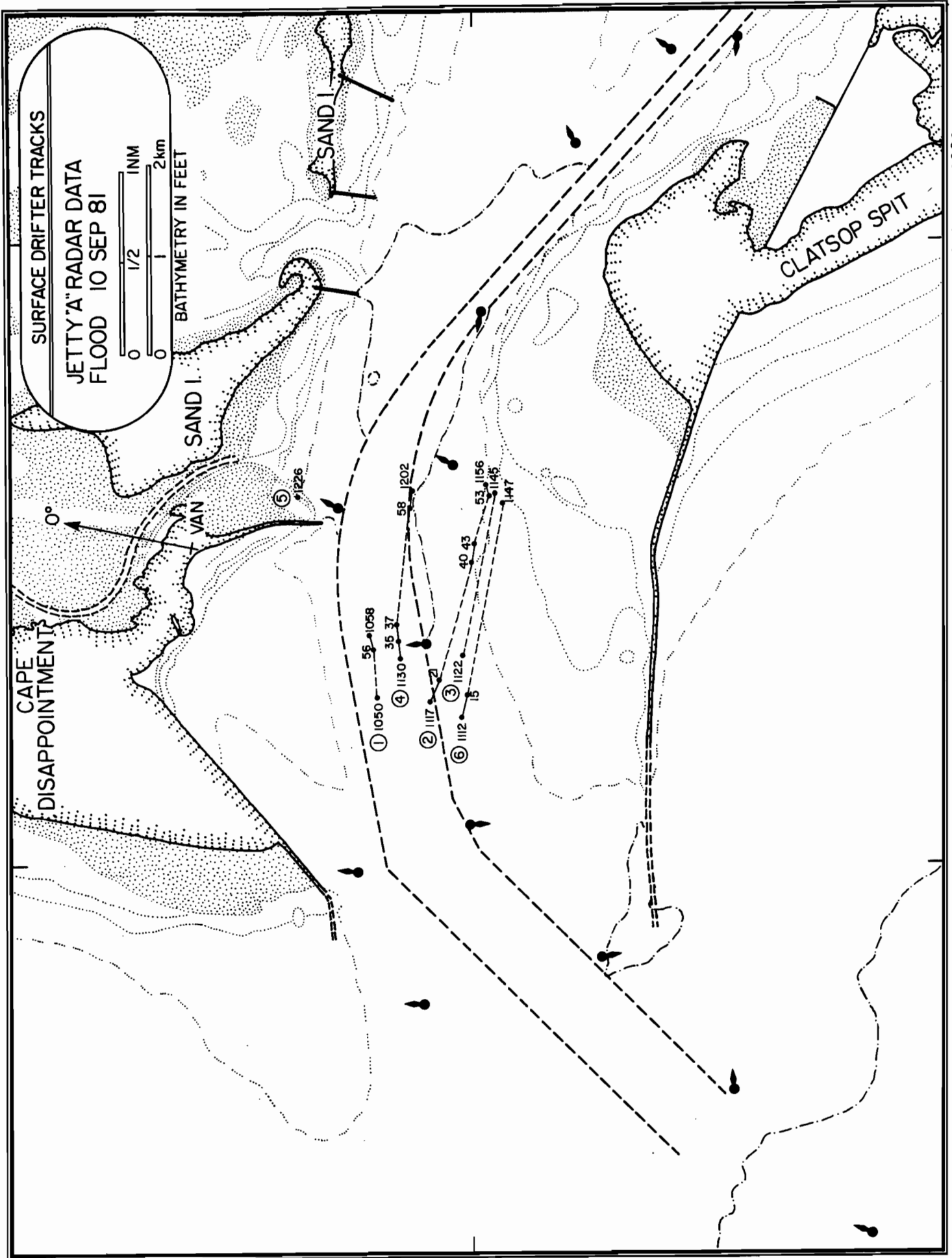


Figure A8. Surface drifter tracks for Jetty A radar data collected during flood of 10 Sept. 1981.



10 September 1981

FLOOD

Waverider LOG (Surface Vessel EGRET)

Time	Hdg.	Sextant Fixes	Objects	Remarks
0930				UW from Hammond Basin
1018				WR in water holding station 100 yards north of Buoy 8  (Drift log 25 m. 17, 18, 19 sec. 1.4 m/sec.)
1030				Begin record holding station.
1032		36°10'	1	100 yards north of No. 8
			2	1½ m. wave,
		35°12'	3	12 second period.
1043	260	36°18'	1	5 foot wave from
			2	echo sounder
		35°14'	3	
		R√ 24°05'	5	
1100		34°15'	1	Begin drift at 1055.
			2	WR ~ 100 yards
		38°57'	3	down-current from boat
1103		33°23'	1	
			2	
		40°46'	3	
1106		32°08'	1	
			2	
		42°55'	3	
1109		30°38'	1	
			2	
		45°23'	3	WR ~ 50 yards NW of boat
		R√ 12°13'	R√ 12	
1112		29°01'	1	
			2	
		48°02'	3	
1115		27°34'	1	WR ~ 50 yards NW of boat
			2	
		50°10'	3	

10 September 1981

FLOOD

Waverider LOG (Surface Vessel EGRET)

Time	Hdg.	Sextant Fixes	Objects	Remarks
1120		24° 39'	1	Stop drifting with WR. underway, towing WR.
			2	
		54° 12'	3	
		30° 30'	R√ 5	
1131		24° 44'	1	On station. 100 yds. N. Buoy 10.
			2	
		64° 44'	3	
		39° 39'	R√ 5	
1153		25° 27'	1	On station.
			2	
		65° 07'	3	
		40° 22'	R√ 5	
1157				Begin drifting from 100 yds. N. of Buoy 10. WR ~ 250 ft. down current from EGRET.
1200		24° 14'	1	
			2	
		67° 00'	3	
1203		19° 53'	1	
			2	
		69° 34'	3	
1206		18° 12'	1	WR ~ 100 ft. NW of EGRET
			2	
		71° 13'	3	
1209		51° 48'	1	
			5	
		36° 52'	3	
		35° 20'	L√ 2	
1213		47° 37'	1	
			5	
		40° 37'	3	

10 September 1981

FLOOD

Waverider LOG (Surface Vessel EGRET)

---

Time	Hdg.	Sextant Fixes	Objects	Remarks
1215		45° 05'	1	WR ~ 100 ft. NW of EGRET.
			5	
		42° 20'	3	
1218		41° 55'	1	
			5	
		44° 39'	3	
1221		27° 06'	2	End drift. Underway for Buoy 14.
			5	
		47° 01'	3	
1232				WR aboard. Underway to Hammond Basin.

---

10 September 1981

FLOOD

CAPE DISAPPOINTMENT RADAR DATA

Buoy No.	Time (PDT)	Range (nm.)	Bearing (deg.)	Remarks
1	1050	1.13	335	
	1055	1.05	325	
	1059	1.03	317	Retrieved Buoy #1
2	1115	1.47	335	
	1120	1.48	328	
	1125	1.45	320	
	1130	1.50	313	
	1135	1.56	307	
	1140	1.67	302	
	1150	1.81	293	
1153	1.87	290	Pick up Buoy #2	
3	1122	1.56	322	
	1125	1.58	317	
	1130	1.64	311	
	1135	1.71	305	
	1140	1.79	300	
	1145	1.87	296	
	1149	1.90	293	Pick up Buoy #3
4	1130	1.20	325	
	1135	1.19	317	
	1140	1.21	310	
	1145	1.24	302	
	1150	1.30	295	
	1155	1.37	289	
	1200	1.47	285	
	1205	1.58	283	
	1210	1.69	280	
	1215	1.79	279	
	1218	1.84	279	Pick up Buoy #4
5	1205	1.19	281	
	1210	1.27	280	
	1215	1.31	279	
	1220	1.33	278	
	1225	1.36	278	Pick up Buoy #5

10 September 1981

FLOOD

CAPE DISAPPOINTMENT RADAR DATA

---

Buoy No.	Time (PDT)	Range (nm.)	Bearing (deg.)	Remarks
6	1110	1.64	335	
	1115	1.61	329	
	1120	1.61	322	
	1125	1.64	315	
	1130	1.71	308	
	1135	1.78	303	
	1140	1.85	299	
	1145	1.91	294	

---

10 September 1981

FLOOD

JETTY A RADAR DATA

---

Buoy No.	Time (PDT)	Range (nm.)	Bearing (deg.)	Remarks
1	104945	1.30	219	
1	105605	1.13	209	
1	105815	1.09	207	Buoy #1 picked up
2	111650	1.57	213	Drifters difficult to see and follow.
2	112030	1.53	208	"
2	113950	1.52	182	"
2	114300	1.54	178	"
2	115250	1.65	169	"
2	115550	1.65	167	"
3	112210	1.60	202	"
3	114525	1.69	174	"
4	113025	1.29	208	"
4	113430	1.23	204	"
4	113700	1.20	200	"
4	115745	1.21	169	"
4	120150	1.25	165	"
5	122623	0.64	153	"
6	111210	1.75	212	"
6	111445	1.71	208	"
6	114715	1.73	171	"

---

10 September 1981

EBB





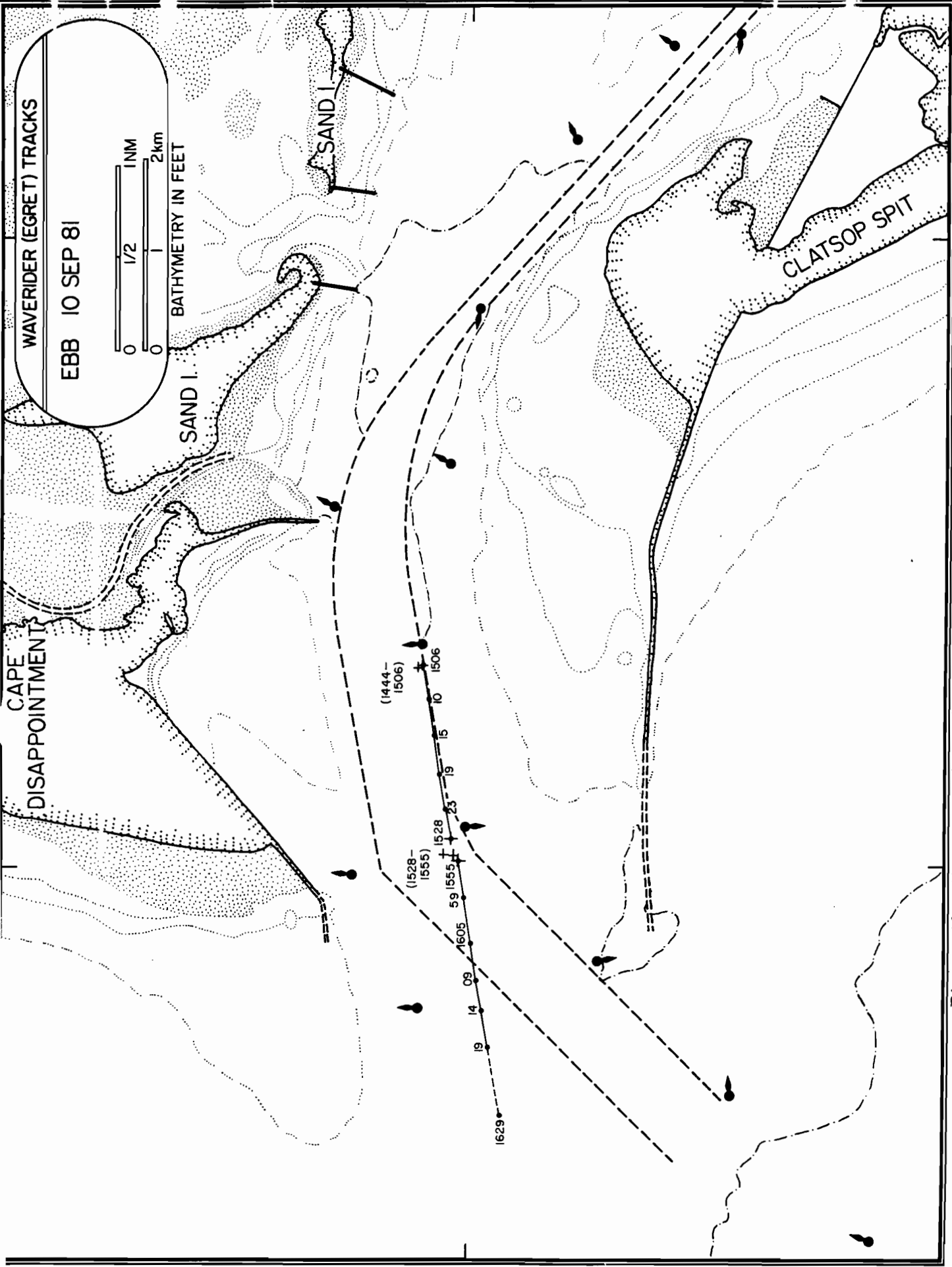


Figure A9. Waverider (EGRET) tracks for ebb period on 10 Sept. 1981.

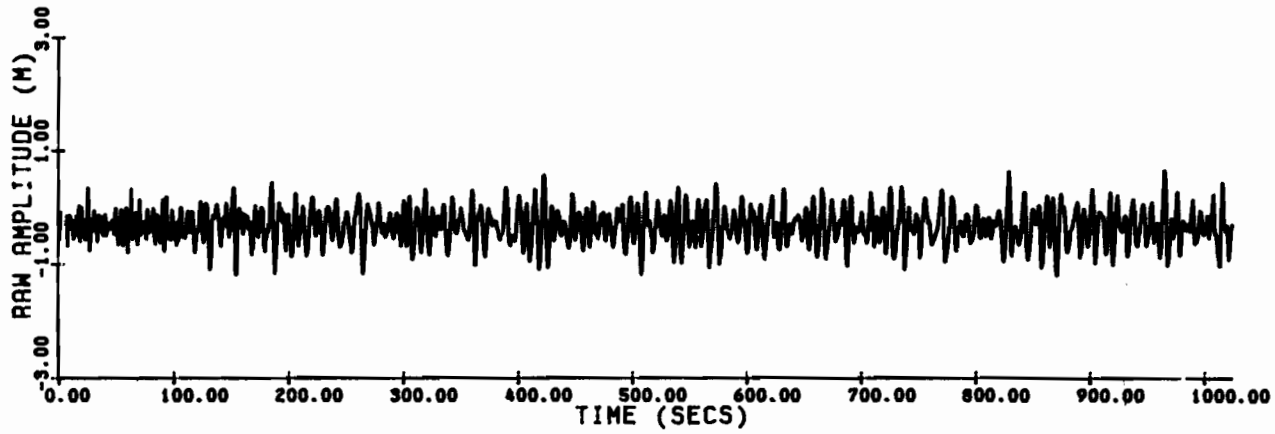
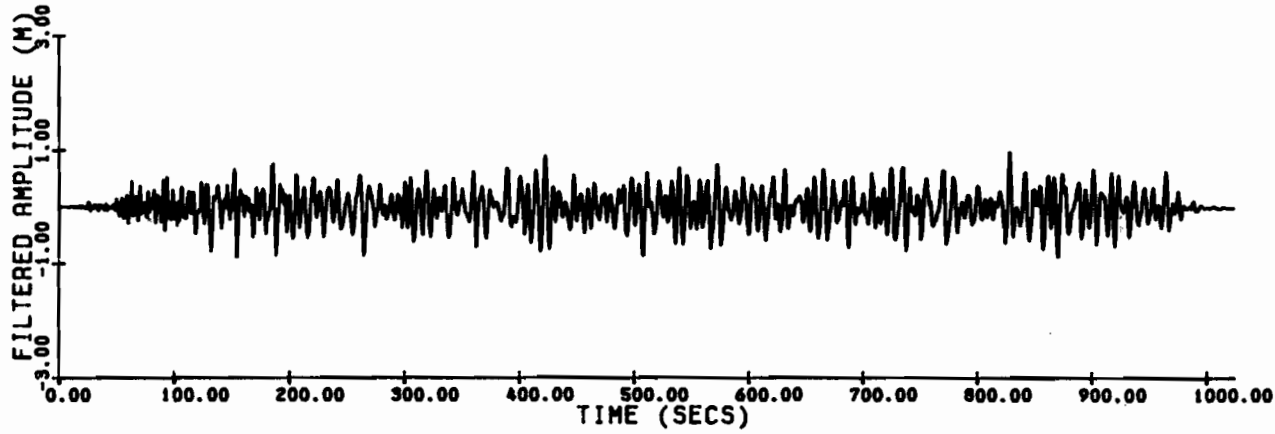
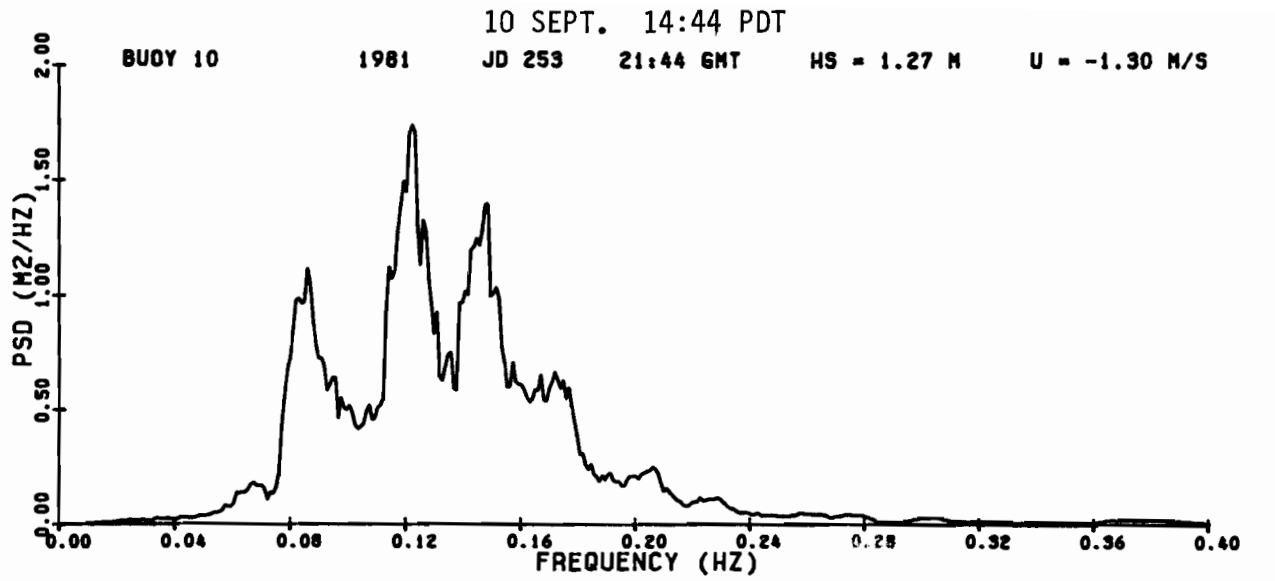


Figure A10. Waverider raw amplitude, filtered amplitude, and power spectral density for 1444 PDT, 10 Sept. 1981.

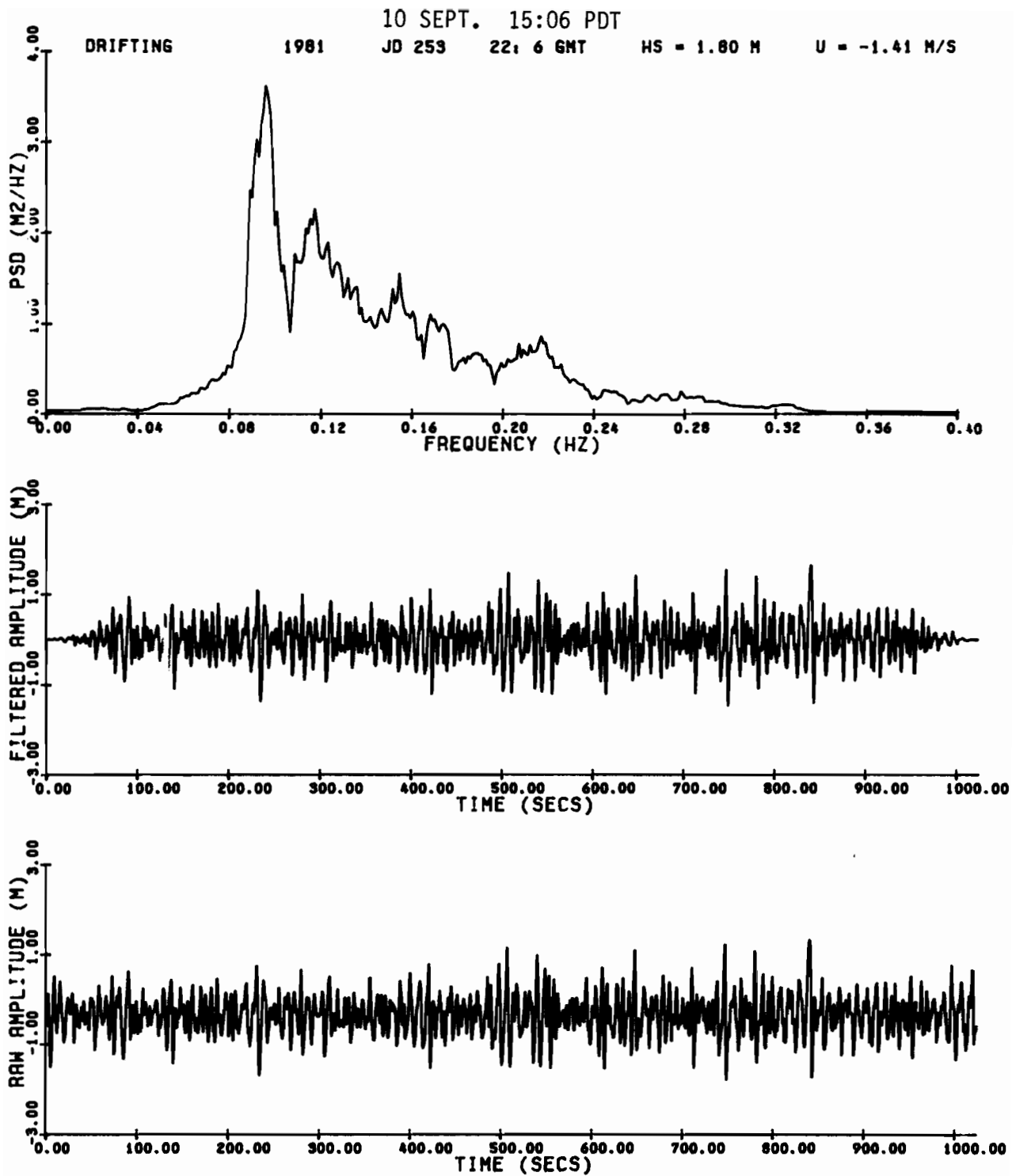


Figure A11. Waverider raw amplitude, filtered amplitude, and power spectral density for 1506 PDT, 10 Sept. 1981.

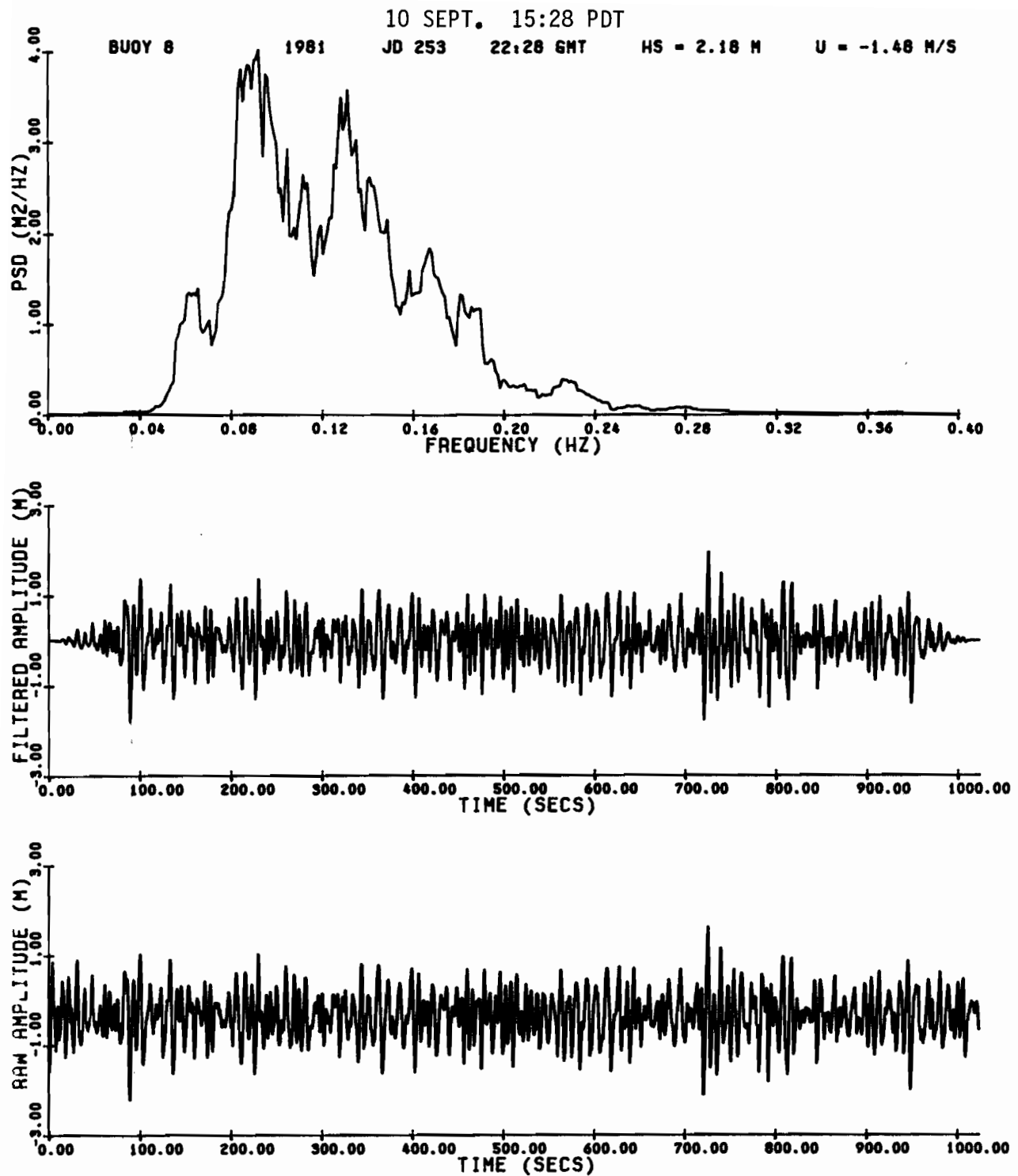


Figure A12. Waverider raw amplitude, filtered amplitude, and power spectral density for 1528 PDT, 10 Sept. 1981.

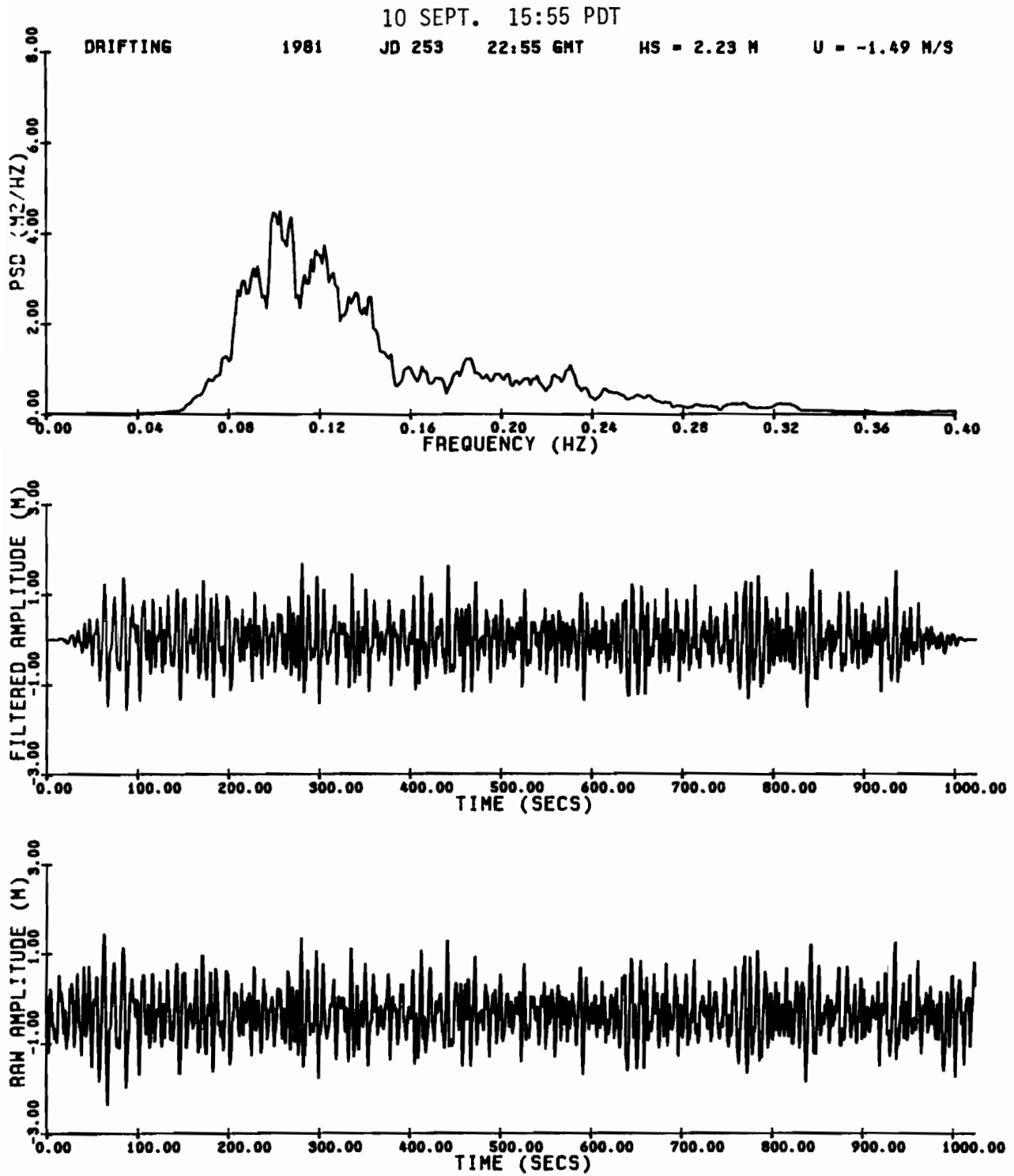


Figure A13. Waverider raw amplitude, filtered amplitude, and power spectral density for 1555 PDT, 10 Sept. 1981.

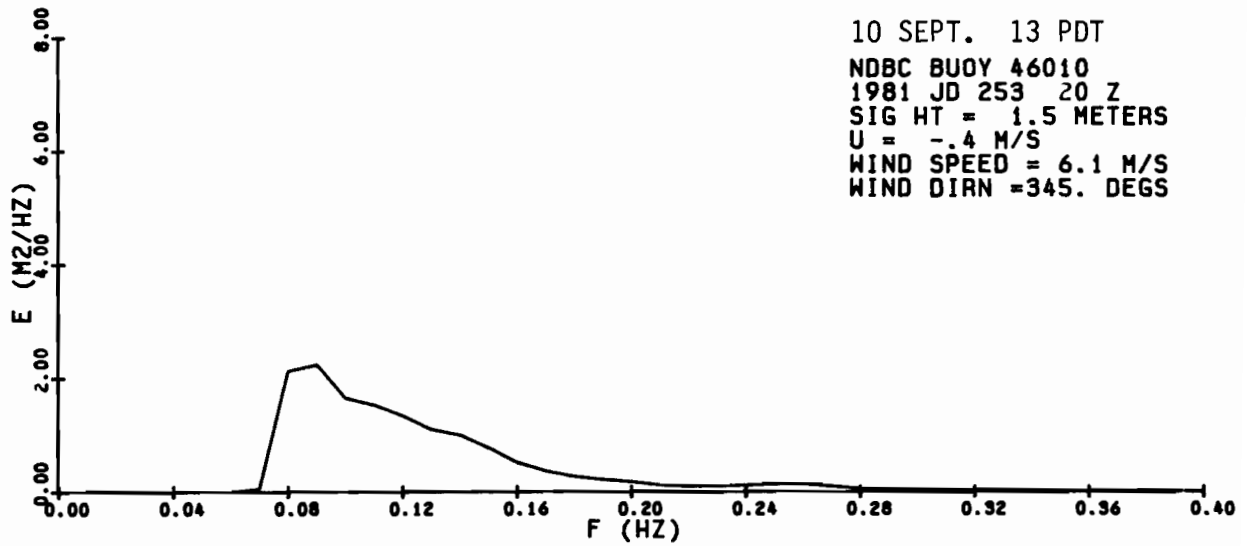
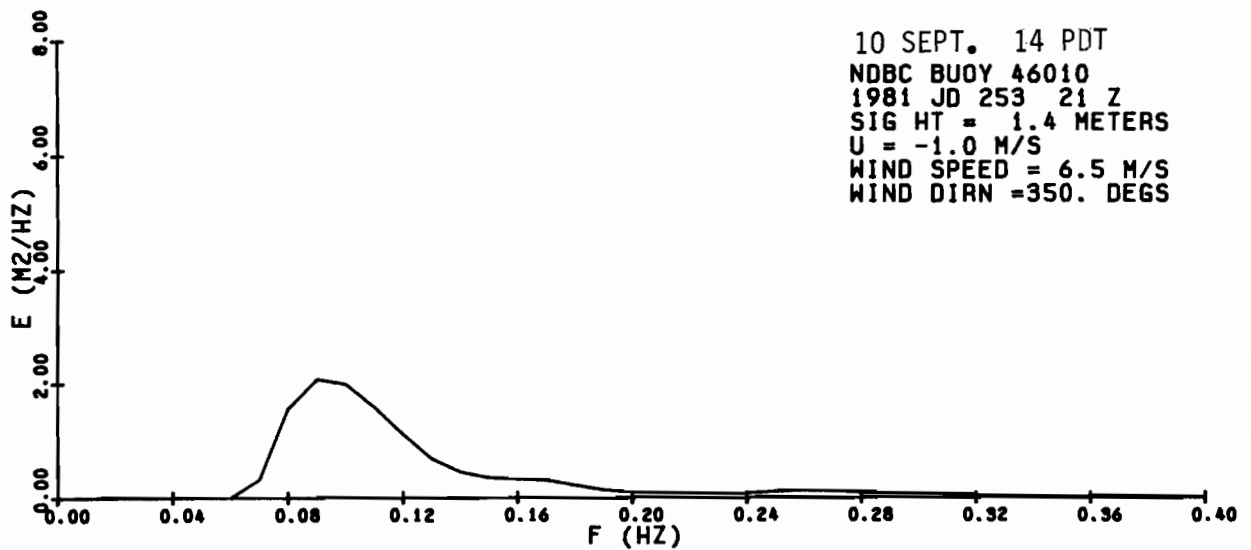
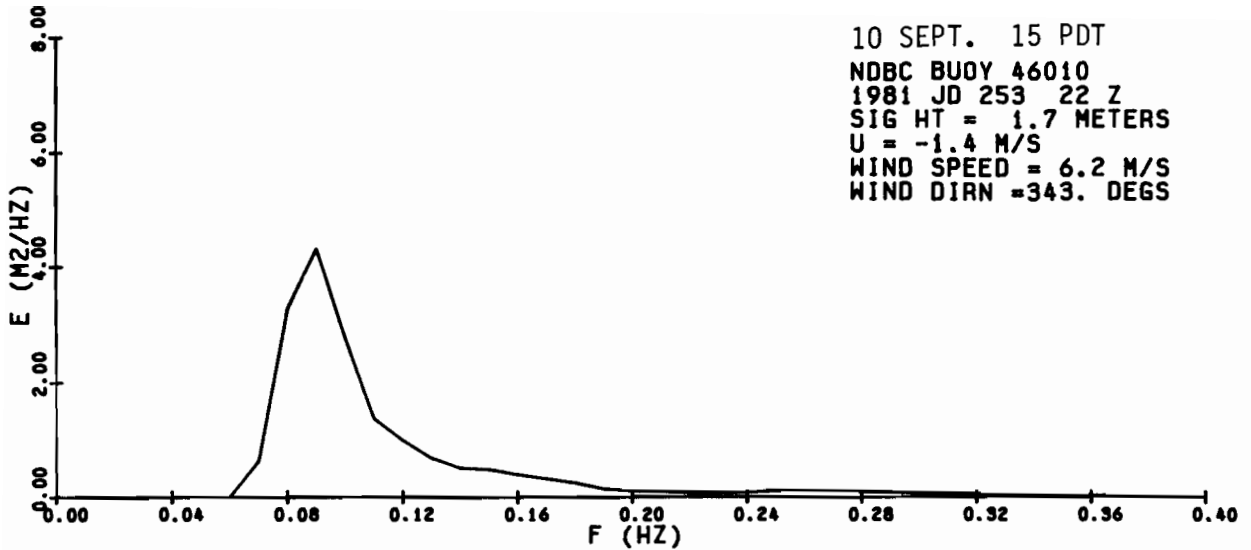


Figure A14. NDBC 46010 power spectral density for 1300, 1400, and 1500 PDT, 10 Sept. 1981.

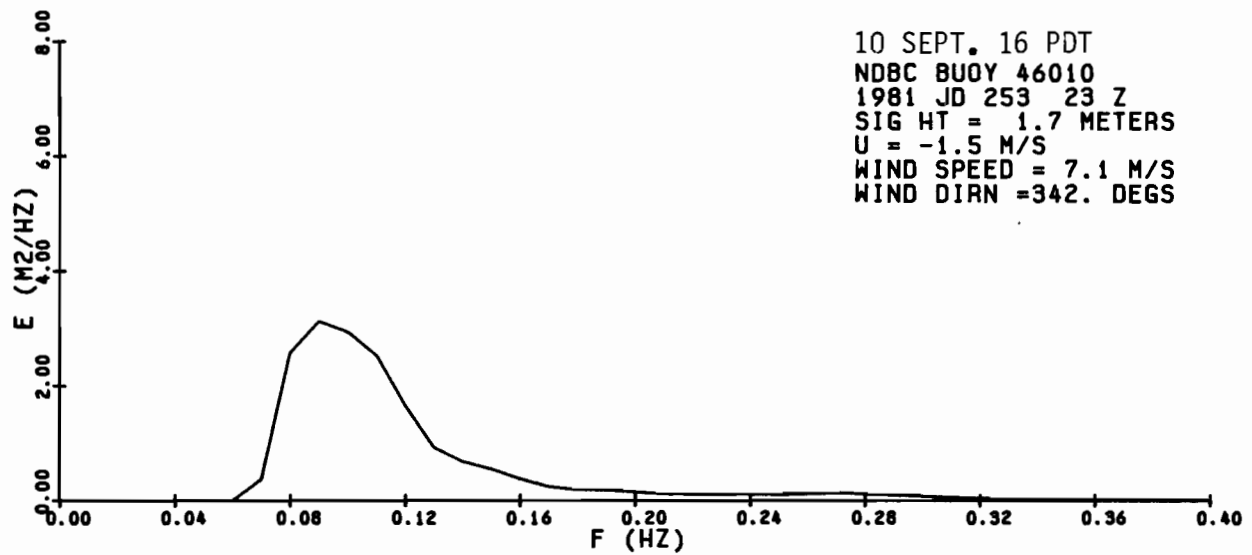
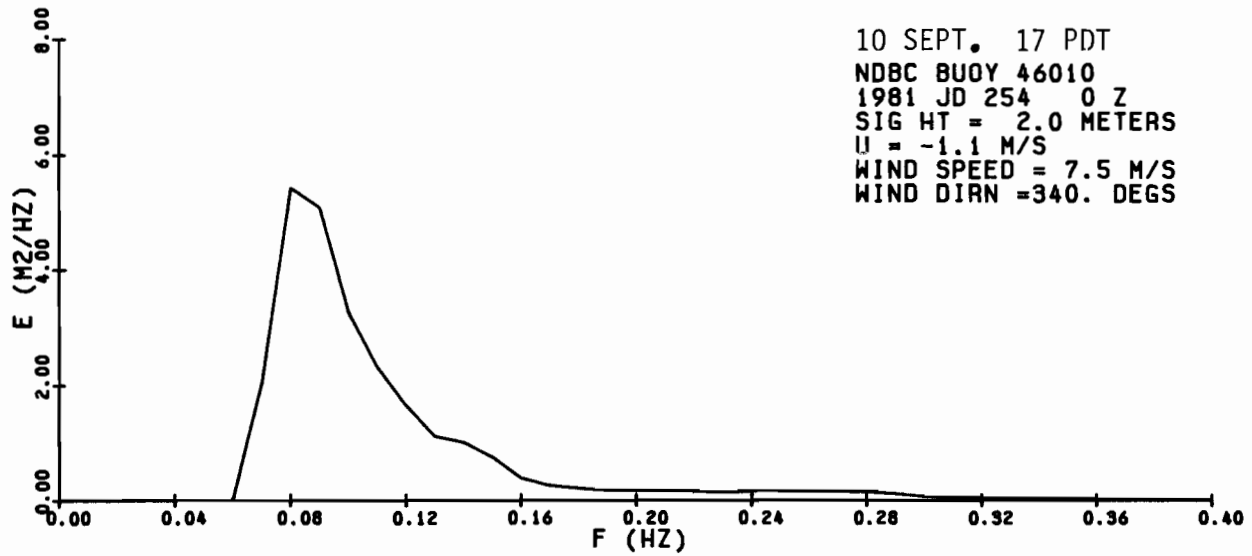
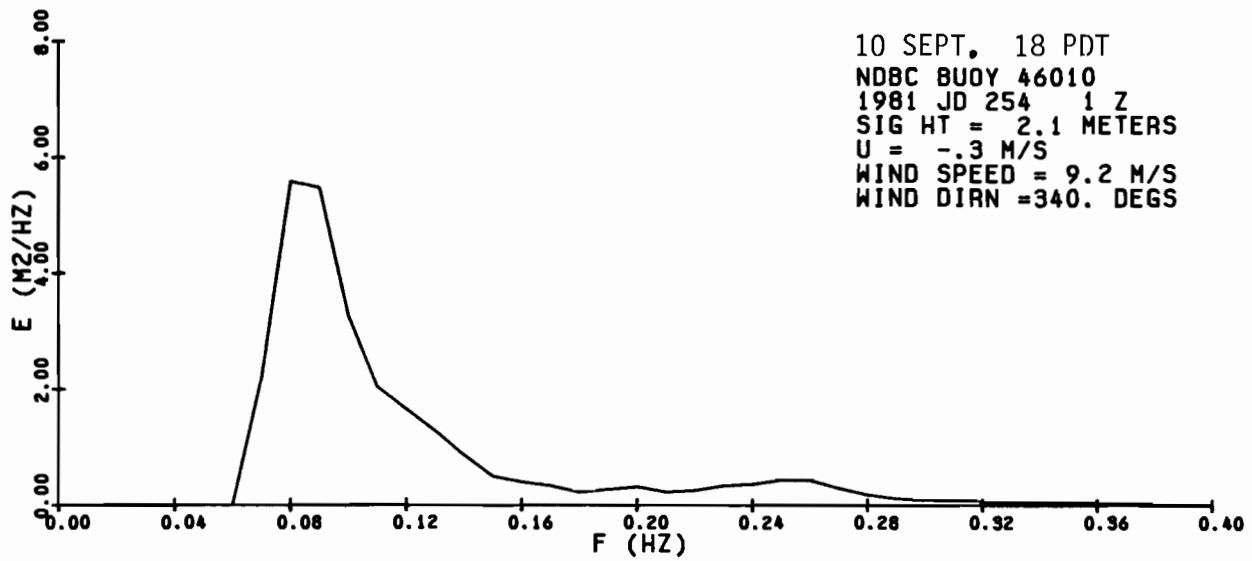


Figure A15. NDBC 46010 power spectral density for 1600, 1700, and 1800 PDT, 10 Sept. 1981.





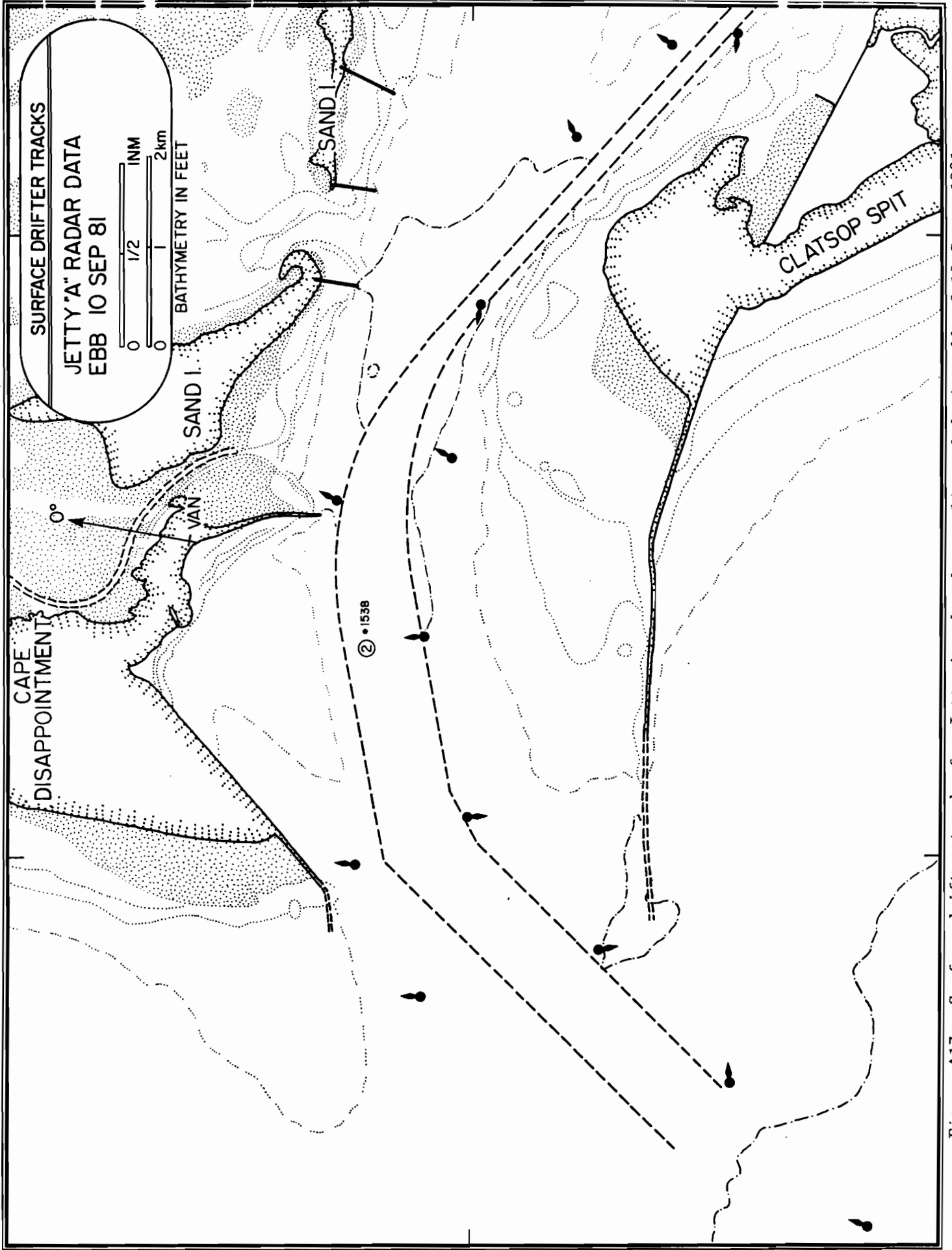


Figure A17. Surface drifter tracks for Jetty A radar data collected during ebb of 10 Sept. 1981.

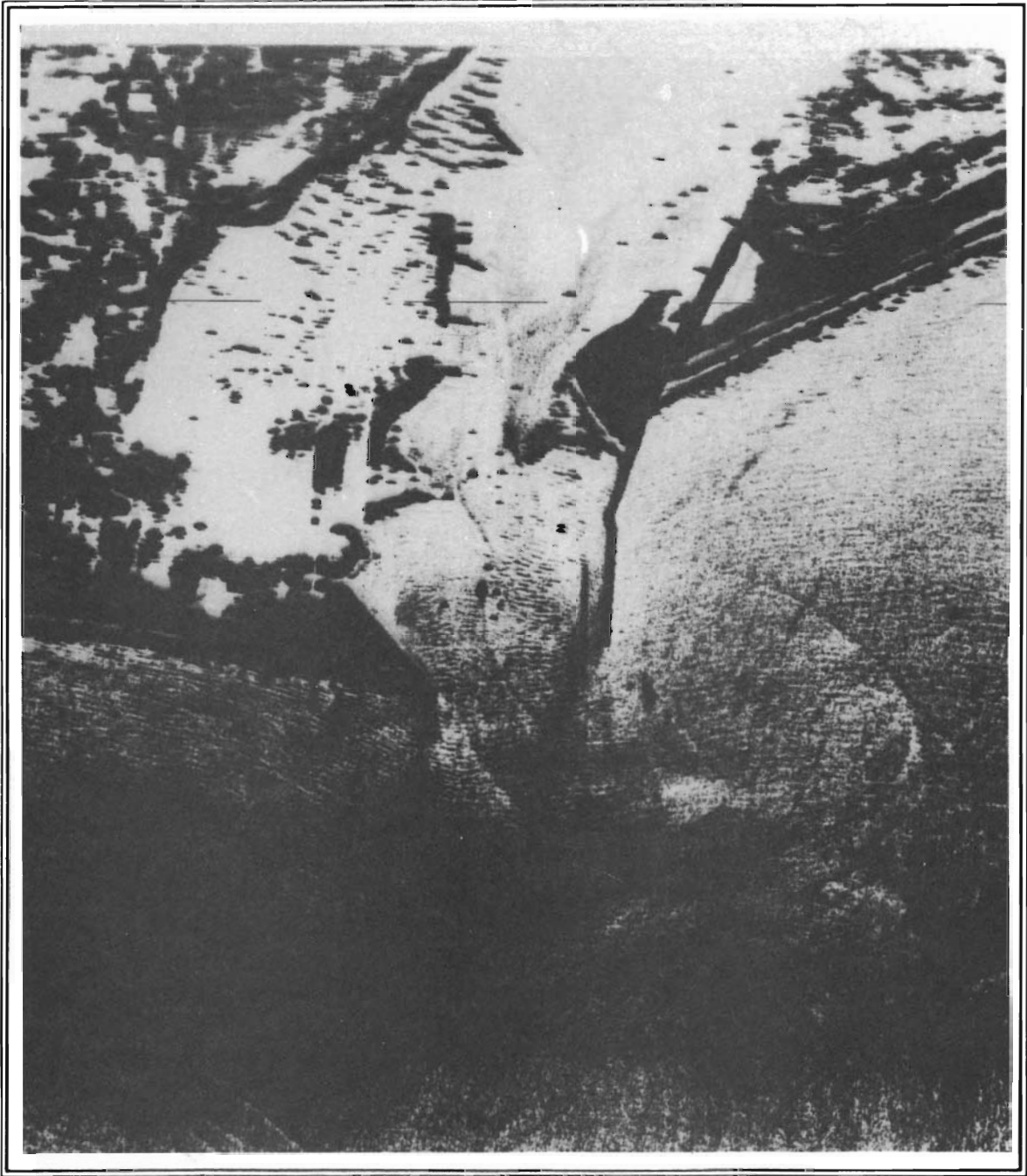


Figure A18. SLAR image of Columbia River entrance obtained on the ebb at 1520 PDT, 10 Sept. 1981.



Figure A19. Blowup of Figure A18, centered on river entrance.

10 September 1981

EBB

Waverider LOG (Surface Vessel EGRET)

Time	Hdg.	Sextant Fixes	Objects	Remarks
1444	060 (into current)			Holding station. WR deployed 100 yds. N of Buoy 10. ~ 100 m line out. ~ 8 sec. 5-8 ft. (current 11, 12 sec./25 m. drift log).
1457	065	27° 38' 60° 38' 38° 31'	1 2 3 5 R√	Holding station.
1501		27° 53' 60° 17'	1 2 3	
1506		27° 27' 60° 04'	1 2 3	Begin drift from on station. WR 100 yds. down current.
1510		30° 37' 54° 00'	1 2 3	
1515		33° 30' 47° 48'	1 2 3	Boat maneuvering to hold WR ~ 200 ft. down current from boat with slack in "towing" cable at all times.
1519		35° 27' 42° 10'	1 2 3	Buoy streaming to leeward ~ 75 m.
152330		36° 33' 37° 44'	1 2 3	

10 September 1981

EBB

Waverider LOG (Surface Vessel EGRET)

Time	Hdg.	Sextant Fixes	Objects	Remarks
152730		36° 34'	1	
			2	
		34° 30'	3	
1528	55- 60° MAG			Holding position ~ 100 yds. NW of Buoy 8. Drifted exactly into position. Waverider submerges with top even with water line but follows the wave pattern very well.
1534		37° 33'	1	In position -
			2	referenced to
		33° 00'	3	Buoy 8.
1542		36° 43'	1	8-10 ft. seas and
			2	8 sec. by visual
		36° 32'	12	and stopwatch.
		36° 10'	13R✓ good	
				(drift log 10 sec. and 10 sec. for 25 m.)
1555		36° 18'	1	Began drifting from
			2	in position N of
		36° 05'	12	Buoy 8.
1559		35° 55'	1	EGRET maneuvering
			2	to stay ~ 150 to
		32° 51'	12	200 ft. up current from WR with slack in cable at all times.
1605		35° 11'	1	
			2	
		26° 03'	14	

10 September 1981

EBB

Waverider LOG (Surface Vessel EGRET)

Time	Hdg.	Sextant Fixes	Objects	Remarks
160930		34° 10'	1	
			2	
		27° 30'	12	
		24° 03'	14 Good	
1614		33° 06'	1	
			2	
		25° 13'	12	
1619		31° 53'	1	
			2	
		20° 15'	14 ✓ Good	
1629				End drift with WR. Underway for Buoy 4 towing WR.
1653		72° 05'	1	
			17 (#4 buoy)	
		58° 50'	16 (#2 buoy)	
		51° 06'	2	
1655		72° 05'	1	Picked up drifter buoy 5 min ago at about 1650.
			17 (#4 buoy)	Cancel plans for record at Buoy 4 due to approach of darkness. Underway for Hammond.
		57° 50'	16 (#2 buoy)	
		52° 12'	2	

10 September 1981

EBB

CAPE DISAPPOINTMENT RADAR DATA

---

Buoy No.	Time (PDT)	Range (nm.)	Bearing (deg.)	Remarks
2	1450	2.4	264	
	1537	1.01	318	
	1540	1.05	328	
	1545	1.16	349	
	1550	1.30	000	
	1555	1.49	005	
	1600	1.72	010	
3	1450	2.4	262	
	1541	1.21	306	
	1545	1.36	317	
	1550	1.53	326	
	1555	1.70	332	
	1600	1.93	338	
	1605	2.14	344	
	1610	2.39	348	
	1615	2.57	352	
	1620	2.80	355	
	1625	2.96	357	
4	1527	0.96	295	
	1530	0.94	305	
	1535	0.92	322	
	1540	1.00	341	
	1545	1.15	001	
	1550	1.30	006	
	1555	1.49	014	
	1600	1.65	015	
5	1523	1.70	281	
	1525	1.61	292	
	1530	1.59	302	
	1535	1.63	312	
	1540	1.74	321	
	1545	1.84	330	
	1550	2.04	335	
	1555	2.28	340	
	1600	2.45	344	

---

10 September 1981

EBB

JETTY A RADAR DATA

---

Buoy No.	Time (PDT)	Range (nm.)	Bearing (deg.)	Remarks
2	153815	1.08	208	Drifters impossible to follow.

---



11 September 1981

SLACK



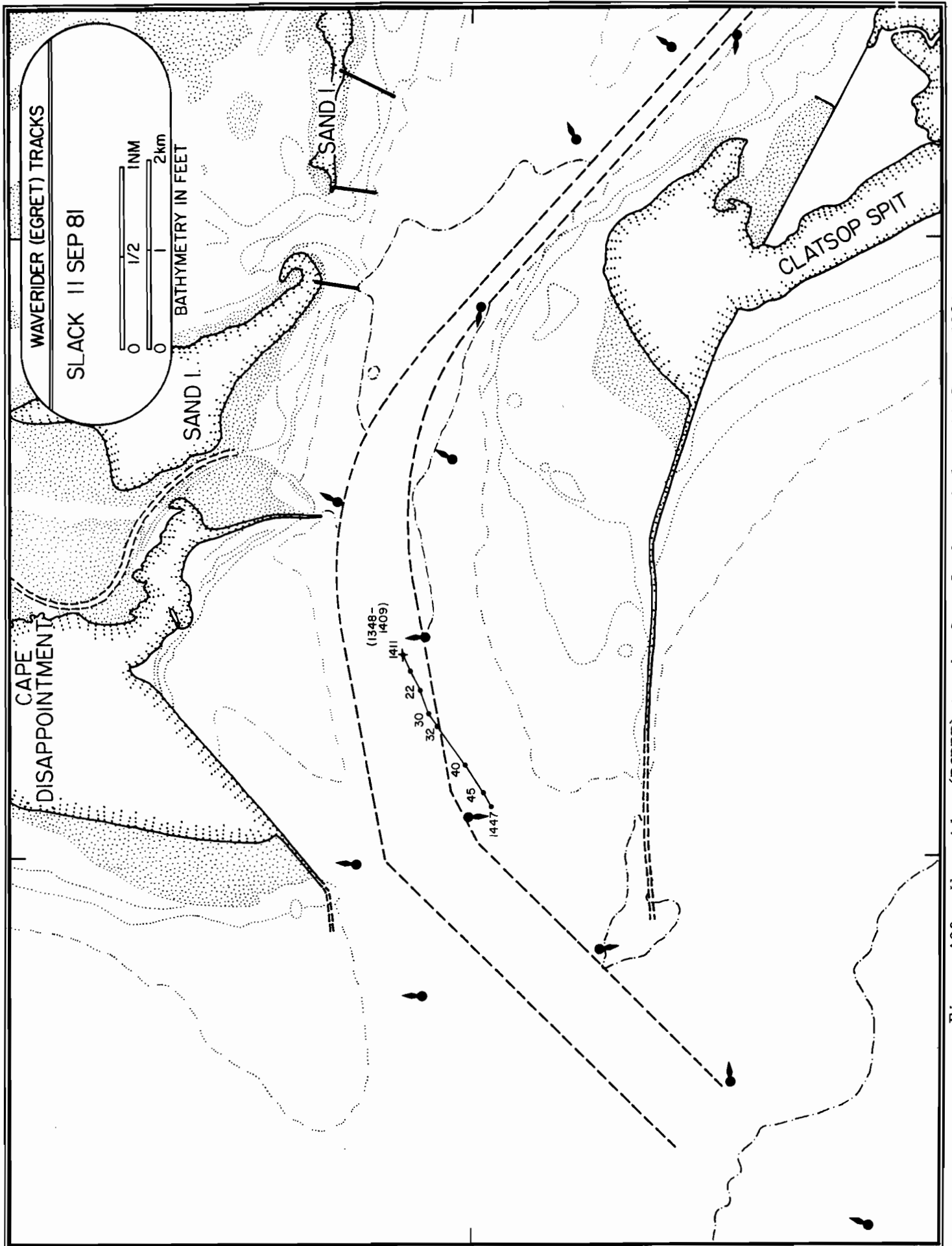


Figure A20. Waverider (EGRET) tracks for slack period on 11 Sept. 1981.

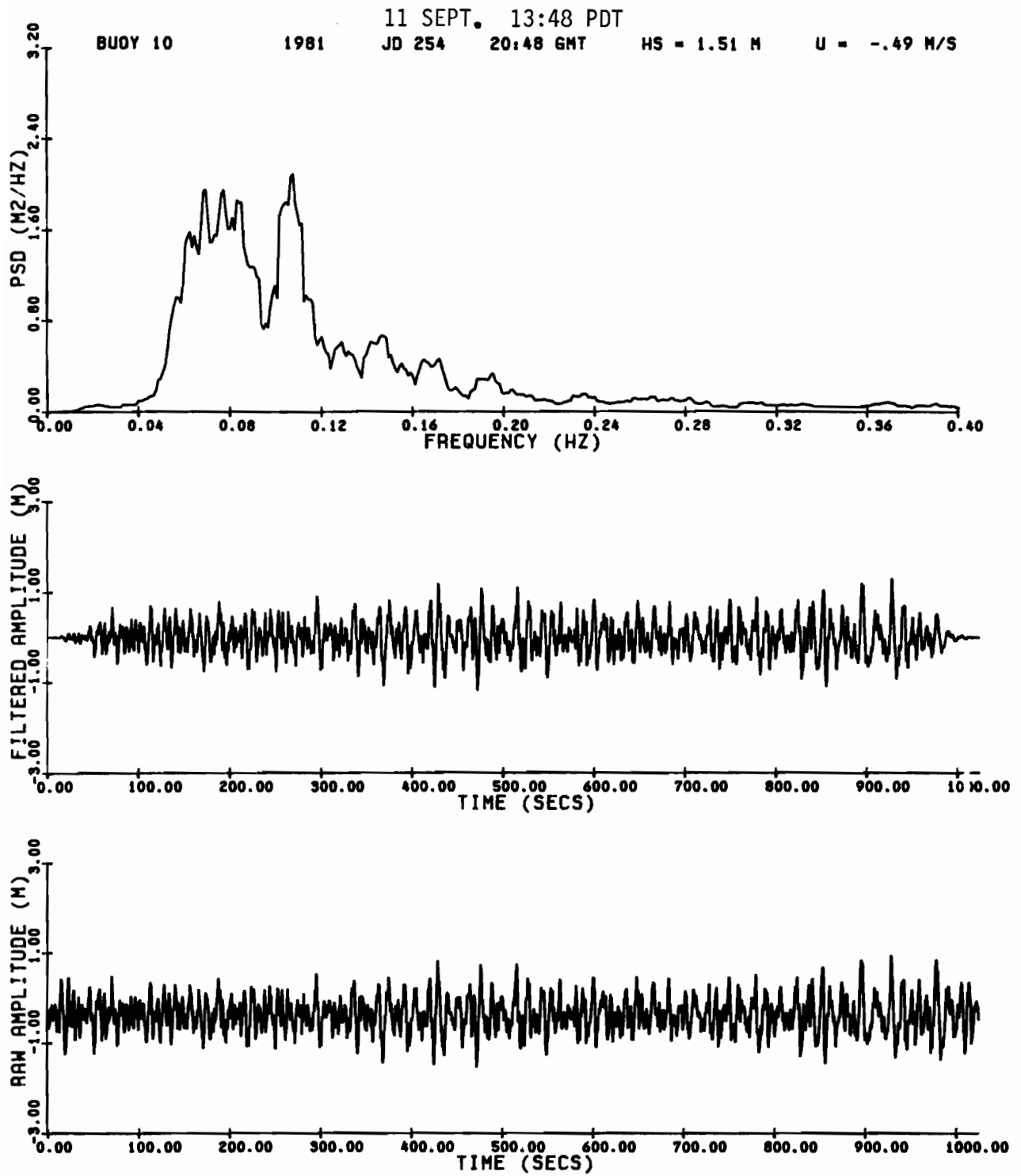


Figure A21. Waverider raw amplitude, filtered amplitude, and power spectral density for 1348 PDT, 11 Sept. 1981.

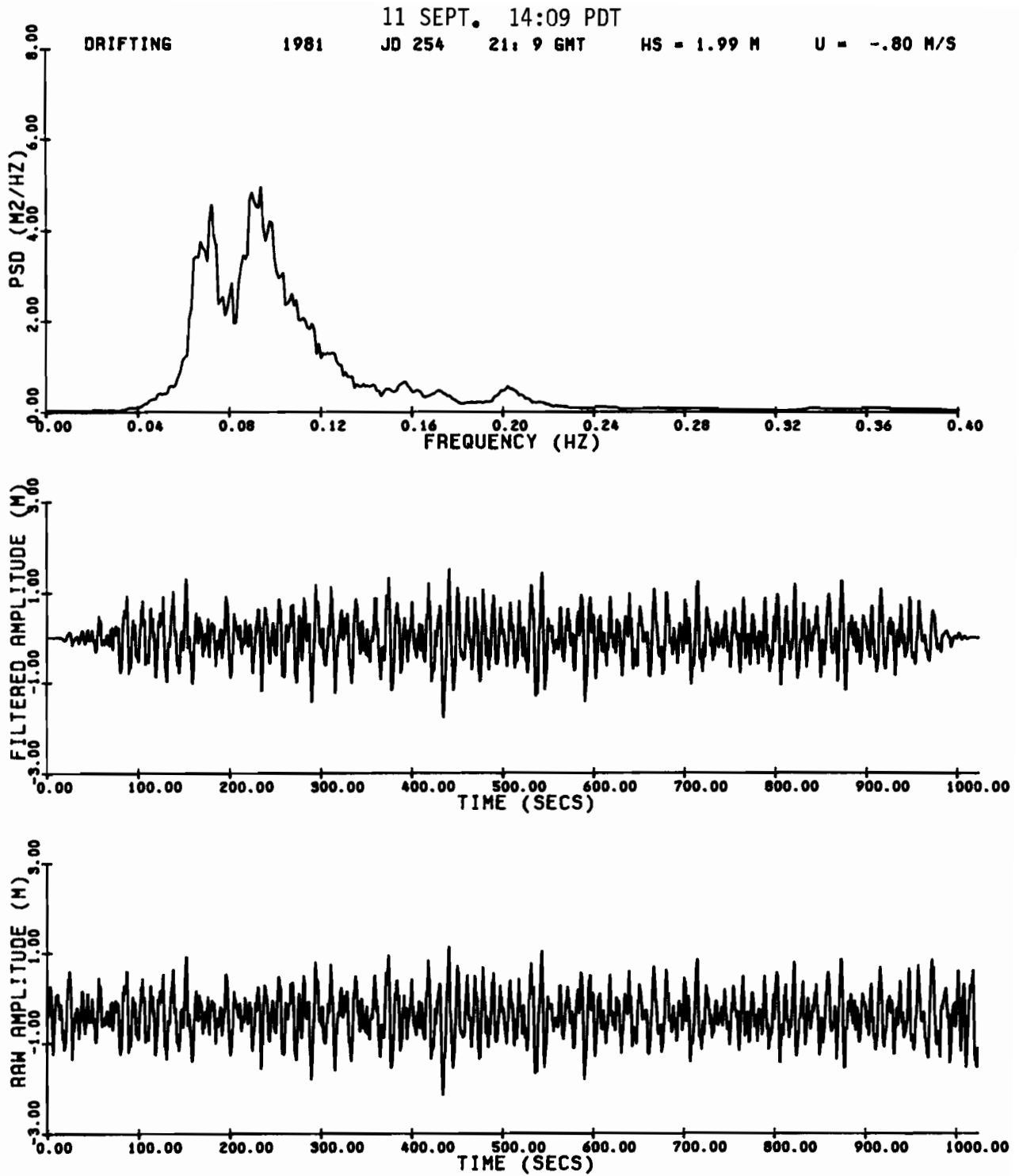


Figure A22. Waverider raw amplitude, filtered amplitude, and power spectral density for 1409 PDT, 11 Sept. 1981.

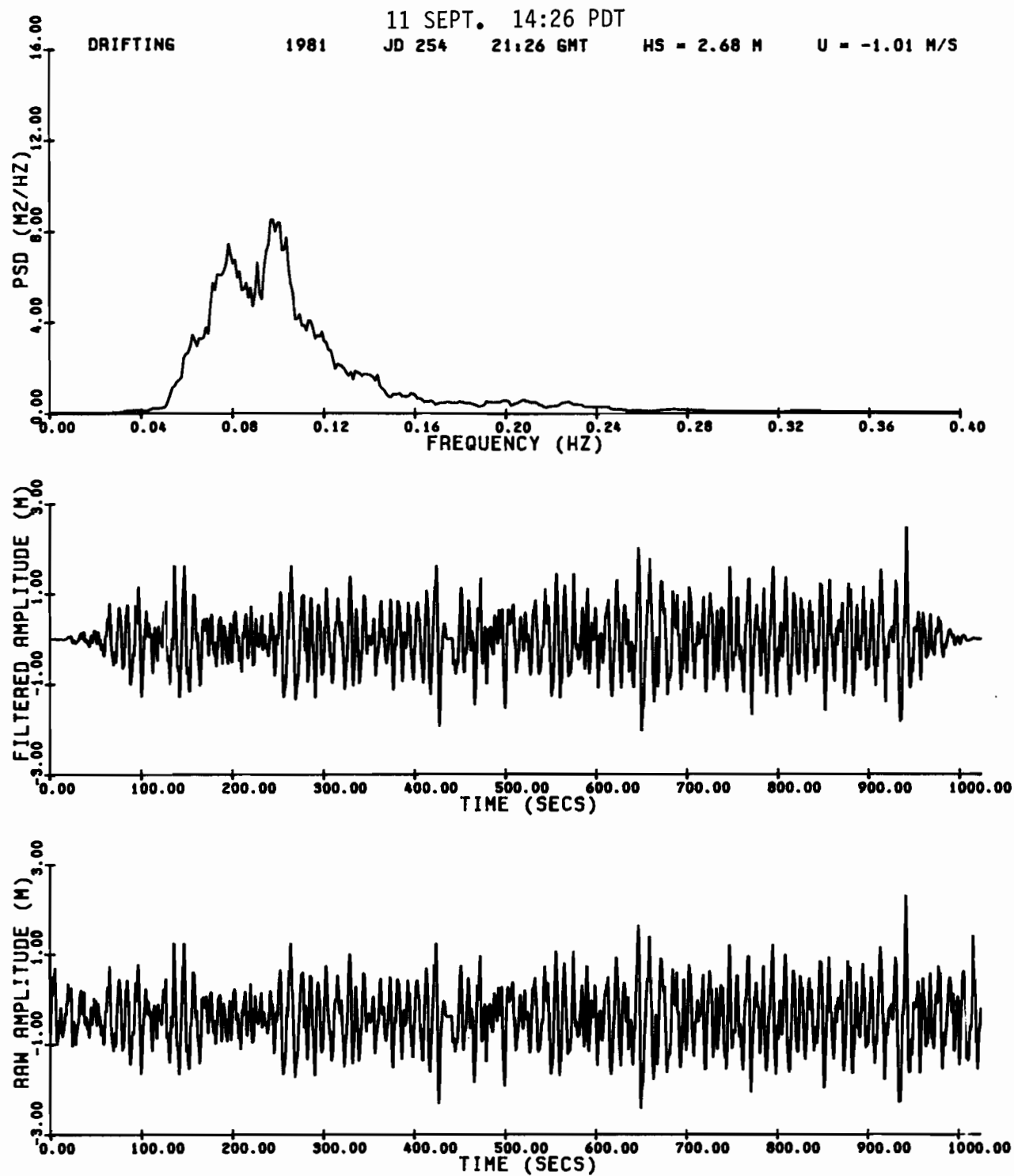


Figure A23. Waverider raw amplitude, filtered amplitude, and power spectral density for 1426 PDT, 11 Sept. 1981.

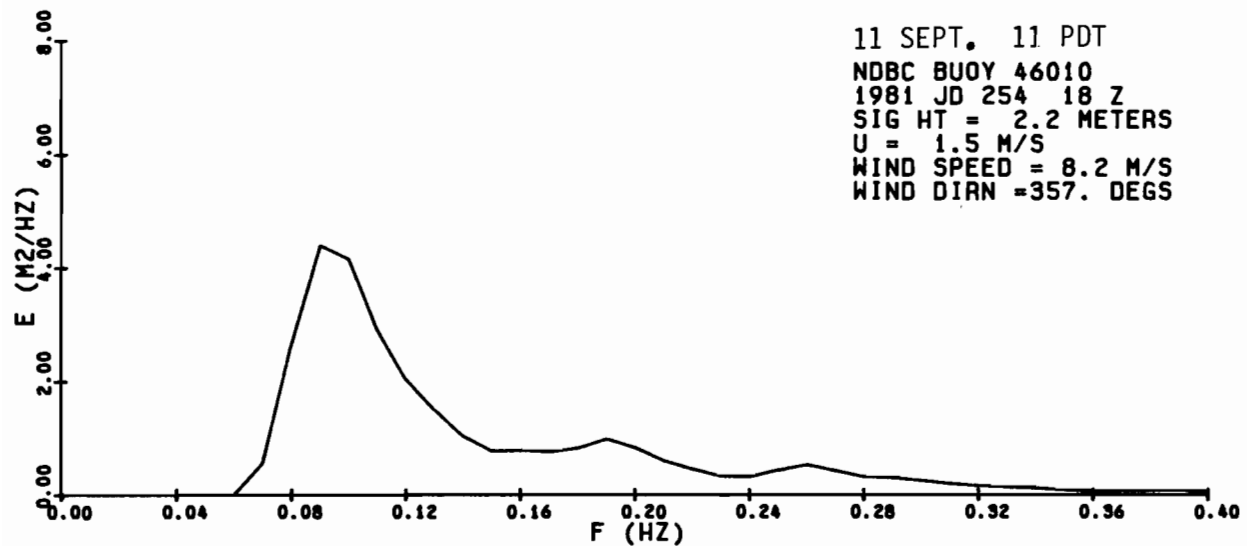
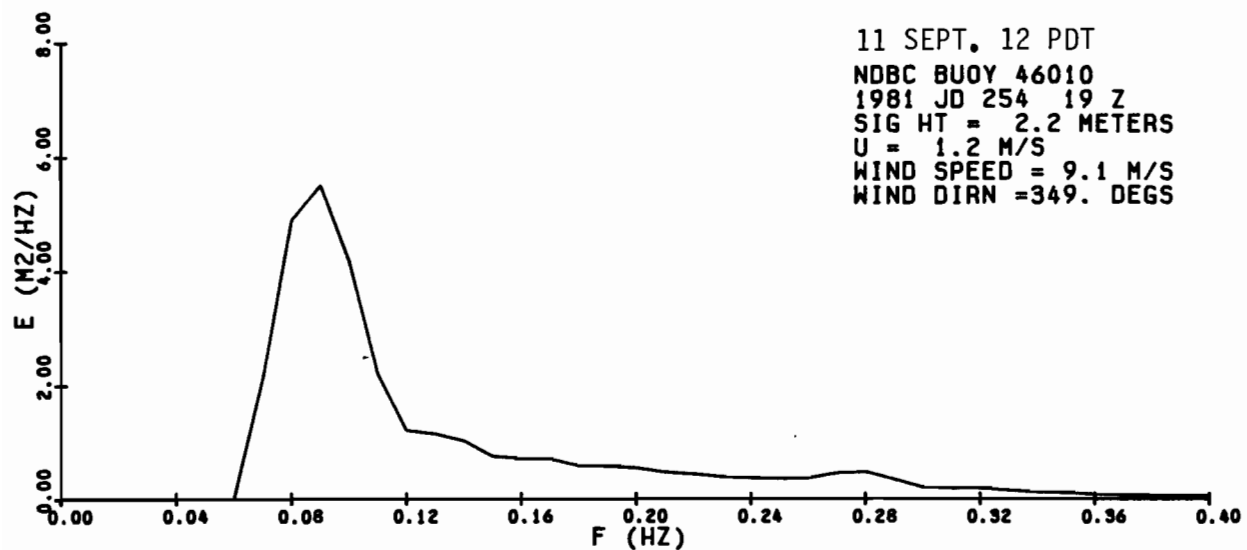
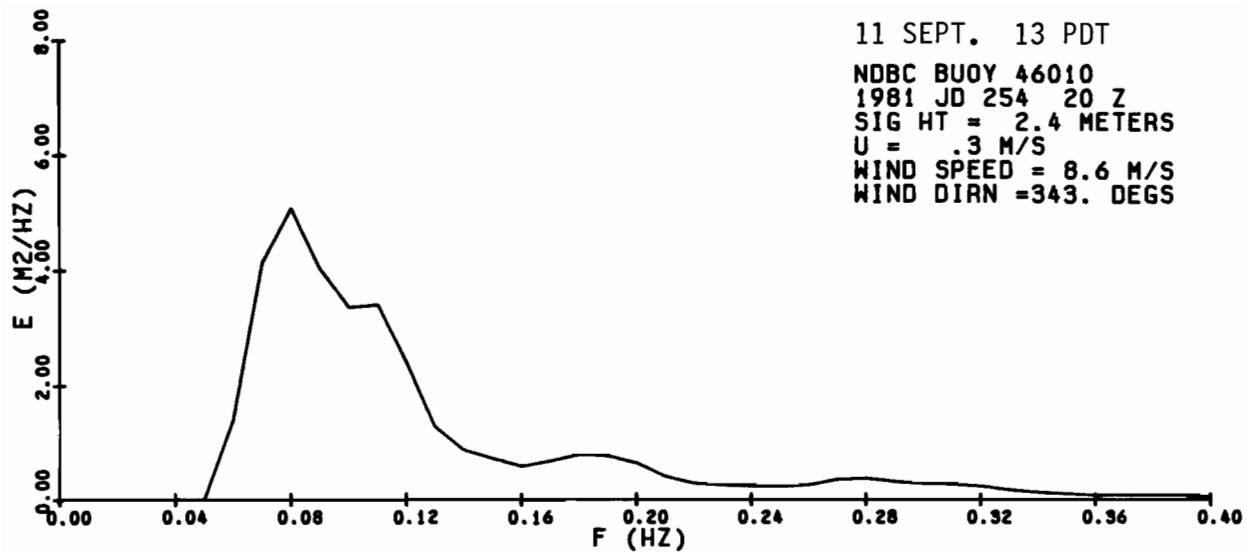


Figure A24. NDBC 46010 power spectral density for 1100, 1200, and 1300 PDT, 11 Sept. 1981.

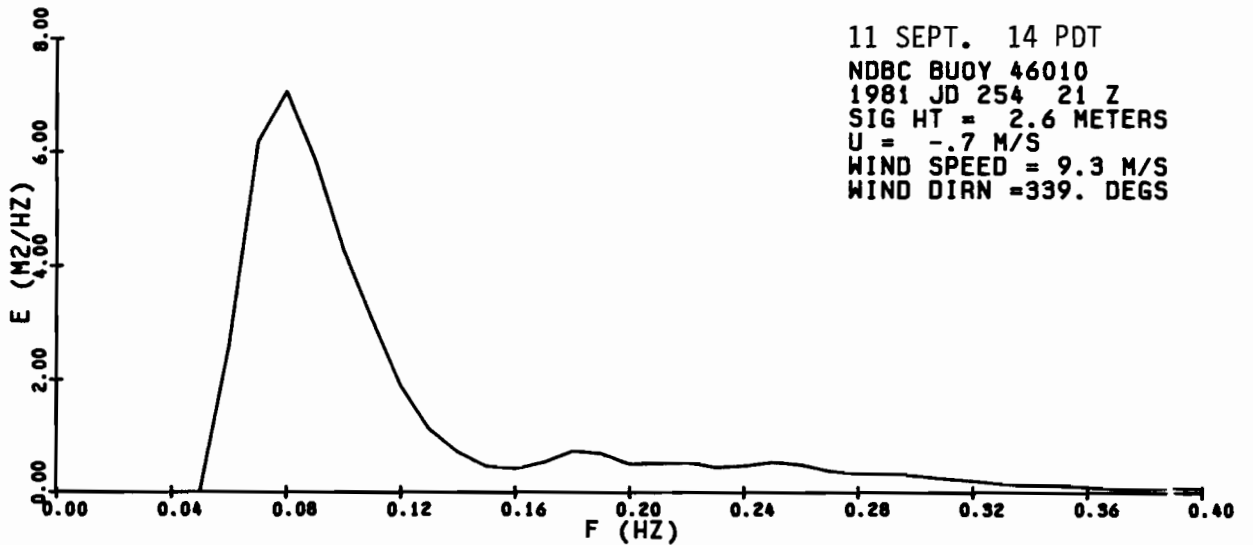
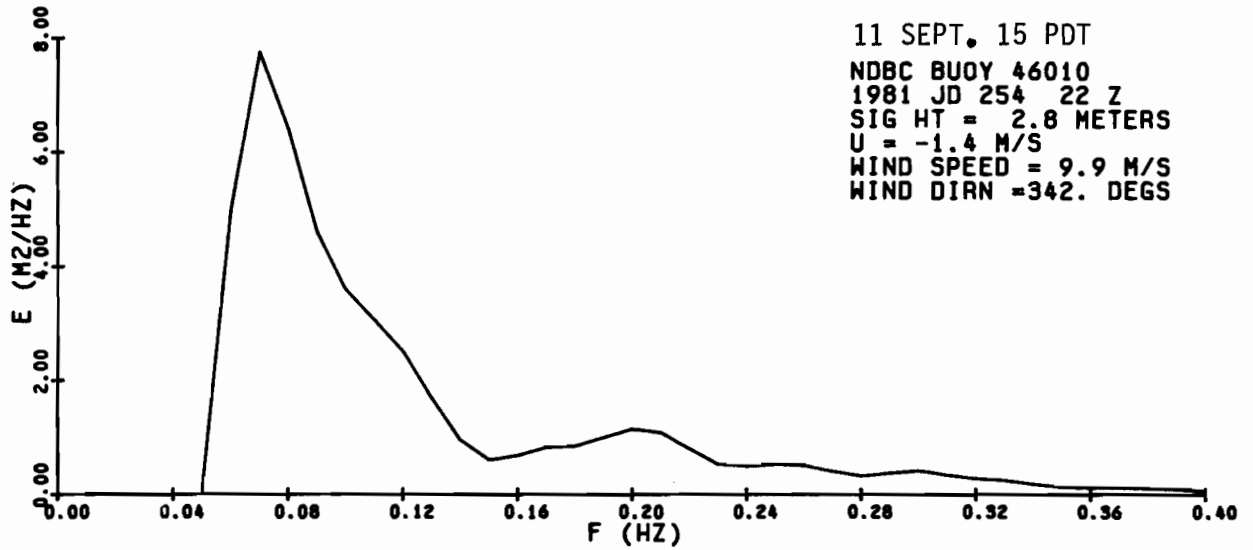
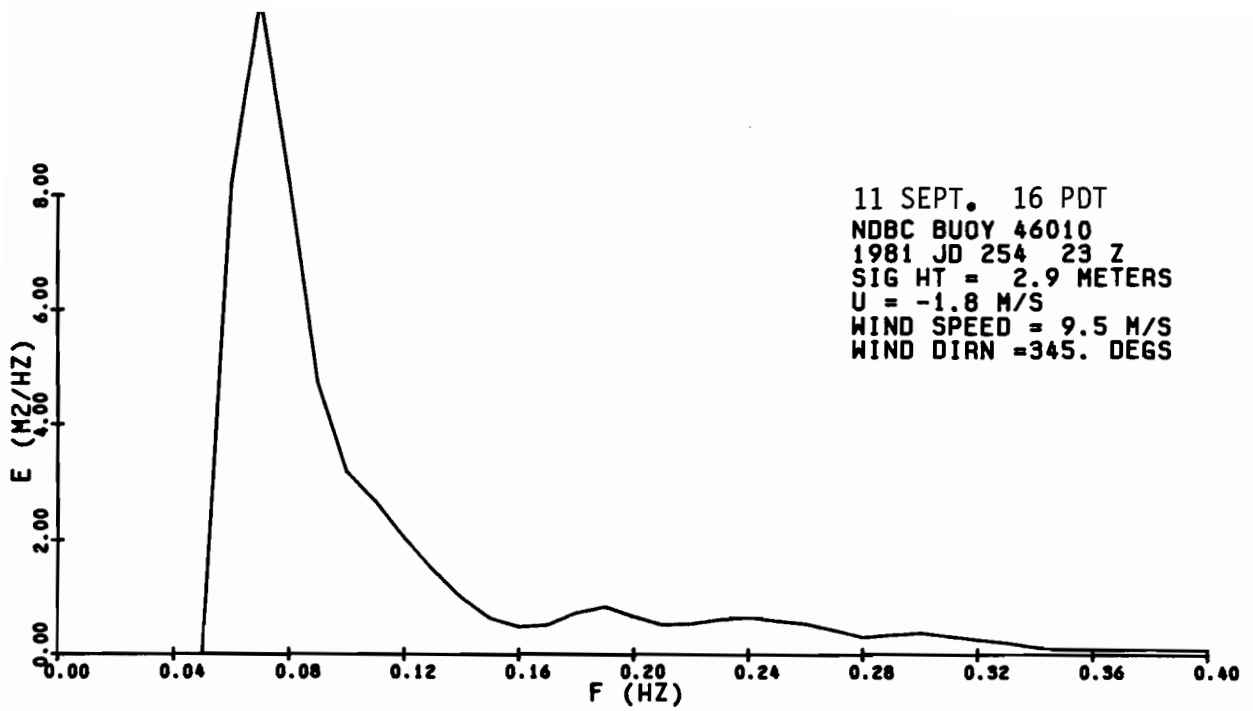


Figure A25. NDBC 46010 power spectral density for 1400, 1500, and 1600 PDT, 11 Sept. 1981.



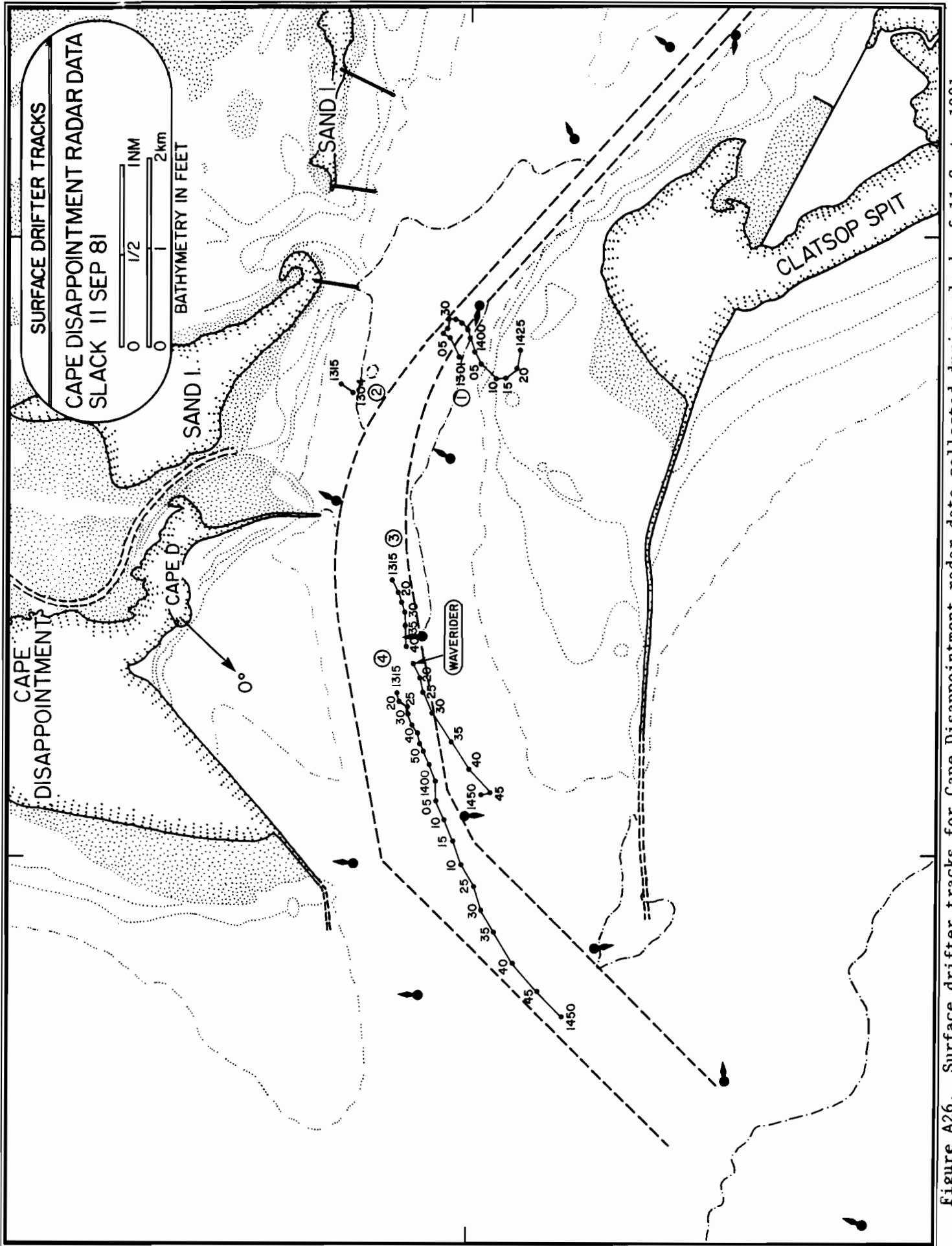


Figure A26. Surface drifter tracks for Cape Disappointment radar data collected during slack of 11 Sept. 1981.

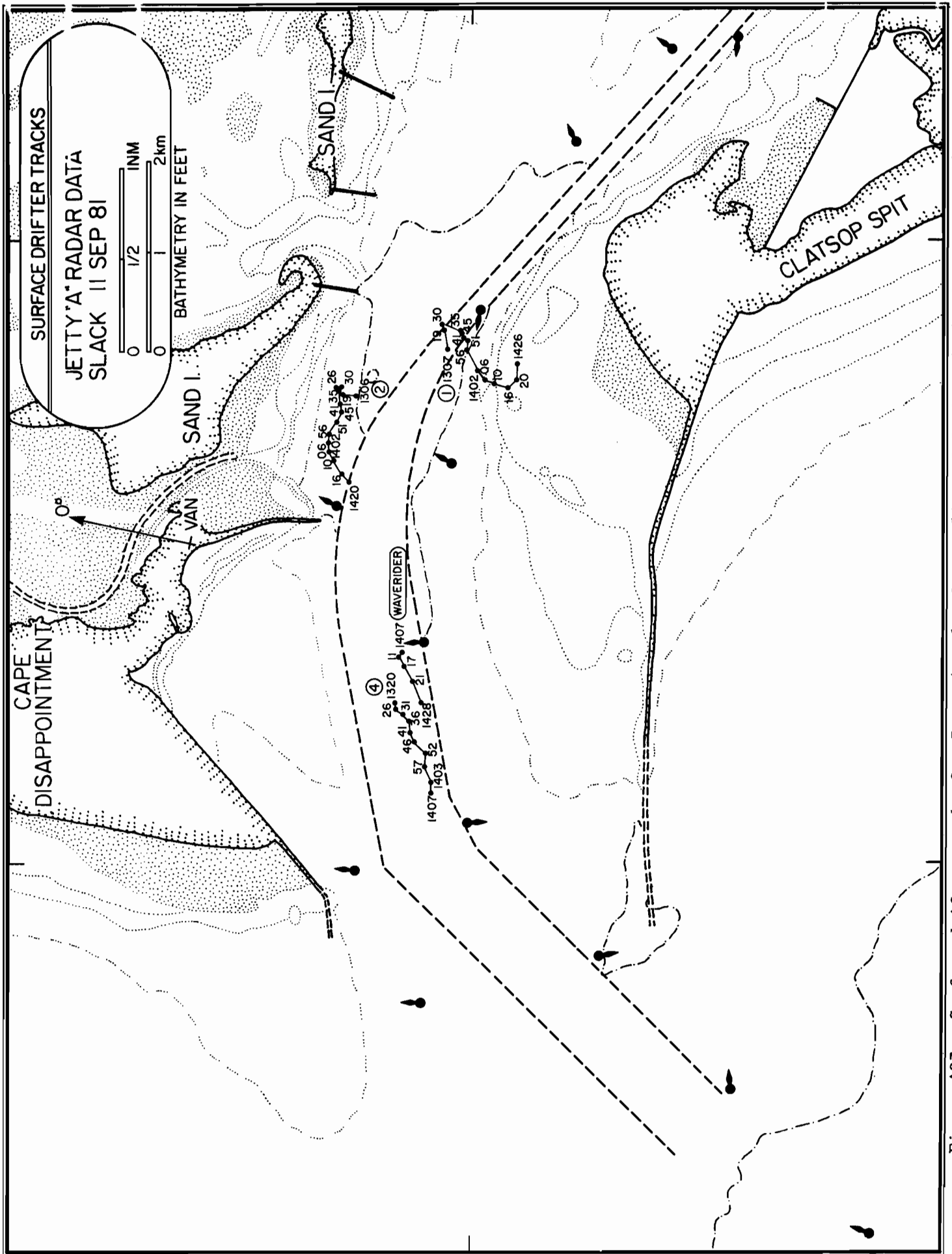
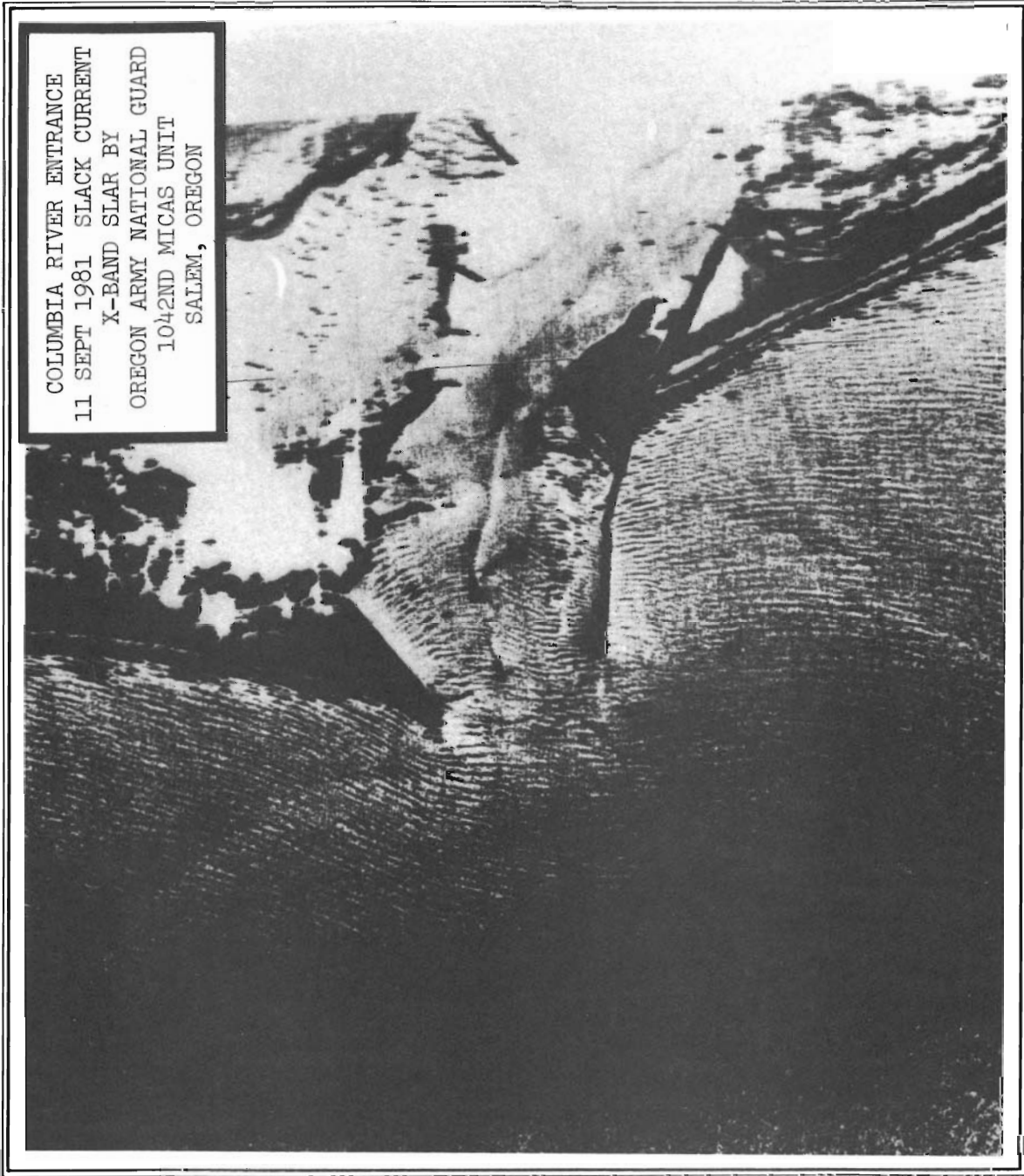


Figure A27. Surface drifter tracks for Jetty A radar data collected during slack of 11 Sept. 1981.



COLUMBIA RIVER ENTRANCE  
11 SEPT 1981 SLACK CURRENT  
X-BAND SLAR BY  
OREGON ARMY NATIONAL GUARD  
1042ND MICAS UNIT  
SALEM, OREGON

Figure A28. SLAR image of Columbia River entrance obtained on the slack at 1315 PDT, 11 Sept. 1981.

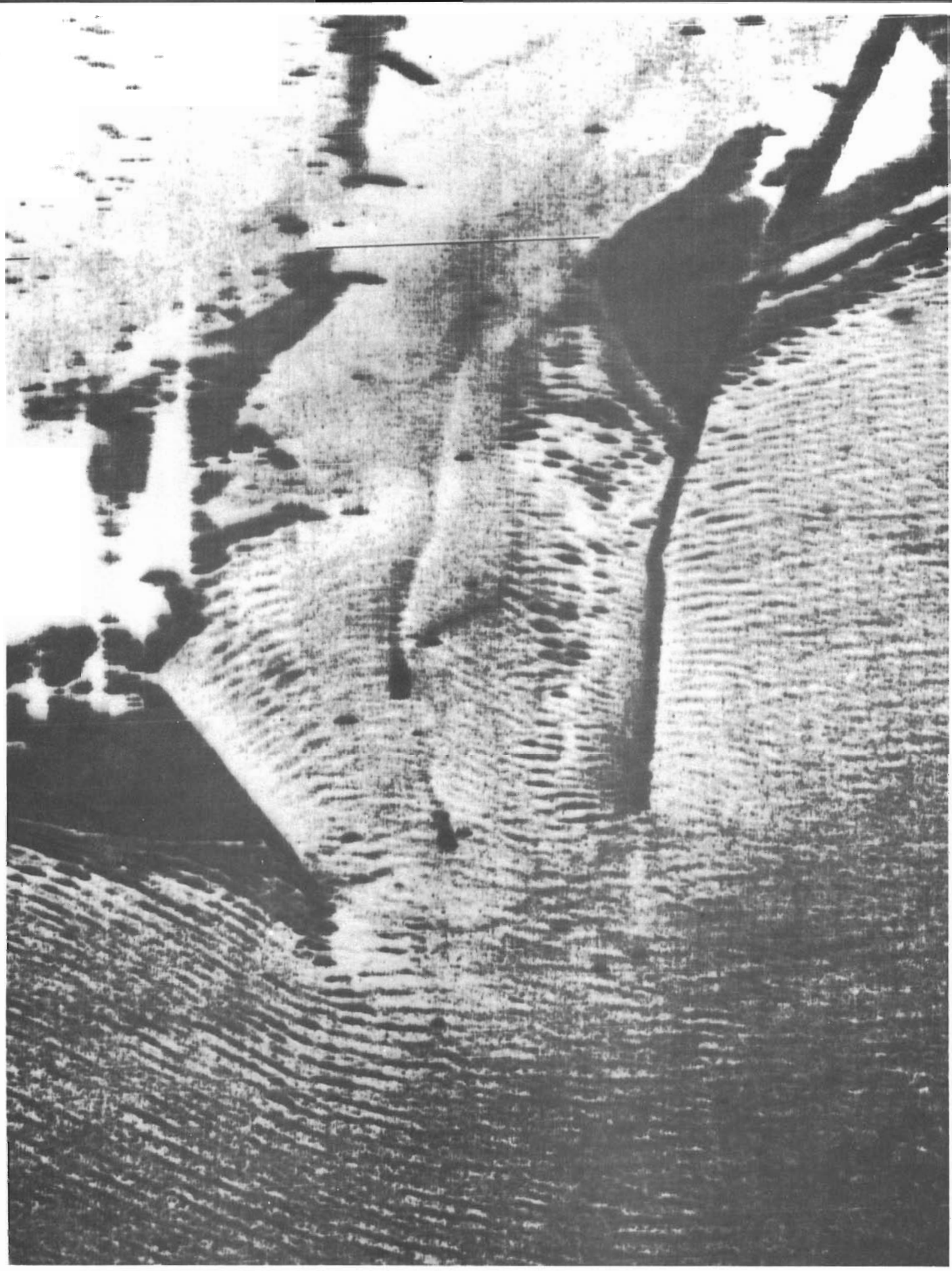


Figure A29. Blowup of Figure A28, centered on the river entrance.

11 September 1981

SLACK

Waverider LOG (Surface Vessel EGRET)

Time	Hdg.	Sextant Fixes	Objects	Remarks
1240				Recorder not on.
1315				WR deployed.
1320				Holding station N of Buoy 10 ~ 100 yds.  Current nearly slack.  ~ 15 kt. NW wind. Drift of buoy almost negligible by visual observation.
1329		22° 01'	1	
			2	
		05° 41'	3	
1337		20° 30'	1	Recorder not on
			2	for above.
		63° 55'	3	Data logger turned on. (At 1342.)
1355		28° 01'	1	Holding position NW
			2	of Buoy 10 very
		62° 30'	3	difficult due to opposed wind/current. Buoy 10 ~ 100 yds.
1358				Ebb increasing rapidly. One engine in gear req'd 50% of time to hold position.
1400		27° 46'	1	WR bears ~ 245 Mag.
			2	
		62° 53'	3	
1408		28° 15'	1	WR bears ~ 245 Mag.
			2	
		62°39'	3	

11 September 1981

SLACK

Waverider LOG (Surface Vessel EGRET)

Time	Hdg.	Sextant Fixes	Objects	Remarks
1409				Begin drift.
1411		28° 30'	1	Wave height
			2	~ 1.4 - 2 m.
		61° 43'	3	~ 13 sec.
1417		30° 05'	1	Free drift very
			2	difficult due to
		58° 25'	3	wind.
1422		31° 18'	1	EGRET may be
			2	putting drag on WR
		54° 26'	3	periodically.
1430		32° 53'	1	Buoy bears 350T.
			2	
		49° 42'	3	
1432		32° 58'	1	Buoy bears 350T.
			2	
		47° 48'	3	
1440		32° 50'	1	8 sec. 3 m.
			2	
		41° 28'	3	
1445		32° 28'	1	WR Buoy bears ~ 340
			2	250 ft.
		38° 00'	3	
1447				Underway to midchannel. End drift.
1507				WR aboard.

11 September 1981

SLACK

CAPE DISAPPOINTMENT RADAR DATA

Buoy No.	Time (PDT)	Range (nm.)	Bearing (deg.)	Remarks
1	1301	2.11	271	
	1305	2.16	268	
	1310	2.15	267	
	1315	2.19	267	
	1320	2.23	266	
	1325	2.21	266	
	1330	2.23	266	
	1335	2.26	267	
	1340	2.26	269	
	1345	2.25	268	
	1350	2.25	269	
	1355	2.22	270	
	1400	2.19	272	
	1405	2.18	274	
	1410	2.19	277	
	1415	2.23	278	
	1420	2.31	277	
1425	2.39	276	Pick up Buoy #1 at 1428	
2	1304	1.57	263	
	1305	1.58	262	
	1310	1.58	259	
	1315	1.57	259	Lost Buoy #2 in blind spot
3	1315	1.17	304	
	1320	1.19	307	
	1325	1.20	310	
	1330	1.21	313	
	1335	1.21	316	
	1340	1.21	322	
	1345	1.28	322	Waverider track starts
	1350	1.26	322	
	1355	1.24	323	
	1400	1.23	323	
	1405	1.25	323	
	1410	1.24	324	
	1415	1.27	326	
	1420	1.33	329	
	1425	1.37	332	
1430	1.46	336		
1435	1.61	340		

11 September 1981

SLACK

CAPE DISAPPOINTMENT RADAR DATA

---

Buoy No.	Time (PDT)	Range (nm.)	Bearing (deg.)	Remarks
	1440	1.78	343	
	1445	1.93	345	
	1450	1.90	346	Pick up Buoy #3
4	1315	1.23	334	
	1320	1.27	336	
	1325	1.32	337	
	1330	1.33	338	
	1335	1.38	340	
	1340	1.42	341	
	1345	1.45	343	
	1350	1.50	344	
	1355	1.56	346	
	1400	1.64	348	
	1405	1.70	351	
	1410	1.81	353	
	1415	1.92	355	
	1420	2.05	357	
	1425	2.18	358	
	1430	2.30	000	
	1435	2.44	001	
	1440	2.63	002	
	1445	2.85	002	
	1450	3.04	002	

---



11 September 1981

SLACK

JETTY A RADAR DATA

Buoy No.	Time (PDT)	Range (nm.)	Bearing (deg.)	Remarks
1	1307	1.79	141	
	1319	1.85	138	
	1330	1.85	137	
	1335	1.91	140	
	1341	1.90	141	
	1345	1.89	140	
	1351	1.90	142	
	135530	1.87	143	
	140130	1.86	147	
	140555	1.87	149	
	140945	1.90	150	
	141603	1.96	152	
	142020	2.02	151	
	142620	2.07	149	
2	1306	1.22	136	
	1319	1.18	133	
	1326	1.20	131	
	1330	1.21	132	
	1335	1.19	132	
	1341	1.13	135	
	1345	1.10	137	
	1351	1.05	138	
	135600	0.99	140	
	140155	0.94	142	
	140620	0.92	145	
	141015	0.91	148	
	141628	0.92	153	
	142032	0.94	157	
"Waverider" (Vessel EGRET) positions from 140635 to 142755:				
	140635	1.31	206	Most likely "Waverider"
	141045	1.30	207	
	141647	1.36	209	Other targets nearby
	142112	1.44	211	
	142755	1.54	214	
4	1320	1.42	217	
	1326	1.46	218	
	1331	1.50	218	
	1336	1.56	218	

11 September 1981

SLACK

JETTY A RADAR DATA

---

Buoy No.	Time (PDT)	Range (nm.)	Bearing (deg.)	Remarks
4	1341	1.60	220	
	1346	1.64	221	
	1352	1.74	221	
	135700	1.78	223	
	140230	1.87	224	
	140710	1.90	225	

---

11 September 1981

EBB



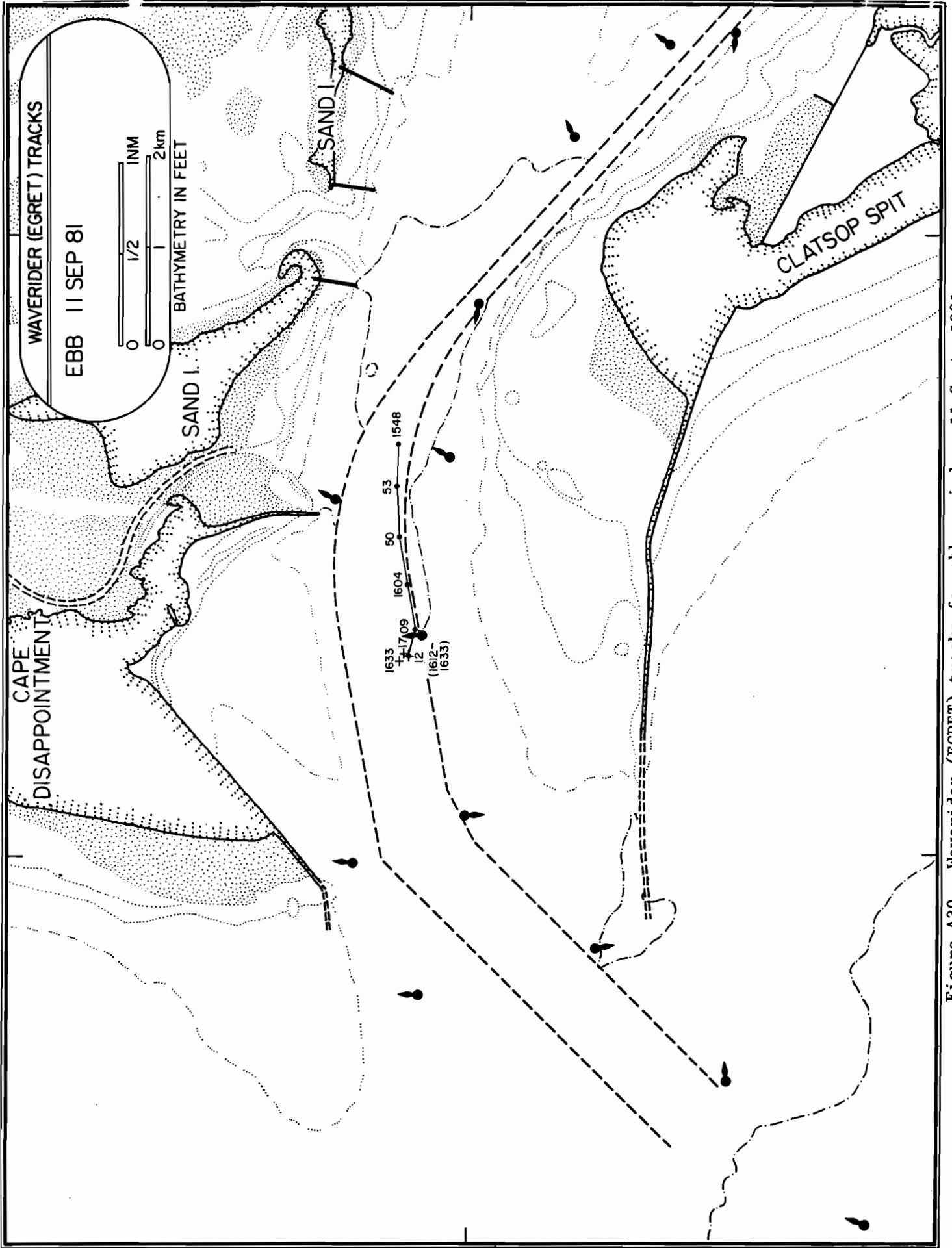


Figure A30. Waverider (EGRET) tracks for ebb period on 11 Sept. 1981.

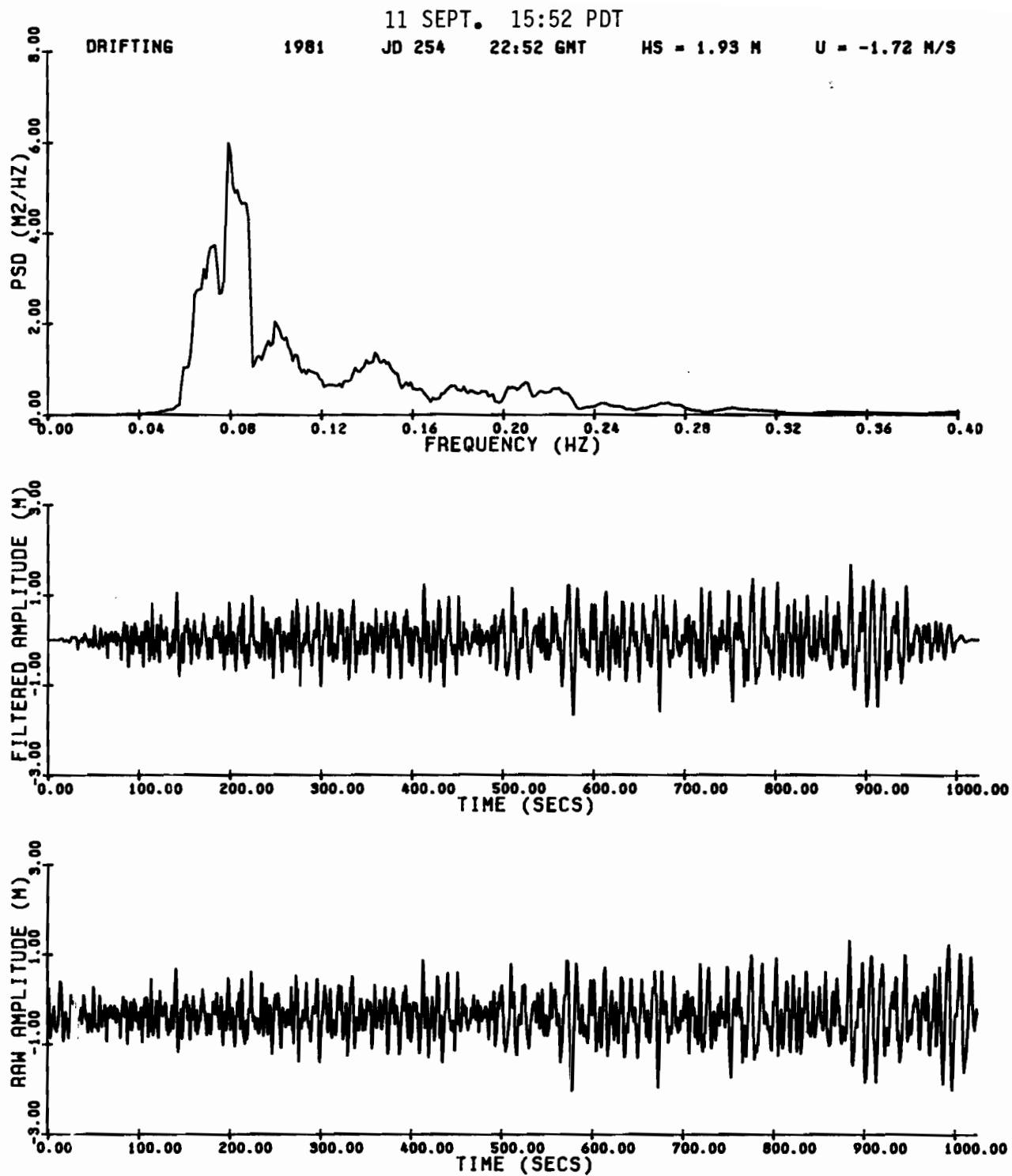


Figure A31. Waverider raw amplitude, filtered amplitude, and power spectral density for 1552 PDT, 11 Sept. 1981.

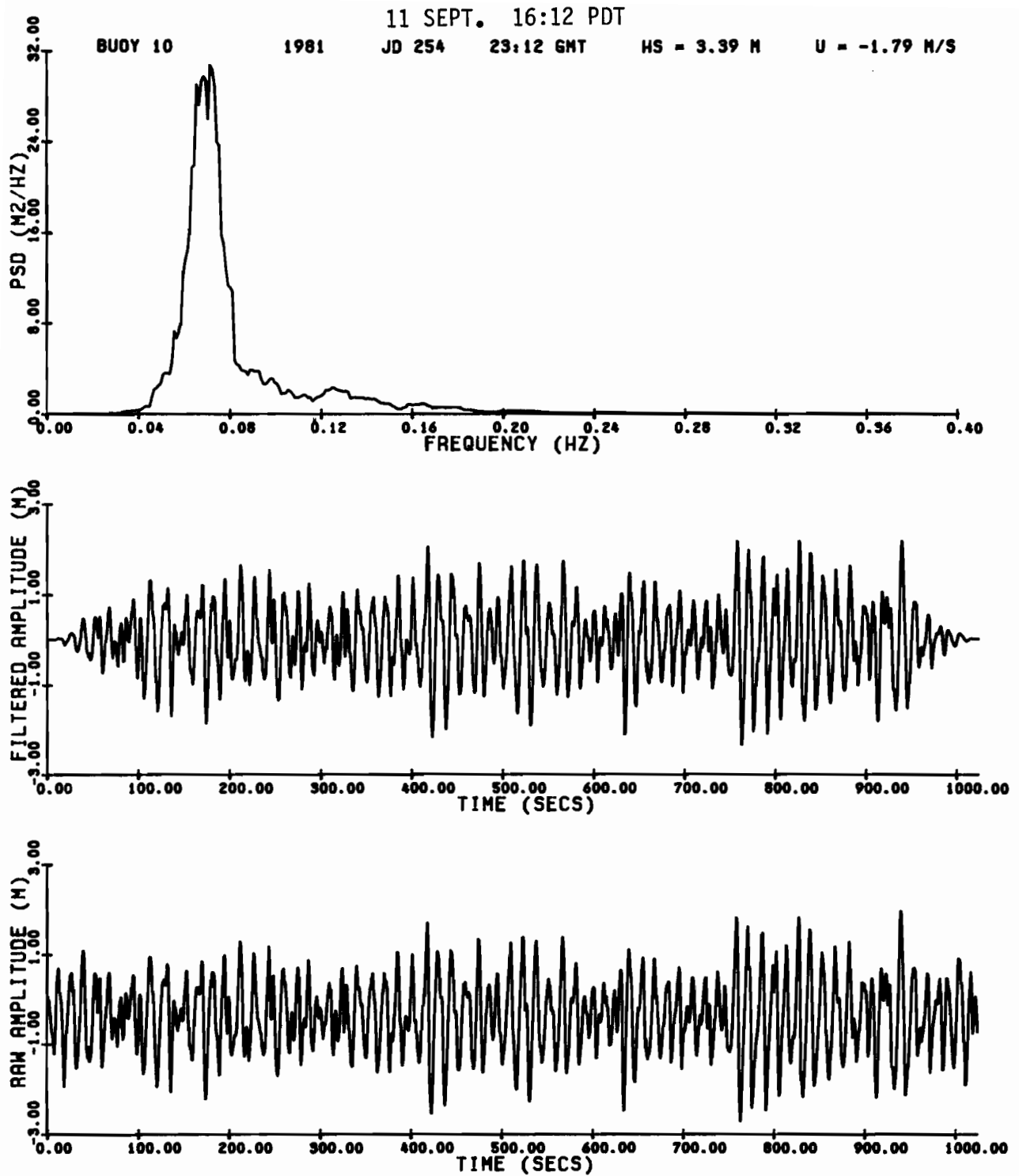


Figure A32. Waverider raw amplitude, filtered amplitude, and power spectral density for 1612 PDT, 11 Sept. 1981.

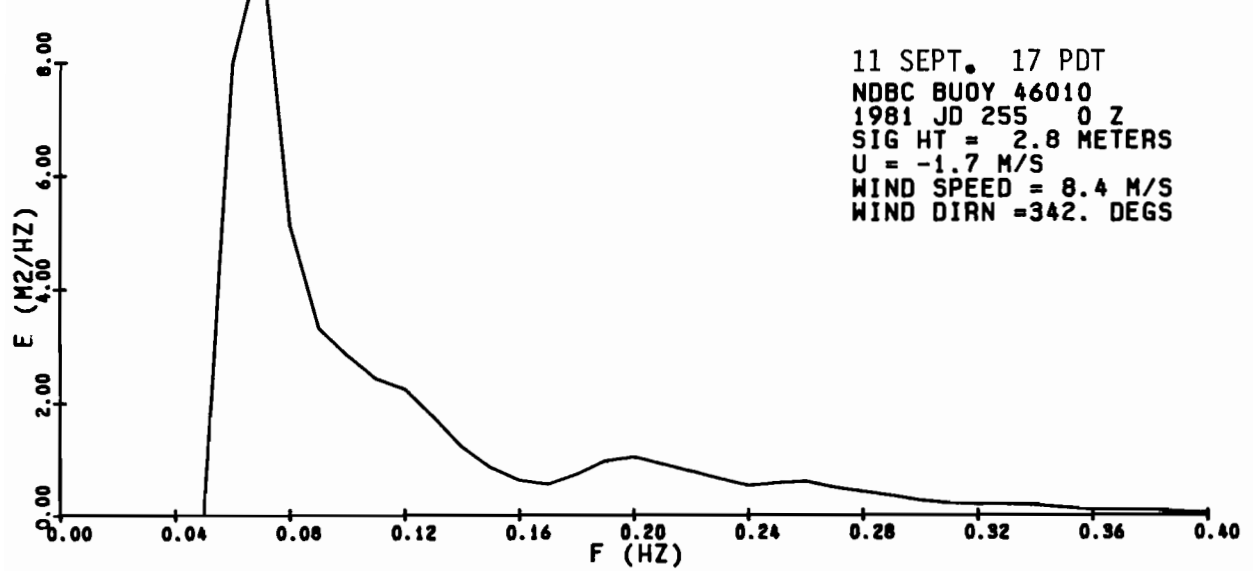
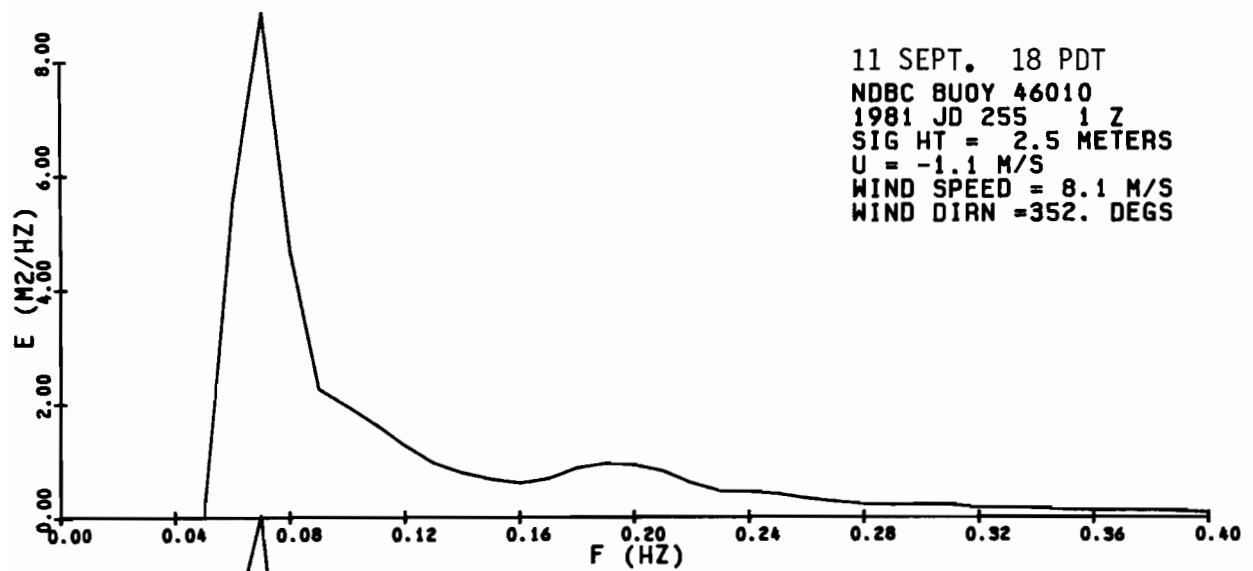
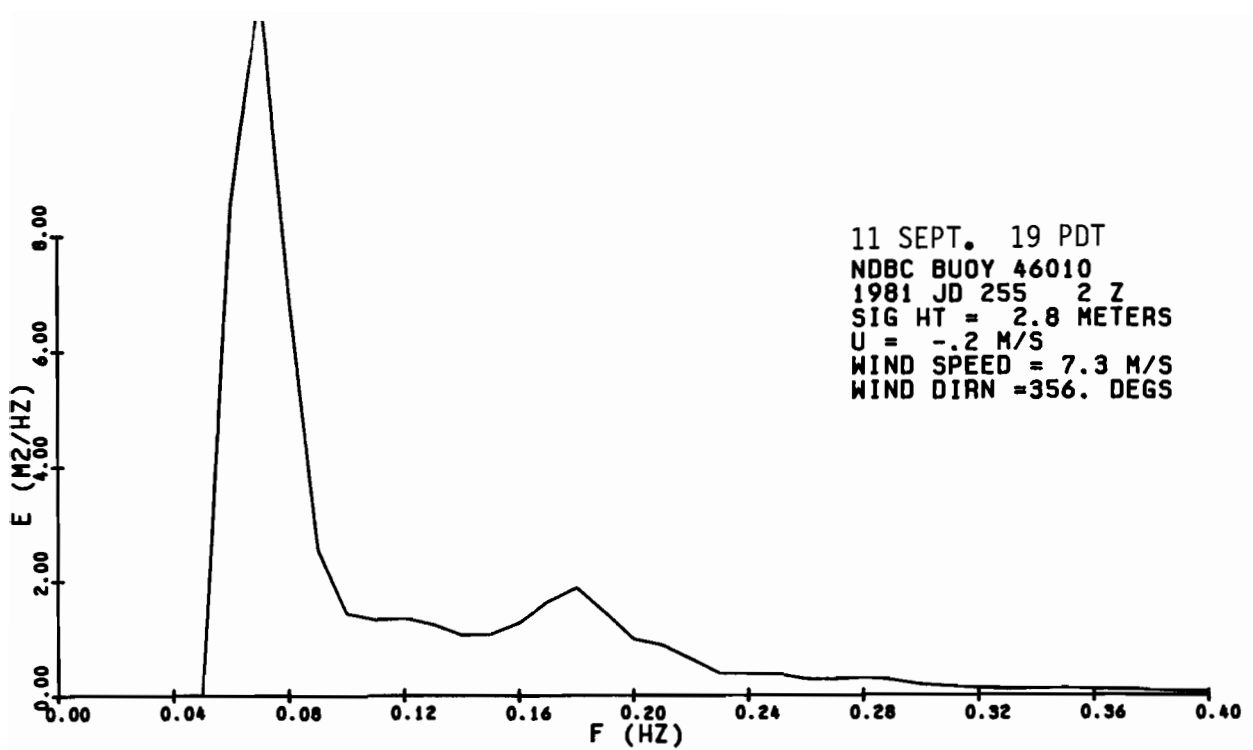


Figure A33. NDBC 46010 power spectral density for 1700, 1800, and 1900 PDT, 11 Sept. 1981.



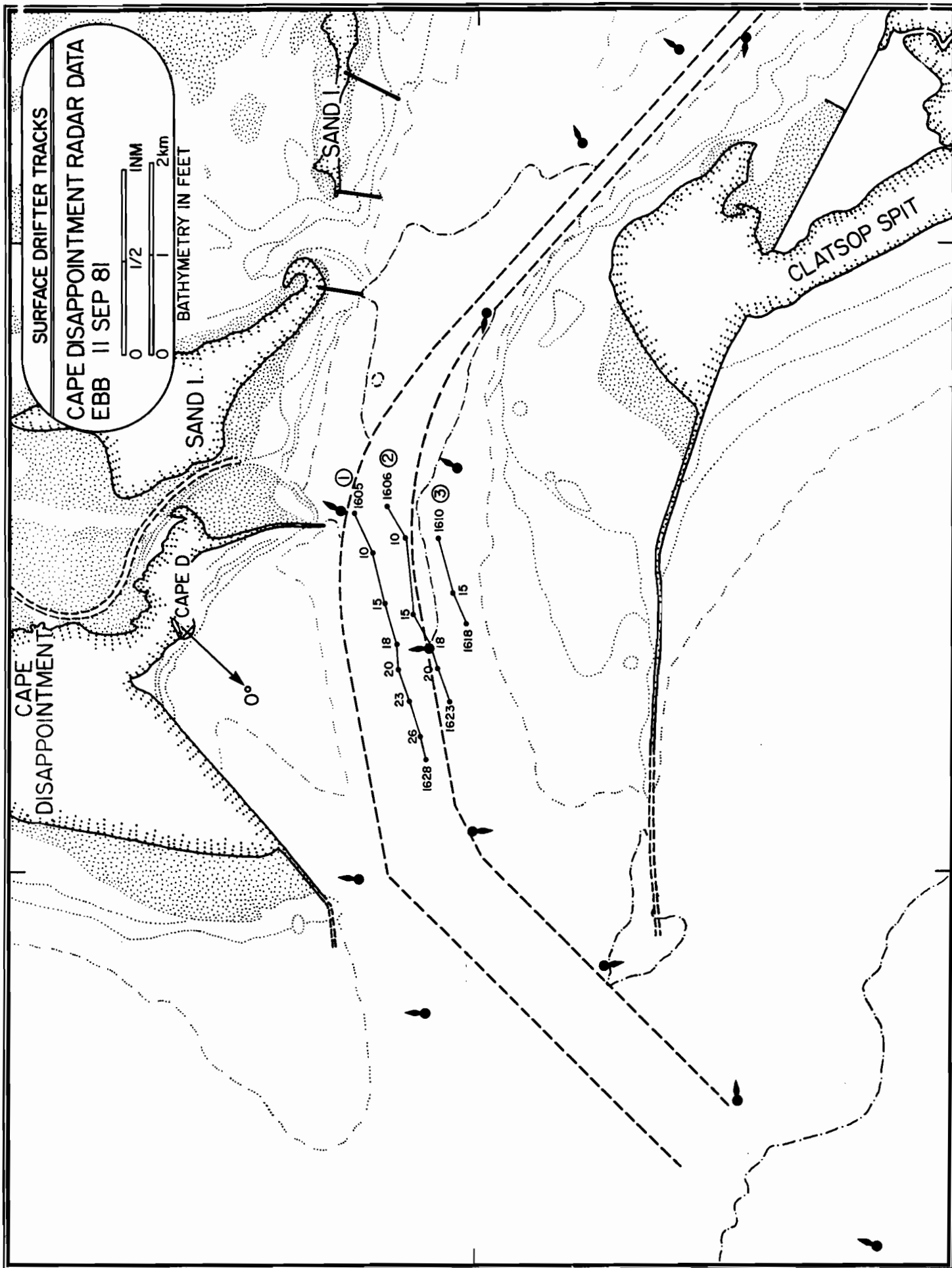
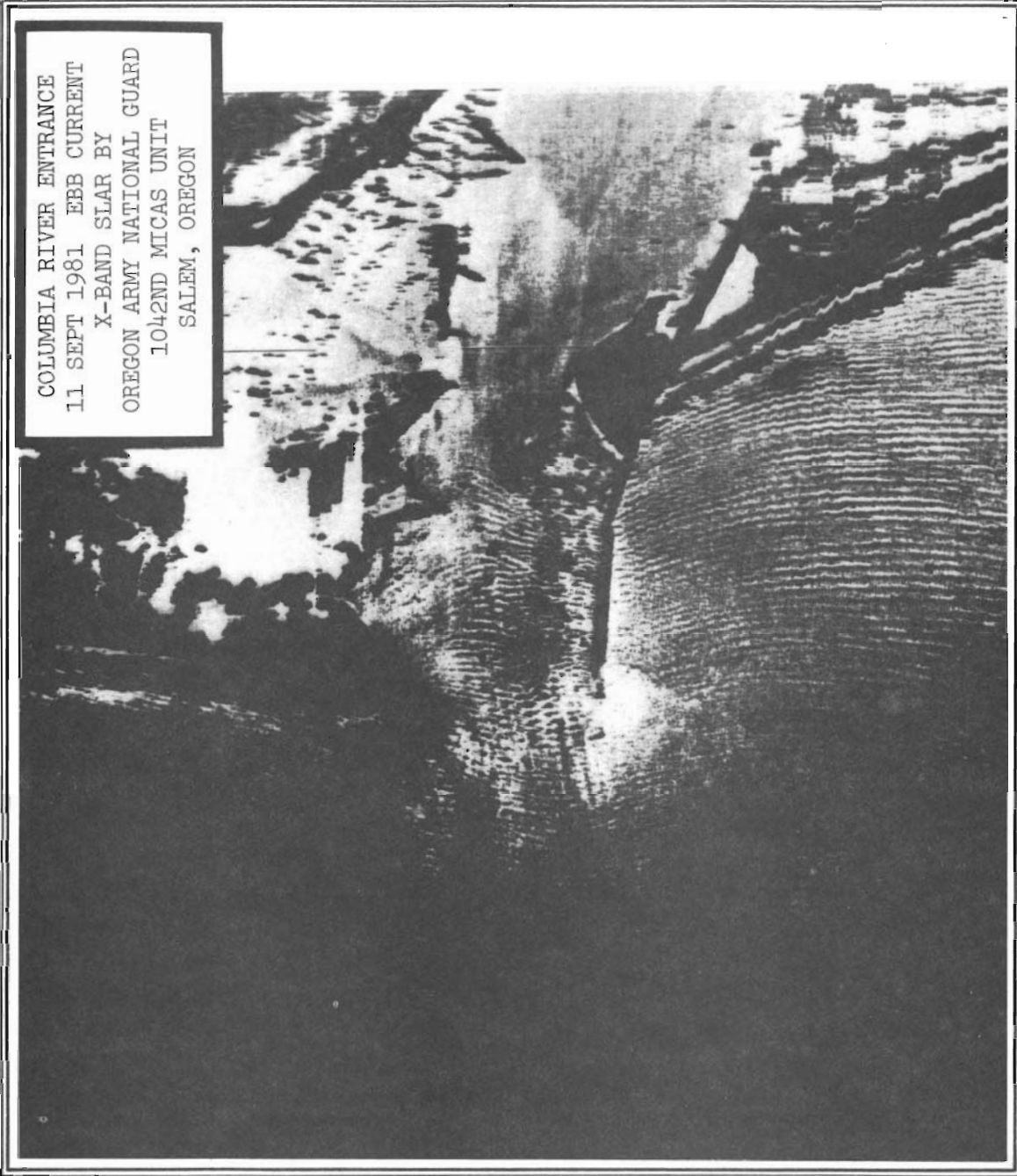


Figure A34. Surface drifter tracks for Cape Disappointment radar data collected during ebb of 11 Sept. 1981.



COLUMBIA RIVER ENTRANCE  
11 SEPT 1981 EBB CURRENT  
X-BAND SLAR BY  
OREGON ARMY NATIONAL GUARD  
1042ND MICAS UNIT  
SALEM, OREGON

Figure A35. SLAR image of Columbia River entrance obtained on the ebb at 1630 PDT, 11 Sept. 1981.

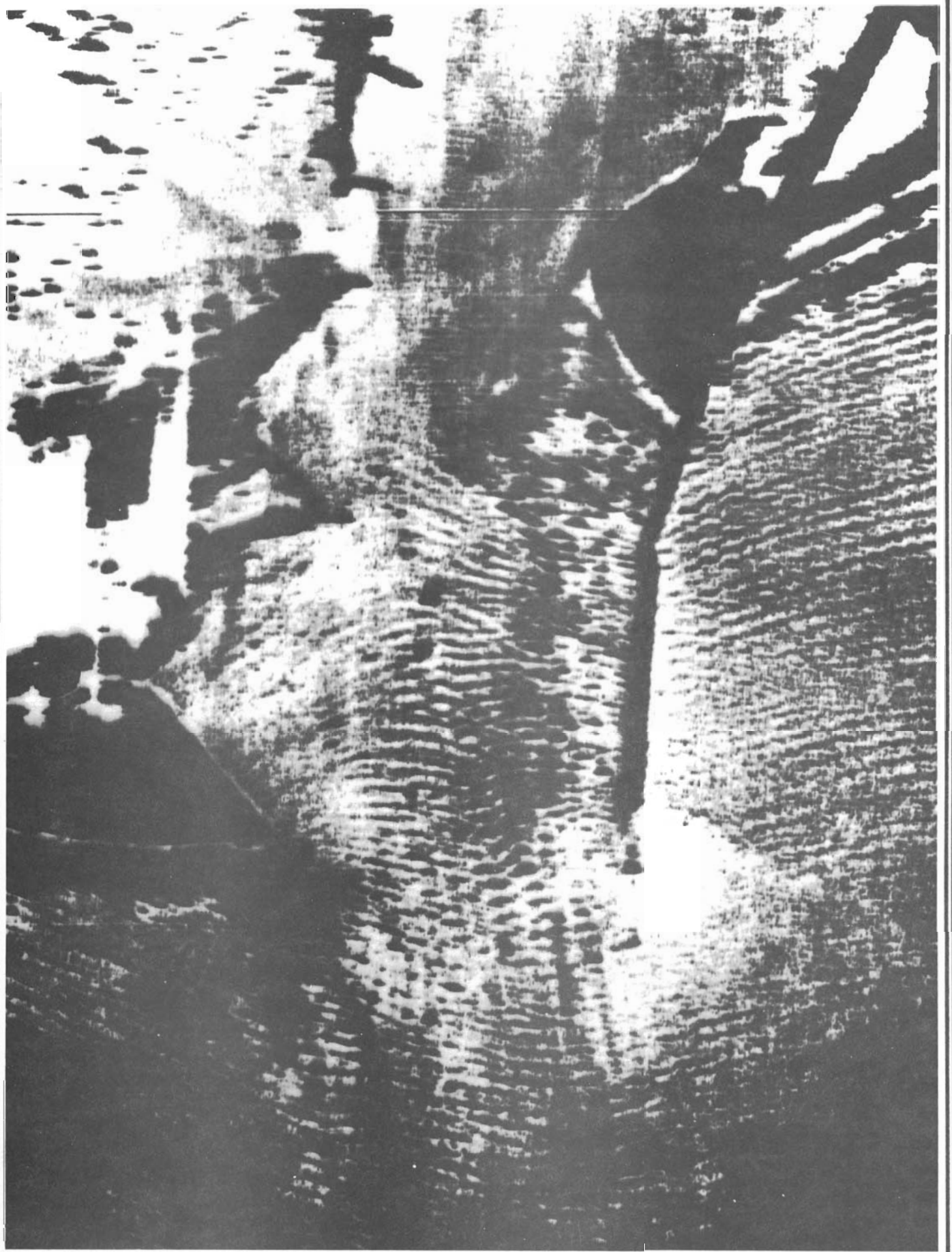


Figure A36. Blowup of Figure A35, centered on the river entrance.

11 September 1981

EBB

Waverider LOG (Surface Vessel EGRET)

Time	Hdg.	Sextant Fixes	Objects	Remarks
1545				WR in water NE of Buoy 12.
1548		79° 39'	5	Begin drift. (1.5 m, 12 sec.) WR buoy W 200 ft.
		19° 50'	3 12	
1553		70° 43'	5	
		13° 51'	3 12	
1559		35° 18'	2	WR buoy NW 200 ft.
		50° 08'	5 3	
1604		40° 27'	2	
		34° 52'	5 3	
1609		39° 37'	2	
		26° 01'	5 3	
1610				Stop drift, maneuver to holding station.
1612		28° 30'	1	On station. (8 sec. 2 m.)
		39° 40'	2 5	
1625		29° 05'	1	(drift log 13, 12, 12 sec. for 25 m.)
			2	
		61° 53'	3	
1633		29° 24'	1	End holding sta.
			2	
		61° 29'	3	
1640				WR aboard.

11 September 1981

EBB

CAPE DISAPPOINTMENT RADAR DATA

---

Buoy No.	Time (PDT)	Range (nm.)	Bearing (deg.)	Remarks
1	1605	1.12	283	
	1610	1.10	296	
	1615	1.08	311	
	1618	1.14	323	
	1620	1.17	330	
	1623	1.26	337	
	1626	1.39	344	
	1628	1.48	348	Picked up Buoy #1
2	1606	1.29	287	
	1610	1.29	296	
	1615	1.23	315	
	1618	1.31	323	
	1620	1.37	328	
	1623	1.47	335	Picked up Buoy #2
	3	1610	1.45	299
1615		1.47	311	
1618		1.51	318	Picked up #3 Targets impossible to follow.

---

11 September 1981

EBB

JETTY A RADAR DATA

---

Buoy No.	Time (PDT)	Range (nm.)	Bearing (deg.)	Remarks
-------------	---------------	----------------	-------------------	---------

---

Targets impossible  
to follow.

12 September 1981

FLOOD





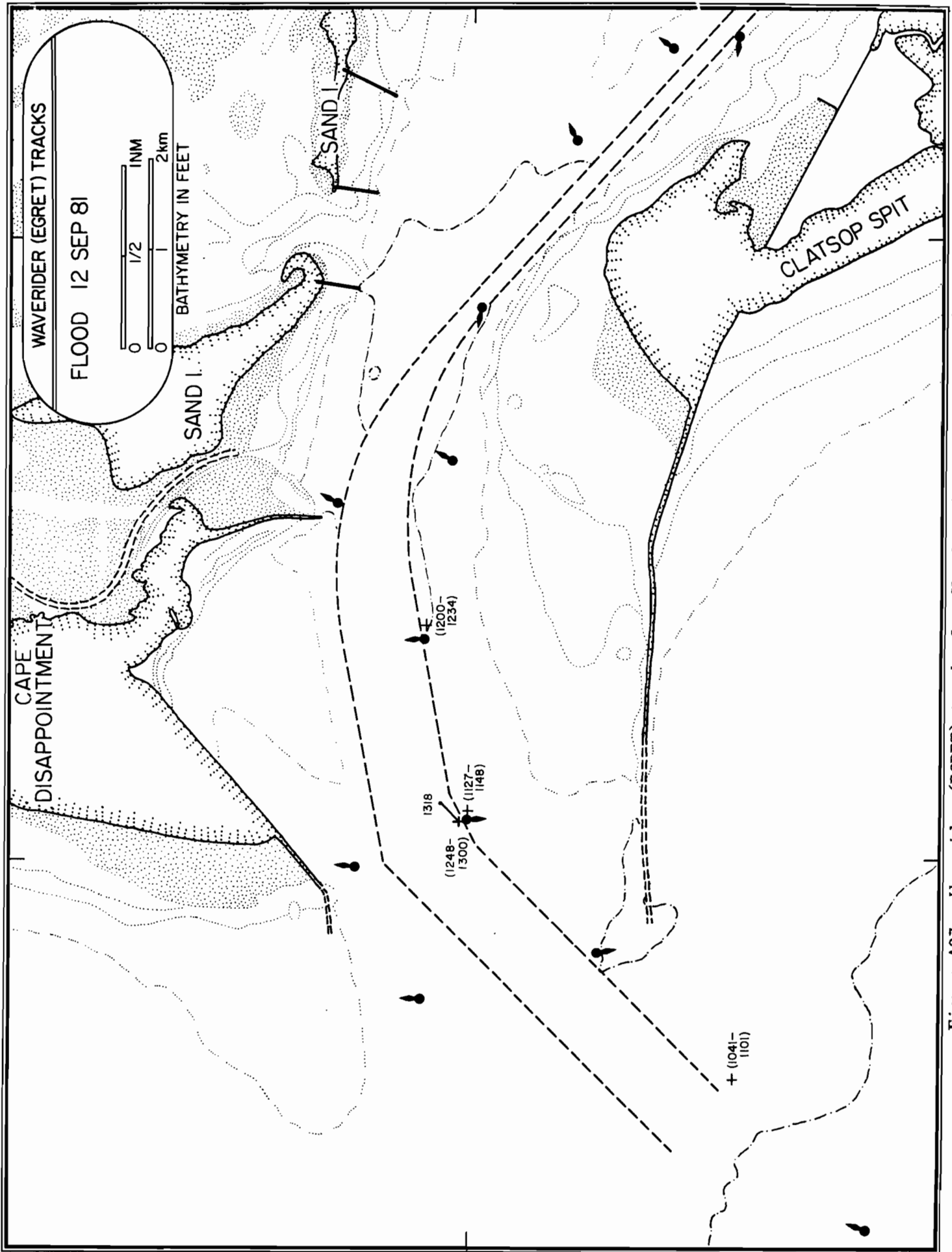


Figure A37. Waverider (EGRET) tracks for flood period on 12 Sept. 1981.

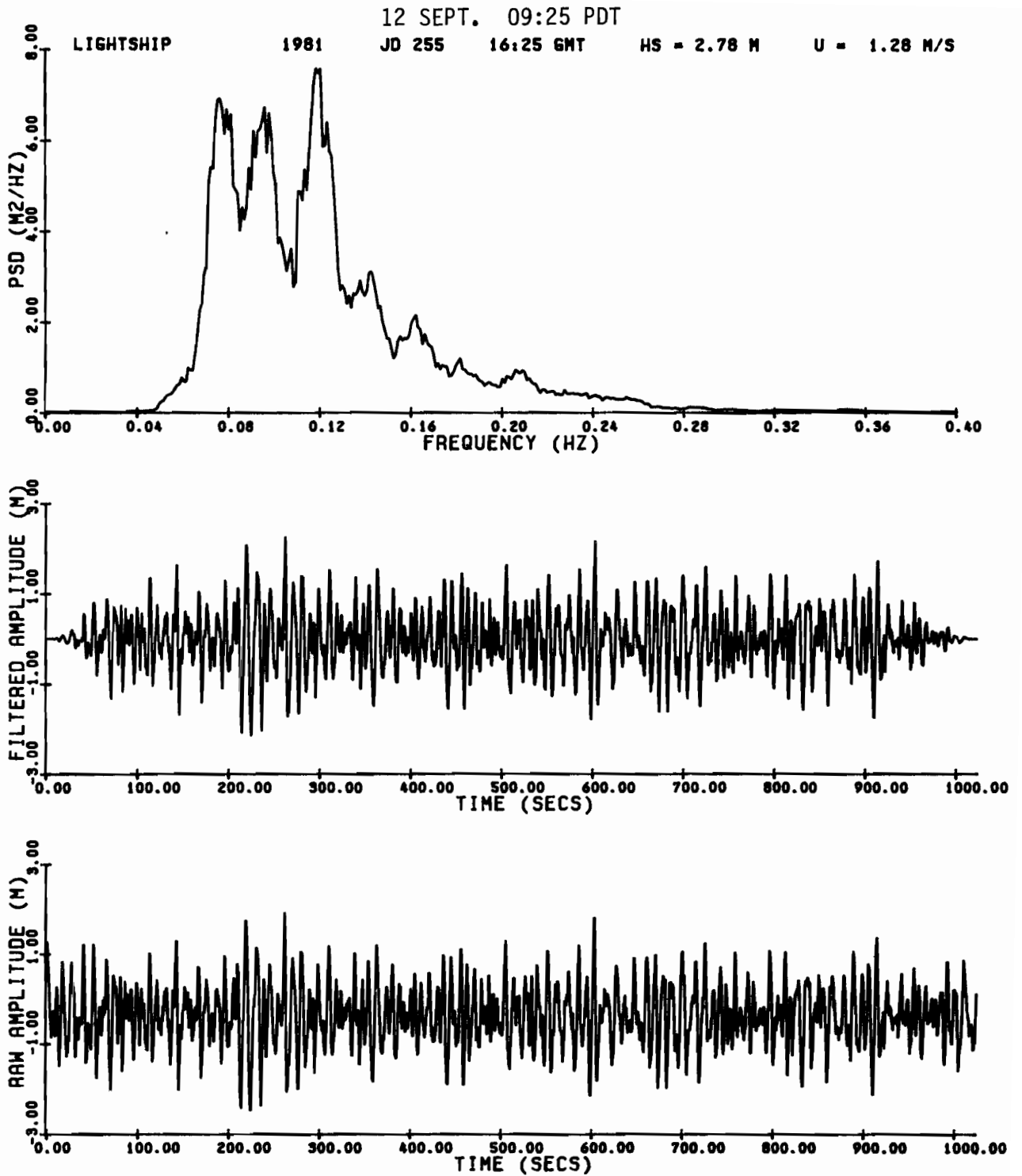


Figure A38. Waverider raw amplitude, filtered amplitude, and power spectral density for 0925 PDT, 12 Sept. 1981.

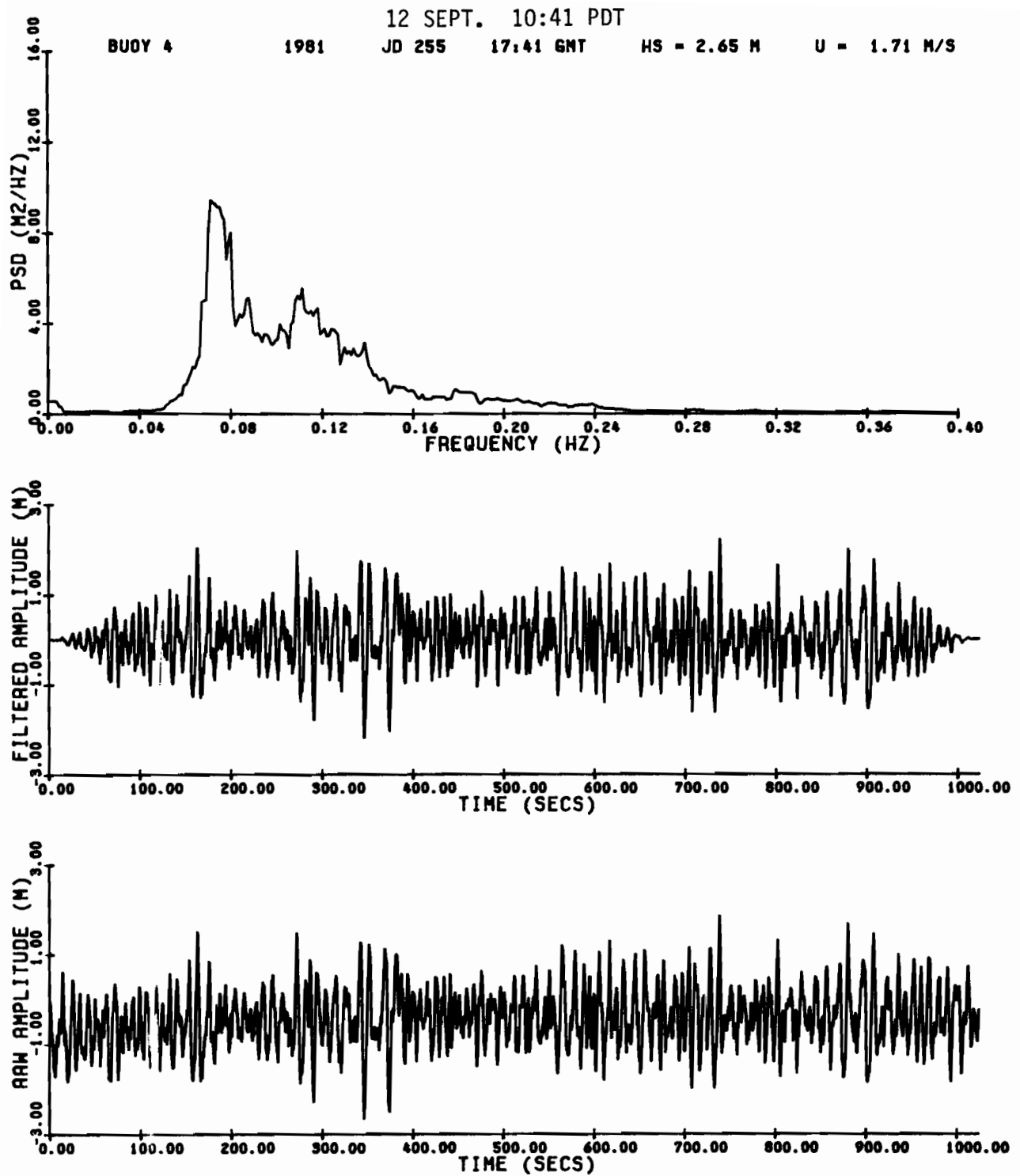


Figure A39. Waverider raw amplitude, filtered amplitude, and power spectral density for 1041 PDT, 12 Sept. 1981.

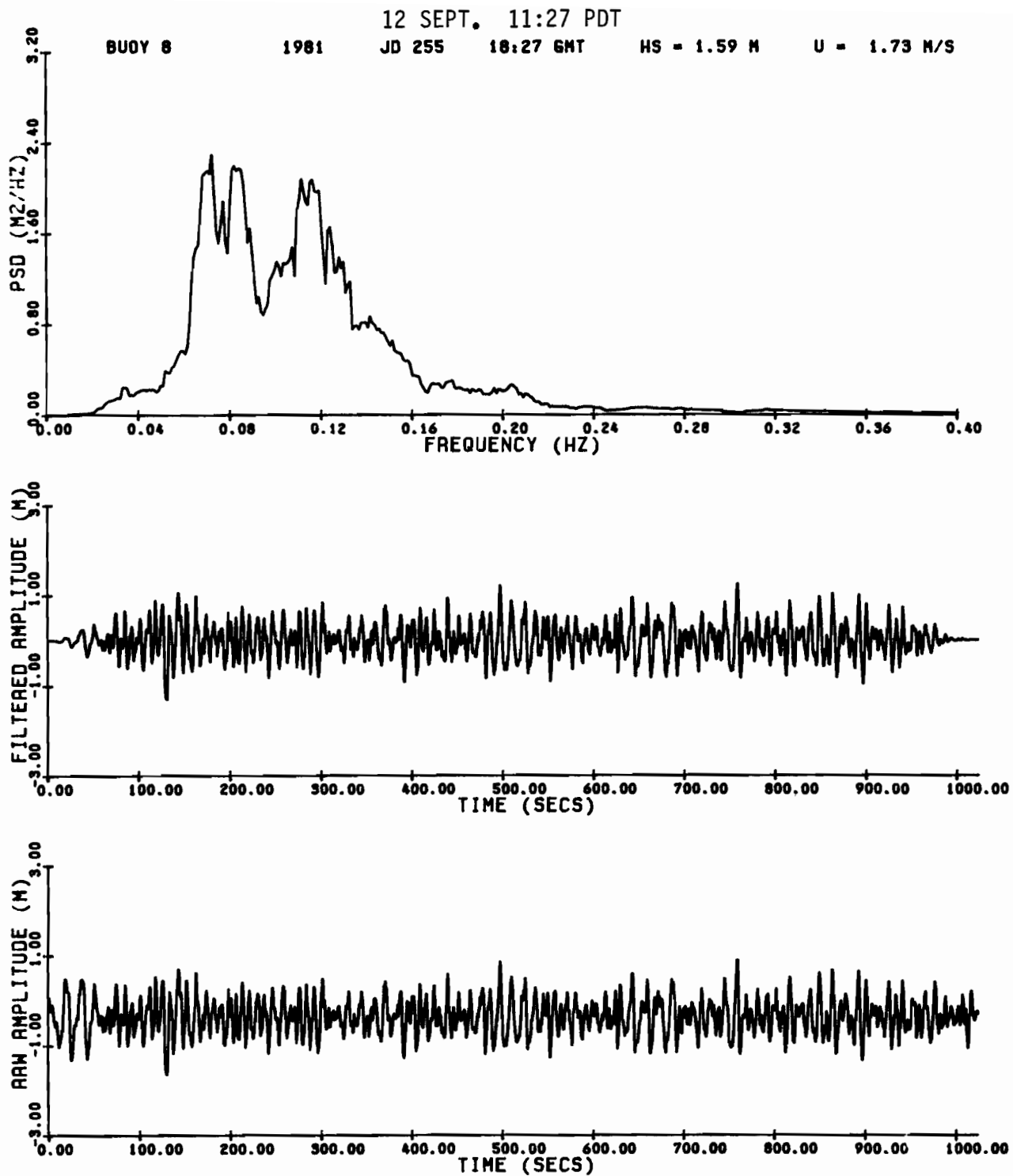


Figure A40. Waverider raw amplitude, filtered amplitude, and power spectral density for 1127 PDT, 12 Sept. 1981.

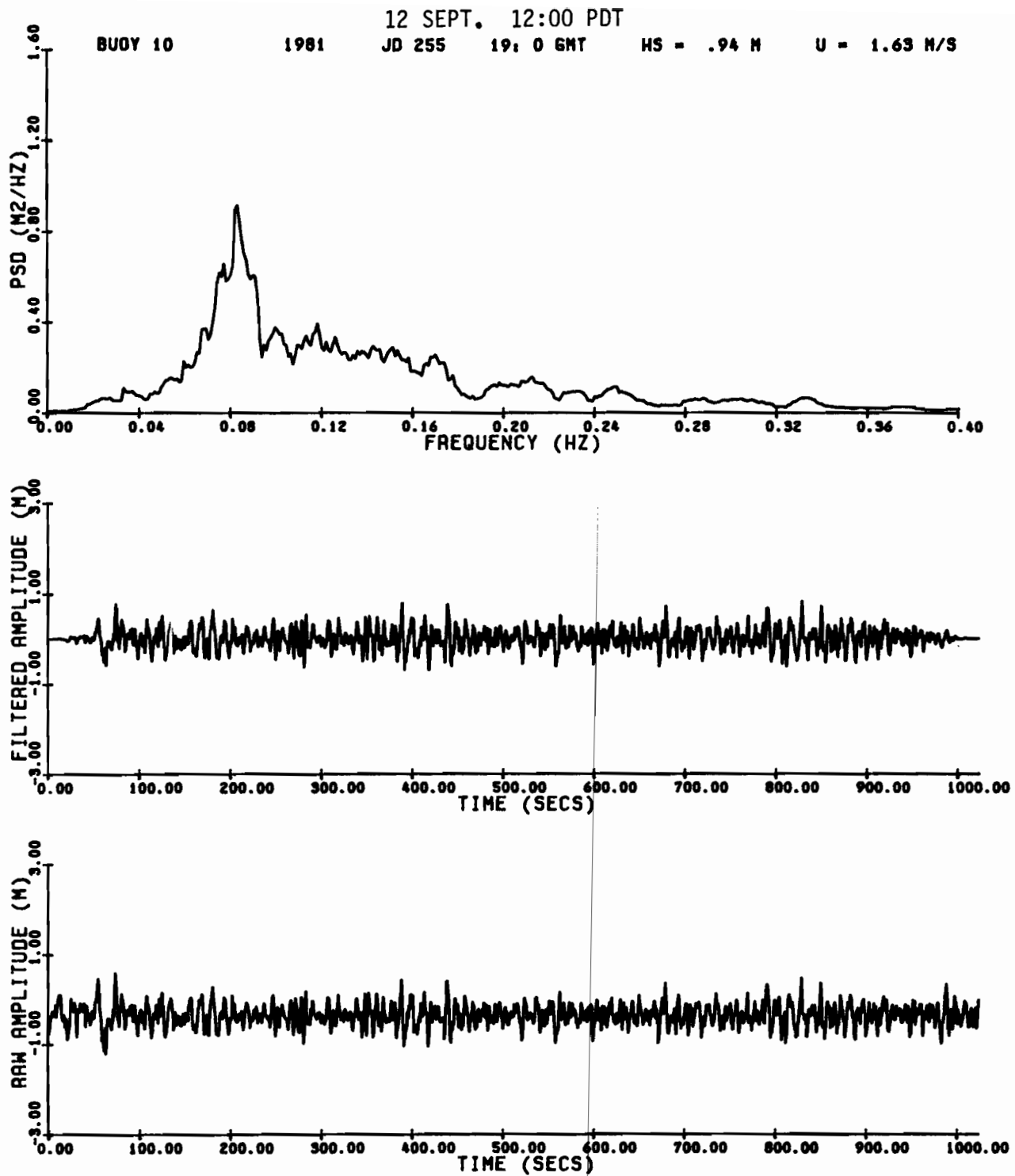


Figure A41. Waverider raw amplitude, filtered amplitude, and power spectral density for 1200 PDT, 12 Sept. 1981.

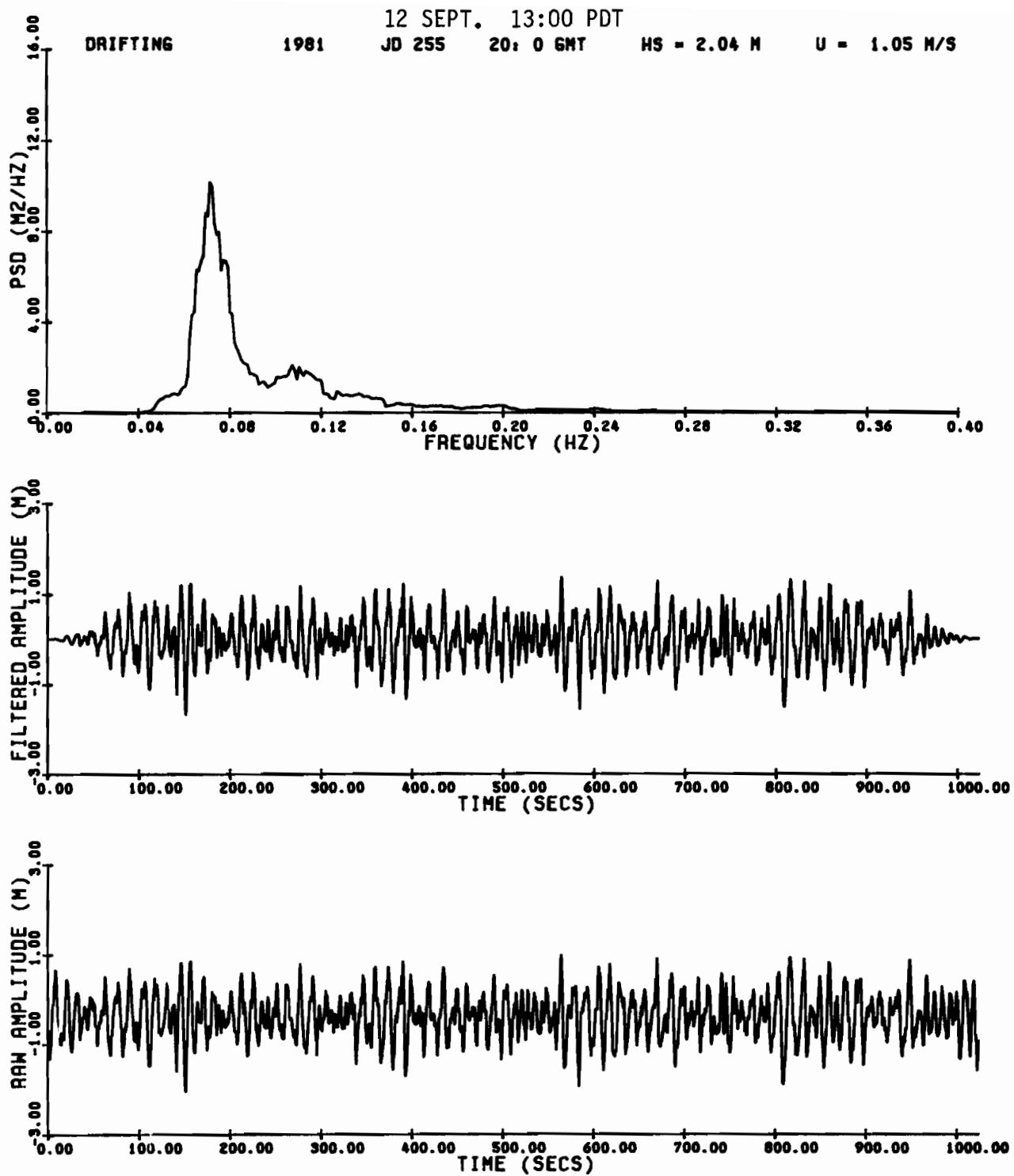


Figure A42. Waverider raw amplitude, filtered amplitude, and power spectral density for 1300 PDT, 12 Sept. 1981.

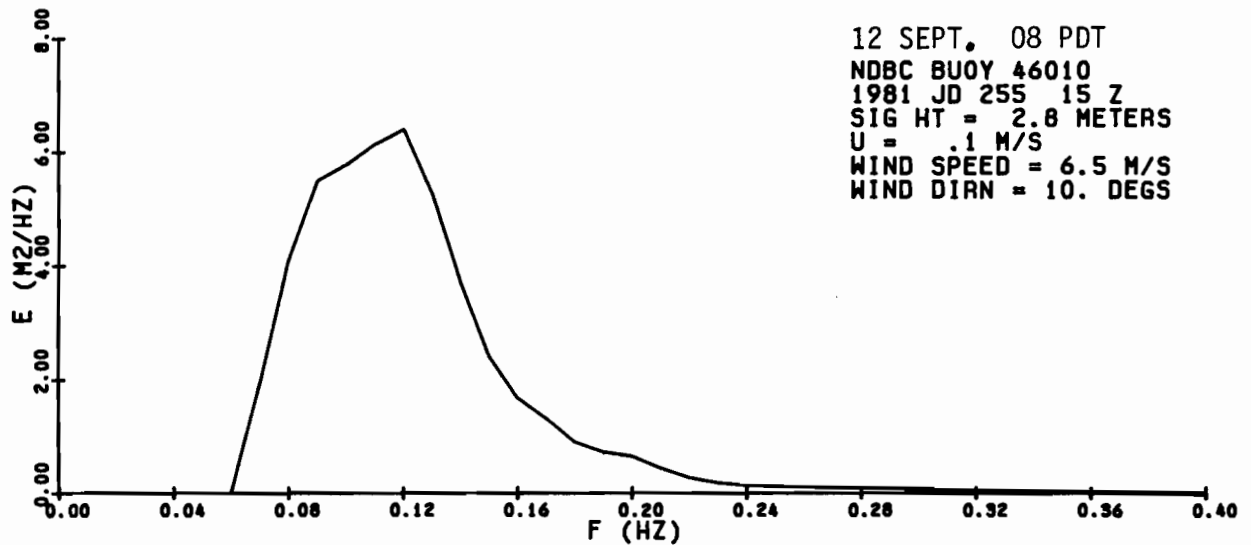
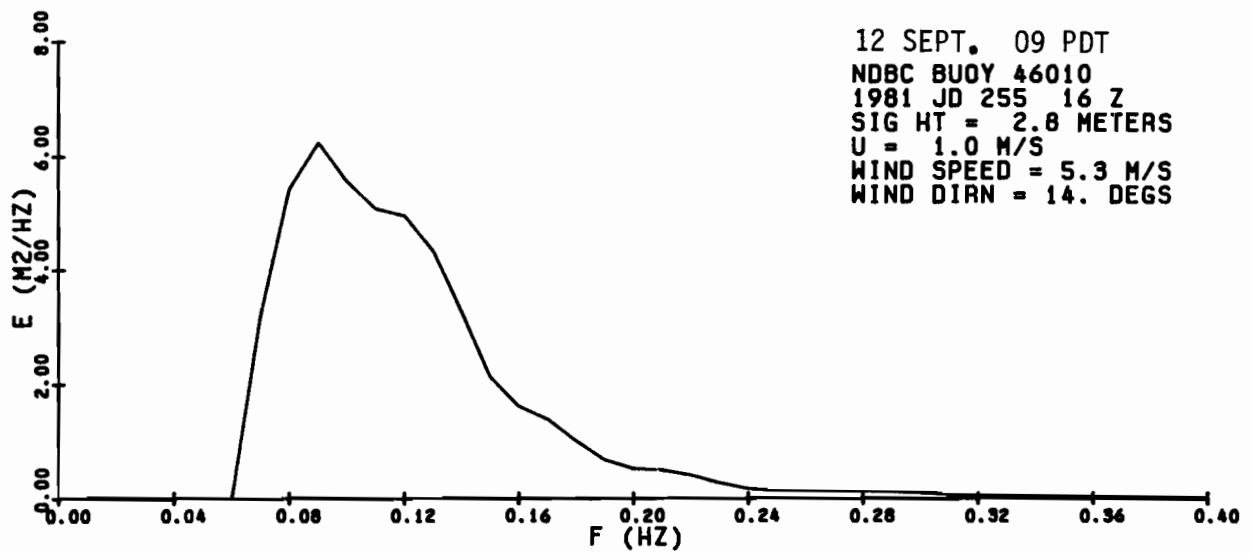
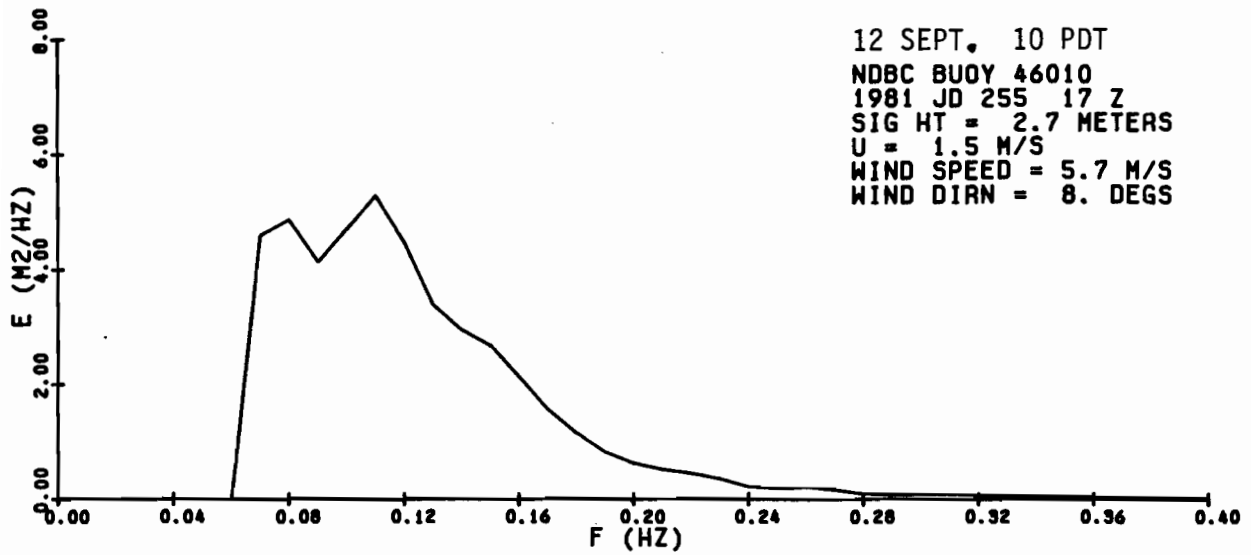


Figure A43. NDBC 46010 power spectral density for 0800, 0900, and 1000 PDT, 12 Sept. 1981.

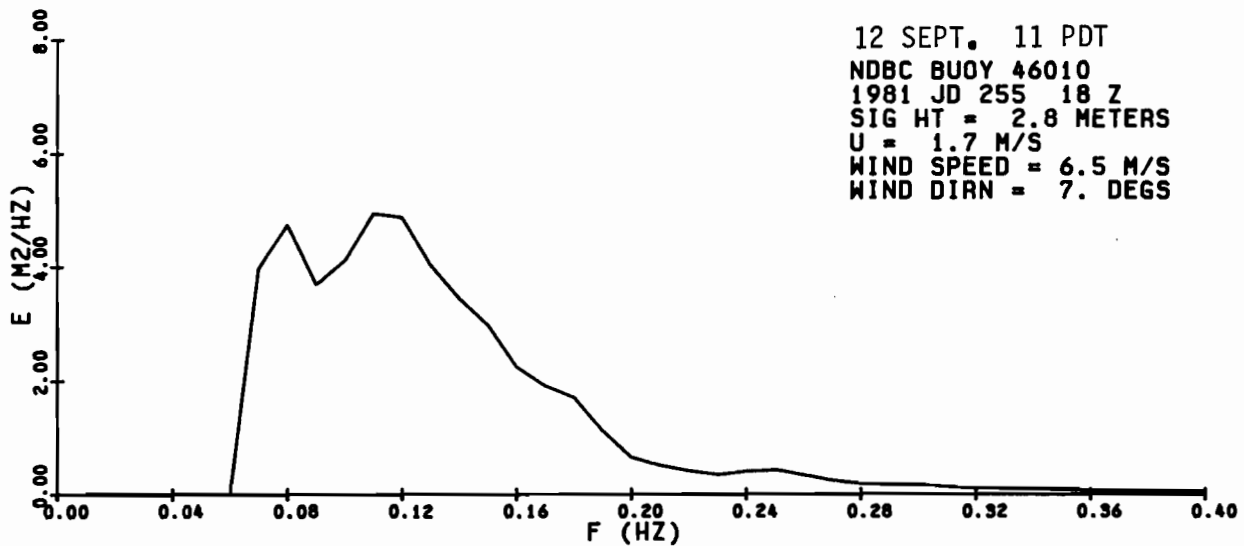
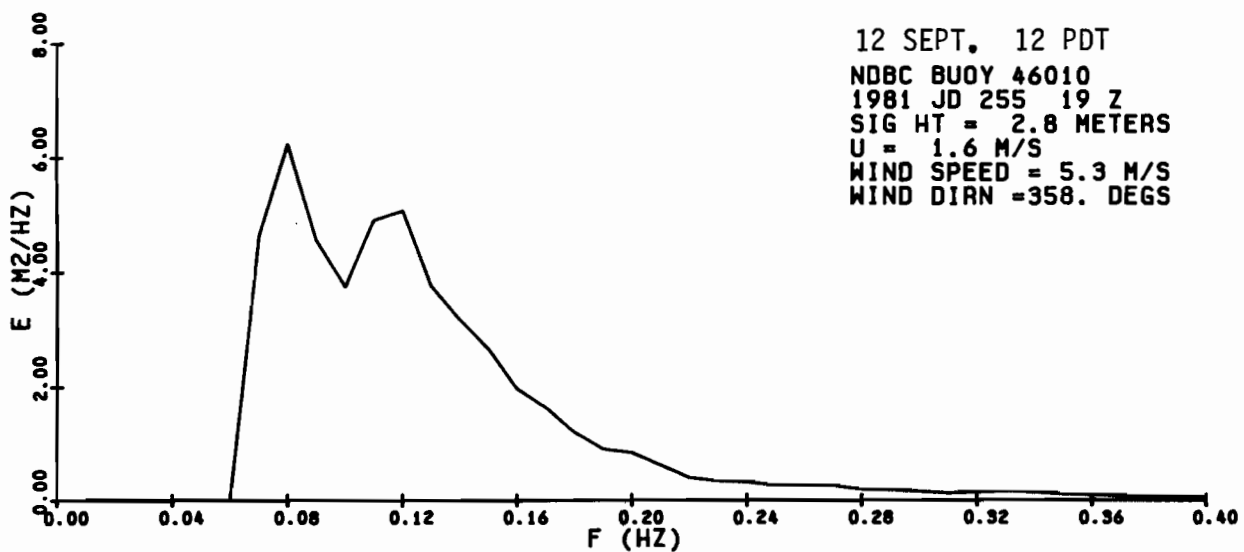
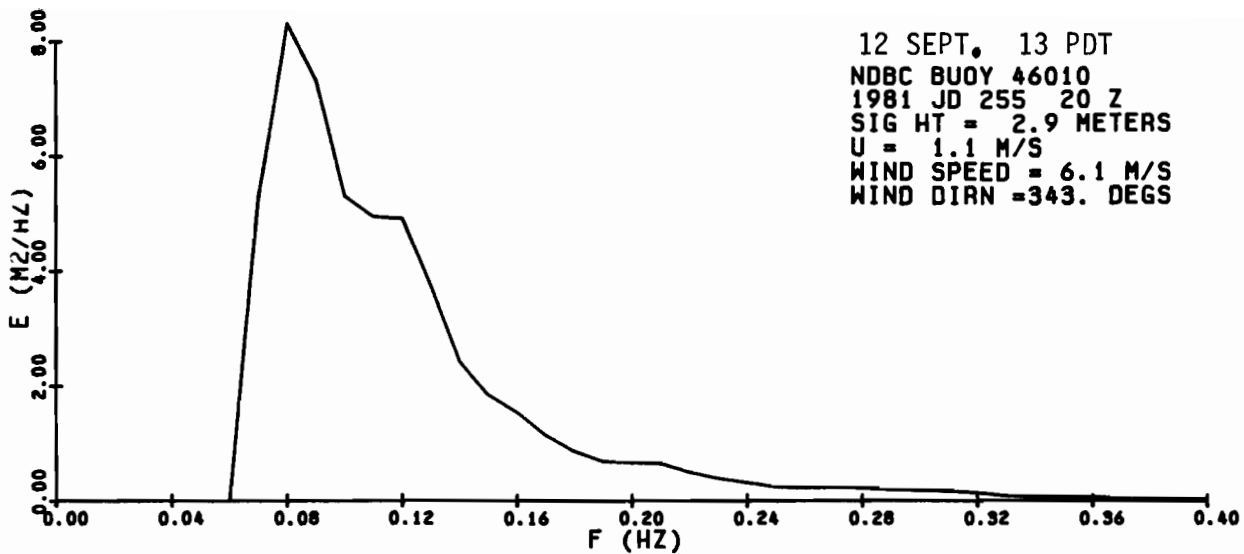


Figure A44. NDBC 46010 power spectral density for 1100, 1200, and 1300 PDT, 12 Sept. 1981.



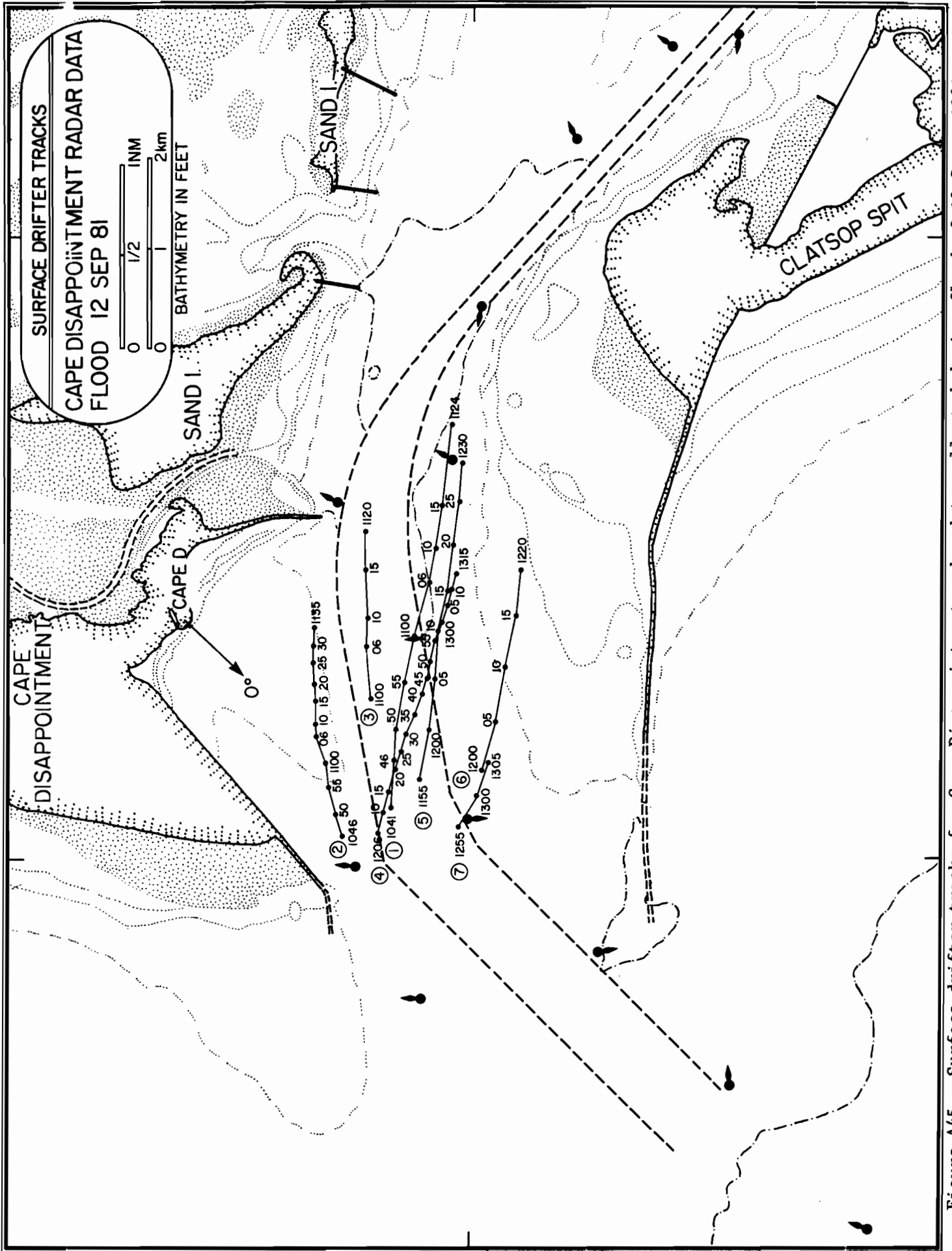


Figure A45. Surface drifter tracks for Cape Disappointment radar data collected during flood of 12 Sept. 1981.

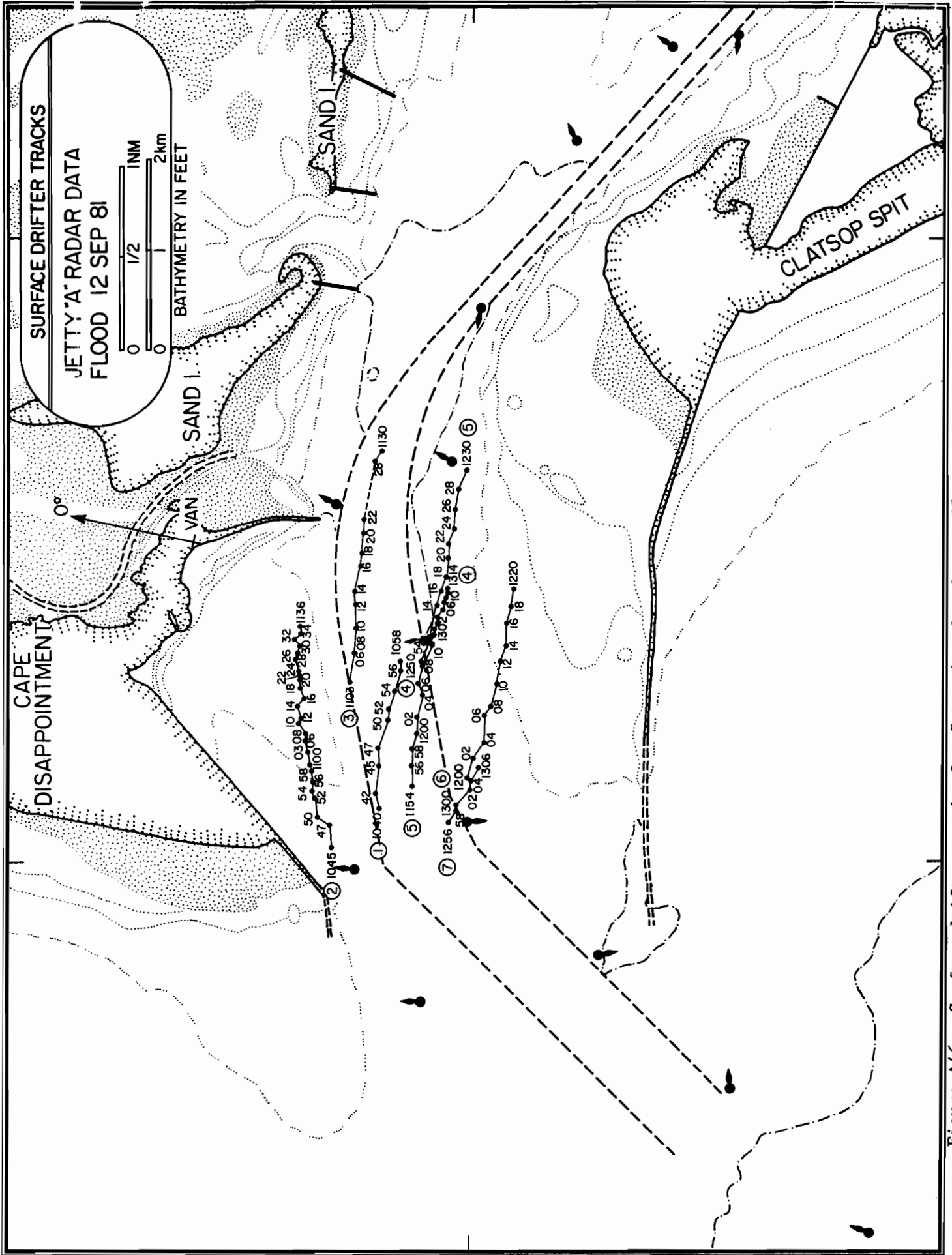


Figure A46. Surface drifter tracks for Jetty A radar data collected during flood of 12 Sept. 1981.

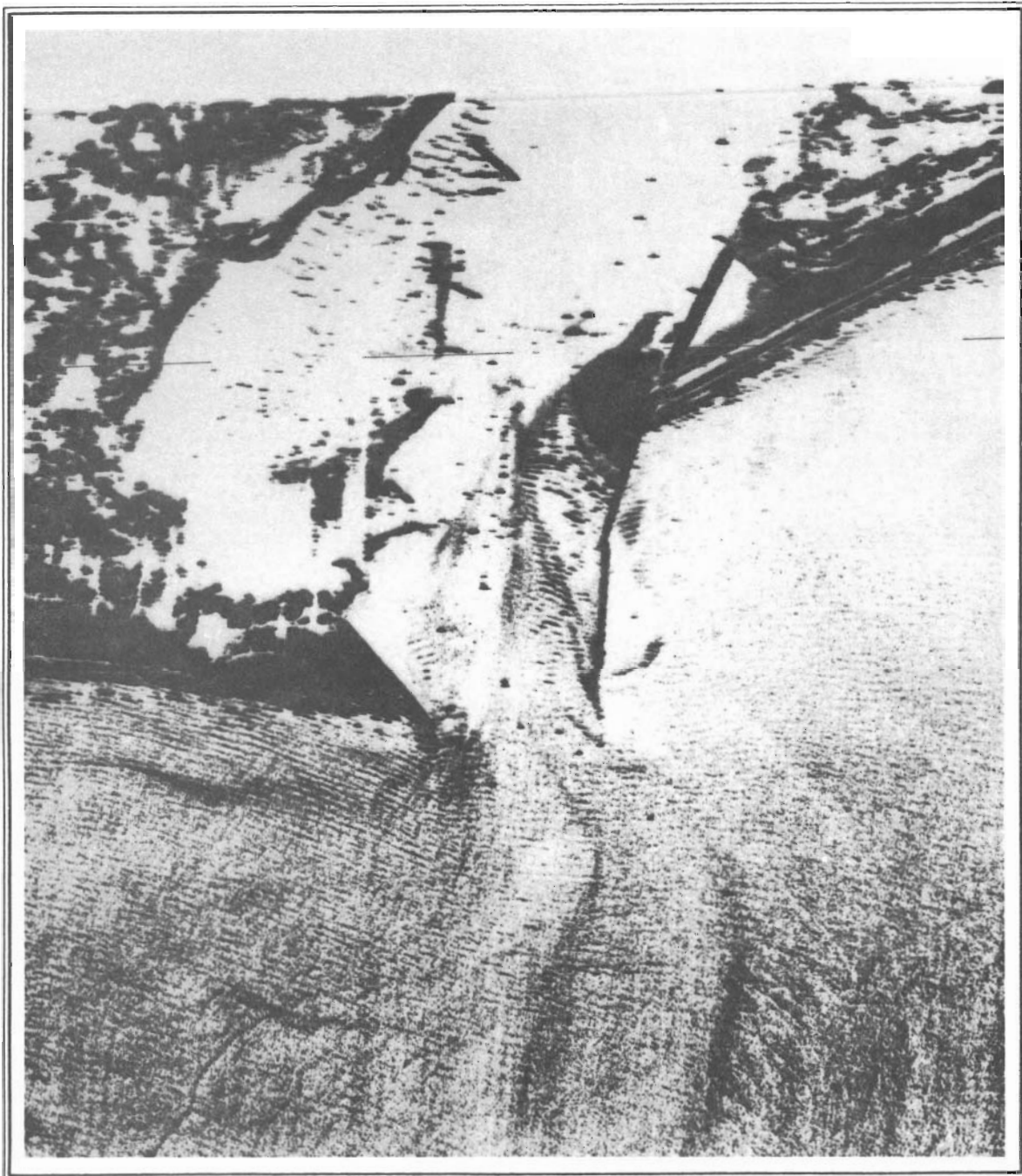


Figure A47. SLAR image of Columbia River entrance obtained on the flood at 1115 PDT, 12 Sept. 1981.

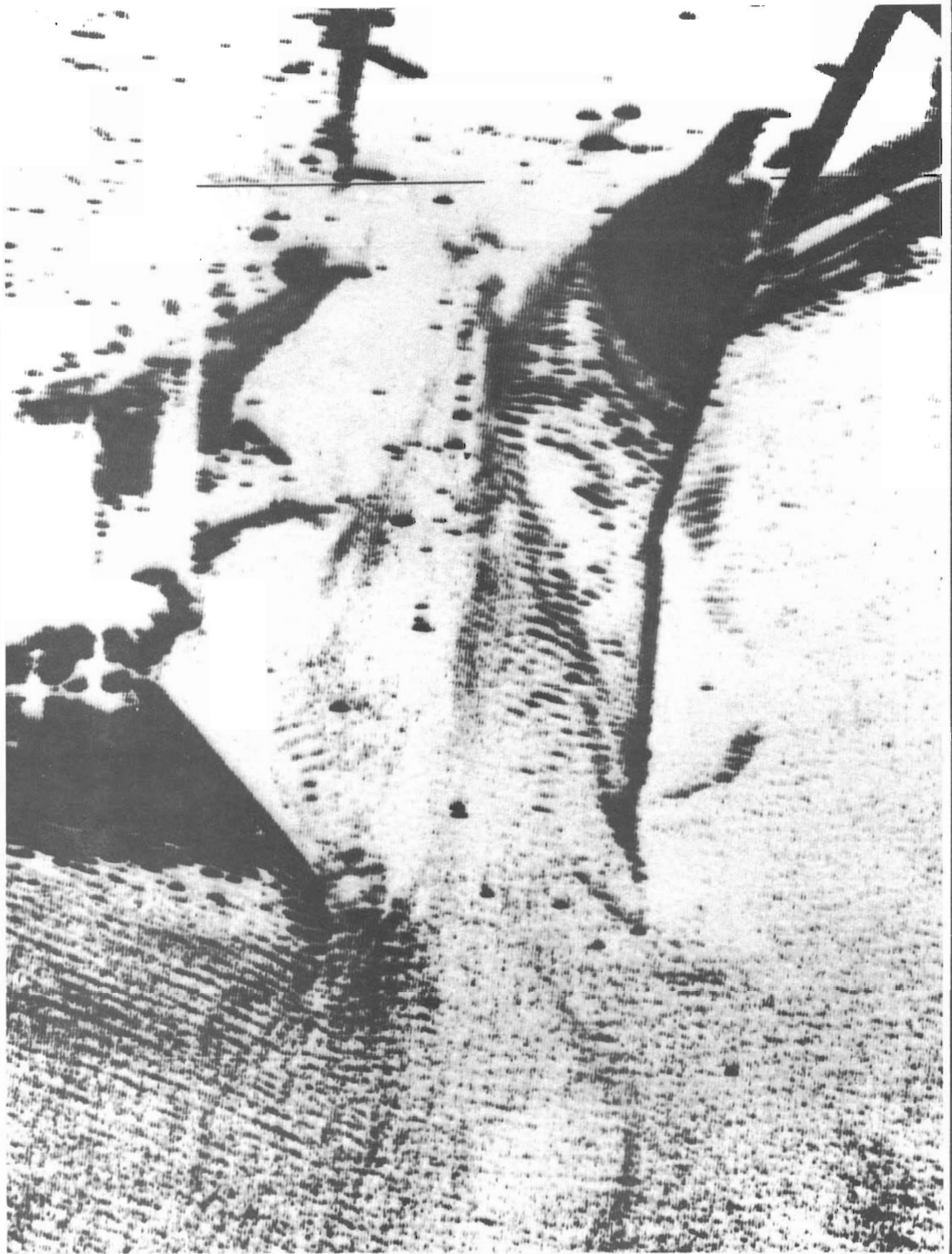


Figure A48. Blowup of Figure A47, centered on the river entrance.

12 September 1981

FLOOD

Waverider LOG (Surface Vessel EGRET)

Time	Hdg.	Sextant Fixes	Objects	Remarks
~0918				WR deployed.
(0921)				(Data logger turned on.)
0925				On station 100 yds. from Buoy CR holding station. (7.5 sec. 2 m.)
0950				Little surface current apparent. WR cable alternates between slack and a little tension. Wind 8-10 kts.  Wave pattern ~ 1.5 m. superimposed on long swell, but wave pattern not very distinct.
0955				Stop holding station.
~1003				Underway for Buoy 2. WR aboard. Fog.
1037				On station Buoy 4. Fog.
1041				Begin record. Buoy 4 bears 270, 150 ft.
1041				Bouy 4 bears NW 100 ft. and Waverider bears E magnetic from EGRET, 100 m. Steady relationship throughout record.

12 September 1981

FLOOD

Waverider LOG (Surface Vessel EGRET)

Time	Hdg.	Sextant Fixes	Objects	Remarks
1041				Light pull on tow line. Drift log (20 m) takes greater than 2 minutes (surface current indefinite) WR position indicates slight flood to NE.
1101				Complete station, begin WR recovery.
1104				WR aboard.
1124				Fog.  WR deployed adjacent Buoy 8.
1127	250			Begin record.  Buoy 8 bears 250, 100 ft (into current). Steady throughout station. (drift log 17, 15.8, 16, 17.8, 18.2 sec for 25 m) Approx. 1 m wave height.
1148				Complete station.
1151				WR aboard. Underway.
1158				WR deployed.
1200	250			On station Buoy 10, EGRET 100 ft. down-current of buoy.

12 September 1981

FLOOD

Waverider LOG (Surface Vessel EGRET)

Time	Hdg.	Sextant Fixes	Objects	Remarks
				Begin record.
				250 mag: into current.
1210				Clear visibility.
1220		37° 56'	2	Steady conditions.
			5	Const. range and
		27° 21'	3	bearing to buoy.
				(drift log 16.20, 16.07, 16.08 sec. per 25 m.)
1234				End sta.
1237				WR aboard.
1248				Fog at Buoy 8. WR deployed. On station a beam Buoy 8. CG Cut- ter SEDGE anchored on Buoy 8 and re- placing buoy. (NOTE: Buoy 8 later removed by Coast Guard.)
1250				Buoy 8 posit. bears S 100 yds. 100 m. cable to WR.
1300				Begin drift.
1318				End sta.

12 September 1981

FLOOD

CAPE DISAPPOINTMENT RADAR DATA

Buoy No	Time (PDT)	Range (nm.)	Bearing (deg.)	Remarks
1	1041	1.52	357	
	1046	1.37	348	
	1050	1.29	341	
	1055	1.24	330	
	1100	1.26	318	
	1106	1.36	305	
	1110	1.43	298	
	1115	1.57	290	
	1120	1.72	282	
	1124	1.84	278	Picked up #1 at 1123 (fix on boat)
2	1046	1.46	009	
	1050	1.34	007	
	1055	1.20	004	
	1100	1.08	000	
	1106	0.96	356	
	1110	0.91	353	
	1115	0.83	346	
	1120	0.78	340	
	1125	0.74	332	
	1130	0.72	325	
	1135	0.71	312	Picked up #2
3	1100	1.10	337	
	1106	1.0	322	
	1110	1.0	313	
	1115	1.03	298	
	1120	1.12	288	Picked up #3 1123
4	1206	1.58	003	
	1210	1.53	359	
	1215	1.45	355	
	1220	1.41	350	
	1225	1.39	346	
	1230	1.36	342	
	1235	1.36	337	
	1240	1.36	332	
	1245	1.36	328	
	1250	1.36	324	
	1255	1.37	319	
	1300	1.41	315	



12 September 1981

FLOOD

CAPE DISAPPOINTMENT RADAR DATA

Buoy No.	Time (PDT)	Range (nm.)	Bearing (deg.)	Remarks
	1305	1.44	311	
	1310	1.48	308	
	1315	1.51	305	Picked up #4
4	1155	1.57	349	
	1200	1.48	339	
	1205	1.40	328	
	1210	1.39	317	
	1215	1.46	308	
	1220	1.54	299	
	1225	1.64	291	
	1230	1.77	285	Picked up #5
6	1200	1.83	342	
	1205	1.80	333	
	1210	1.79	323	
	1215	1.82	314	
	1220	1.88	306	Picked up #6
7	1255	1.89	352	
	1300	1.88	346	
	1305	1.85	340	Picked up #7

12 September 1981

FLOOD

JETTY, A RADAR DATA

Buoy No.	Time (PDT)	Range (nm.)	Bearing (deg.)	Remarks
1	1040	1.78	234	
	1042	1.71	233	
	1045	1.60	229	
	1047	1.53	227	
	1050	1.45	221	
	1052	1.41	219	
	1054	1.38	215	
	1056	1.33	210	
	1058	1.31	208	
2	1045	1.84	244	
	1047	1.72	243	
	1050	1.66	244	
	1052	1.56	243	
	1054	1.52	243	
	1056	1.48	242	
	1058	1.42	241	
	1100	1.38	241	
	110230	1.32	240	
	1106	1.24	239	
	1108	1.21	238	
	1110	1.14	238	
	1112	1.13	237	
	1114	1.06	236	
	1116	1.05	233	
	1118	0.99	232	
	1120	0.95	231	
	1122	0.94	229	
	1124	0.91	228	
	1126	0.86	226	
1128	0.85	224		
1130	0.82	221		
1132	0.78	221		
1134	0.78	217		
1136	0.76	216		
3	1102255	1.17	220	
	1106	1.08	212	
	1108	1.04	208	
	1110	1.01	205	
	1112	0.96	198	
	1114	0.93	194	

12 September 1981

FLOOD

JETTY A RADAR DATA

Buoy No.	Time (PDT)	Range (nm.)	Bearing (deg.)	Remarks
	1116	0.92	186	
	1118	0.92	181	
	1120	0.93	175	
	1122	0.94	170	
	1128	1.11	154	Position confirmed as Nerka approached
	1130	1.16	152	Drifter picked up
4	1250	1.40	206	
	1254	1.40	203	
	1256	1.40	201	
	1258	1.40	199	
	1300	1.40	198	
	1302	1.40	196	
	1304	1.39	195	
	1306	1.41	193	
	1308	1.41	191	
	1310	1.41	190	
	1312	1.41	189	
	1314	1.41	188	
5	1154	1.80	227	
	1156	1.72	224	
	1158	1.66	222	
	1200	1.61	219	
	1202	1.56	216	
	1204	1.51	212	
	1206	1.45	210	
	1208	1.42	206	
	1210	1.42	201	
	1212	1.39	199	
	1214	1.38	192	
	1216	1.38	189	
	1218	1.40	185	
	1220	1.40	181	
	1222	1.40	178	
	1224	1.44	174	
	1226	1.45	170	
	1228	1.49	166	
	1230	1.55	163	Drifter retrieved

12 September 1981

FLOOD

JETTY A RADAR DATA

---

Buoy No.	Time (PDT)	Range (nm.)	Bearing (deg.)	Remarks
6	1200	1.99	219	
	1202	1.93	216	
	1204	1.93	213	
	1206	1.86	209	
	1208	1.86	207	
	1210	1.83	203	
	1212	1.80	199	
	1214	1.80	196	
	1216	1.77	192	
	1218	1.77	189	
	1220	1.78	186	Drifter retrieved
7	1256	2.08	226	
	1258	2.08	224	
	1300	2.04	223	Buoy 7?
	1302	2.04	220	
	1304	2.01	219	
	1306	2.00	217	

---

12 September 1981

EBB



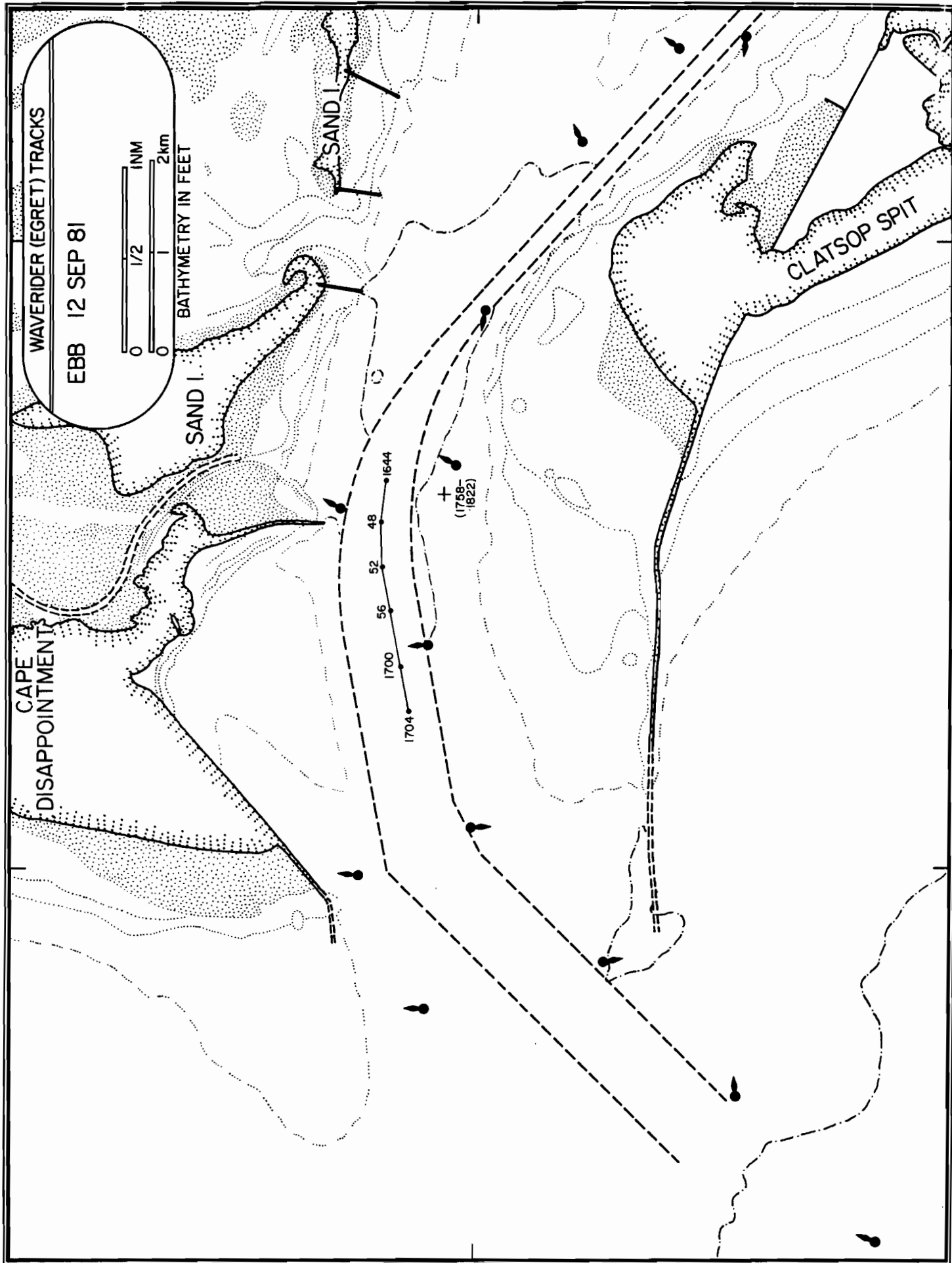


Figure A49. Waverider (EGRET) tracks for ebb period on 12 Sept. 1981.

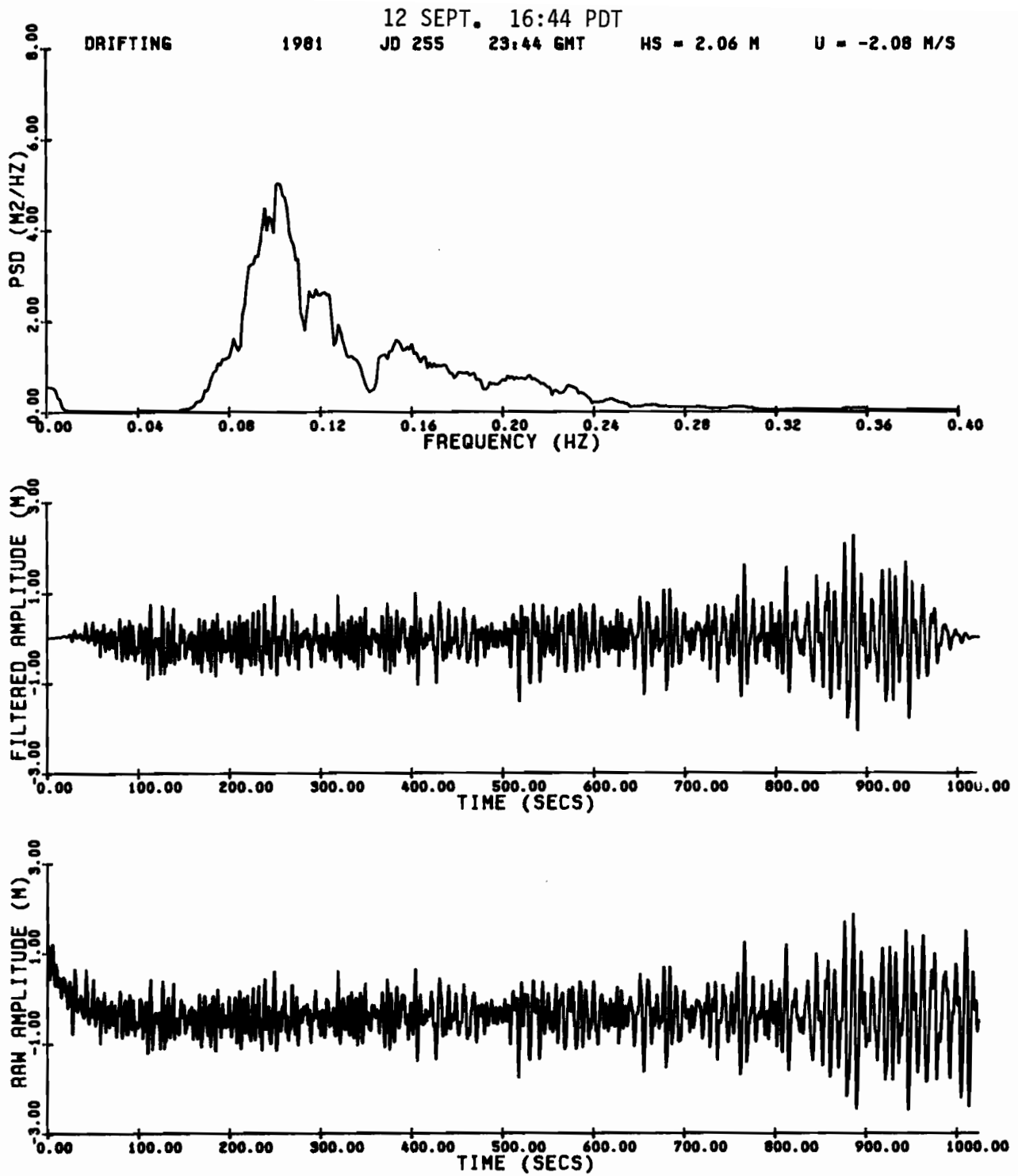


Figure A50. Waverider raw amplitude, filtered amplitude, and power spectral density for 1644 PDT, 12 Sept. 1981.



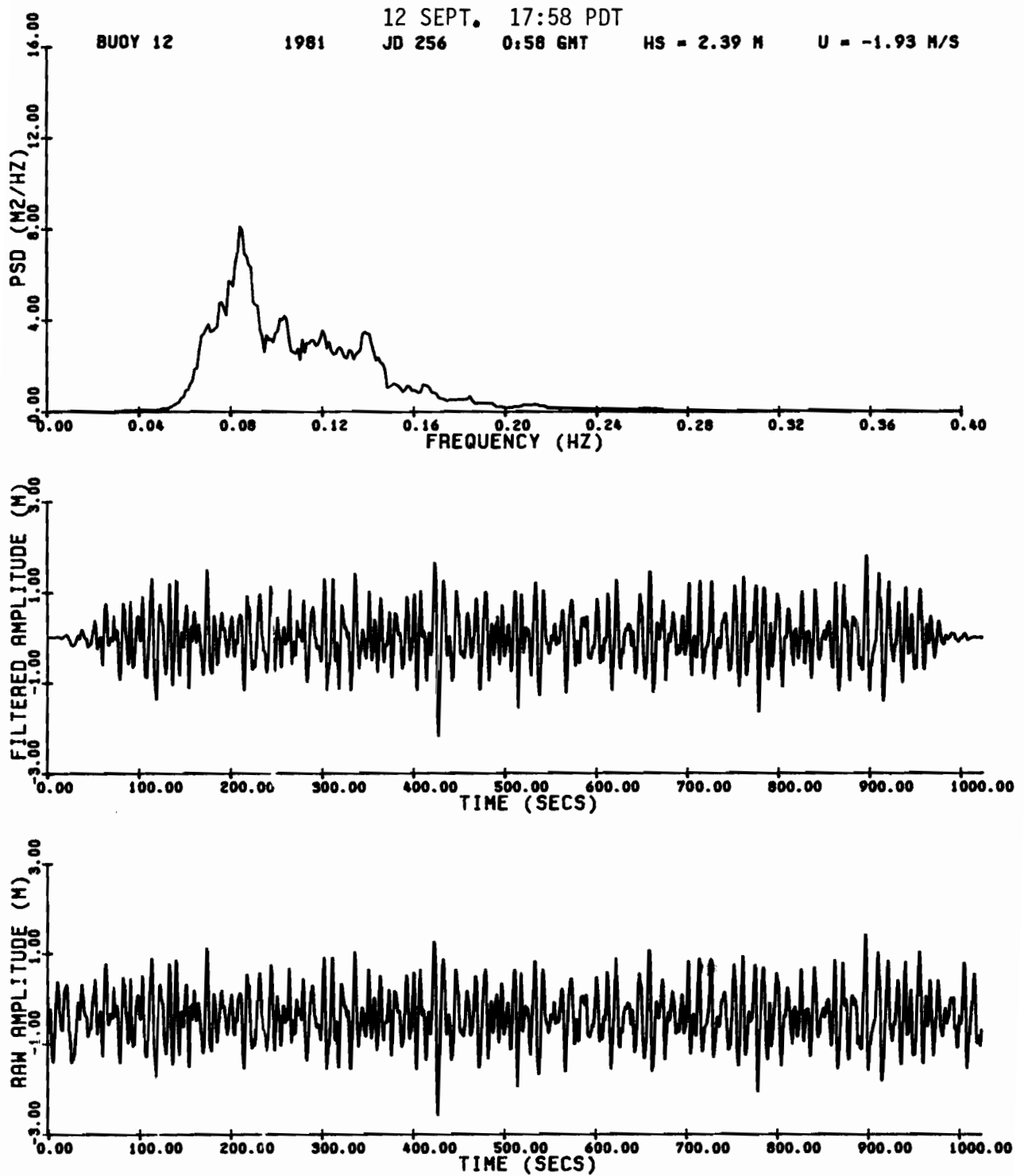


Figure A51. Waverider raw amplitude, filtered amplitude, and power spectral density for 1758 PDT, 12 Sept. 1981.

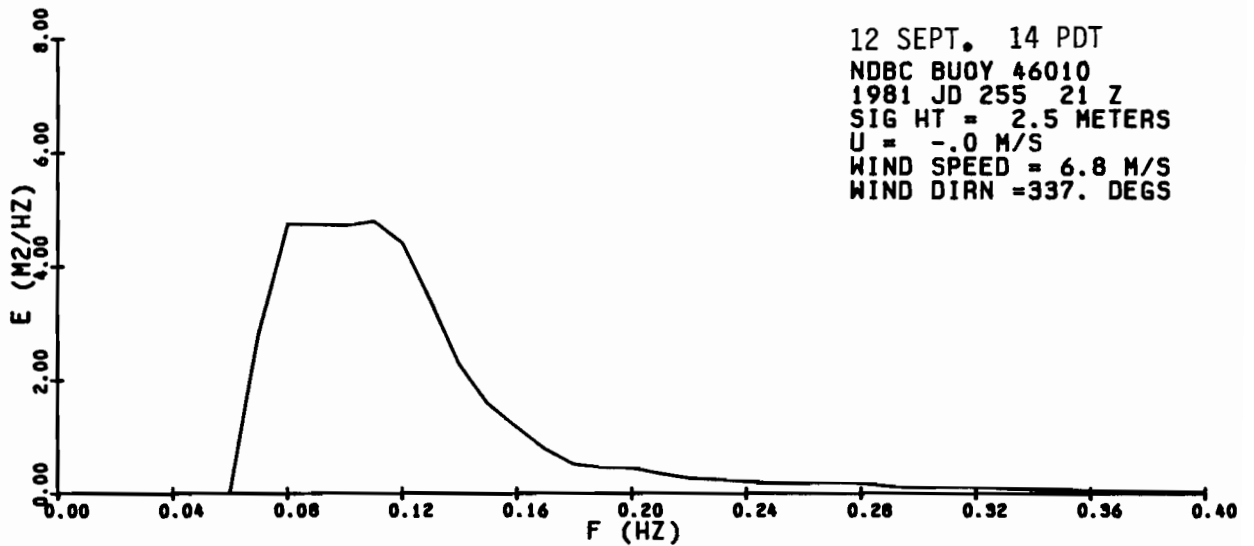
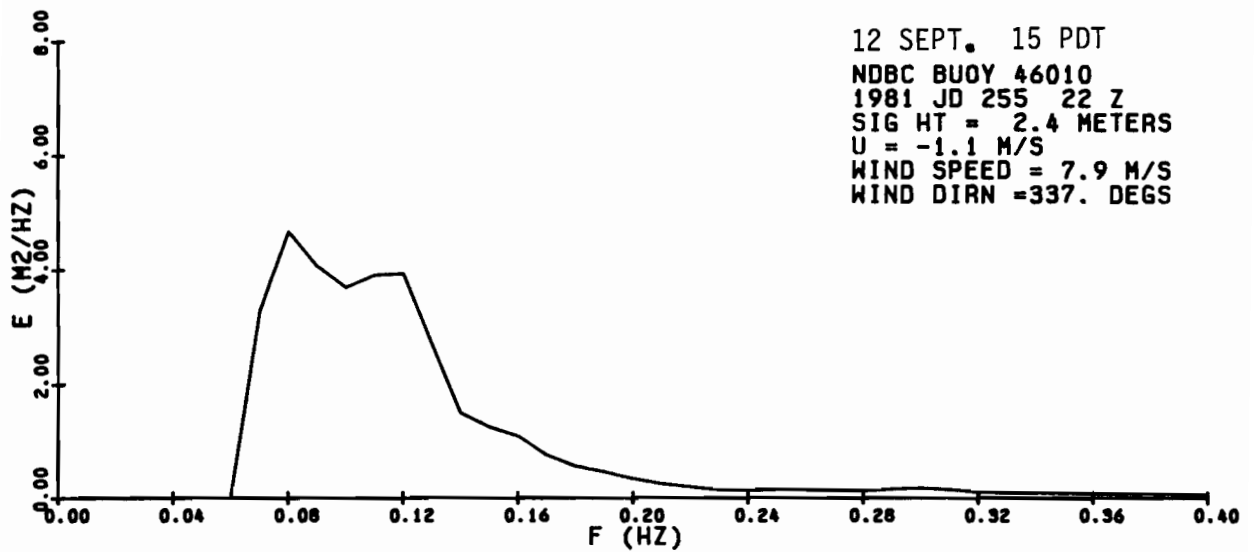
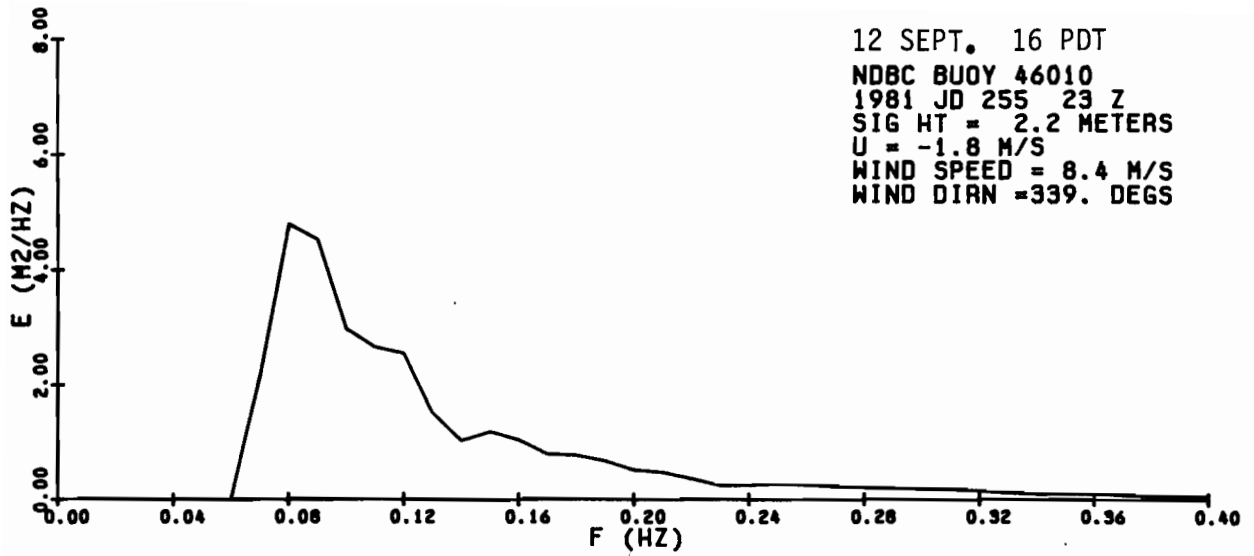


Figure A52. NDBC 46010 power spectral density for 1400, 1500, and 1600 PDT, 12 Sept. 1981.

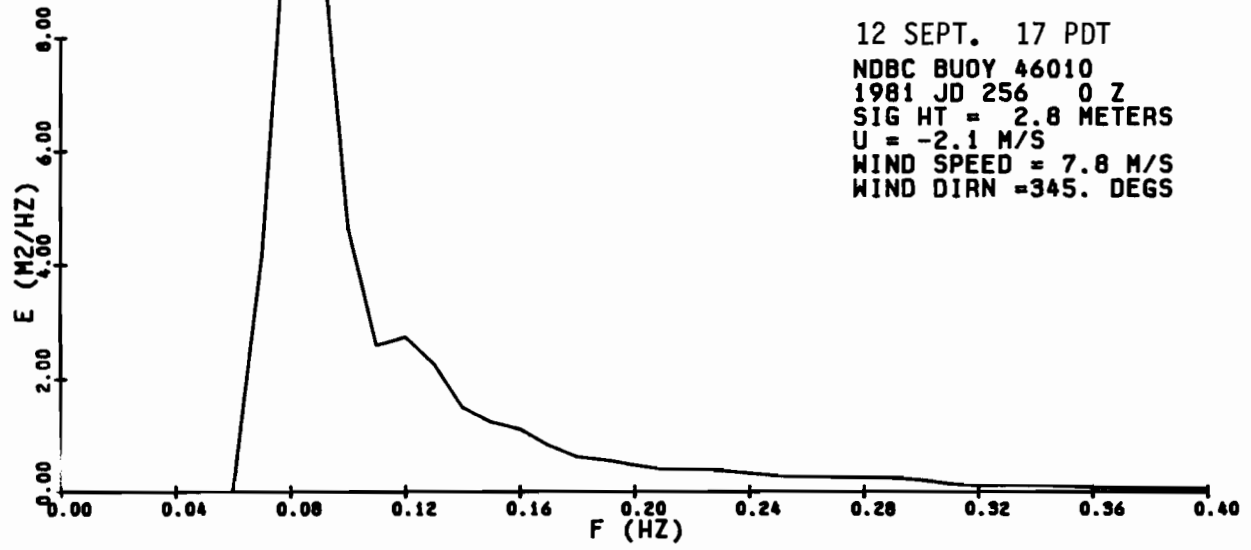
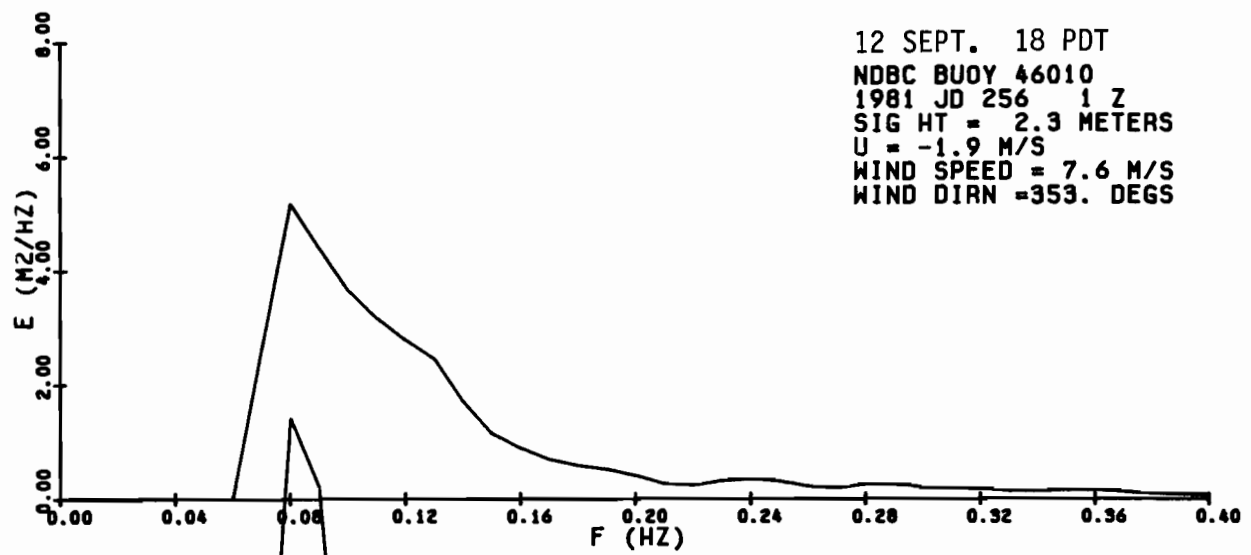
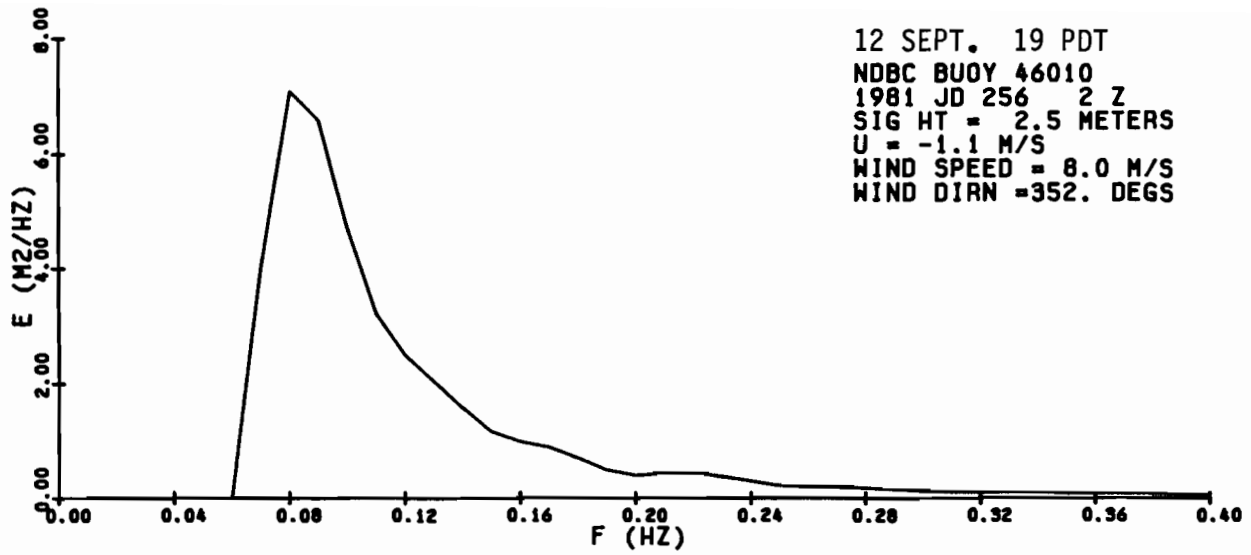


Figure A53. NDBC 46010 power spectral density for 1700, 1800, and 1900 PDT, 12 Sept. 1981.

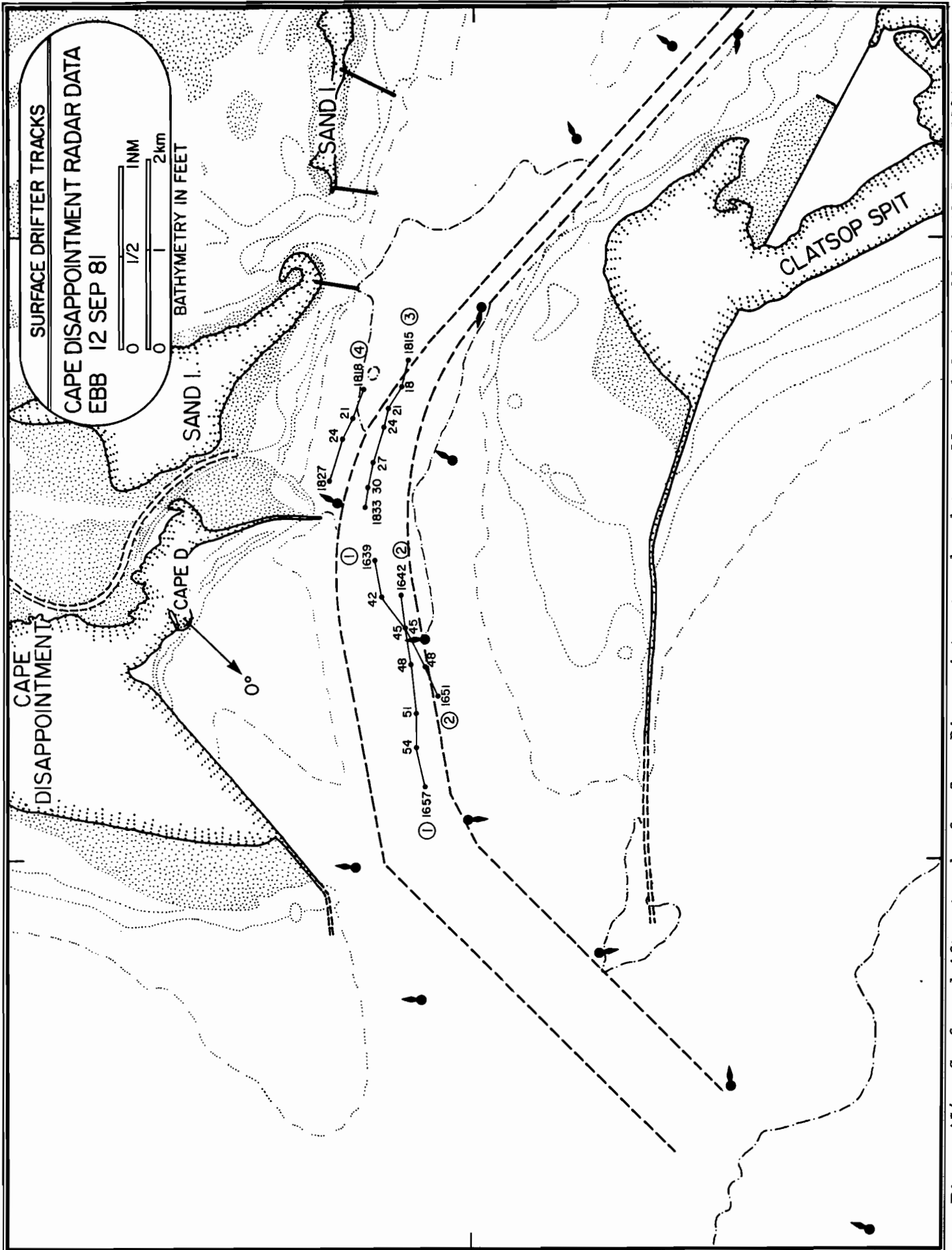


Figure A54. Surface drifter tracks for Cape Disappointment radar data collected during ebb of 12 Sept. 1981.

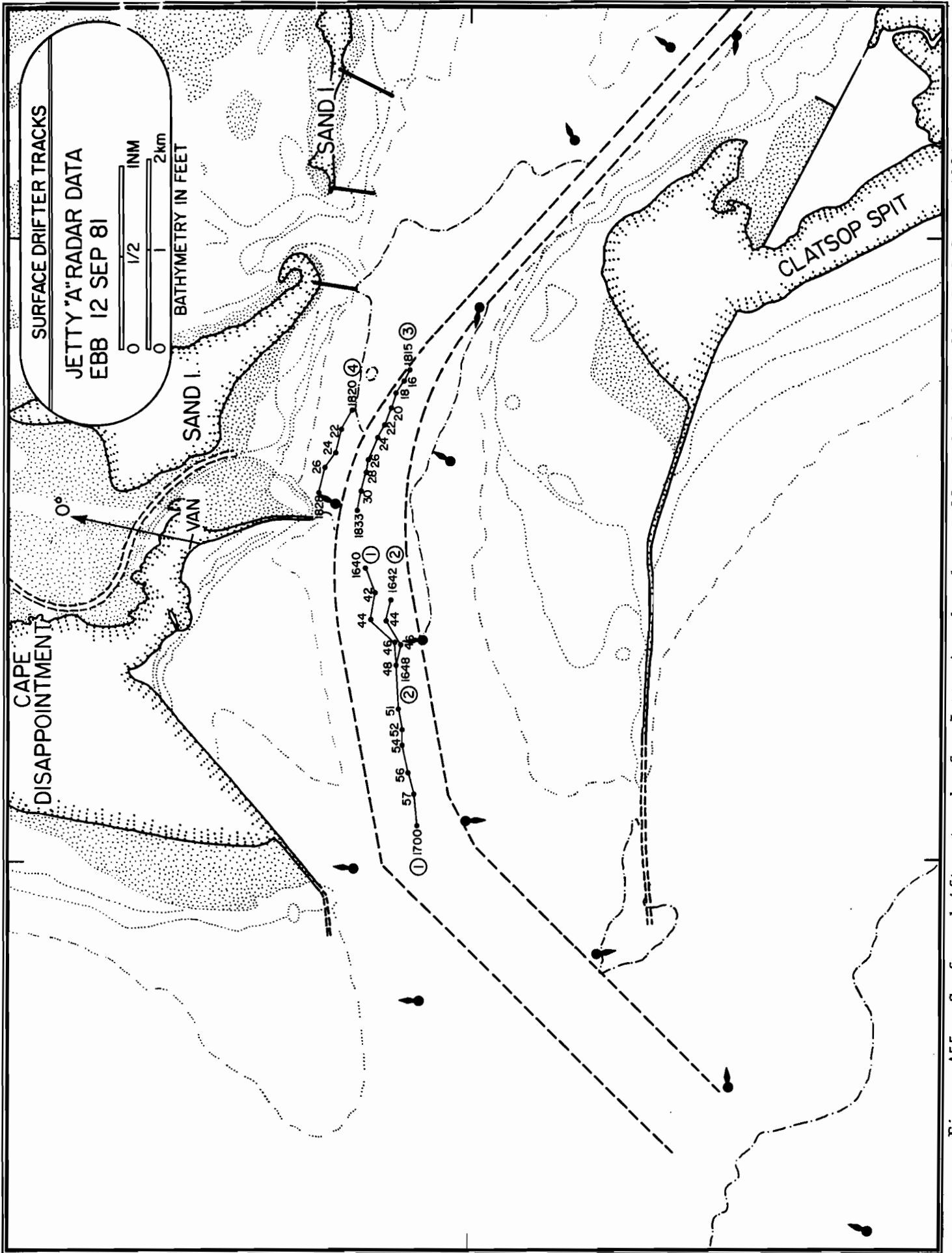


Figure A55. Surface drifter tracks for Jetty A radar data collected during ebb of 12 Sept. 1981.

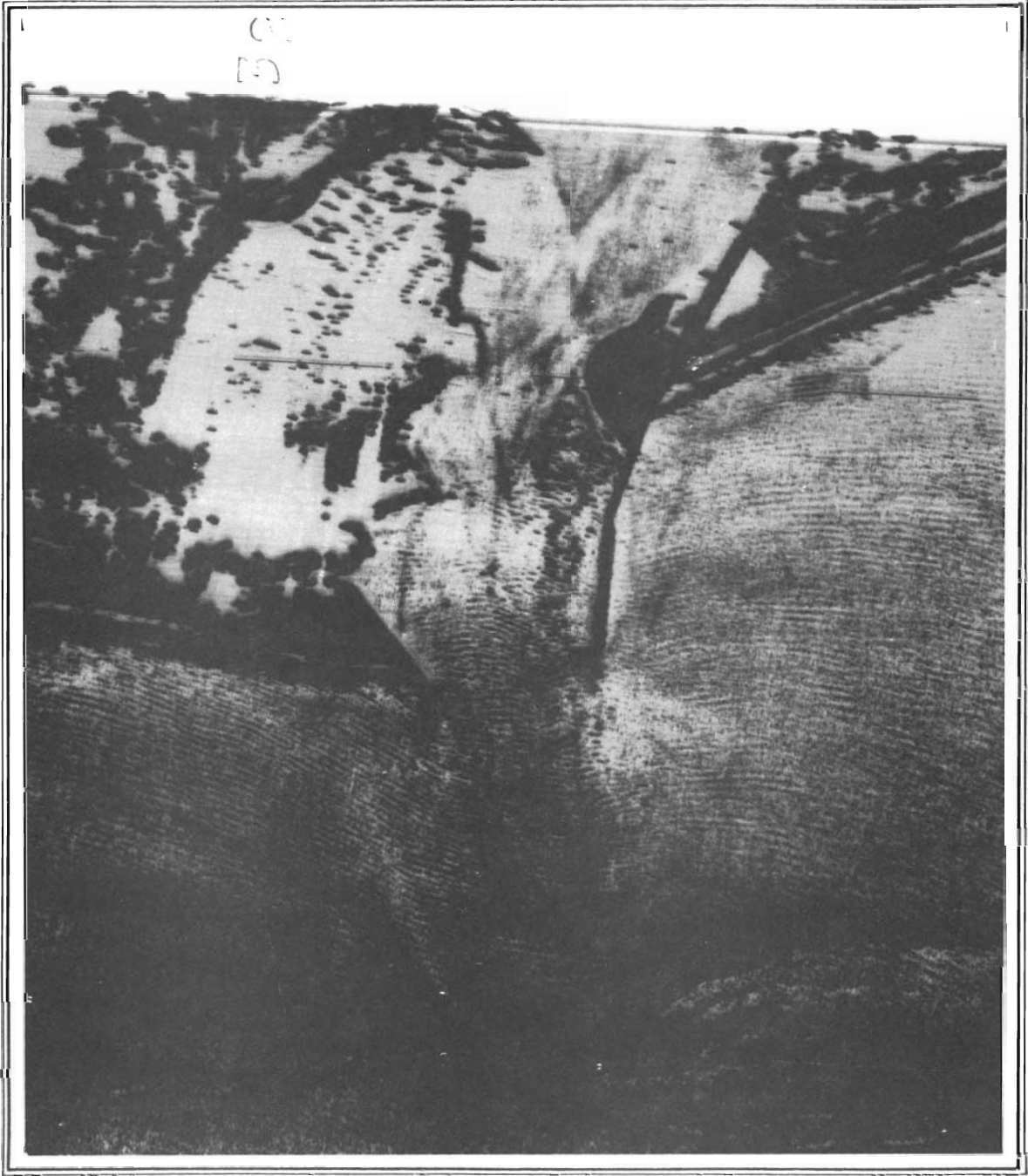


Figure A56. SLAR image of Columbia River entrance obtained on the ebb at 1645 PDT, 12 Sept. 1981.



Figure A57. Blowup of Figure A56, centered on the river entrance

12 September 1981

EBB

Waverider LOG (Surface Vessel EGRET)

Time	Hdg.	Sextant Fixes	Objects	Remarks
1641				WR deployed.
1644		16° 48'	2	Begin record drifting. WR bears 270 150 ft.
			5	
		82° 56'	3	
1648		32° 40'	2	
			5	
		64° 42'	3	
1652		46° 20'	2	WR bears 270 150 ft. (8 sec., 2 m. vis. obs.)
			5	
		42° 20'	3	
1656		47° 23'	2	
			5	
		29° 12'	3	
			1	
			2	
		42° 48'	5	
1704		34° 50'	1	End drift. Wave leading edges very steep. Waves 4 to 5 more wavelengths offshore appear to be beginning to break. Towing WR to Buoy 10. Continue towing up- stream.
			2	
		37° 15'	5	
~1745				WR aboard.
1758				WR deployed 100 yds. on channel side of Buoy 12.
1811				On station, record. (10.6, 11.6, 11.6/ 25 m.)



12 September 1981

EBB

Waverider LOG (Surface Vessel EGRET)

---

Time	Hdg.	Sextant Fixes	Objects	Remarks
1822		19° 54'	2	End station.
		58° 35'	5	Position steady
			3	throughout station.
1828	72			End station.
1832				WR aboard.

---

12 September 1981

EBB

CAPE DISAPPOINTMENT RADAR DATA

---

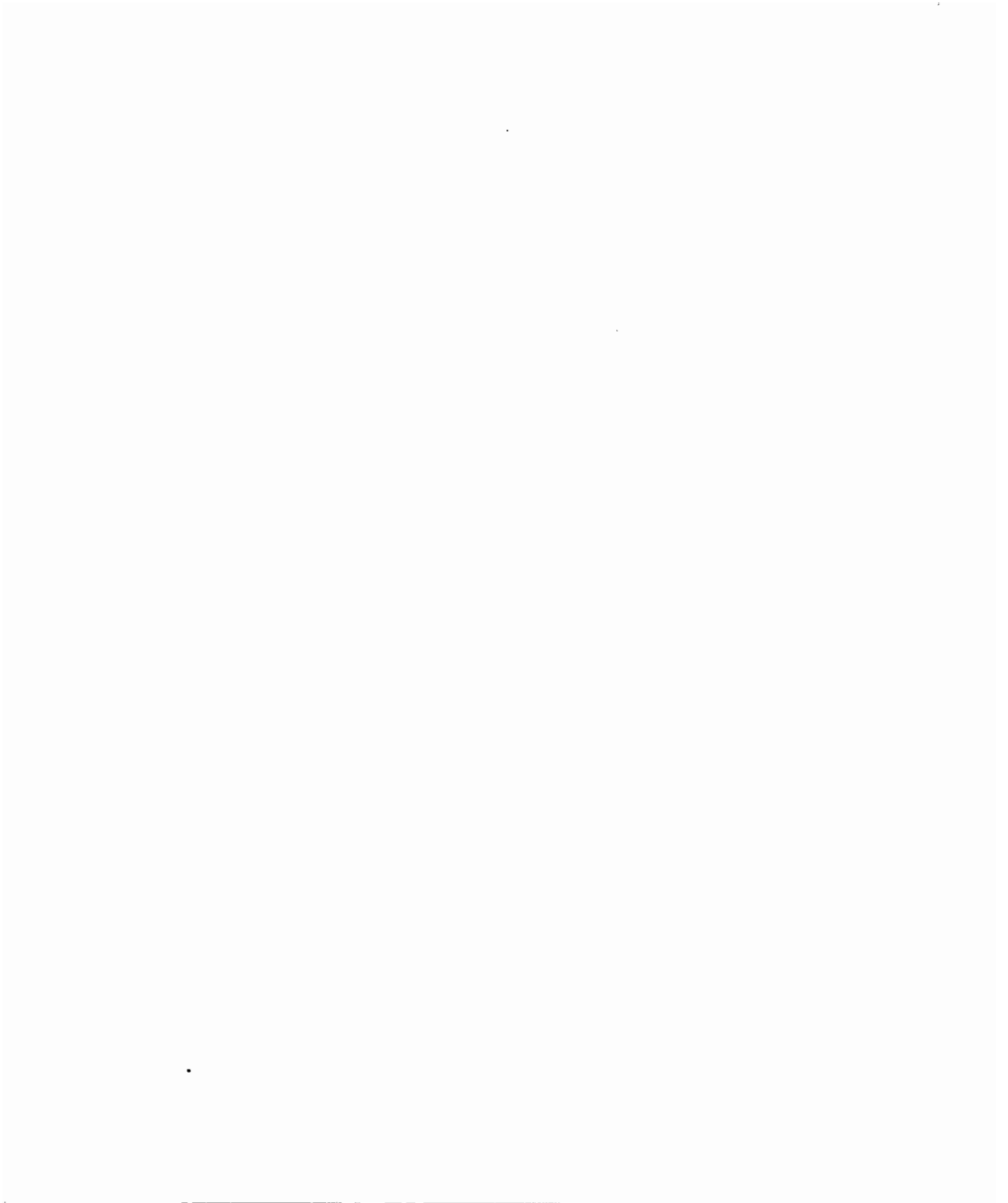
Buoy No.	Time (PDT)	Range (nm.)	Bearing (deg.)	Remarks
1	1639	1.10	296	
	1642	1.09	307	
	1645	1.21	316	
	1648	1.26	326	
	1651	1.36	336	
	1654	1.44	343	
	1657	1.60	349	Picked up #1
2	1642	1.20	307	
	1645	1.21	316	
	1648	1.33	325	
	1651	1.44	331	Picked up #2
3	1815	1.91	265	
	1818	1.78	267	
	1821	1.63	268	
	1824	1.55	270	
	1827	1.37	274	
	1830	1.25	278	
	1833	1.19	282	Picked up #3
4	1818	1.63	262	
	1821	1.46	264	
	1824	1.33	265	
	1827	1.12	270	Picked up #4

12 September 1981

EBB

JETTY A RADAR DATA

Buoy No.	Time (PDT)	Range (nm.)	Bearing (deg.)	Remarks
1	1640	0.97	186	
	1642	1.06	193	
	1644	1.08	201	
	1646	1.25	204	
	1648	1.32	209	
	1651	1.47	217	
	1652	1.57	220	
	1654	1.61	222	
	1656	1.74	225	
	1657	1.84	227	
	1700	2.00	230	
2	1642	1.14	194	
	1644	1.16	200	
	1646	1.28	204	
	1648	1.32	209	Buoy retrieved
3	1815	1.54	140	
	1816	1.49	141	
	1818	1.40	142	
	1820	1.34	144	
	1822	1.26	147	
	1824	1.19	149	
	1826	1.09	153	
	1828	1.04	156	
	1830	0.98	161	
	1833	0.94	167	
4	1820	1.16	139	
	1822	1.04	141	
	1824	0.94	147	
	1826	0.86	149	
	1828	0.77	156	Buoy in radar shadow.



13 September 1981

FLOOD



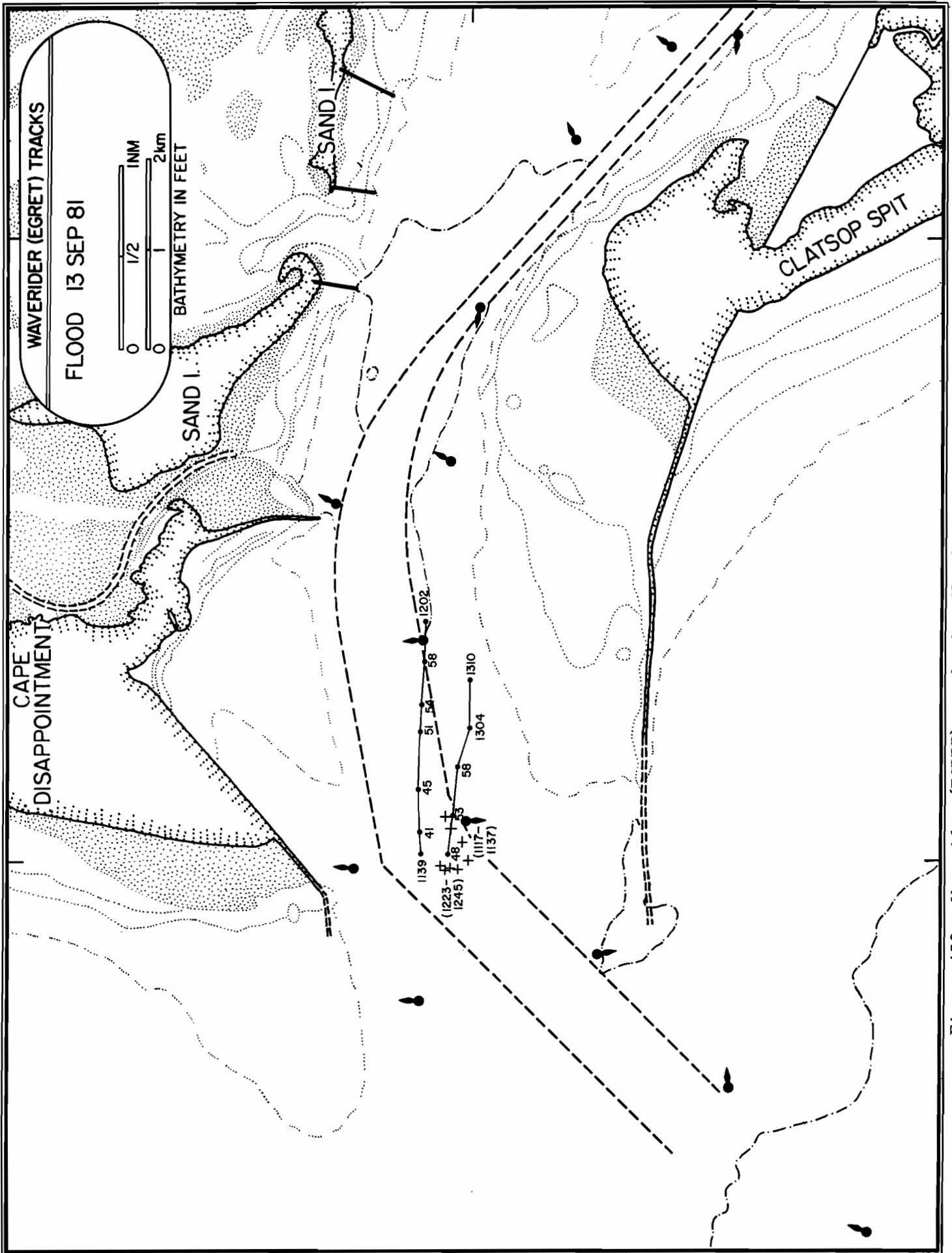


Figure A58. Waverider (EGRET) tracks for flood period on 13 Sept. 1981.

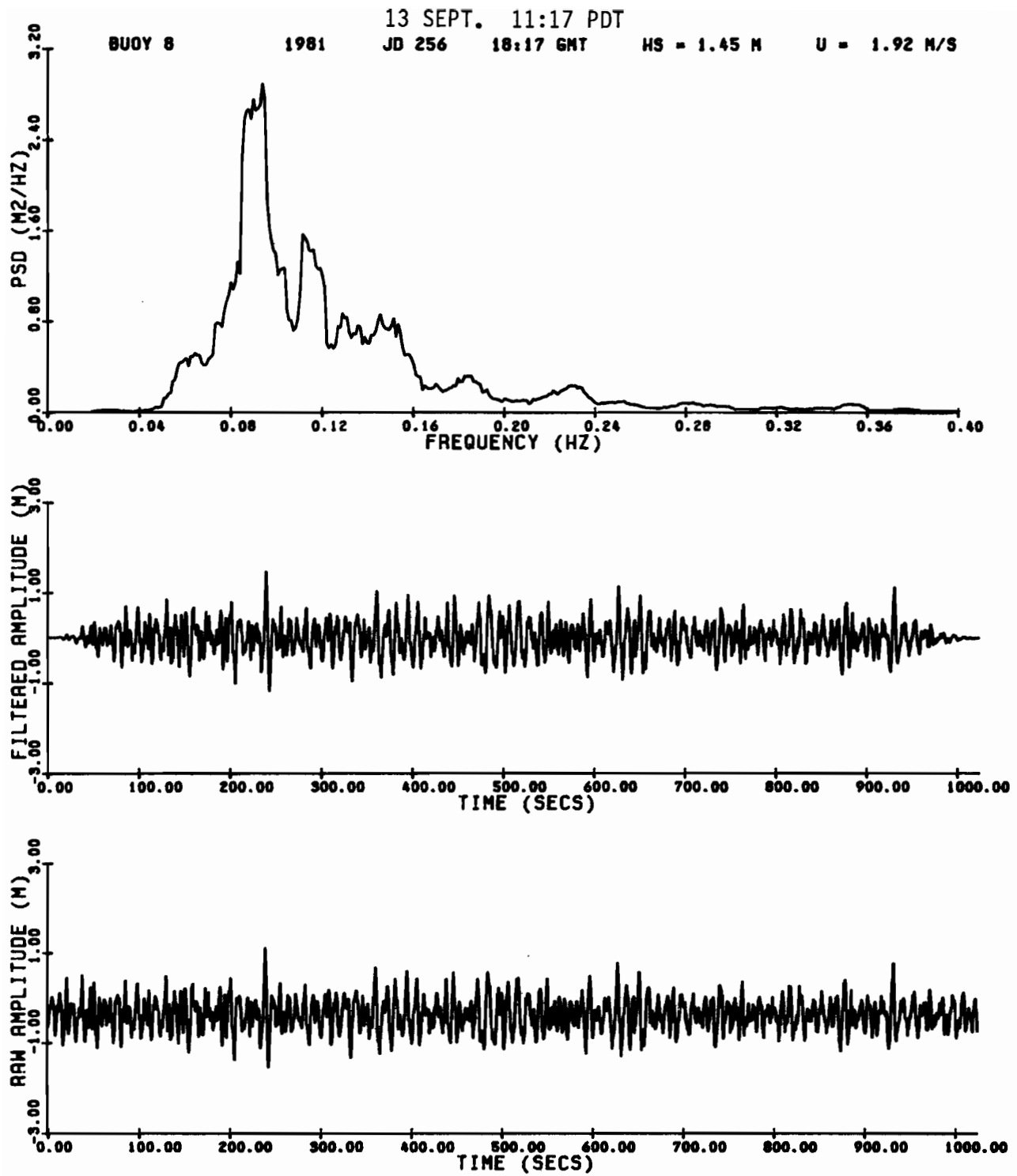


Figure A59. Waverider raw amplitude, filtered amplitude, and power spectral density for 1117 PDT, 13 Sept. 1981.



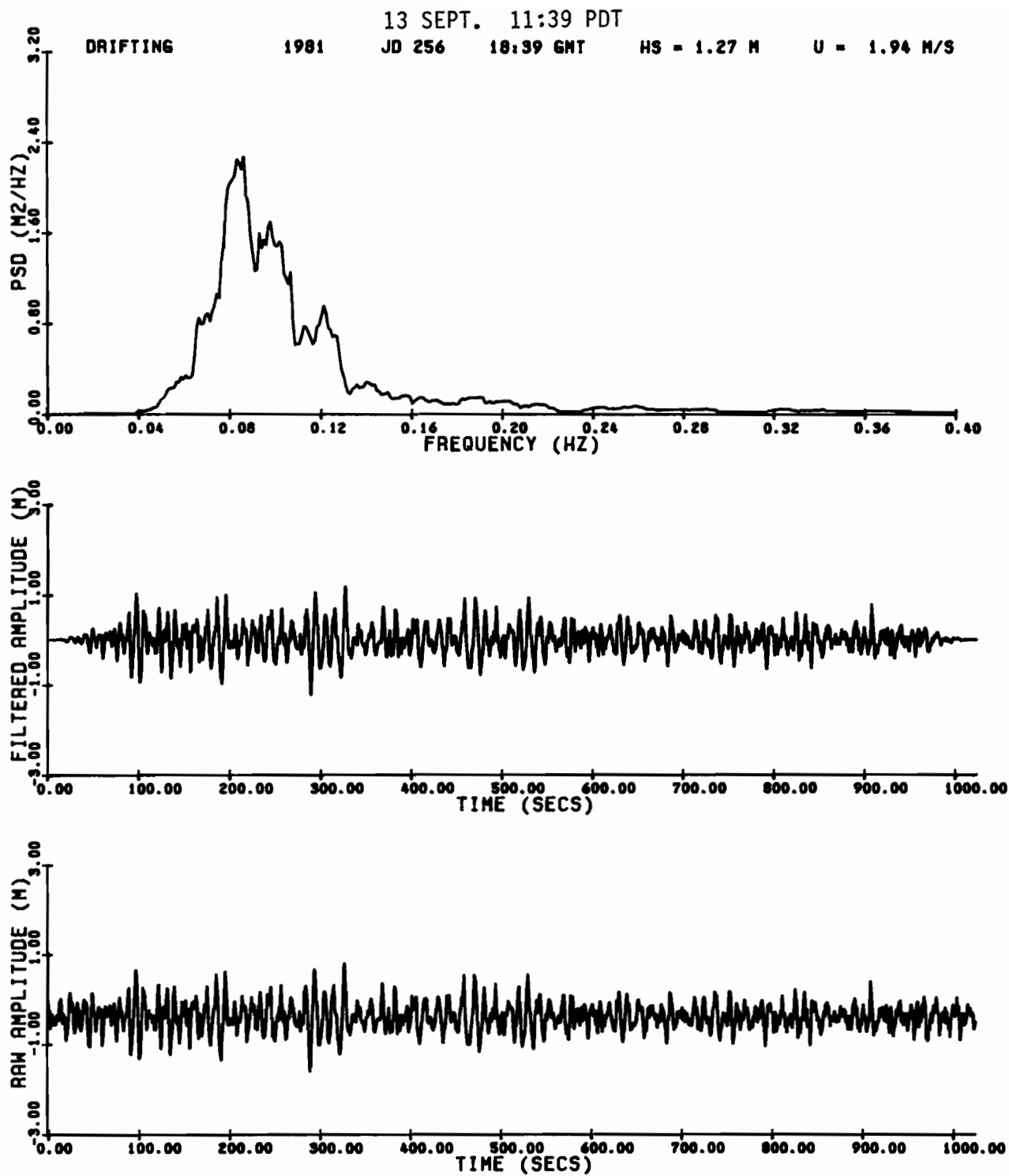


Figure A60. Waverider raw amplitude, filtered amplitude, and power spectral density for 1139 PDT, 13 Sept. 1981.

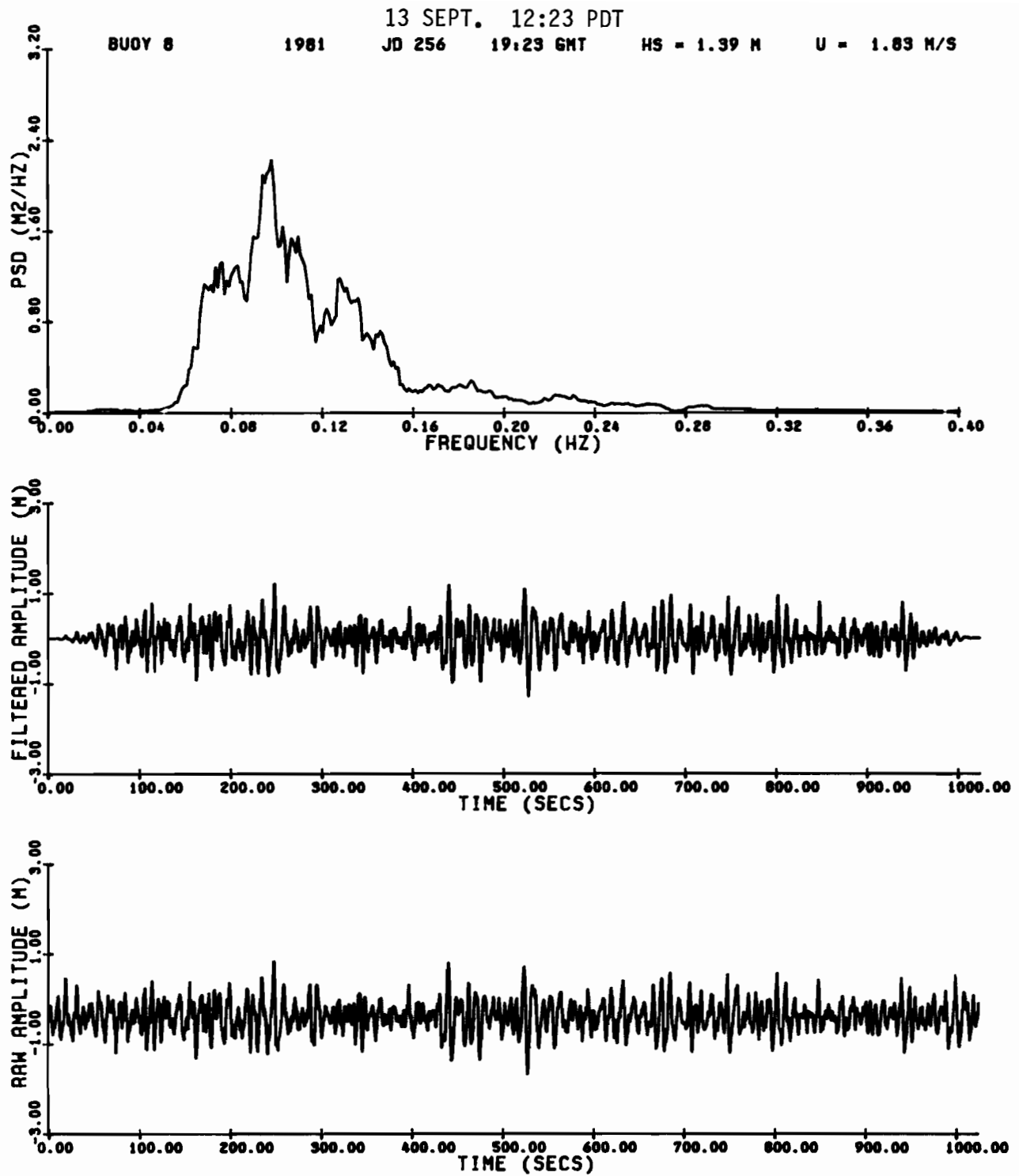


Figure A61. Waverider raw amplitude, filtered amplitude, and power spectral density for 1223 PDT, 13 Sept. 1981.

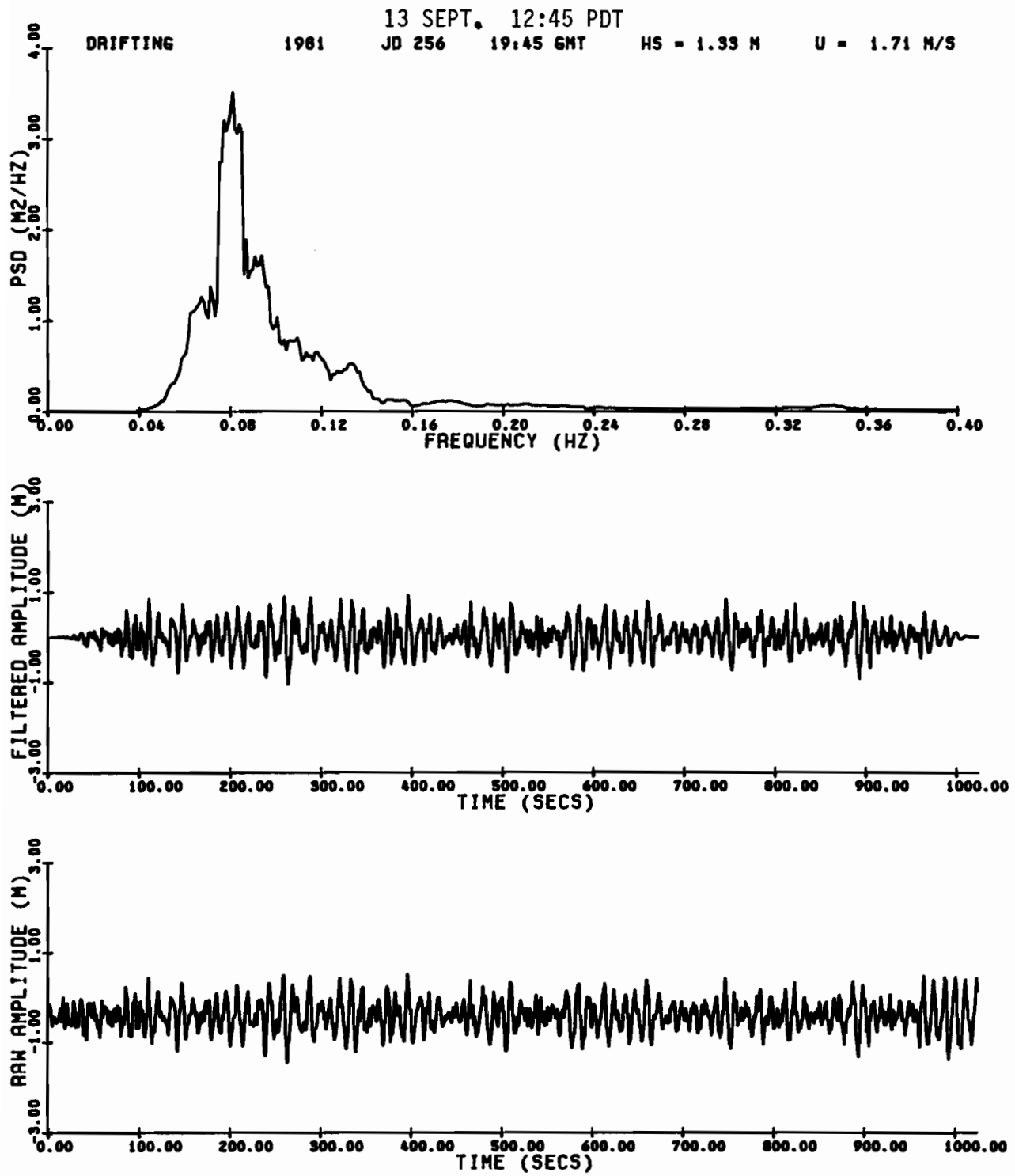


Figure A62. Waverider raw amplitude, filtered amplitude, and power spectral density for 1245 PDT, 13 Sept. 1981.

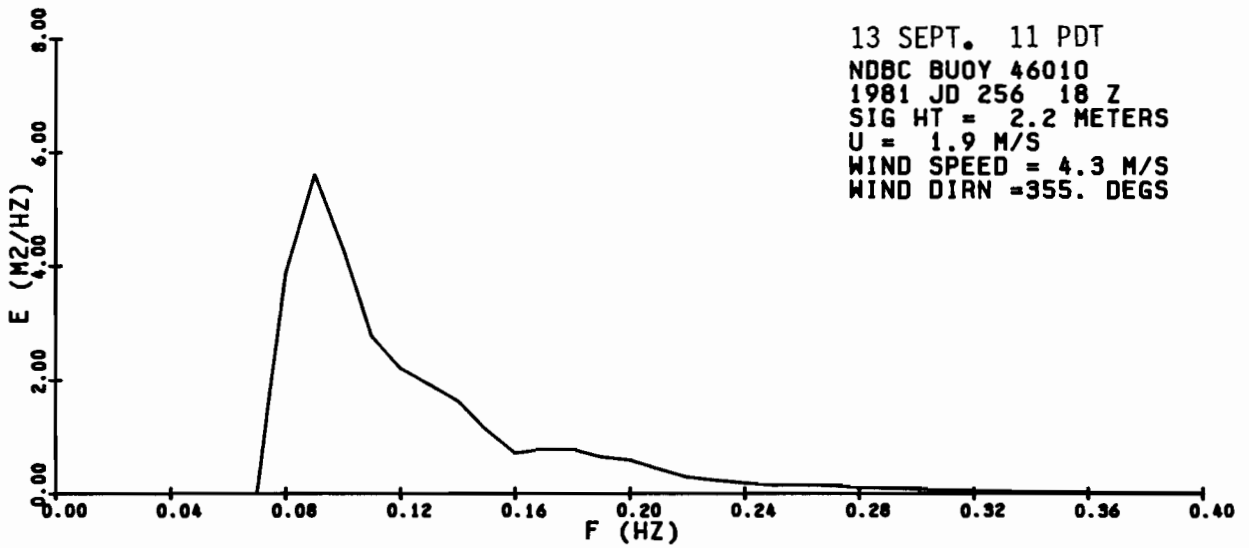
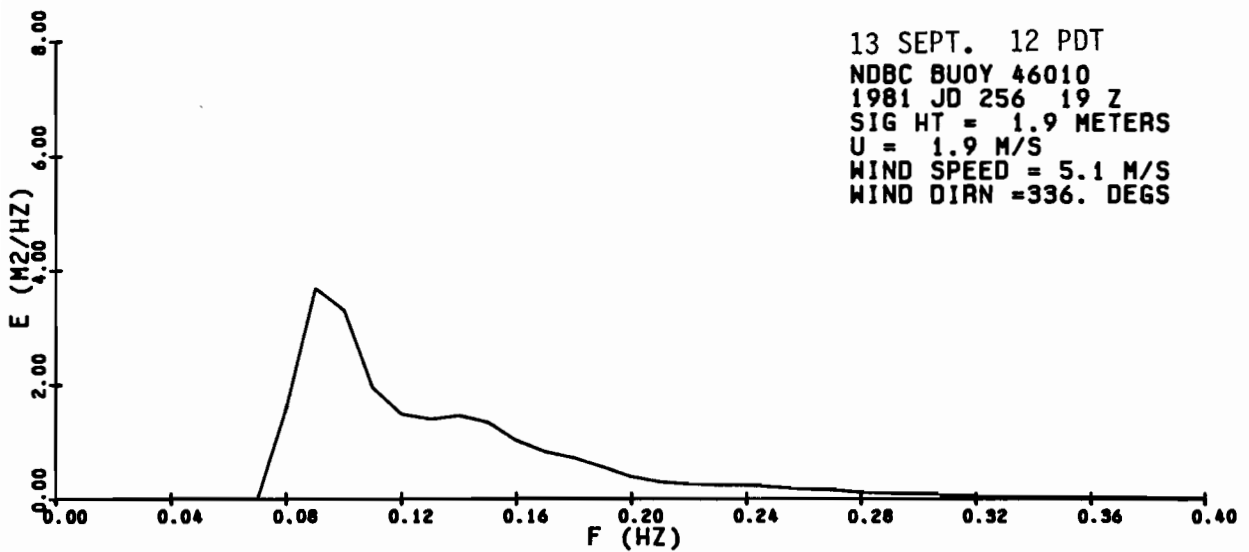
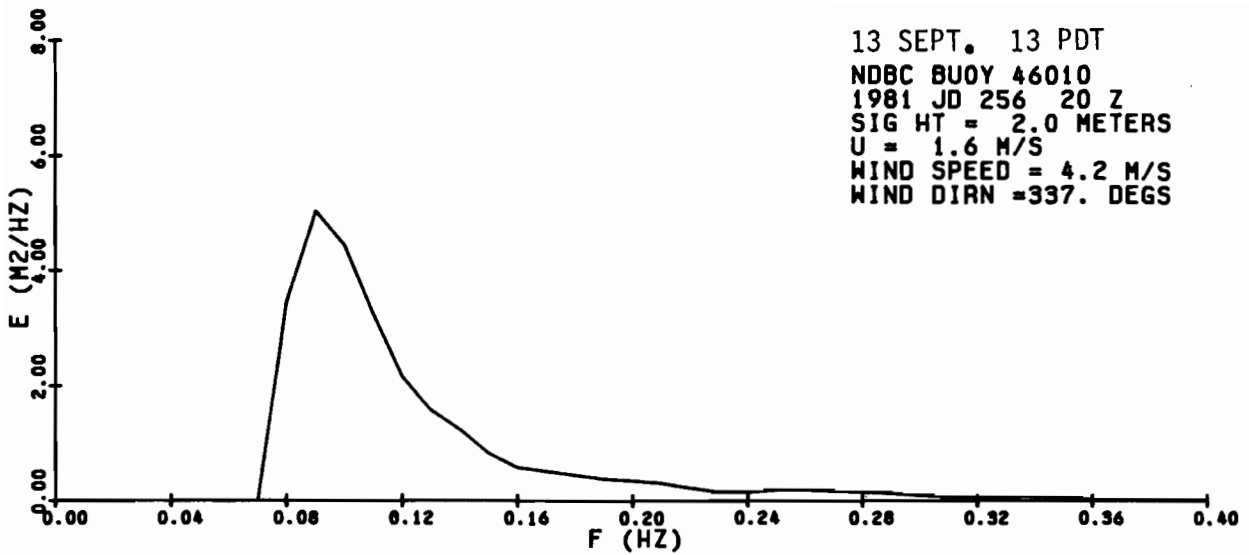


Figure A63. NDBC 46010 power spectral density for 1100, 1200, and 1300 PDT, 13 Sept. 1981.

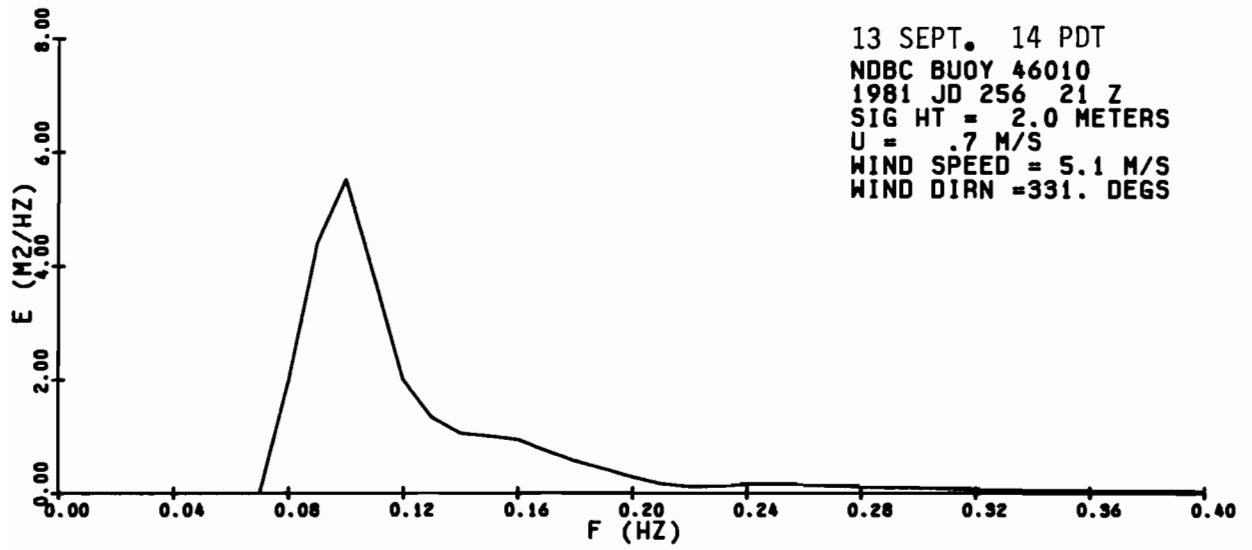
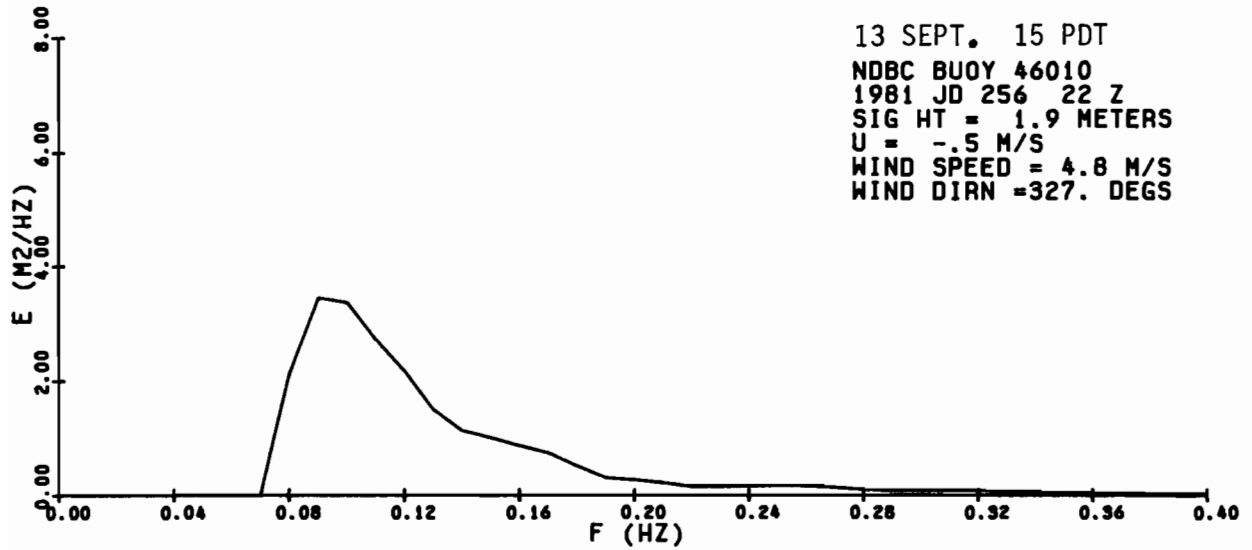
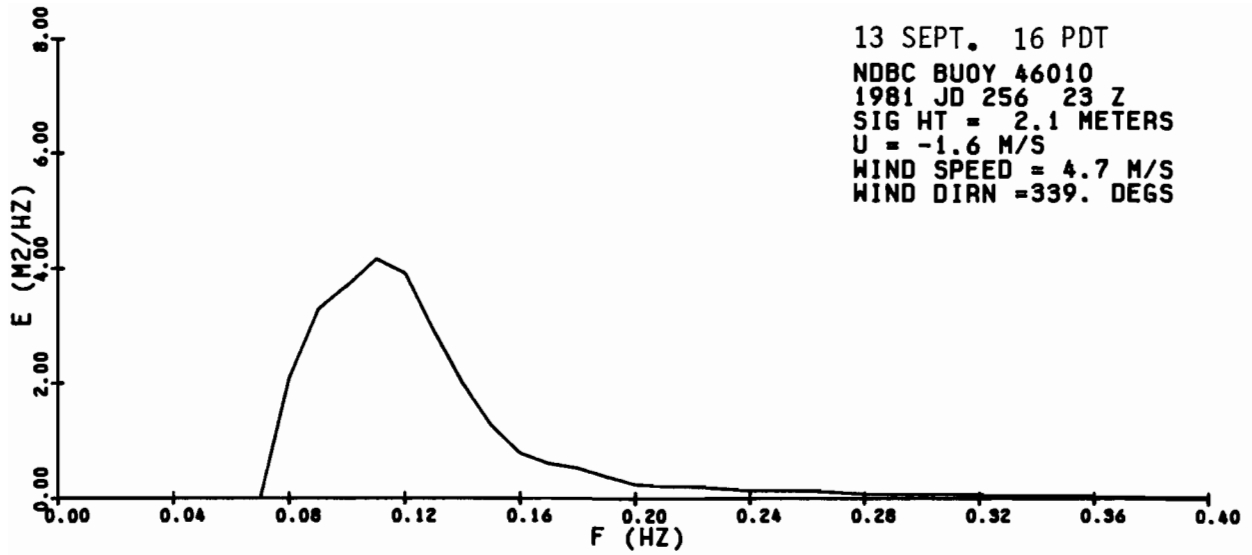


Figure A64. NDBC 46010 power spectral density for 1400, 1500, and 1600 PDT, 13 Sept. 1981.

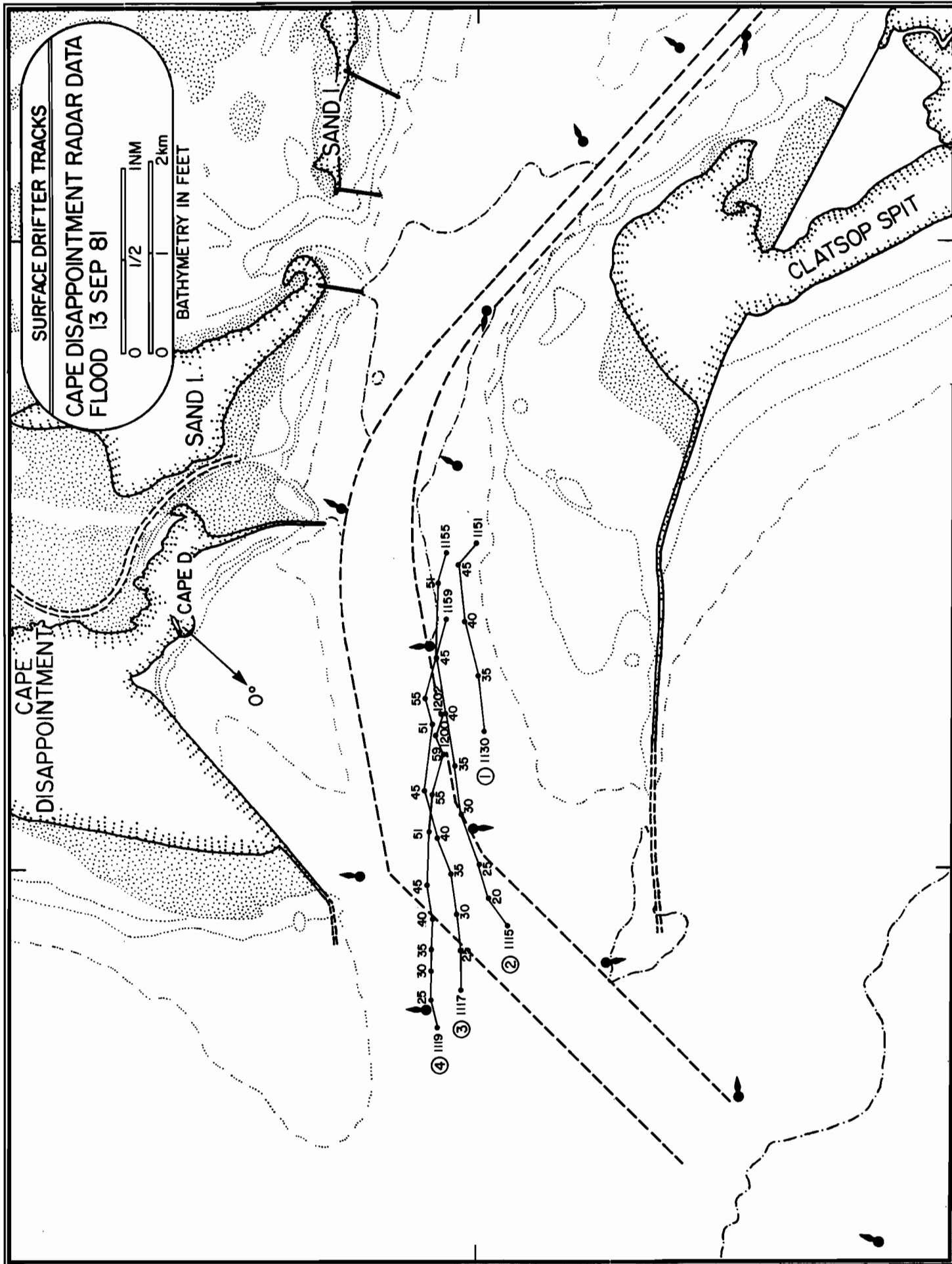


Figure A65. Surface drifter tracks for Cape Disappointment radar data collected during flood of 13 Sept. 1981.

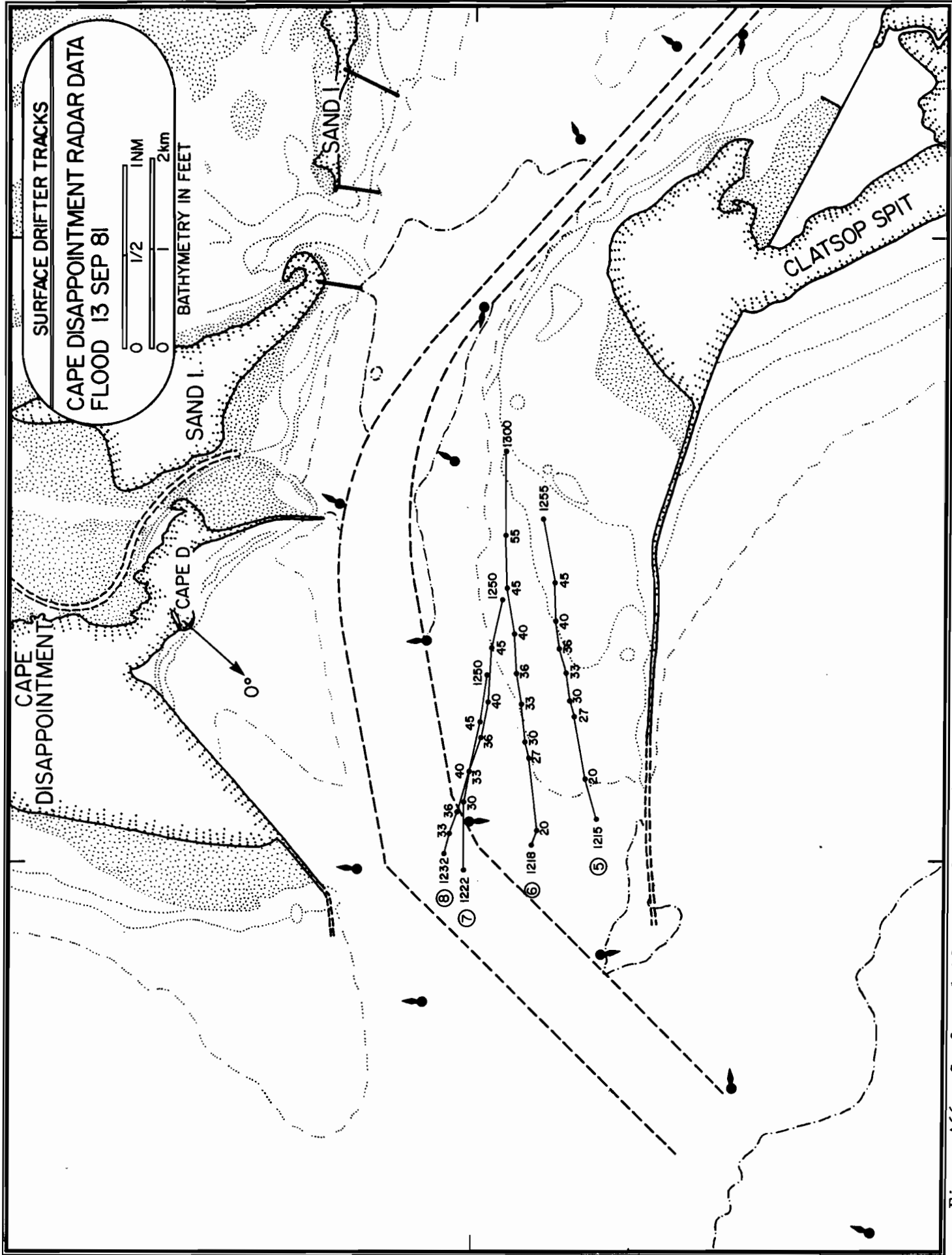


Figure A66. Surface drifter tracks for Cape Disappointment radar data collected during flood of 13 Sept. 1981.

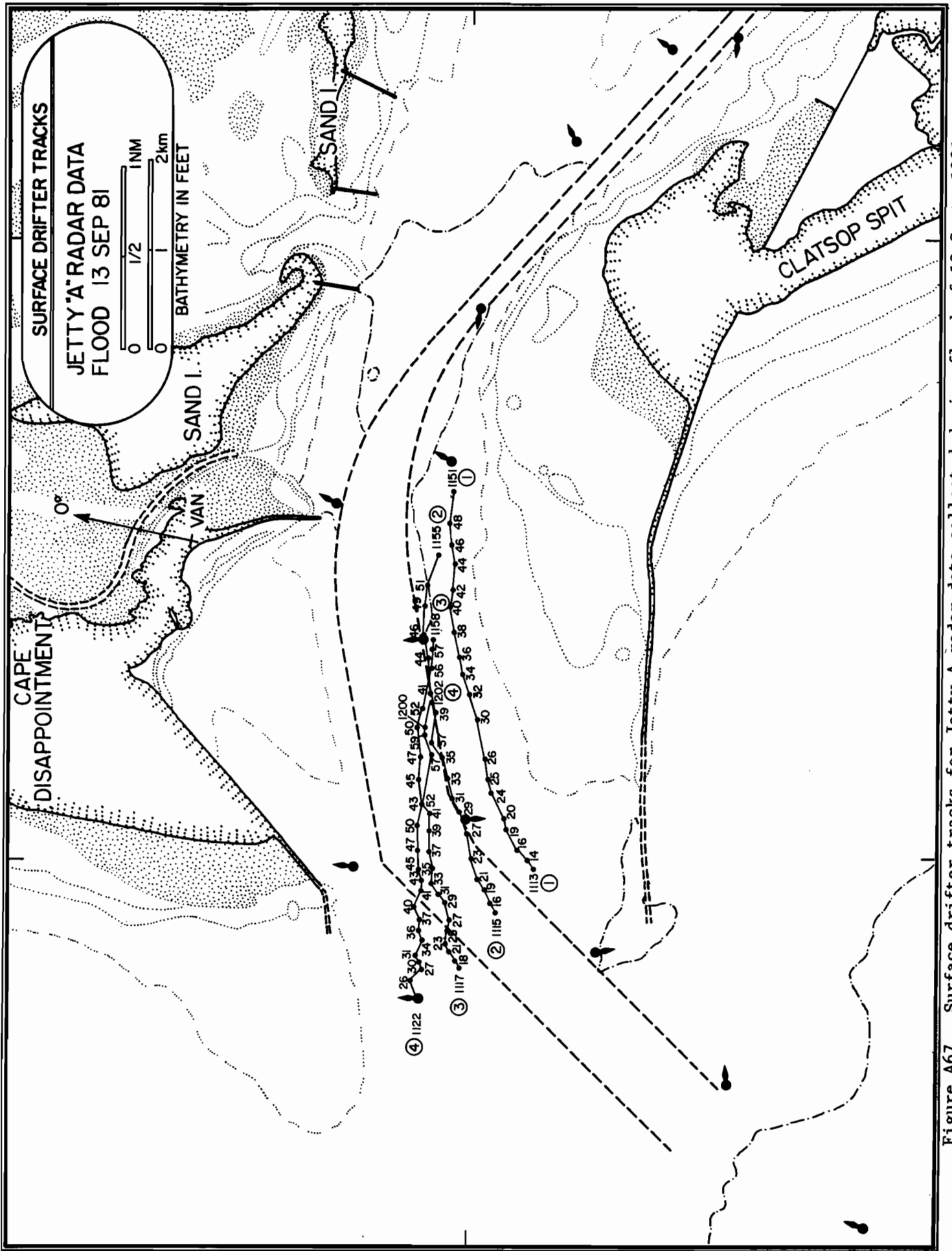


Figure A67. Surface drifter tracks for Jetty A radar data collected during flood of 13 Sept. 1981.



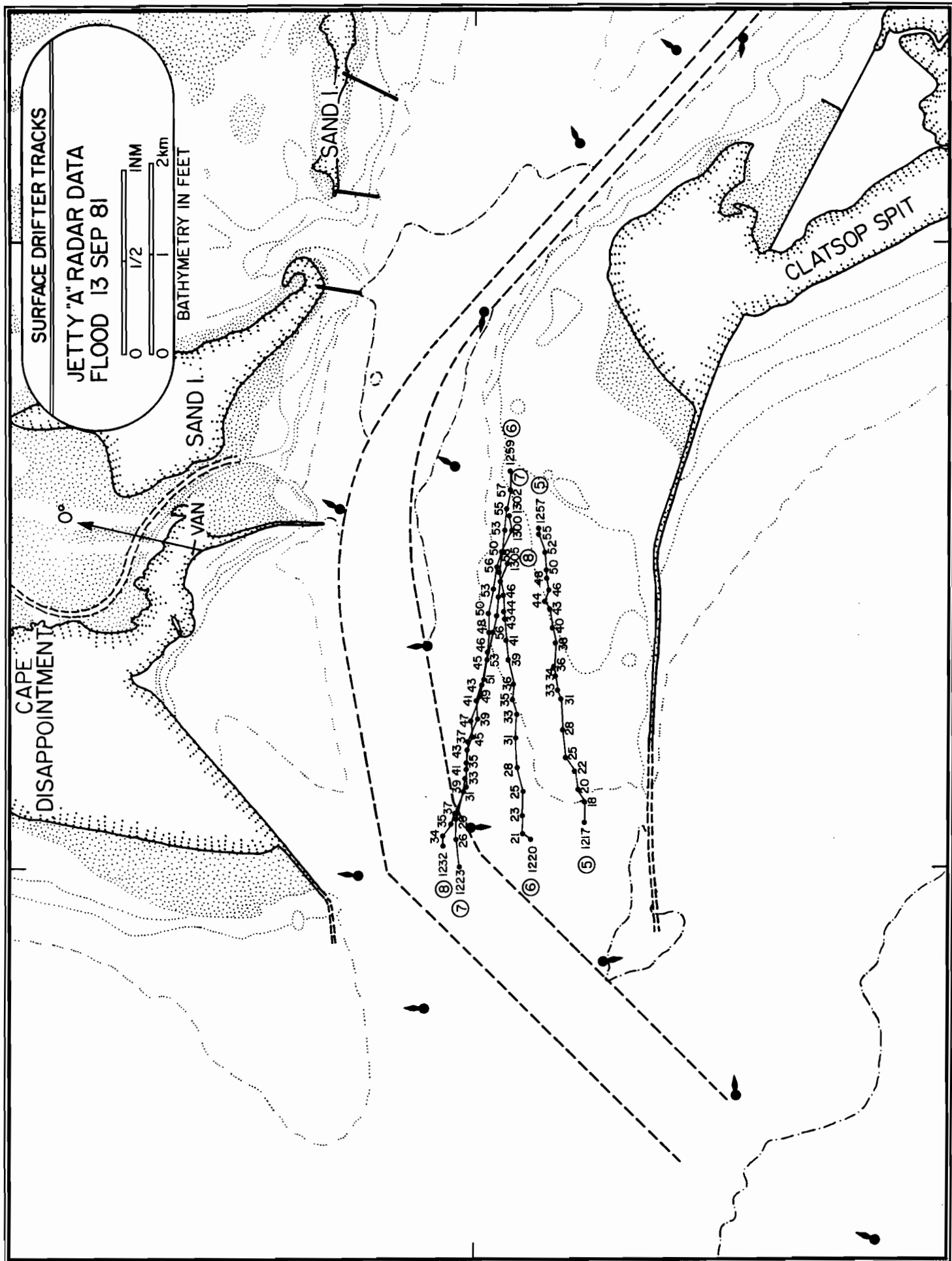


Figure A68. Surface drifter tracks for Jetty A radar data collected during flood of 13 Sept. 1981.

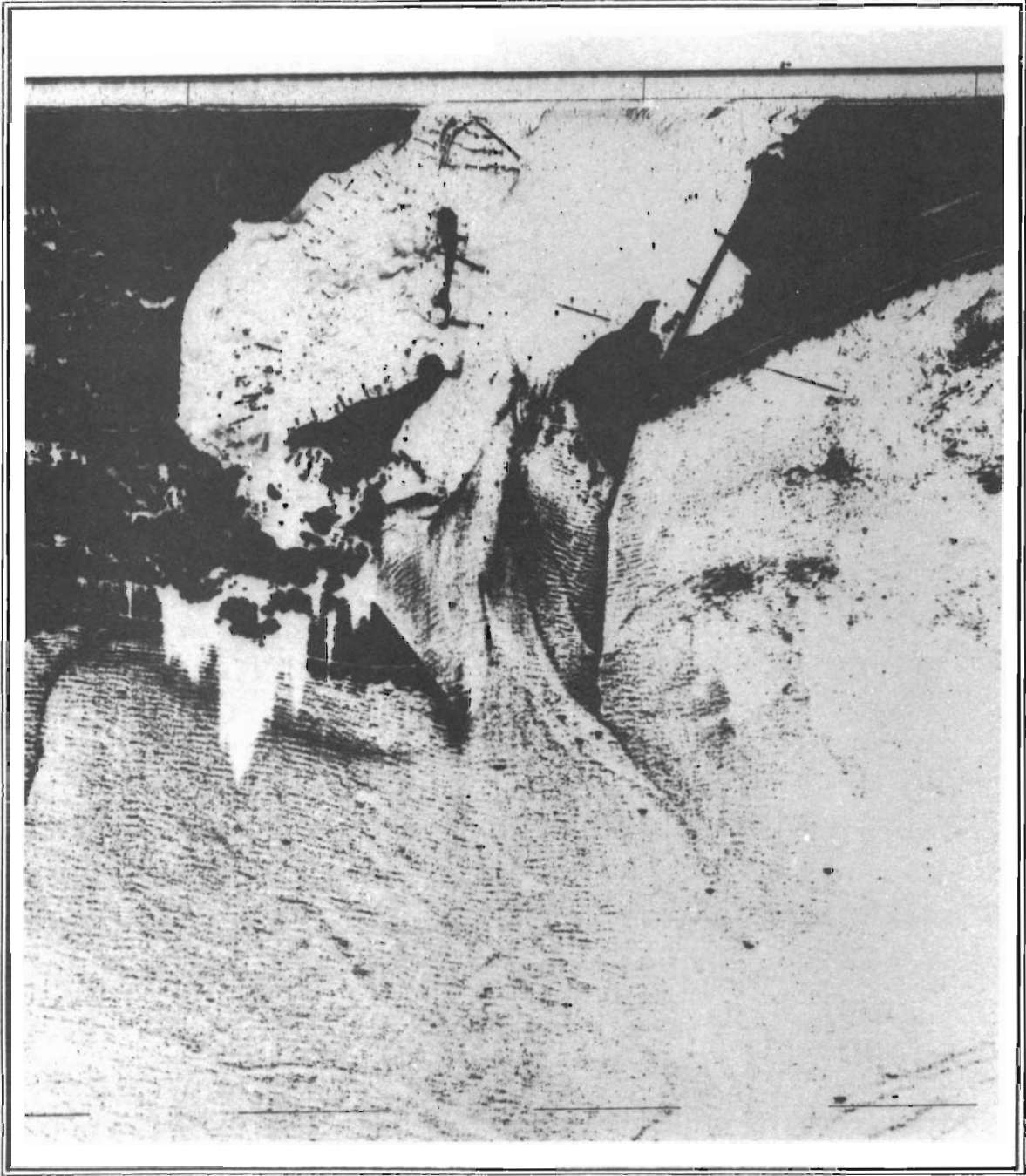


Figure A69. SLAR image of Columbia River entrance obtained on the flood at 1140 PDT, 13 Sept. 1981.



Figure A70. Blowup of Figure A69, centered on the river entrance.

13 September 1981

FLOOD

Waverider LOG (Surface Vessel EGRET)

Time	Hdg.	Sextant Fixes	Objects	Remarks
				NOTE: Buoy 8 has been removed by the Coast Guard.
1117				WR deployed. Begin record. Approx. position of Buoy 8.
1121		35° 36'	1	WR bears 060, 100 yds.
			2	
		23° 17'	15	
1125		35° 57'	1	
			2	
		24° 30'	15	
1129		36° 41'	1	(7-8 sec, ½ to 1 m)
			2	
		25° 42'	15	
1134		38° 06'	1	
			2	
		26° 23'	15	
1137				Underway for vessel traffic. End record.
1139				Begin drift, begin record.
1141		39° 52'	1	WR bears 060, 100-150 ft
			2	
		26° 30'	15	
1145		38° 55'	1	Drifter buoy 200 ft south of WR.
			2	
		29° 57'	15	
1151		35° 06'	1	
			2	
		34° 55'	15	

13 September 1981

FLOOD

Waverider LOG (Surface Vessel EGRET)

Time	Hdg.	Sextant Fixes	Objects	Remarks
1154		32° 24'	1	Drift buoy ~ 200 yds S of WR.
			2	
		36° 58'	15	
		35° 28'	5	
1158		27° 01'	1	
			2	
		39° 40'	15	
1200				Buoy 8 100 ft South.
1202		21° 45'	1	End drift.
			2	
		40° 07'	15	
1204				WR aboard.
~1218				WR deployed.
1223		38° 18'	1	On station.
			2	Begin record.
		23° 28'	15	
1230		36° 39'	1	10.5 sec.
			2	
		23° 02'	15	
				WR bears E 090 100 m, steady.
				(drift log 25 m 16.4, 16.4, 19.2 sec.)
1238		37° 45'	1	(12.5 sec., 1.5 m)
			2	
		23° 21'	15	
1243		38° 12'	1	
			2	
		23° 25'	15	
1245				End station, begin drift station.

13 September 1981

FLOOD

Waverider LOG (Surface Vessel EGRET)

Time	Hdg.	Sextant Fixes	Objects	Remarks
1248		37° 21'	1	WR 200 ft. bears E.
			2	
		24° 20'	15	
1253		36° 01'	1	WR bears E 100 ft.
			2	
		26° 16'	15	
1258		33° 40'	1	
			2	
		29° 05'	15	
				12 sec ~ $\frac{1}{2}$ m.
1304		30° 00'	1	
			2	
		30° 25'	15	
1310		26° 16'	1	End drift.
			2	
		32° 12'	15	
1312				WR aboard.

13 September 1981

FLOOD

CAPE DISAPPOINTMENT RADAR DATA

Buoy No.	Time (PDT)	Range (nm.)	Bearing (deg.)	Remarks
1	1130	1.70	334	
	1135	1.60	324	
	1140	1.50	313	
	1145	1.52	301	
	1151	1.65	288	Picked up #1
2	1115	2.38	258	
	1120	2.21	357	
	1125	2.05	354	
	1130	1.80	349	
	1135	1.63	342	
	1140	1.48	333	
	1145	1.36	321	
	1151	1.39	304	
1155	1.47	298	Picked up #2	
3	1117	2.48	008	
	1125	2.31	005	
	1130	2.15	002	
	1135	1.97	358	
	1140	1.78	355	
	1145	1.57	349	
	1151	1.42	336	
	1155	1.34	331	
	1159	1.40	312	Picked up #3
4	1119	2.59	013	
	1125	2.43	012	
	1130	2.31	010	
	1135	2.20	008	
	1140	2.07	005	
	1145	1.91	002	
	1151	1.71	355	
	1155	1.60	349	
	1159	1.50	341	
	1200	1.46	338	
	1202	1.46	333	Picked up #4
5	1215	2.51	341	
	1220	2.38	337	
	1227	2.20	329	
	1230	2.16	327	

13 September 1981

FLOOD

CAPE DISAPPOINTMENT RADAR DATA

---

Buoy No.	Time (PDT)	Range (nm.)	Bearing (deg.)	Remarks
	1233	2.11	323	
	1236	2.06	319	
	1240	2.03	315	
	1245	2.03	309	
	125530	2.03	299	Picked up #5
6	1218	2.27	348	
	1220	2.26	346	
	1227	2.03	337	
	1230	1.99	335	
	1233	1.90	329	
	1236	1.85	324	
	1240	1.81	317	
	1245	1.78	309	
	1250	1.82	300	
	1300	2.00	287	Picked up #6
7	1222	2.06	357	
	1230	1.83	348	
	1233	1.77	343	
	1236	1.74	337	
	1240	1.71	330	
	1245	1.69	320	
	1250	1.74	311	
	1302			#7 picked up
8	1232	1.91	357	
	1233	1.87	354	
	1236	1.84	350	
	1240	1.77	343	
	1245	1.70	334	
	1250	1.69	325	
	1307			#8 picked up

---



13 September 1981

FLOOD

JETTY A RADAR DATA

---

Buoy No.	Time (PDT)	Range (nm.)	Bearing (deg.)	Remarks
1	111240	2.61	224	
	111410	2.55	224	
	111600	2.47	224	
	111840	2.36	223	
	112020	2.30	222	
	112340	2.15	220	
	112440	2.10	219	
	112620	2.00	217	
	113020	1.84	212	
	113235	1.72	209	
	113420	1.64	206	
	113610	1.59	203	
	113810	1.52	199	
	114020	1.46	194	
	114200	1.45	190	
	114400	1.43	184	
	114550	1.41	180	
	114800	1.41	175	
	115040	1.46	168	1 retrieved
2	111430	2.65	231	
	111620	2.58	231	
	111830	2.51	230	
	112030	2.45	230	
	112320	2.33	229	
	112640	2.21	227	
	112840	2.10	226	
	113030	2.01	225	
	113250	1.91	223	
	113440	1.81	221	
	113630	1.72	220	
	113830	1.63	215	
	114040	1.54	213	
	114410	1.43	206	
	114610	1.37	202	
	114910	1.31	195	
115123	1.30	190		
115440	1.34	182	2 retrieved	

---

13 September 1981

FLOOD

JETTY A RADAR DATA

---

Buoy No.	Time (PDT)	Range (nm.)	Bearing (deg.)	Remarks
3	111640	2.79	238	
	111820	2.75	238	
	112110	2.68	238	
	112250	2.64	238	
	112520	2.58	237	
	112710	2.53	236	
	112920	2.45	235	
	113100	2.39	235	
	113320	2.31	235	
	113500	2.24	234	
	113710	2.16	233	
	113850	2.07	231	
	114100	1.99	229	
	114230	1.91	229	
	114430	1.80	227	
	114640	1.72	224	
	114930	1.60	220	
	115140	1.56	216	
115530	1.46	208		
115710	1.43	204		
115810	1.41	202	3 retrieved	
4	112220	2.83	244	
	112540	2.71	243	
	112720	2.69	242	
	112940	2.65	242	
	113120	2.61	242	
	113350	2.55	240	
	113530	2.49	240	
	113720	2.44	239	
	113930	2.37	239	
	114120	2.31	237	
	114250	2.27	236	
	114510	2.20	236	
	114650	2.11	234	
	114950	1.99	232	
	115210	1.91	229	
	115650	1.75	222	
115840	1.65	220		
120000	1.63	219		
120150	1.57	214	4 retrieved	

---

13 September 1981

FLOOD

JETTY A RADAR DATA

Buoy No.	Time (PDT)	Range (nm.)	Bearing (deg.)	Remarks
5	121640	2.63	215	
	121810	2.56	213	
	122020	2.49	212	
	122210	2.43	210	
	122440	2.34	209	
	122800	2.27	206	
	123040	2.19	202	
	123240	2.14	201	
	123410	2.10	199	
	123600	2.08	198	
	123810	2.05	194	
	124020	2.01	192	
	124230	1.98	189	
	124410	1.95	188	
	124540	1.95	186	
	124800	1.93	184	
	124940	1.93	183	
	125210	1.91	180	
	125450	1.89	177	
	125640	1.89	176	5 retrieved
6	121930	2.45	221	
	122030	2.40	221	
	122230	2.34	219	
	122500	2.25	216	
	122810	2.15	214	
	123110	2.04	210	
	123310	1.99	207	
	123430	1.93	205	
	123620	1.90	203	
	123830	1.82	199	
	124040	1.79	196	
	124250	1.74	192	
	124430	1.73	191	
	124600	1.71	188	
	124810	1.68	184	
	125000	1.69	180	
	125230	1.71	176	
	125500	1.73	172	
	125720	1.77	169	
	125910	1.78	166	6 retrieved

13 September 1981

FLOOD

JETTY A RADAR DATA

Buoy No.	Time (PDT)	Range (nm.)	Bearing (deg.)	Remarks
7	122250	2.28	230	
	122620	2.16	228	
	122830	2.07	226	
	123130	2.00	222	
	123320	1.95	220	
	123450	1.90	218	
	123630	1.85	215	
	123900	1.81	211	
	124100	1.76	208	
	124300	1.74	205	
	124450	1.71	201	
	124620	1.71	199	
	124830	1.68	195	
	125020	1.65	192	
	125250	1.67	187	
	125530	1.67	183	
	125740	1.69	180	
	130010	1.73	176	
	130140	1.72	173	7 retrieved
8	123210	2.13	230	
	123340	2.10	229	
	123510	2.08	227	
	123650	2.05	225	
	123920	1.98	221	
	124120	1.92	219	
	124320	1.86	216	
	124500	1.84	214	
	124630	1.79	212	
	124840	1.76	207	
	125050	1.74	204	
	125320	1.71	200	
	125550	1.70	195	
	125800	1.69	192	
	130030	1.69	188	
	130230	1.69	185	
130430	1.72	182	8 retrieved	

13 September 1981

EBB



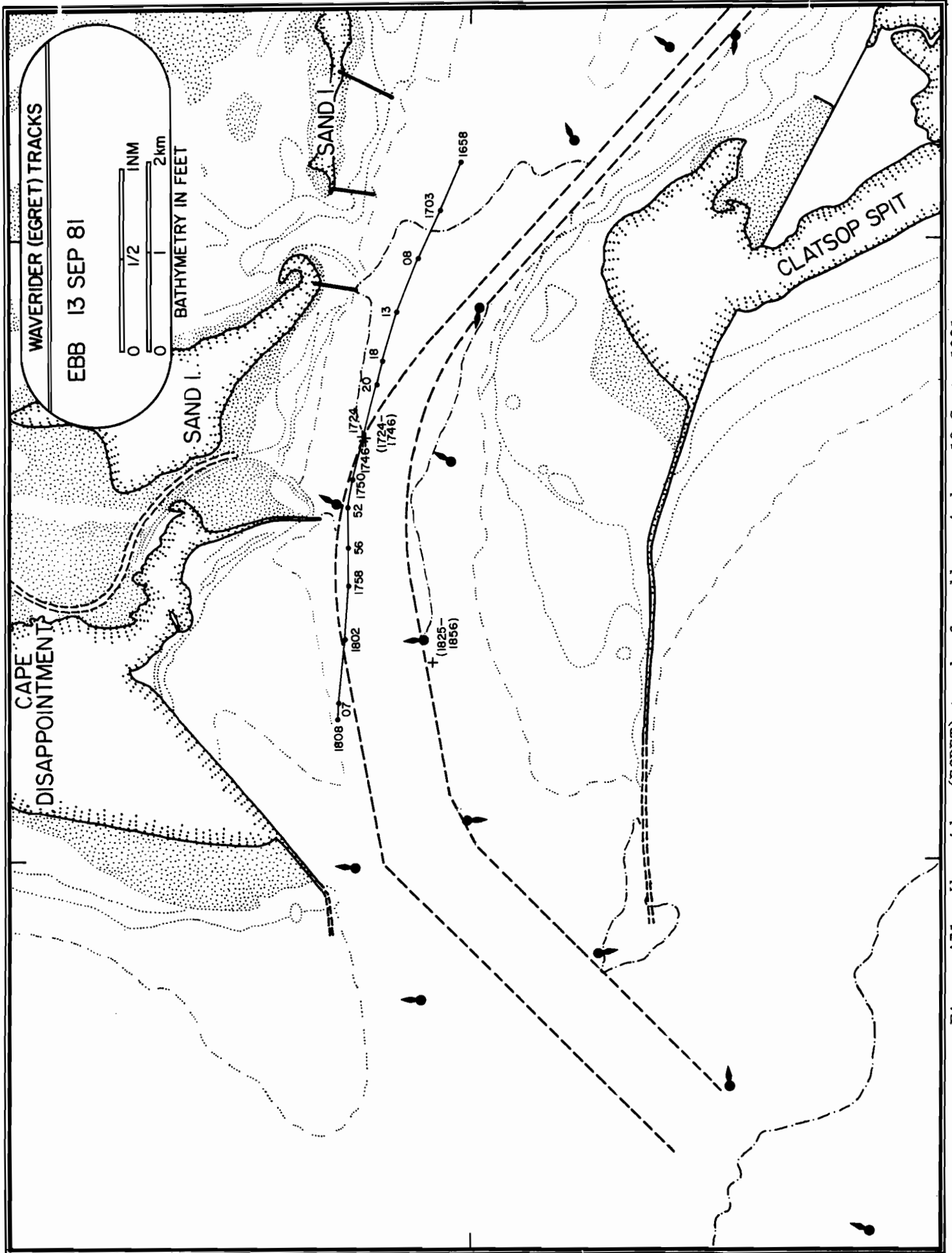


Figure A71. Waverider (EGRET) tracks for ebb period on 13 Sept. 1981.

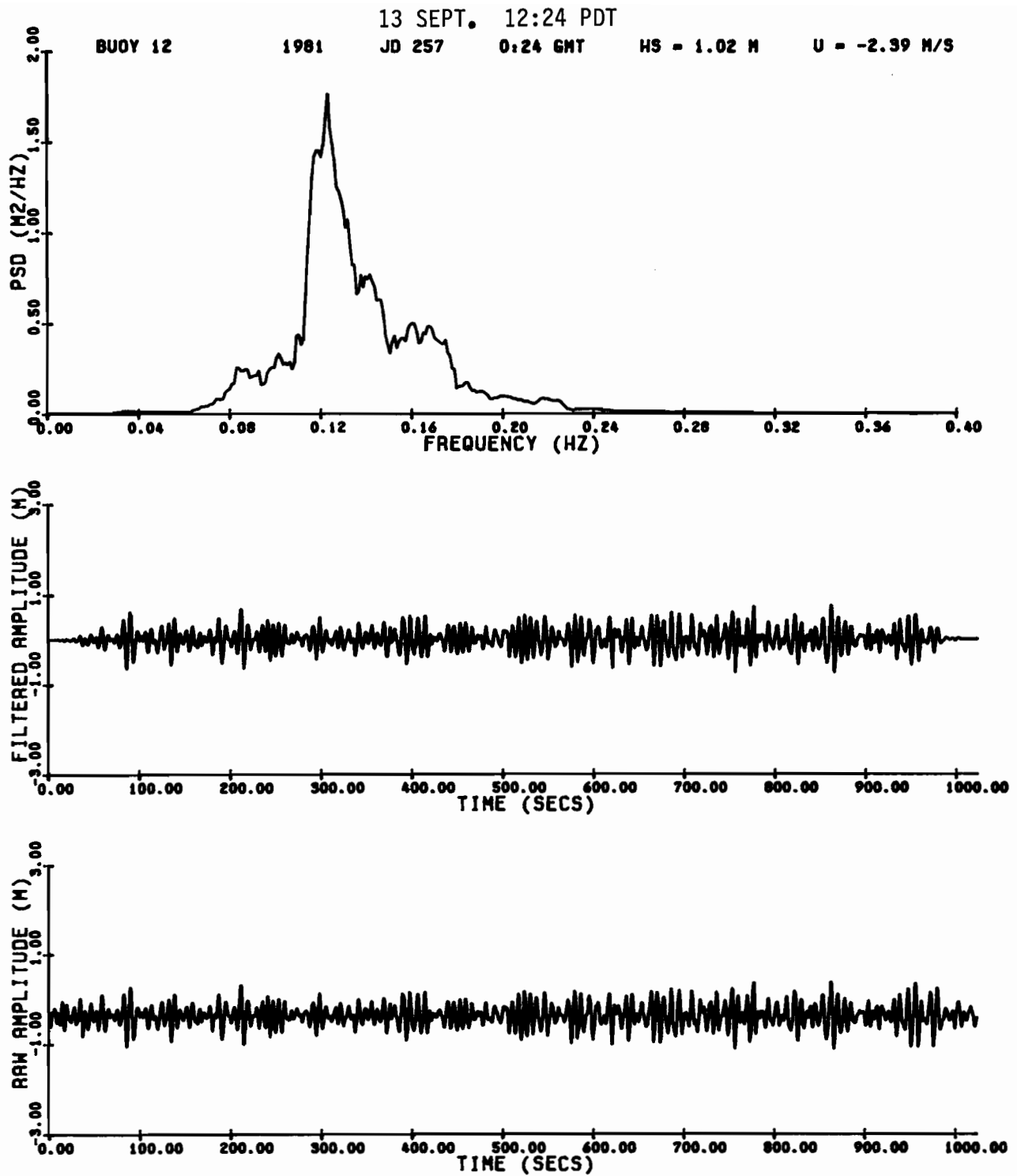


Figure A72. Waverider raw amplitude, filtered amplitude, and power spectral density for 1724 PDT, 13 Sept. 1981.



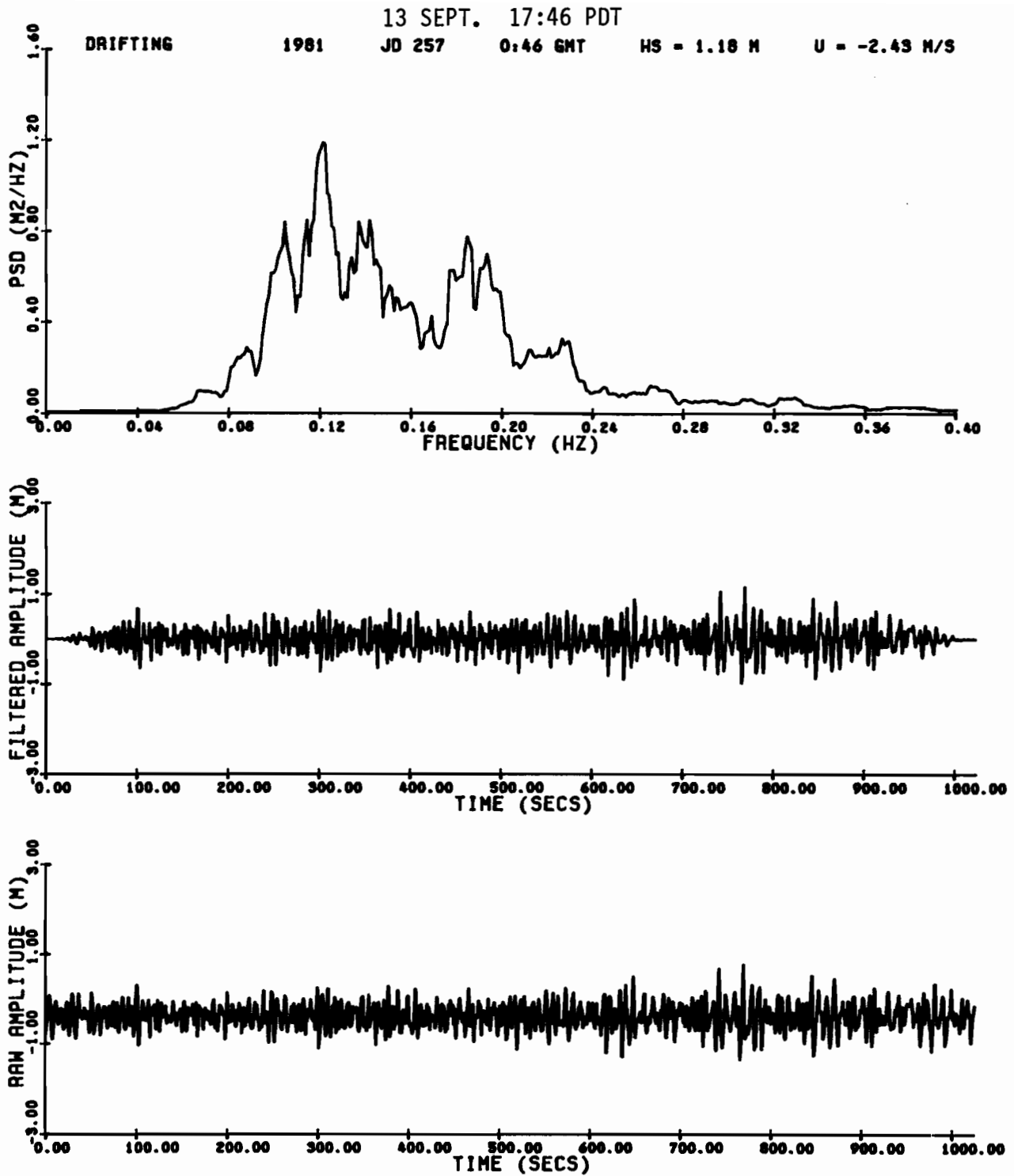


Figure A73. Waverider raw amplitude, filtered amplitude, and power spectral density for 1746 PDT, 13 Sept. 1981.

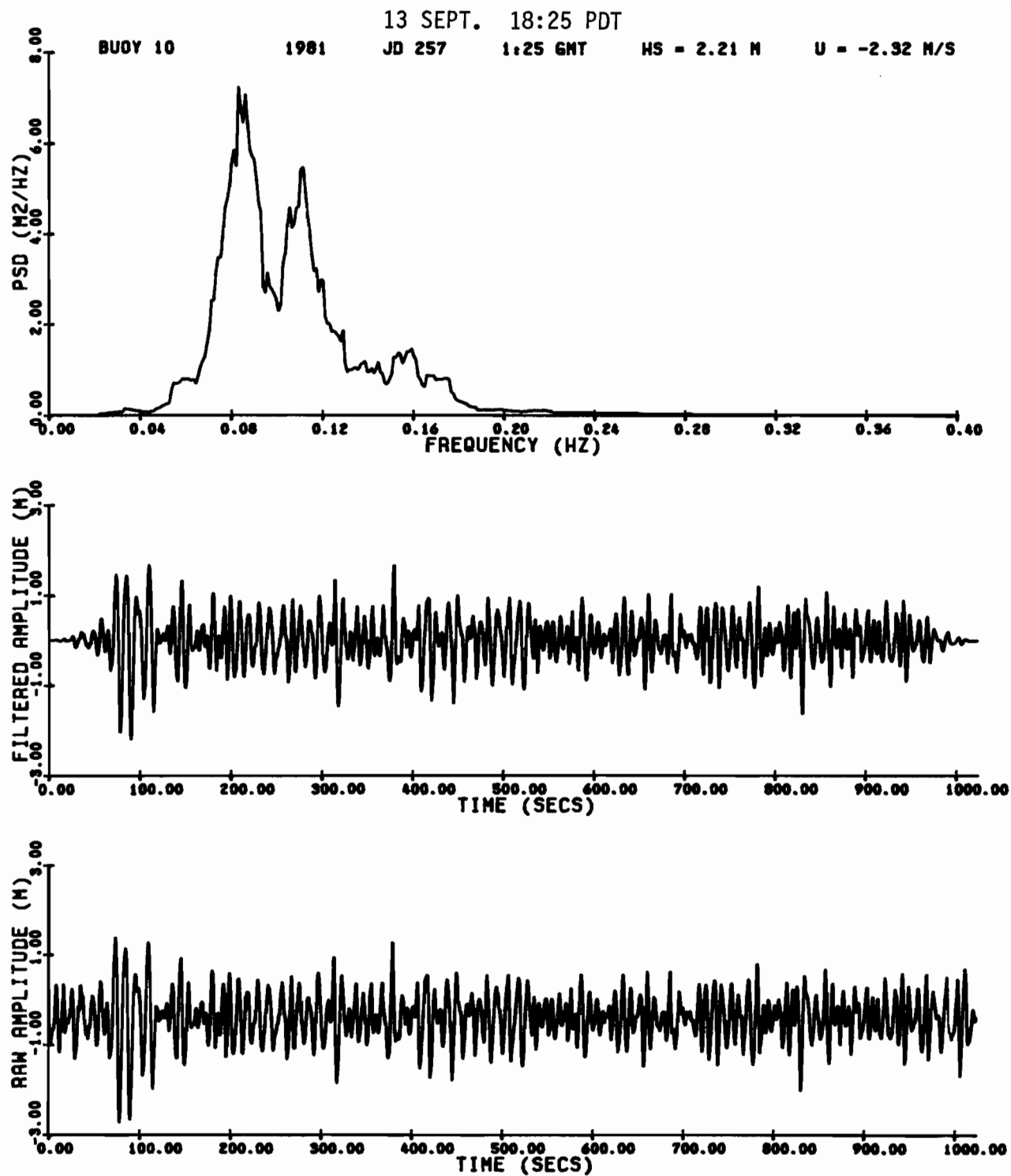


Figure A74. Waverider raw amplitude, filtered amplitude, and power spectral density for 1825 PDT, 13 Sept. 1981.

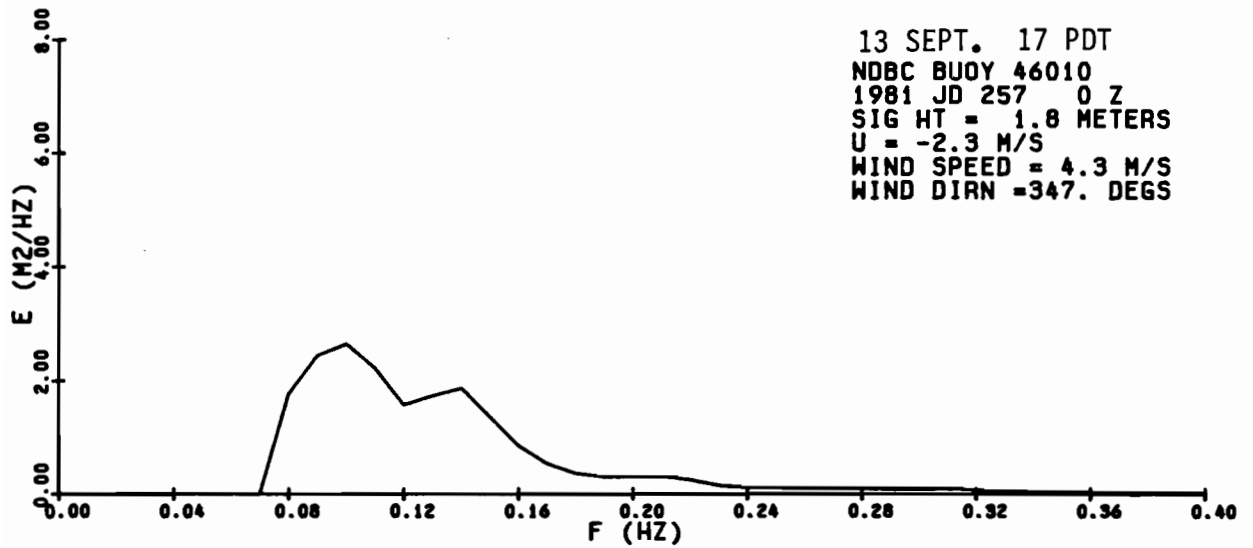
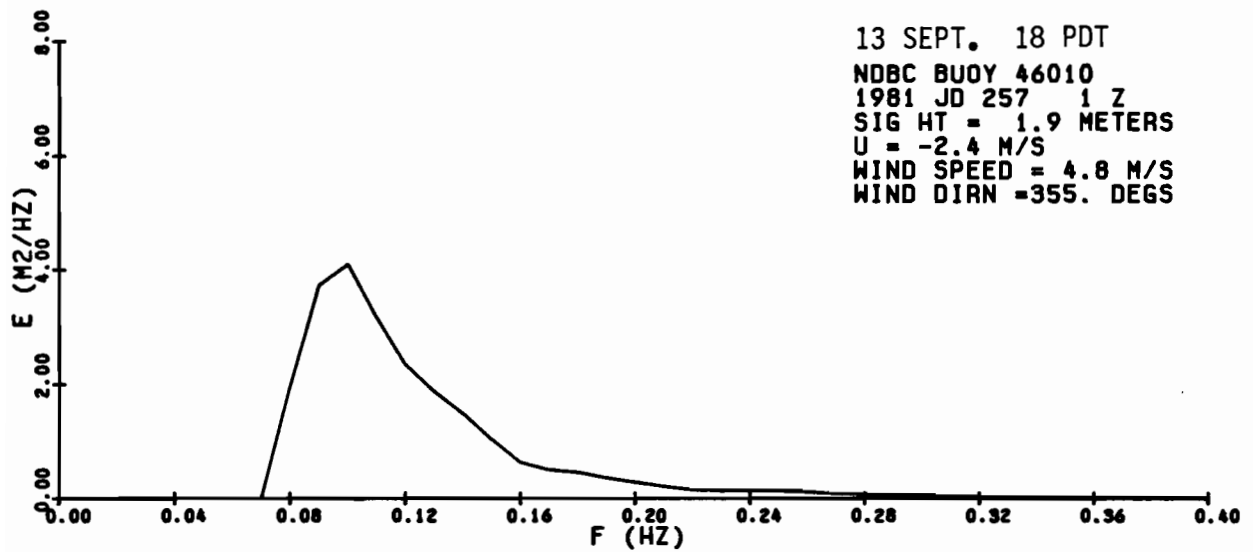
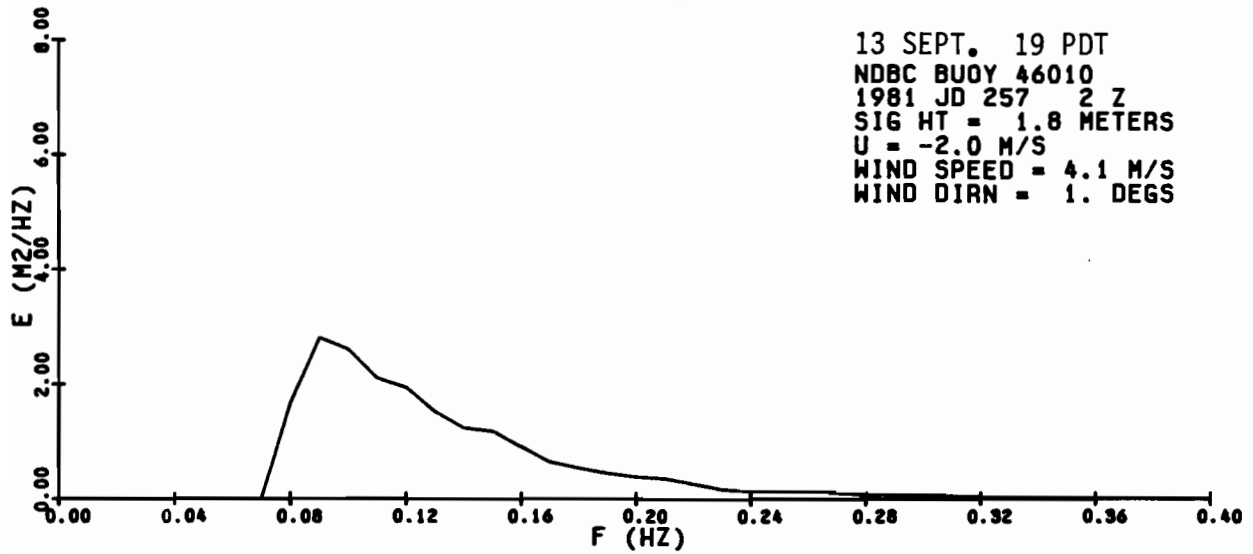


Figure A75. NDBC 46010 power spectral density for 1700, 1800, and 1900 PDT, 13 Sept. 1981.

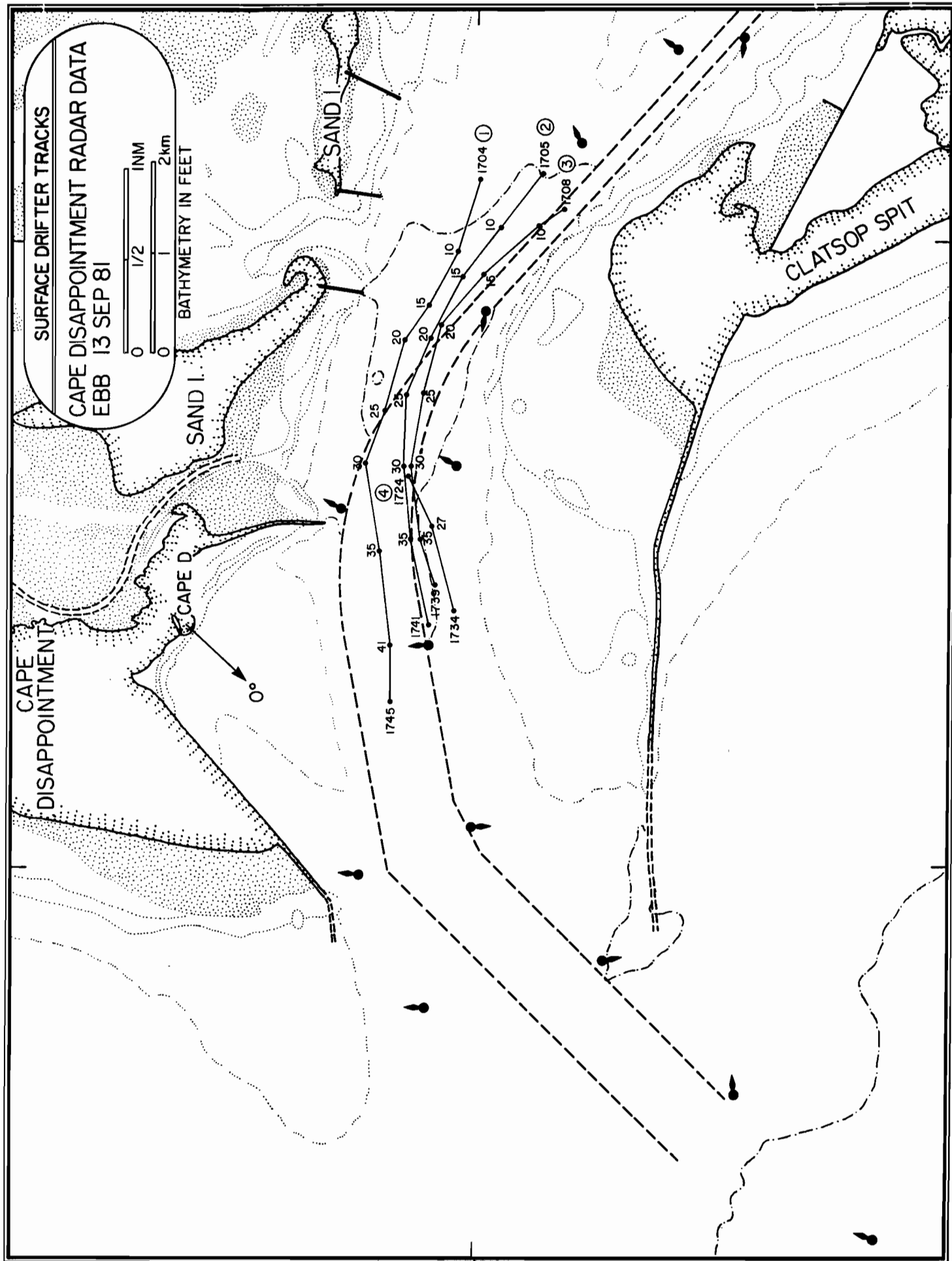


Figure A76. Surface drifter tracks for Cape Disappointment radar data collected during ebb of 13 Sept. 1981.

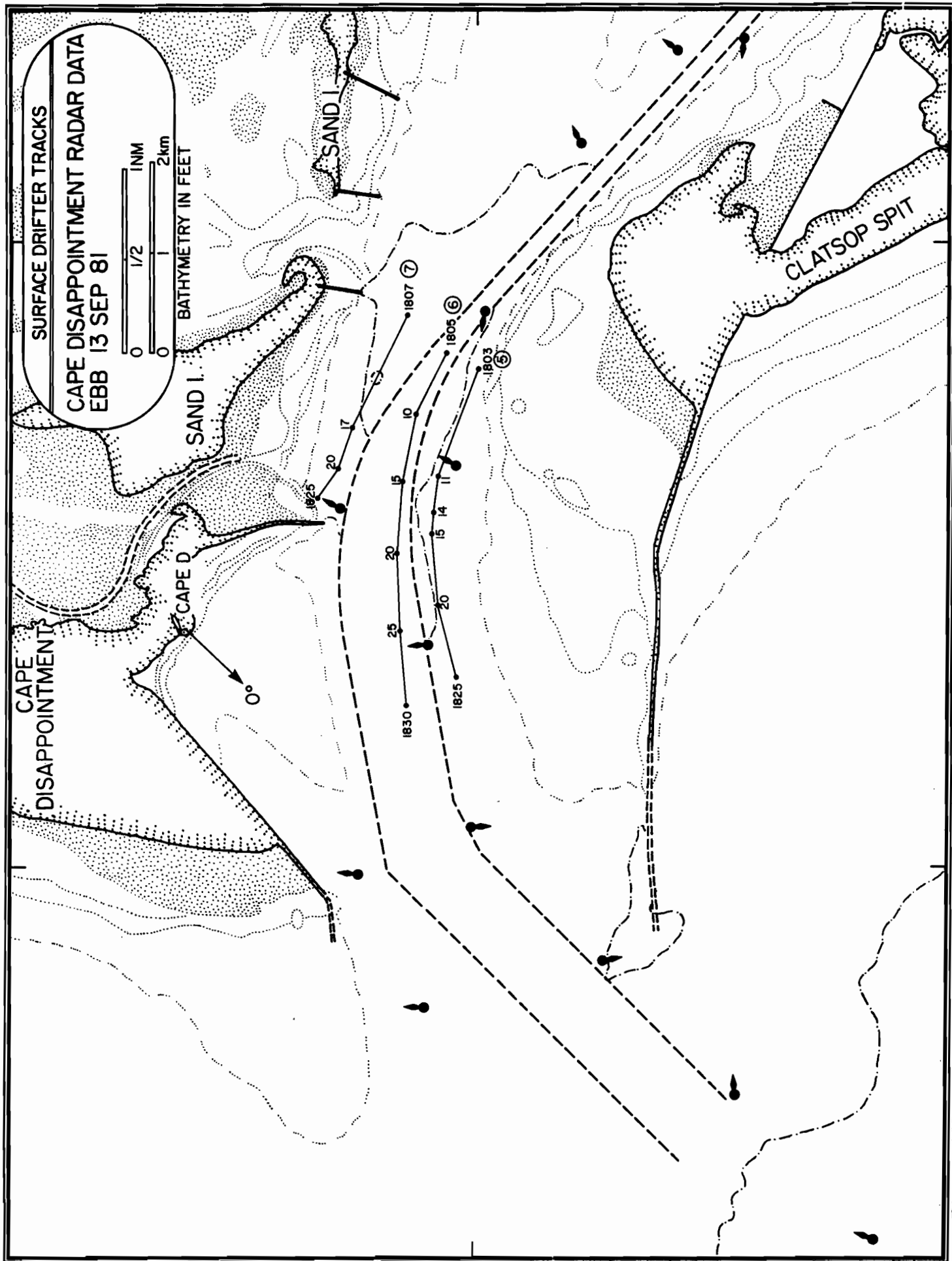


Figure A77. Surface drifter tracks for Cape Disappointment radar data collected during ebb of 13 Sept. 1981.

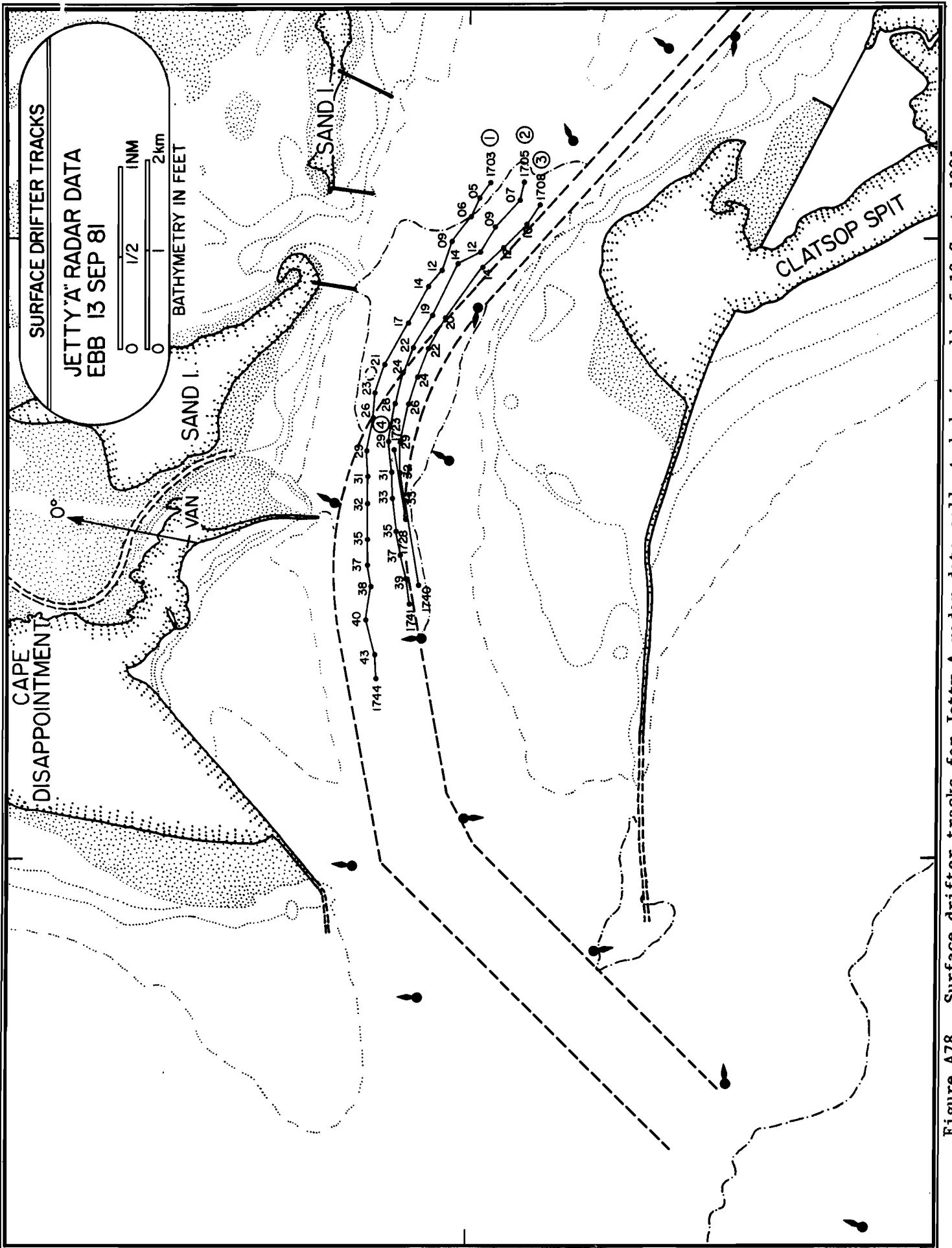


Figure A78. Surface drifter tracks for Jetty A radar data collected during ebb of 13 Sept. 1981.

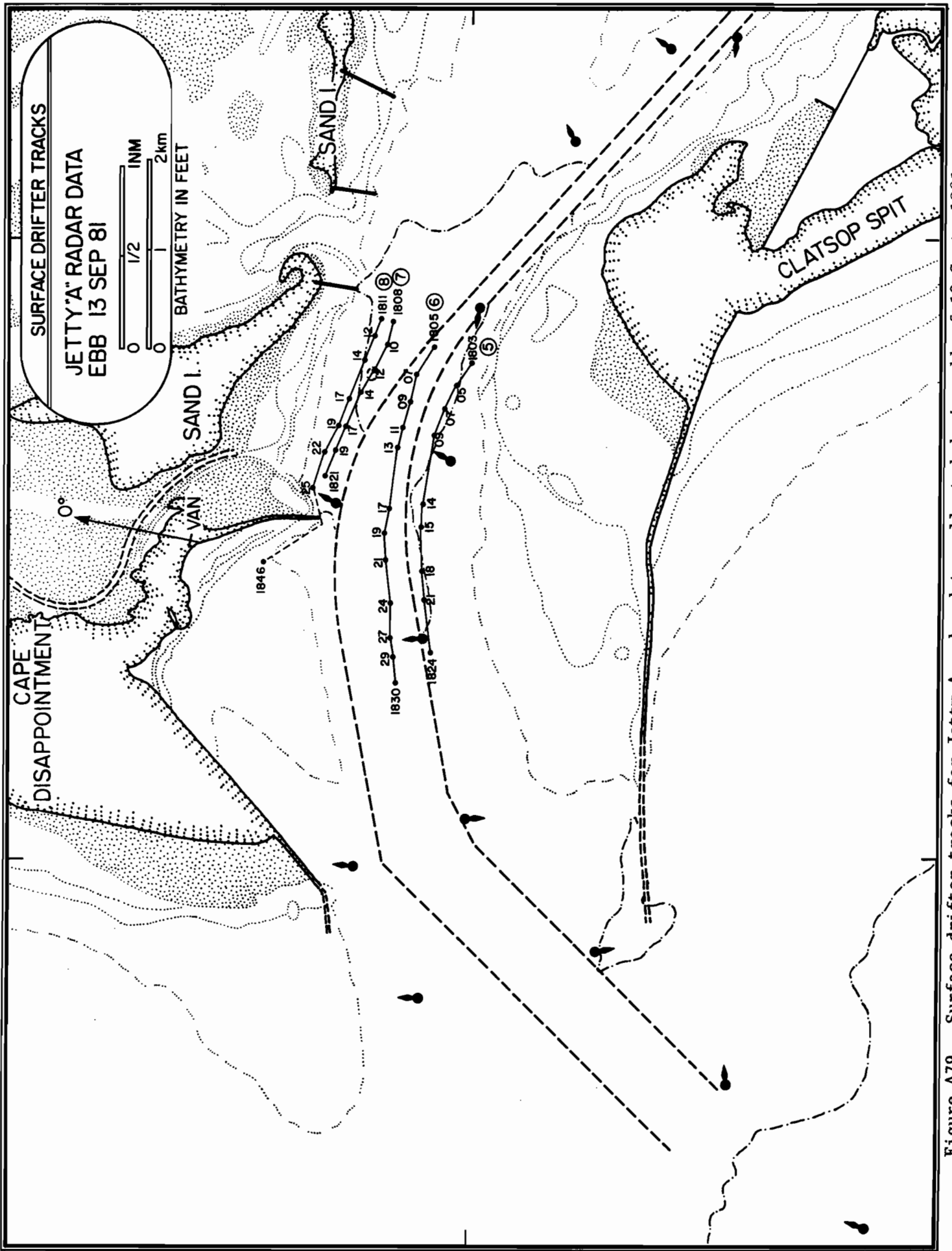


Figure A79. Surface drifter tracks for Jetty A radar data collected during ebb of 13 Sept. 1981.

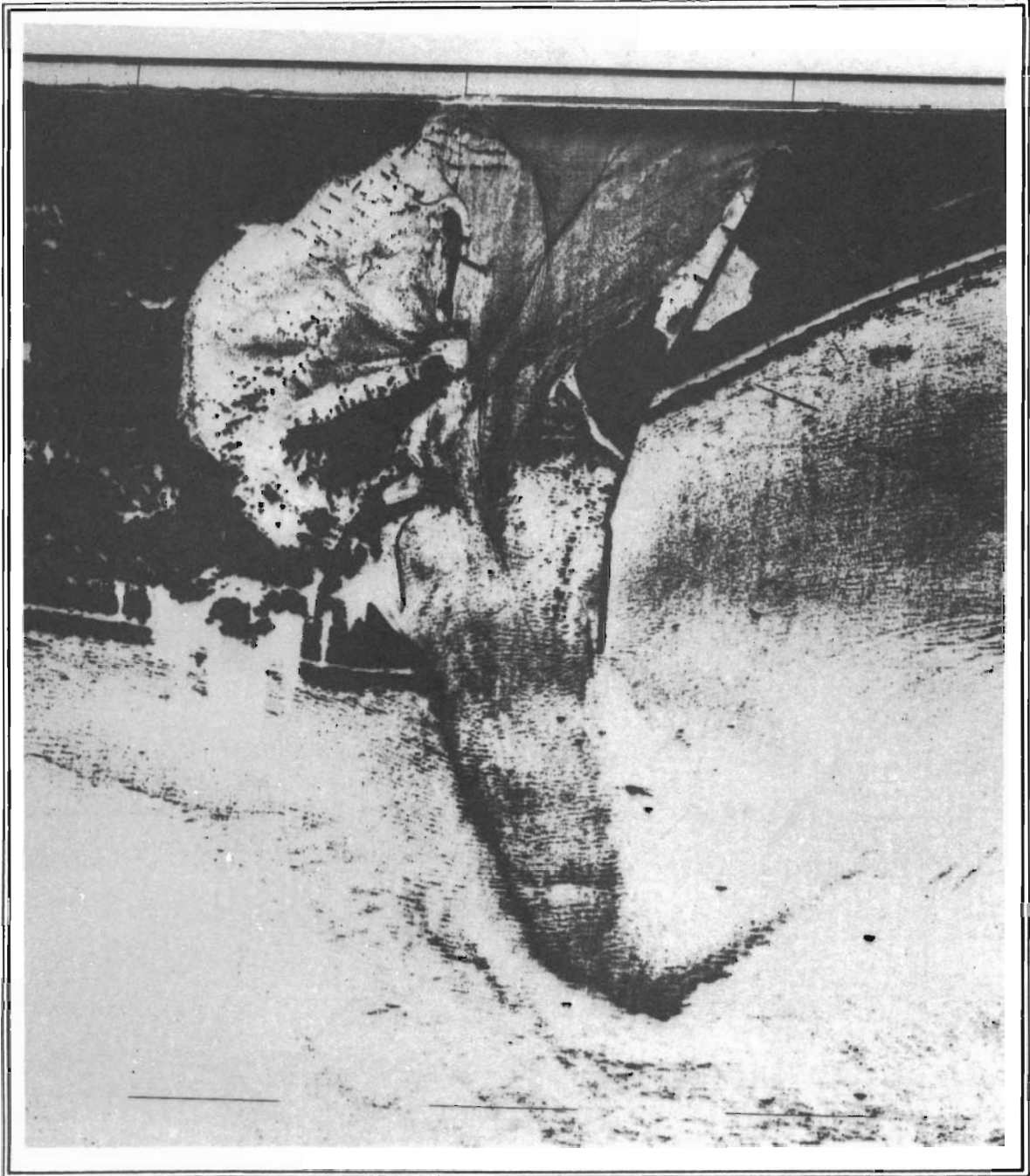


Figure A80. SLAR image of Columbia River entrance obtained on the ebb at 1730 PDT, 13 Sept. 1981.





Figure A81. Blowup of Figure A80, centered on the river entrance.

13 September 1981

EBB

Waverider LOG (Surface Vessel EGRET)

Time	Hdg.	Sextant Fixes	Objects	Remarks
1656				WR deployed.
1658		60° 01'	2	Begin drift.
			4	
		20° 30'	12	
		44° 00'	L√ 3	
1659				McArthur CM Station. 200 ft N.
				WR bears W 200 ft.
1703		21° 47'	2	
			3	
		73° 32'	12	
1708		32° 23'	2	WR bears NW 150 ft.
			3	
		76° 11'	12	
1713		53° 18'	2	WR bears NW 150 ft.
			3	
		65° 15'	12	
1718		82° 03'	2	
			3	
		48° 14'	11	
1720		92° 03'	2	
			3	
		31° 26'	12	
1724				End drift. Holding station.
1726		107° 25'	2	Steady on station. WR bears W 100 m.
			3	
		15° 08'	12	
1730		108° 15'	2	
			3	
		14° 34'	12	

13 September 1981

EBB

Waverider LOG (Surface Vessel EGRET)

Time	Hdg.	Sextant Fixes	Objects	Remarks
1734				Apparent current increase.
1736		100° 09'	2	
			3	
		18° 15'	12	
1744				Drift log 25 m. 11.0, 4.7, 10.7 sec.
1746		107° 27'	2	Begin drift from station.
			3	
		15° 06'	12	
1750		16° 30'	2	
			5	
		95° 50'	3	
1752		33° 53'	2	
			5	
		77° 18'	3	
1753				100 ft. S of Buoy 11.
1756		55° 53'	2	
			5	
		46° 01'	3	
1757				WR bears SW 100 ft.
175830		62° 32'	2	WR bears SW 100 ft.
			5	
		29° 27'	3	
1802		29° 57'	1	
			2	
		58° 55'	5	
1807		43° 18'	1	
			2	
		45° 56'	5	
1808				End drift. Underway. Move to position near Buoy 10.

13 September 1981

EBB

Waverider LOG (Surface Vessel EGRET)

---

Time	Hdg.	Sextant Fixes	Objects	Remarks
1825				On sta. 100 ft. W of Buoy 10. Begin record. 2 m., approx. 8 and 12 sec. WR bears W 100 m.  Drift log 10.4, 9.7, 10.8
1843		26° 50'	1	
			2	
		36° 56'	5	
1856				End station, end project.

---

13 September 1981

EBB

CAPE DISAPPOINTMENT RADAR DATA

Buoy No.	Time (PDT)	Range (nm.)	Bearing (deg.)	Remarks
1	1704	2.96	258	
	1710	2.56	261	
	1715	2.22	262	
	1720	1.90	262	
	1725	1.62	267	
	1730	1.33	272	
	1735	1.15	293	
	1741	1.10	320	
	1745	1.19	335	Picked up #1
2	1705	3.18	263	
	1710	2.8	263	
	1715	2.46	263	
	1720	2.09	265	
	1725	1.76	268	
	1730	1.49	278	
	1735	1.31	293	
	1741	1.32	314	Picked up #2 after 1741 fix
3	1708	3.05	267	
	1710	2.94	266	
	1715	2.54	265	
	1720	2.18	266	
	1725	1.84	270	
	1730	1.51	279	
	1735	1.37	294	
	1739	1.38	305	Picked up #3
4	1724	1.48	280	
	1727	1.36	292	
	1734	1.47	311	Picked up #4
5	1803	2.14	273	
	1811	1.62	283	
	1814	1.49	289	
	1815	1.43	293	
	1820	1.37	309	
	1825	1.49	325	Pick up #5
6	1805	2.09	268	
	1810	1.73	271	
	1815	1.43	280	

13 September 1981

EBB

CAPE DISAPPOINTMENT RADAR DATA

---

Buoy No.	Time (PDT)	Range (nm.)	Bearing (deg.)	Remarks
	1820	1.22	295	
	1825	1.16	315	
	1830	1.26	334	Pick up #6
7	1807	2.12	260	
	1817	1.44	264	
	1820	1.21	268	
	1825	1.01	269	Pick up #3

---

13 September 1981

EBB

JETTY A RADAR DATA

Buoy No.	Time (PDT)	Range (nm.)	Bearing (deg.)	Remarks
1	1703	2.60	129	
	170440	2.50	129	
	170620	2.38	130	
	170900	2.21	130	
	171140	2.06	132	
	171330	1.93	132	
	171650	1.71	134	
	172100	1.45	137	
	172320	1.32	140	
	172530	1.22	145	
	172830	1.10	152	
	173100	1.05	159	
	173220	1.00	167	
	173510	0.98	178	
	173700	0.99	186	
	173830	1.03	193	
	174020	1.07	203	
	174250	1.20	211	
174410	1.28	216	1 picked up	
2	170520	2.73	132	
	170640	2.64	133	
	170920	2.44	133	
	171150	2.28	134	
	171350	2.15	133	
	171830	1.84	136	
	172140	1.63	138	
	172340	1.50	141	
	172550	1.37	145	
	172850	1.23	152	
	173120	1.18	160	
	173250	1.14	167	
	173520	1.14	176	
	173720	1.16	183	
	173850	1.21	189	
	174050	1.27	195	2 picked up
3	170740	2.69	135	
	170940	2.57	136	
	171210	2.39	136	

13 September 1981

EBB

JETTY A RADAR DATA

Buoy No.	Time (PDT)	Range (nm.)	Bearing (deg.)	Remarks
	171420	2.23	136	?
	171950	1.88	138	Found buoy 3. Previous fix in error?
	172200	1.70	140	
	172410	1.55	143	
	172610	1.43	147	
	172910	1.28	154	
	173140	1.21	161	
	173320	1.21	168	3 lost radar reflector after this
	173940	1.29	190	3 picked up
4	172250	1.25	155	
	172800	1.20	173	
5	180310	1.84	146	
	180500	1.70	148	
	180650	1.58	151	
	180900	1.46	155	
	181340	1.29	169	
	181510	1.27	175	
	181820	1.27	186	
	182030	1.32	193	
	182340	1.45	204	
6	180440	1.72	140	
	180710	1.55	142	
	180920	1.44	146	
	181130	1.32	150	
	181300	1.24	154	
	181640	1.10	169	
	181840	1.06	176	
	182050	1.06	184	
	182400	1.13	196	
	182640	1.20	205	
	182830	1.28	209	
	183020	1.36	214	6 picked up
7	180750	1.66	131	
	180940	1.54	133	
	181200	1.38	135	



13 September 1981

EBB

JETTY A RADAR DATA

---

Buoy No.	Time (PDT)	Range (nm.)	Bearing (deg.)	Remarks
	181400	1.26	137	
	181700	1.07	142	
	181900	0.94	146	
	182110	0.82	152	
8	181050	1.63	129	
	181210	1.53	130	
	181420	1.40	132	
	181720	1.18	136	
	181920	1.04	140	
	182130	0.89	144	
	182440	0.73	154	
	184600	0.42	193	

---